DTU Library

Model Predictive Control in Urban Systems

Svensen, Jan Lorenz

[Link back to DTU Orbit](#)

Model Predictive Control in Urban Systems

Jan Lorenz Svensen

DTU

Summary (English)

This dissertation is about Model Predictive Control (MPC) and its application to sewer networks.

Our main interest is to control sewer networks, such that the wastewater is kept inside the network and not overflowing into the nearby environments, if possible. Towards this goal, we consider the use of the predictive abilities of MPC, an optimal control method, to account for the coming rain inflow to the network; provided through known forecasts.

An outline of the physics of sewer networks is presented, such as the Saint-Venant equations and overflows from weirs, including an outline of the general goals for the operation of the network. An outline is given for different approaches to formulating design models for the control of the sewer. We show different methods of how overflow from weirs can be included in MPC for linear designs, and discuss the benefits of each approach

For more realistic scenarios, we assume the presence of uncertainty in the rain forecasts applied to the MPC. We outline different approaches to MPC with handling of uncertainty; such as tube-based MPC and Chance-constrained MPC(CC-MPC). We show how the probabilistic formulation of CC-MPC can be adapted to handle the presence of weirs; by the addition of constraints for defining the expected overflows, and probabilistic constraints on the avoidment of overflow. A discussion on the different approaches to uncertainty is given; showing how similar and different they are.

We outline how the stochastic distributions of the constraints utilized by CC-

MPC can be estimated, based on the usage of ensemble forecasts. We show how the estimation can be applied to CC-MPC, to obtain computational simpler optimization programs.

Summary (Danish)

Denne afhandling handler om Model Predictive Control (MPC) og dens anvendelse i kloaknetværk.

Et af grund punkterne ved kontrol af kloakker er at holde spildevandet nede i selve kloakken, således at der ikke sker forurening ved overløb til nærliggende områder. Et andet er at lede spildevandet til rensningsanlæggene.

For at bedre opnå dette mål og tage højde for fremtidige regnvejr, anvender vi den optimale kontrol metode MPC; for dens evner til at forudsige den rette kontrol baseret på vejrudsigter.

I afhandlingen giver vi en beskrivelse af fysikken bag kloakker, såsom Saint-Venant ligningerne og overløb. Vi diskuterer også de generelle driftsmål for kloakker, og hvordan de kan blive realiseret i kontrol design.

Selve modellerne brugt i kontrol design, bliver diskuteret for hvordan de kan formes fra fysikken eller estimeringer.

En del af diskussionen omkring kontrol design, er fokuseret på inklusionen af overløb i MPC med lineær designs. Vi diskuterer flere tilgange til overløb og de tilhørende fordele og ulemper.

Da realistiske vejrudsigter som udgangspunkt ikke er eksakte, må MPCen tage højde for en vis grad af usikkerhed i de anvendte prognoser. Fra forskningen, beskrive vi kort nogle af de forskellige tilgange til MPC der kan håndterer usikkerhed, f.eks. tube-baseret MPC og Chance-begrænset MPC (CC-MPC). Vi

beskriver hvordan CC-MPC's probabilistiske formulering kan blive tilpasset til-stedeværelsen af overløb; ved indførelsen af ekstra overløb definerende begræns-ninger, samt probabilistisk begrænsninger til undgåelse af overløb.

Vi belyser de forskellige MPC metoders tilgange til usikkerhed, deriblandt dis-kuterer vi hvor ens og forskellige de er.

Som en del af diskussionen om brugen af CC-MPC i kloak, diskuterer vi brugen af distribution estimering, og hvordan dette kan benyttes til simplificering af CC-MPC ved brug af ensemble prognoser.

Preface

This thesis was prepared at DTU Compute in fulfillment of the requirements for acquiring the ph.d. degree. The work has been carried out at the section for Dynamical Systems at the Department of Applied Mathematics and Computer Science (DTU Compute) at the Technical University of Denmark, under the supervision of the following team of supervisors:

1. Assoc. Prof. Niels Kjølstad Poulsen, DTU (Main, Now Prof. Emeritus)

2. Assoc. Prof. Hans Henrik Niemann, DTU

3. Res. Sci. Anne Katrine Vinther Falk, DHI

4. Tech. Dir. Henrik Madsen, DHI

5. Prof. Henrik Madsen, DTU (substitute main)

The main subject of this project is Model Predictive Control in Sewer Networks. A basic understanding of statistics and linear algebra are beneficial to acquire before reading this dissertation.

This dissertation is based on seven papers, whereof one is a conference paper, one is an unpublished article, and five are journal papers (1 published and 4 submitted).

Lyngby, 14-October-2020

Not Real

Jan Lorenz Svensen

Acknowledgements

I would like to thank my supervisors; now Prof. Emeritus Niels Kjølstad Poulsen, Assoc. Prof. Henrik Niemann, and DHI Researcher Anne Katrine Vinther Falk for their guidance and feedback during my project, and to Prof. Henrik Madsen (DTU) for both guidance and stepping into the role of main supervisor during the last period of the project.

I will also thank Prof. Vicenç Puig, Sr. Researcher Gabriela Cembrano and Dr.(post-doc) Congcong Sun for their collaboration and inputs during/after my research stay at UPC, and for allowing me to visit them in Barcelona during the last three months of 2019.

I would like to thank my colleagues at the section for Dynamical Systems for providing a welcoming and varying workspace during the last three years, with nice talks and sparrings. I am also grateful for the conversations and sparrings with my collaborators in the Water Smart Cities project.

Last but not least a thanks to my family for their support during my studies, especially my parents who have had to put up with my venting in some of the more frustrating periods of the ph.d. project.

Contents

Nomenclature

Abbriviations:

CDF	Cummalative Distribution Function
MPC	Model Predictive Control
CC-MPC	Chance Constrained Model Predictive Control
T-MPC	Tube-based Model Predictive Control
MI	Mixed Integer
QP	Quadratic Program
LP	Linear Program
PID	Proportional-Integral-Differential
ELS	Extended Least Square
ARMAX	**A**uto**R**egressive-**M**oving **A**verage with e**X**ogenous input
WWTP	Waste Water Treatment Plant
CSO	Combined Sewer Overflows
w.r.t	with respect to / with regards to
s.t	such that
def.	definition
fig.	figure
WSC	Water Smart Cities

Mathematics / Symbols

$f(\cdot)$	a function f of an unspecified set of variables
$\mathbf{X}$	Variable/function X is a column vector
$diag(\mathbf{X})$	a diagonal matrix where the diagonal is the elements of the vector $\mathbf{X}$
$\mathcal{X}$	A workspace / constraint set for variable X
$\|\|\mathbf{X}\|\|_1$	the 1st norm of $\mathbf{X}$ defined as $\|\|\mathbf{X}\|\|_1 = \sum_{i=1}^{n_X} \|X_i\|$
$\|\|\mathbf{X}\|\|_Q^2$	the weighted 2nd norm of $\mathbf{X}$ defined as $\|\|\mathbf{X}\|\|_Q^2 = \mathbf{X}^T Q \mathbf{X}$
$X \sim F$	Stochastic variable X following distribution F
$E\{X\}$	The expecation of X
$\sigma^2\{X\}$	The variance of X
$\sigma^2\{X,Y\}$	The cros-covariance of X and Y
$Pr\{X \leq y\}$	The probability of X being less than y
$\Phi_X\{y\}$	The CDF of X for value y
$\mathbb{R}$	The set of real numbers
$\oplus$	the Minkowsky sum; addition of two sets
$[x,y]$	the closed interval from x to y, e.q. $[0,1]$ includes every number between 0 and 1, and 0 and 1.
(x,y)	the open interval from x to y, e.q. $(0,1)$ includes every number between 0 and 1, without 0 and 1.
$\{x,y,z,...\}$	the set including x,y,z and etc., e.q. the set $\{0,1\}$ only includes 0 and 1.
$\in$	included in, e.g. $X \in \mathcal{X}$
$\forall$	for all
$\exists$	there exist at least one / for some
k	sample number / discrete time
V_k	Tank volume at time k
β	Volume-flow coefficient
q	flow / flow-rate
q_k^{in}	Inflow at time k

q_k^{out} Outflow at time k

q_k^u Controlled flow at time k

q_k^w CSO flow at time k

ΔT Sampling time

CHAPTER 1

Introduction

The ph.d. project of this dissertation was a part of the Water Smart City(WSC) project between several institutions and industries in Denmark. The participants were DTU Environment, DTU Compute, DHI, Krüger Veolia, Rambøll, DMI, Aarhus Vand, Biofoss, Hofor, and Vand Center Syd.

The WSC project was concerned with the future of urban water system management; from the initial design to the operation. This resulted in research into weather forecasts, city planning, chemical process management in Waste Water Treatment Plants (WWTP), sensors, and the management of sewer networks, which this dissertation focuses on.

1.1 Background

Part of the motivation behind the ph.d. study, and the WSC project, is the concern for the effect of climate change, such as increases in the frequency of heavy rain events, which has been observed during the last decades[Gre15]. Heavy rain events include weather phenomenons such as cloudbursts (min. 15mm in 30 minutes, [NAP17]). The main thoughts and concerns on the future for the sewer networks of the cities under increased rain load are primarily on the capacity of the sewers to keep the water inside the sewers, without any flows to the

neighboring environments, such as rivers, fields, harbors, roads or the Mayor's Basement.

The main issues with such overflows, especially in cities, are the sewer networks are usually decades old, from a time where the rain- and waste flows were transported in a single pipe; commonly referred to as a combined sewer, as in opposition to newer pipes known as separated sewers; a pipe for rain flow and a pipe for waste flow. The use of combined sewer networks means that any overflow will be polluted by the sewer waste to some degree. An overflow occurs if a section of the sewer network is full, but still receives more flow than it sends to other sections, similar to pouring to much water in a cup and it flows over the edge.

While it is simple to think of solutions to deal with this problem in the long term such as changing the combined sewer networks into separated sewer networks and/or expanding the pipe and reservoir dimensions to increase the storage capacity of the system; all of the simple solutions require investments into the physical structures of the network, which is both expensive and time-consuming; can be on the order of decades for a large city, if the general live and discomfort of the population is to be taken into account.

Other solutions could be investing in devices to limit the rain flow into the sewers, such as controlled closing of the gratings to the sewer during larger rain events[LBM+19]. While the solutions suggested above all consist of investing time and money in updating the current infrastructure of the sewer networks; in the research of this dissertation, the focus has been given to how to utilize the current infrastructure to avoid these issues, possibly avoiding unnecessary investments or decreasing the urgency of updating the current network, allowing for more consideration for the population.

1.2   Previous Research

In the research, the approach to improve utilization of the infrastructure is done through improving the overall control of the network. One common way to control sewer networks is to use rule-based control, where a set of rules are defined to direct the system under different scenarios[GBGE+15]. For complex systems and/or scenarios, this requires a lot of rules to cover all of the details of the system, as well as expert knowledge of the exact system to design and update the rules. Another approach to the control of the sewer networks is Model Predictive Control (MPC)[GR94], where the network is described by a model and the control is the optimum control of that model w.r.t. the given

definition of optimum; such as minimum control or overflow. While a model requires expert knowledge for the exact system to formulate; changes to the goal of the control, e.g. due to legal changes, do not require a system expert to formulate the new definition of optimum.

MPC is a control method that has been developed over the last several decades. The method is based on constrained optimization over a finite horizon, performed repeatedly as the horizon is receding. MPC's performance and formulation with the presence of uncertainty have in recent years been researched; resulting in several methods within MPC to handle uncertainty. One class of methods are the Robust MPCs, such as Tube MPC, where the goal is to find a solution to the control, which is applicable under all realizations of the uncertainty. Another class of methods is the Stochastic MPCs, such as Chance-Constrained MPC, where the goal is to find a solution which covers a statistic portion of realizations of the uncertainty, based on stochastic knowledge.

Several formulations of MPC without uncertainty have been proposed for sewer networks; discussing how to model the dynamics, especially the overflows from weir structures.

1.3   Research Outline

In the research of this dissertation, the control of the sewer networks has only considered the aspects of flow and volume of the sewer network, while other aspects such as the concentration of pollution and sedimentation have been set aside.

The research focuses on how to formulate the MPC optimization program utilizing linear models, while still encompassing the important dynamical structures of the real sewer network. One focus is which of the previously suggested description of weirs provides a better MPC formulation and in which sense is it better?

Another focus of the research has been MPC under the presence of uncertainty, primarily focused on forecast uncertainty in sewer networks. The chance-constrained MPC(CC-MPC) method is utilized as the approach to handling uncertainty. A main point in the research is how CC-MPC operates in comparison to MPC in sewer systems? Another point of the study is how to formulate CC-MPC for sewer networks when overflows from weirs are considered? such that the probabilistic constraints are meaningful. Besides the formulation of CC-MPC, the how to apply the stochastic knowledge is also of interest in the

research.

1.4   Publications

Several publications have been published/submitted during the ph.d. project, this dissertation has its foundation based on the following publications:

- Article A: Model Predictive Control of Overflow in Sewer Networks - A comparison of two methods, Systol 2019, Casablanca, Morocco

- Article B: An MPC-Enabled SWMM Implementation of the Astlingen RTC Benchmarking Network, Water, April 2020

- Article C: Stochastic Model Predictive Control and Sewer Networks, unpublished article, Januar, 2020

- Article D: Chance-Constrained Model Predictive Control - A reformulated approach suitable for sewer networks, Journal of Advanced Control for Applications, submitted: July 2020

- Article E: Chance-constrained Stochastic MPC of Astlingen Urban Drainage Benchmark Network, Journal of Control Engineering Practice, submitted: August 2020

- Article F: Towards Robust & Stochastic MPC: a comparison of Tube-Based and Chance Constrained MPC methods, Journal of Control Engineering Practice, submitted: September 2020

- Article G: Sewer Orientated Framework for Ensemble-based Chance-Constrained MPC, unpublished

Other publications published during the project, but not included as a basis for this dissertation, are the following extended abstracts from conference proceedings:

- Extended abstract: "Model Predictive Control: A case study of Trøjborg", Novatech 2019, Lyon, France

- Extended abstract: "Model Predictive Control of Overflow in Sewer Networks", Watermatex 2019, Copenhagen, Denmark

- Extended abstract: "A SWMM Model For The Astlingen Benchmark Network", IWA WWC 2021, Copenhagen, Denmark, accepted.

where the last two are sister publications to paper A and B respectively.

1.5   Outline of dissertation

In the following chapters, we will go through the current status of knowledge as well as some basic knowledge for the uninitialized. Before following with the research results of this project.

Chapter 2 of the dissertation presents aspects of sewer networks, such as the mathematical description of the physical networks, the different types of structures present in the networks, and the common management objectives.

Chapter 3 contains a short discussion on modeling approaches, and the different case studies utilized in my research.

Chapter 4 will introduce the reader to Model Predictive Control, from the basic theory of optimization to specific applications in sewer networks and more advanced formulation regarding uncertainty, such as the robust Tube MPC and the stochastic chance-constrained MPC.

Chapter 5 is a summary of the papers used as this dissertation's foundation; outlying the context of each paper, both in relation to the content in chapters 2, 3, and 4 and in relation to the novelty of the research presented by the paper.

Chapter 6 will provide the reader with the conclusion of the dissertation; providing a summary of the results of the research, as well as thoughts on future research to be considered along the lines of the research presented in this dissertation.

The Appendices A-G contains the foundational papers of the dissertation, and their background information, such as time and place of publication.

Sewer systems – Physics & Manegement

Sewer systems are dynamical systems constructed by a network of pipes and storage tanks, designed to transport sewage and rain down to the Waste Water Treatment Plant (WWTP). The network systems are either designed as separated sewers, a network for sewage and one for rain, or as combined sewers, where they flow in the same network.

In this chapter, we will discuss the physical dynamics, and commonly observed features found in sewer networks. The discussion will provide the mathematical models of the structures, which are used in high-fidelity simulators, such as DHI's Mike Urban[DHI17] or EPA's SWMM[Ros17].

2.1   Saint-Venant & Pipes

The physical dynamics or hydraulics of sewer systems are different for the different components of the system (tanks, pipes, etc.). Pipes are possibly the most abundant component of the sewer system, both in sheer numbers and possibly also in total volume capacity. The dynamics of a pipe can, under suitable assumptions, be described by the Saint Venant equations for gradually-varied

unsteady flow in open channels[BD11]. The Saint Venant equation is based on the following assumptions among others:

- Flow through the pipe is 1-dimensional; only changing along the pipe length, and being uniform across the flooded cross-area of the pipe.

- Small bottom slope of the pipe, with pipe bed being fixed; changes such as accumulation of solids are negligible.

- The effect of friction is comparable to steady flow.

For pipes, where this is only applicable piece-wised over the pipes, the pipes can be described as a cascade of pipe sections, for which the assumptions hold for each section.

The Saint-Venant equations also called the shallow water equations for the 3-dimensional version, can be derived from the more general Navir-Stokes equations for viscous fluids, through integration over depth.

The Saint Venant equations can also be derived from Newton's second law of motion, Conservation of mass, and Reynolds transport theorem, see [CMM88]. The equations themself consist of a continuity equation and a momentum equation, discussed below.

Continuity equation   If we consider a general pipe section of fixed length dx as seen in Fig. 2.1, then from conservation of mass, the continuity equation can be formulated as below

$$0 = \frac{\partial \rho A}{\partial t} + \rho \frac{\partial Q}{\partial x} - \rho q_L \tag{2.1}$$

where A is the average cross-area of the pipe section, ρ is the fluid density, q_L is the lateral inflow per unit length of the pipe and Q is the inflow to the pipe

Momentum equation   From Newton's second law of motion, the momumentum equation given below can be obtained. The external forces affecting the momentum of the pipe are in general due to gravity, friction, pressure, eddy losses due to abrupt changes in pipe size, and wind shear due to the winds frictional resistance; though only applicable for open channels and not pipes.

$$\frac{\partial Q}{\partial t} + \frac{\partial \beta_m Q^2/A}{\partial x} + gA(\frac{\partial y}{\partial x} - S_0 + S_f + S_e) - \beta_m q v_x + W_f B = 0 \tag{2.2}$$

a) Elevation   b) Plan   c) Cross section
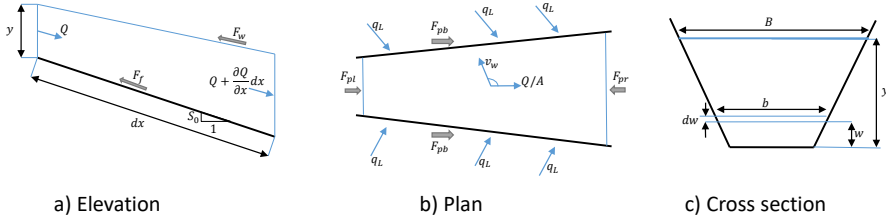
Figure 2.1: An example of a simple channel, with notations for the derivation of the Saint-Venant equations from [CMM88]; F being forces and v being velocity.

where v_x is the x-directional velocity of the lateral inflow, and β_m is the momentum/Boussinesq coefficient. while S_0 is the bed slope of the pipe (gravity term), S_f is the friction slope given by the manning equation (friction term), S_e is the eddy loss slope (eddy term), W_f is the wind shear factor with B is the surface width (wind shear term). The pressure term is given by the spatial change in depth $\partial y / \partial x$.

2.2 Reservoir Tanks

Besides pipes, reservoir tanks are the other big element of sewer networks, w.r.t volume capacity. Tanks are storage elements and are defined by mass conservation, usually formulated in terms of reservoir volume with the density assumed constant:

$$\frac{dV}{dt} = q^{in} - q^{out} - q^{cso} \tag{2.3}$$

where the temporal change in volume equals the difference between inflow, outflow, and weir flow[MP05].

2.3 Bernoulli & Features

Other than pipes and tanks, sewer networks consist of several other structural features, usual connections between the pipes and tanks, directing the flows of the system. In hydraulics, such features are described using Bernoulli's principle, which is a variation of the conservation of energy given in head (energy per unit weight, [meters])[BD11]. In sewer systems, the liquids are generally assumed

to be incompressible, so using Bernoulli in the case of liquid flow between one section of a pipe/structure to another, gives:

$$\frac{p_1}{\rho g} + \frac{v_1^2}{2g} + z_1 - h_L = \frac{p_2}{\rho g} + \frac{v_2^2}{2g} + z_2 \tag{2.4}$$

where h_L is the head(energy) loss between the two sections, due to pipe friction and local features, such as changes in pipe geometry. Using (2.4), the flow between chosen sections in the sewer system can be formulated by an algebraic relation, with the order depending on the head loss and velocity-flow relations. The velocity-flow relation, at a given section i, is $v_i = q_i/A_i$, where A_i is the flooded cross-sectional area of the section, in the flow direction. In hydraulics based on Bernoulli's Principle, the pipes generally operate in one of two modes, full and part-full; full pipes correspond to a pipe, where the liquid occupies the entire pipe and A_i is maximized and constant at any point i along the pipe. In Contrast, part-full pipes still have empty space in the pipe and a cross-area A_i depending at the flow height at the given point i along the pipe. In sewers, the common mode of operation is the part-full mode.

2.3.1   Orifice Plate / Penstock

One of the features in the sewer networks is the orifice plates or penstocks, which is used to limit the inflow into a pipe, with the latter term being a controllable variant[BD11]. Physically, an orifice feature is any type of plate used to reduce the inflow cross-area of the pipe, as illustrated in Fig. 2.2.

A simple approach to define the flow through an orifice plate is to utilize Bernoulli's principle, focusing on the system just before and after the plate. Under the assumption of equal pressure in both sections, and velocity v_1 and head loss being negligible (e.g. tanks), the orifice flow is defined as

$$q_2 = C_d A_o \sqrt{2gH}, \quad H = z_1 - z_2 \tag{2.5}$$

where A_o is the flow area of the orifice, and C_d is the orifice coefficient; correcting for the assumptions affect on accuracy.

2.3.2   Weir

Another feature is the weirs; weirs are structures that allow flows from one element to another when the latter has reached a given capacity load, as illustrated
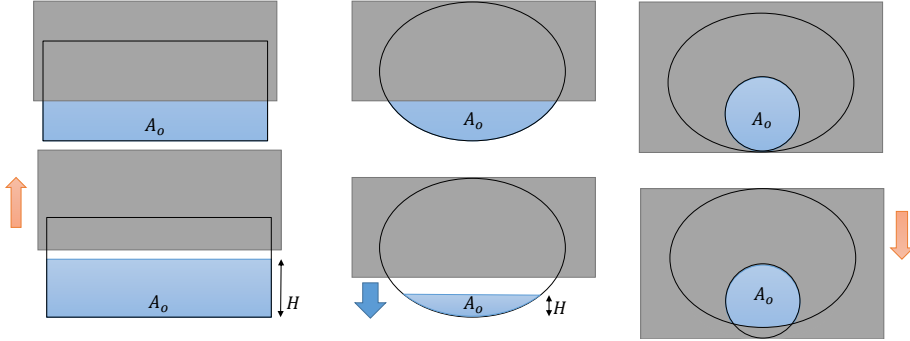
Figure 2.2: An illustration of different orifices and pipes; upper row showing orifices with openings fully flooded. Lower row shows the same orifices with either changes in orifice position (in direction of the orange arrow) or water level H (in direction of the blue arrow)

in Fig. 2.3. For a rectangular weir[BD11], the weir flow can be derived from the Bernoulli equations:

$$q^{cso} = C_d \frac{2}{3} b \sqrt{2g \max(h - h_w, 0)^3} \tag{2.6}$$

where b is the width of the weir, h is the height of water above the channel bed. The height h_w is the height the weir crest is located above the channel bed, and C_d is the discharge coefficient correcting for assumptions, with a usual value: $C_d \in [0.6, 0.7]$. The weir flow in (2.6) is equivalent to the piece-wise function:

$$q^{cso} = \begin{cases} C_d \frac{2}{3} b \sqrt{2g(h - h_w)^3}, & \text{if } h \geq h_w \\ 0, & \text{otherwise} \end{cases} \tag{2.7}$$

or given in term of a logical variable $\delta \in \{0, 1\}$

$$\delta = 1 \Leftrightarrow h \geq h_w \tag{2.8}$$

$$q^{cso} = \delta C_d \frac{2}{3} b \sqrt{2g(h - h_w)^3} \tag{2.9}$$

2.4 Controlled features

As mention above, pipes and tanks are not the only elements of sewer systems, other structural features exist; wherefrom we already have discussed the orifice
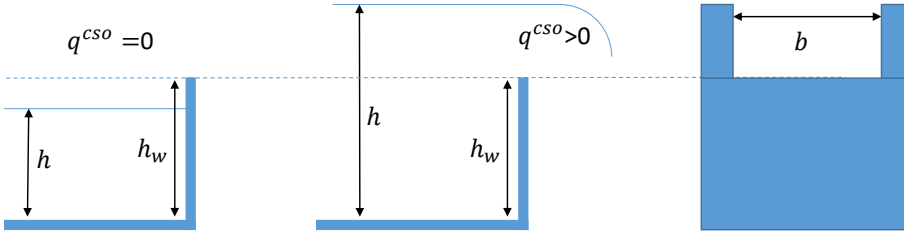
Figure 2.3: An illustration of a weir; left picture showing the condition for no weir flow, central picture showing the condition for weir flow, and right picture illustrating a rectangular weir

plate and the weir. Some of these features are the different types of controllers used to affect the behavior of the sewer system.

One type of controllers commonly found in sewer systems is pumps[SCC$^+$03], commonly used to fill and/or empty reservoir tanks, or shifting volume/flow to other sections of the network. Another controller type is the redirection gates, where an inflow is split into two outflows; this split can both be at a ratio r or one outflow being filled completely before the other. In the latter case, a redirection gate would behave like a weir on a pipe with a controllable weir crest q^r. Consider the outflows q^a and q^b, then the two descriptions would be defined as

$$q^a = rq^{in} \qquad\qquad q^a = \begin{cases} q^{in} & q^{in} \leq q^r \\ q^r \end{cases} \qquad (2.10)$$

$$q^b = (1-r)q^{in} \qquad\qquad q^b = q^{in} - q^a \qquad\qquad (2.11)$$

A third common type of controllers is the retention gates, which are used to hold back volume in certain parts of the system. Retention gates can be constructed with penstock orifice plates.

2.4.1   Control Levels

The control of sewer systems comes in many variants, but can generally be categorized in local and global control strategies, as illustrated in Fig. 2.4. In a local control strategy, each controller is operated independently of each other, using measurements of its nearby system and a reference of thwe desired local operation. In the case of a global control strategy, the controllers are operated collectively; using measurements from the entire system, with overall operation goals in mind.

A global controller can be controlling the equipments directly or by dictating the references to the local controllers. The reference used in local control is either fixed mechanically or controlled manually by a remote operator/global controller.

For most real systems, the local controllers are constructed as classical P, PI, or PID controllers, given that they can be made both analog or digital. Another benefit is that they can be designed to provide the desired response to changes in the reference, both w.r.t. time and behaviors, such as overshoot.

If we consider the equipment a system given by $G_p(s)$, then a local PID controller $G_c(s)$ and the resulting closed-loop system $G_{cl}(s)$ can be defined as below in accordance with [JS09].

$$G_c(s) = K_p \frac{1 + \tau_i s + \tau_i \tau_d s^2}{\tau_i s} \tag{2.12}$$

$$G_{cl}(s) = \frac{G_c(s) G_p(s)}{1 + G_c(s) G_p(s)} \tag{2.13}$$

where the tuning parameters K_p, τ_i, and τ_d are the control gain, integration time, and derivative time of the PID. In the case of P and PI control, the derivative time is zero, with the addition for the P controllers of the integration time being infinite. The exact way to tune the parameters depends on the equipment's dynamics $G_p(s)$ and the desired behavior of the system; which has been researched extensively, [O'D09] provides an extensive compendium of tuning rules for 1st to 5th order systems with or without delays as well as generalized approaches, non-model specific ones, and zero-order systems with delays.

The global controllers can be designed in various ways, such as rule-based or model-based, we will discuss this further in chapter 3 and chapter 4.

2.5   Manegement in Sewer Operation

In Chapter 4, we will be discussing the control design of the system. In this section, we will therefore be discussing some of the operational goals commonly seen in the management of sewer systems[SCC$^+$03], at least in the context of MPC design.

The different management objectives discussed below, are not necessarily used in the control of all systems or even over the entire system equally but are chosen
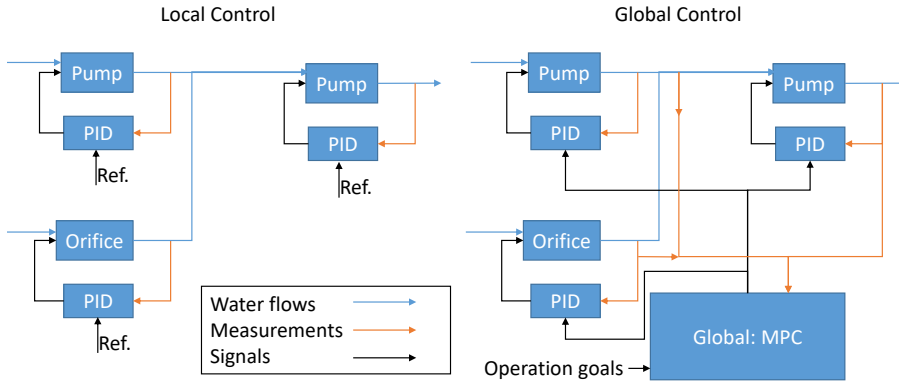
Figure 2.4: An illustration of local and global control schemes. The local PID controllers (left) can be seen to operate independently according to given references, while in the global controller (right), the local controllers are given their references from a higher level MPC controller; observing the entire system

to fit the desired behavior of the specific system, possibly with other objectives not discussed here.

2.5.1   Reference flow

A common objective is for some flows in the system, to follow a reference in some sense. The desired behavior can be understood as simply following the reference with divergence in both directions being undesirable, or with staying either below or above the reference being the desirable behavior.

A commonplace for a reference objective is the outflow of the entire system towards a WWTP. Some WWTP desire a limited, but predictable input for their processes.

2.5.2   Maximum flow & Minimum volume

The objective of maximum flow is simply the desired behavior being the flow from or to a section in the system being as large as possible. The minimum volume objective is similarly just the desire for having empty tanks in the system, such that the volume capacity of the sewer is ready to receive large rain inflows.

In some cases, the two objectives have the peculiar behavior of being equivalent, while in other cases they are counteracting each other. An example is a maximum outflow and minimum volume objectives considering the same tank, here the operational results would be identical, making the objectives equivalent and dualities of each other.

Similar to the reference objective above, the usage of maximum flow objectives can be seen in the flow to the WWTP, due to some WWTP desire as much flow as possible.

2.5.3 Control usage

Minimum control is a management objective usually associated with active controllers such as pumps, in order to reduce the monetary cost of operation. The active controllers require a power source to be operational, while passive controllers only require a power source to change operation setting; e.g. a pump without electricity will not pump and therefore will not generate a flow through it, while an open orifice plate without electricity will still allow flow through it.

Other operation goals can also promote the usage of a minimum control objective, such as a controller alternative to a weir, therefore emulating CSO minimization.

2.5.4 Control change

In the operation of sewer systems, maintenance is usually an expense to be reduced if possible. Maintenance is needed when the system is worn down to some degree. Wear occurs due to aging, usage, and other factors. For sewer systems, smooth changes in operation usually lead to less wear on the system. this also applies directly to the controllers, where sudden changes in operation generate more force in the mechanical structures, therefore leading to more wear in the controllers.

This is usually mitigated by the objective of smooth control through minimization of the change in control usage or control roughness. similar objectives can be used for specific flows in the system, whether they are control or not, to fulfill operational desired of smoothness; such as e.g. the outflow towards a WWTP.

2.5.5   CSO avoidance / minimization

An important management objective is whether one's aim is to avoid CSO or minimize it. The subtle difference in the objective is important for the design model discussed earlier; if the aim is on avoidance, then the dynamics of CSO are excluded from the system dynamics and replaced with a constraint at the crest level. In the case of CSO minimization being the aim, then the dynamics of CSO is included in the system dynamics.

The reservoir tanks and pipes with weirs leading to the external environment are the usual place for these objectives but are not excluding its usage on internal weirs in the system, e.g. CSO from one tank to another.

CHAPTER 3

Sewer Systems - Modelling

In the previous chapter, we discussed how the physics of sewer networks is described mathematically and which objectives are commonly used to manage the sewer networks. In section 2.4, we discussed how the different control equipments are controlled by a local PID controller given a setpoint to operate at. The actual management of sewer networks is commonly done as a global controller; providing the references to all the individual local controllers in the networks[SCC+03].

In many sewer networks, the global controller is based on rules, if-then statements, to define the references[GBGE+15]. For more complex systems, rule-based controllers can become a massive collection of rules to cover each scenario of the system w.r.t the management objectives. When a system is changed a little, many rules might be affected and needing change, deletion, or even brand new rules in order to work properly. An alternative to rule-based control is model-based control, where the references are computed using a model of the system. The model provides a mathematical description, describing the system adequately enough, such that it covers all non-negligible dynamics affecting the intended purpose of the model.

Models used for control design are generally a simplified description of the system. Otherwise for sewer systems, one would have to solve the partial differential equations of the Saint-Venant equations discussed in section 2.1 to compute the

prober control input to the system.

There are many methods for generating and describing a model for a given system. In this chapter, we will discuss two ways to formulate models, and we will discuss the physical limitation there exist in sewer systems and needs to be included in the models. We will end this chapter discussing the different case studies of sewer networks utilized in the research in this ph.d. project.

The two methods considered are discrete methods w.r.t time[HJS08], where the system is assumed stationary between time samples. The k-th sample of a variable $x(t)$ can be written as

$$x_k = x(t_0 + k\Delta T) \tag{3.1}$$

where t_0 is the time where samples are counted from, and ΔT is the sampling time; the period between each sample.

3.1   Transfer functions

The first modeling approach we will discuss is an external description of a system[Pou07, Mad07], also called a transfer function; relating input and output. Transfer function models only consider four things to describe a system: 1) the control variables 2) the external disturbances 3) the system outputs and 4) the structure of the model.
The system outputs are the elements of the system, which are measured for the management of the system, e.g. specific flows in a sewer system, such as the flow to WWTP and CSOs.

For a linear model structure; the transfer function of the i-th system output $y_{k,i}$ at time k can be described by an ARMAX model:

$$y_{k,i} + \sum_{j=1}^{n}\sum_{l=1}^{n_y} a_{j,l,i}y_{k-j,l} = \sum_{j=0}^{m}\left(c_{i,j}\epsilon_{k-j} + \sum_{l=1}^{n_u} b_{i,j,l}u_{k-j,l} + \sum_{l=1}^{n_d} f_{i,j,l}d_{k-j,l} \right) \tag{3.2}$$

where u is the controlled variables, d is the external deterministic disturbances and ϵ is the stochastic disturbances, assumed to be a white noise zero-mean signal independent of the output at previous times, with $c_{i,0} = 1$.

The benefit of these models is the lack of system knowledge needed; if enough data of the desired outputs are available together with the corresponding control and disturbance inputs, then the best parameters of any desired model structure to describe the system can be estimated, without knowing the underlying physics

of the system. It will, of course, help to know the physics, when one decides on a given model structure.

One possible way of estimating the parameters are extended least-square(ELS) estimation[Pou07]. The linear model can be rewritten in terms of the stochastic noise at time k or its residual as

$$\epsilon_k = y_k - \boldsymbol{\phi}_k^T \boldsymbol{\theta} \tag{3.3}$$

where $\boldsymbol{\theta}$ is a vector of model parameters and $\boldsymbol{\phi}_k$ is a vector of known inputs (control, disturbances, and previous outputs) at time k, given as

$$\boldsymbol{\theta} = [a_{i,1,1}, ..., a_{i,n,n_y}, b_{i,1,1}, ..., b_{i,m,n_u}, f_{i,1,1}, ... f_{i,m,n_d}, c_{i,1}, ... c_{i,m}] \tag{3.4}$$

and

$$\boldsymbol{\phi}_k = [y_{k-1,1}, ..., y_{k-n,n_y}, u_{k,1}, ..., u_{k-m,n_u}, d_{k,1}, ..., d_{k-m,n_d}, \epsilon_{k-1}, ..., \epsilon_{k-m}] \tag{3.5}$$

For ELS estimation of the parameter, we assume that the previous residuals in (3.5), can be estimated close enough by (3.3), where the parameters $\boldsymbol{\theta}$ are replaced by an estimate $\hat{\boldsymbol{\theta}}$. By using the information of N known temporal data sets of inputs and outputs, we can formulate an iterative estimation of the parameters

$$\hat{\boldsymbol{\theta}}_{n+1} = \hat{\boldsymbol{\theta}}_n + \left(\sum_{i=1}^{N} \boldsymbol{\phi}_i \boldsymbol{\phi}_i^T \right)^{-1} \sum_{i=1}^{N} \boldsymbol{\phi}_i \epsilon_i \tag{3.6}$$

where the parameter estimate $\hat{\boldsymbol{\theta}}_n$ can be updated until it settles to stationary values; with repeated estimations every time new data sets becomes available.

3.2 Virtual Tanks

The second method we will discuss for modeling a system is known as a lumped model, or specifically for sewer systems: a Virtual tank model[OM10]. A lumped model is a description of a larger system, where the detailed dynamics are collected into higher level interconnected parts; with each part corresponds to a collection of system elements and is described collectively by simpler dynamics.

For the sewer systems, such a separation would correspond to splitting the network into subnetworks of reservoir tanks and pipes. As illustrated in Fig. 3.1, the subnetworks can be assumed to be described sufficiently by the collective volume capacity of each element in it; a virtual tank, see def. 3.1, where the subnetwork is treated as a reservoir tank[GR94].
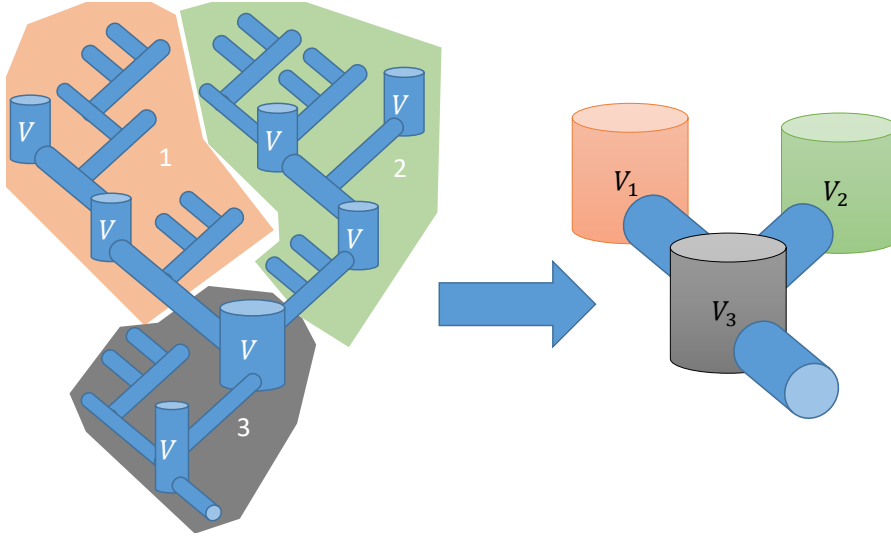
Figure 3.1: An illustration of system simplification by lumping dynamics into simpler units

DEFINITION 3.1 (VIRTUAL TANKS) For any given section of a system at any given time, a virtual tank would be a volume storage element representing the total volume stored inside the section; pipes, reservoir, etc. The element is purely described by mass balance; current volume, inflows, and outflows[OM10].

The discrete dynamics of the reservoir and virtual tanks can be obtained through discretization of the mass balance in (2.3), and are given by

$$V_{k+1} = V_k + \Delta T(q_k^{in} - q_k^{out} - q_k^{cso}) \tag{3.7}$$

If the outflow of a linear tank model is driven by gravity through an orifice (controlled or not), then the outflow can be assumed proportional to the tank volume:

$$q_k^{out} = \beta V_k \tag{3.8}$$

where β is the volume-flow coefficient, [Sin88].

3.3   Constraints

While the real physical dynamics describe the system in its entirety, simplified models do not. In general, especially for linear models, one of the things not

included in the model structure is the existence of physical limits on the different parts of the system. To describe the workspace of a given element, we can extend the models with constraints to include the physical limits of the dynamics. In the next chapter, we will discuss control with constraints.

For the volume of the reservoir tanks (virtual or not), the physical limits can be defined as an upper and lower bound for each tank

$$0 \leq V_k \leq \overline{V} \tag{3.9}$$

The general controlled flows are likewise constrained by an upper and lower bound

$$\underline{q}^u \leq q_k^u \leq \overline{q}^u \tag{3.10}$$

where the exact formulation of the bounds is dependent on the type of control device used. In sewer systems, several types of control devices are used. The commonly used types include penstocks and pumps.

If the pumps are bidirectional (pumps in both directions), then the above constraint is applicable. If the pump is only unidirectional, then the pump constraints are given by

$$0 \leq q_k^u \leq \overline{q}^u \tag{3.11}$$

For both types of pumps, there would be specific pump model dynamics and limitations, which one might have to include in the MPC design in order to describe the dynamics of the sewer, similar to our discussion on the orifice plates.

For the penstock devices (orifice plates), it is common to assume that backwater flow does not occur such that the flow through an orifice is unidirectional, being constraint as above. For the penstocks controlling tank outflow (virtual or real), the orifices are driven by the upstream volume through gravity; meaning the control flow in a penstock is limited by the volume. If we consider the discussed linear tank outflow in (3.8), then the constraints of the penstock can be formulated as

$$0 \leq q_k^u \leq \beta V_k \tag{3.12}$$

or as a combination of both of the above.

This discussion on the physical constraints of sewer systems are by no means a complete list, but an attempt on a short overview of the most generally used. Combinations and/or more complex constraints might be more applicable for specific systems.

3.4   Case Studies / Models

In the research of sewer systems, many different case studies have been proposed and used during the years[SCC⁺03, GGSvO14, PCR⁺09]. During this ph.d. project, three case study systems have been utilized:

- Barcelona Sewer model

- Astlingen Benchmark model

- Aarhus Sewer model

The systems include different features and have different size and layout. The contents of each case study model will be discussed in the remainder of this chapter.

3.4.1   Barcelona

The Barcelona sewer model from [OM10] is a model of a subset of the sewer network of the city of Barcelona in Catalonia, Spain. The model is defined using virtual tanks, and consists of 12 tanks; one real tank and 11 virtual tanks, each corresponding to a catchment area of Barcelona, as seen in Fig. 3.2. Furthermore, the model consists of 22 weirs, where most generates CSO, and a few redirect the flows internally in the sewer. The single real tank does not have CSO capability, and both the inflow and outflow is controlled, by a redirection gate and a retention gate, respectively. Most of the CSOs in the system flow back into the system, after flooding the surface of the catchments, those who don't flow back, flows into the Mediterranean sea; permanently exiting the system.

The thresholds for when a CSO occurs is given by the volume capacity of the virtual tanks and the outflow capacity of the weir elements. The dimensions of each tank and weir element can be seen in Table 3.1, where the volume and outflow capacity of each element is given. In the Barcelona model, the controllers are three redirection gates and a retention gate.
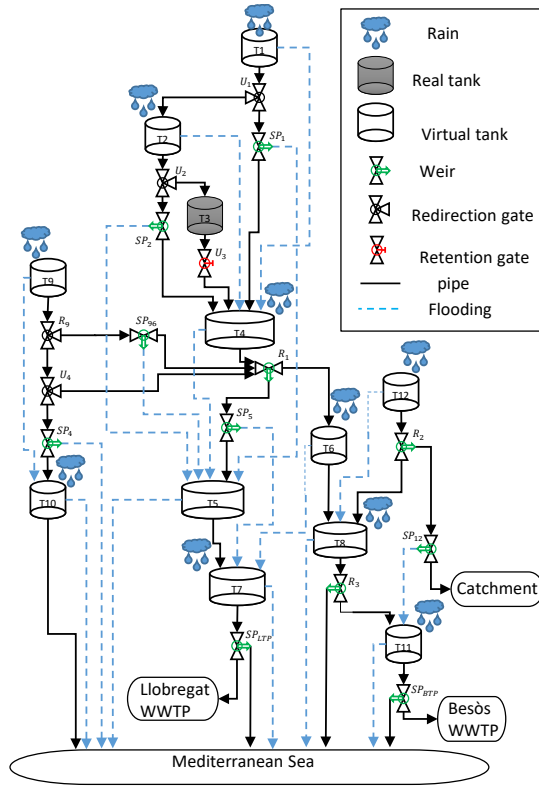
Figure 3.2: A schematic of the Barcelona sewer model, on the tank level. The labels T, SP, R, and U stands for tanks, sewer pipes, internal structures, and control respectively.

element	T1	T2	T3	T4	T5	T6
volume m^3	16901	43000	35000	26659	27854	26659
outflow m^3/s	12.00	24.94	7.00	2.66	3.34	14.40
element	T7	T8	T9	T10	T11	T12
volume m^3	79229	87407	91988	175220	91442	293248
outflow m^3/s	27.73	47.20	11.96	71.84	45.72	146.62
element	SP_1	SP_2	SP_4	SP_5	SP_{12}	SP_{96}
outflow m^3/s	9.14	3.40	32.80	13.36	60.00	10.0
element	SP_{LTP}	SP_{BTP}	R1	R2	R3	R9
outflow m^3/s	7.30	9.00	24.60	63.40	30.00	24.00

Table 3.1: Dimensions of the Barcelona Model, indicating the thresholds for CSO and other weir flows
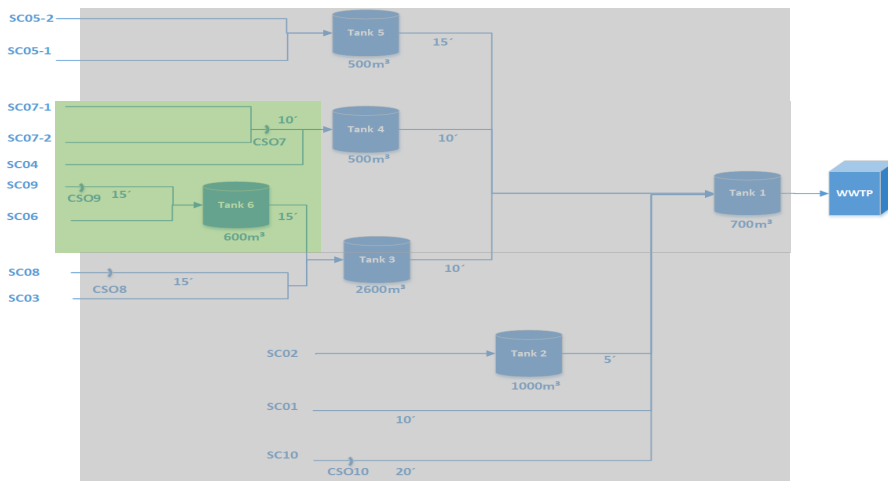
Figure 3.3: A schematic of the Astlingen Benchmark model, with the receiving bodies illustrated by the colored background, green for the creek, and grey for the river. The external flows from catchments are noted by SCxx and SCxx-y, while the CSO from tanks is excluded in the schematic and from pipes denoted by CSOX. The delays in pipes are by x' in minutes

3.4.2 Astlingen

The Astlingen benchmark model from [SLPH18] is a designed artificial sewer system, designed to include the most common aspect of sewer systems. It was originally proposed to give an accessible and fully described benchmark system for research and comparison of control practices in the sewer system communities, regardless of simulation software choice and model data accessibility from utility companies. In Fig. 3.3, a layout of the Astlingen system is given in terms of reservoir tanks as proposed in [SLPH18].

The system consists of six tanks and four pipe weirs, which all can produce CSO to the nearby environments. An important feature about the Astlingen is its environment; it is supposed to represent a city with a river and a creek going through it. The river and creek act as the recipients for the CSO of the sewer system. Given the smaller size and flow in the creek, the river is the preferred CSO recipient of the system. The recipient of the CSO from each weir is shown in Table 3.2, together with volume- and outflow capacities of the tanks and pipe weirs. As with the Barcelona model, the CSO threshold is defined by volume/outflow capacities.

element	T1	T2	T3	T4	T5	T6
volume m^3	700	1000	2600	500	500	600
outflow m^3/s	271.28	140.00	190.00	80.00	39.00	175.00
recipient	river	river	river	river	river	Creek
element	CSO7	CSO8	CSO9	CSO10		
outflow m^3/s	85.50	485.33	129.17	203.67		
recipient	creek	river	creek	river		

Table 3.2: Dimensions of the Astlingen Model

element	T1	T2	T3	T4	T5	T6	T7	T8
volume m^3	300	20	350	844	200	200	100	10
outflow m^3/s	1.50	0.60	1.00	1.80	0.50	0.80	0.10	0.04
delay out min	-	20	10	4	-	-	-	-
CSO type	Ext	Ext	Back	Back	Ext	Ext	Int	Ext
element	T9	T10	T11	T12	T13	T14	T15	T16
volume m^3	10	10	150	10	10	10	10	10
outflow m^3/s	1.00	0.20	0.35	0.10	0.80	0.20	0.40	0.70
delay out min	-	2	5	-	-	-	20	3
CSO type	Ext	Ext	Ext	Ext	Ext	Ext	Ext	Ext
element	T17	T18	T19	T20	T21	T22	T23	T24
volume m^3	70	50	85	13001	10001	3501	90	3001
outflow m^3/s	0.80	0.15	0.98	0.22	0.40	0.18	1.20	0.09
delay out min	14	-	-	-	-	-	-	-
CSO type	Ext	Int	Ext	Ext	Ext	Ext	Ext	Ext
element	T25	T26	T27	T28	T29	T30	T31	T32
volume m^3	6699	3503	200	60	100	85	200	100
outflow m^3/s	1.50	0.10	0.20	0.70	0.20	0.10	0.20	0.04
delay out min	-	-	-	-	-	-	-	-
CSO type	Ext	Ext	Int	Ext	Int	Int	Back	Int
element	T33	T34	T35	T36	T37	T38		
volume m^3	32	25	12	80	90	10		
outflow m^3/s	0.50	0.50	0.50	0.30	0.40	0.10		
delay out min	-	-	-	-	-	-		
CSO type	Int	Int	Int	Int	Int	Ext		

Table 3.3: Dimensions of the Aarhus Model[Dre20]
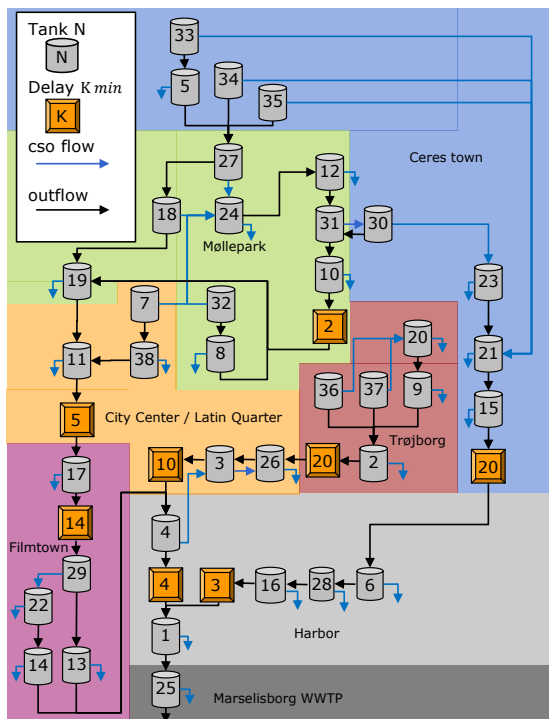
Figure 3.4: A schematic of the Aarhus sewer model, displaying the interconnection and spatial distribution of the virtual tanks relating them to their corresponding real world area by the colored background.

The flow in the interconnection between the tanks, pipe weirs, and catchments is given as the delay of the inbetween flow of each element set. The controllers in the system are retention gates at the outflow of each tank.

3.4.3   Aarhus

The Aarhus model is based on the section of the Marselisborg sewer system covering the city of Aarhus in Denmark. It is an autogenerated design model for MPC based on a MIKE URBAN high fidelity model of the Marselisborg sewer network[DH20]. The autogeneration has reduced the Saint-Venant based MIKE model to a linear virtual tank based design model as illustrated in Fig. 3.4, based on pre-selected criteria such as controller location.

The model consists of 38 virtual tanks, which in some cases includes real reser-

voir tanks. Every tank has the ability to produce an overflow, whereas twenty-four of them correspond to CSO to the external environment, eleven corresponds to internal overflows in the system, and the last three corresponds to internal backwater flows towards the previous tank. The interconnection in the model also consists of flow delays between the tanks. The details of each tank are shown in Table 3.3, where the CSO thresholds are the tanks' volume capacities.

The controllers of the system are placed at the outflow of every tank and include controllers such as pumps and retention gates.

Model Predictive Control

Model Predictive Control (MPC) is a control method that has been developed since 1963, where it was originally proposed in [Pro63]. It has been applied to a great number of different fields of applications[QB03, Lee11, HH15, Kim13, SSR14, RSvdGvO14], one of these is, of course, sewer networks[GR94, CQS$^+$04, OM10, MP05].

MPC is an optimal control method, usually for discrete systems, using a receding horizon approach; where the optimal control is computed over a prediction horizon N_{h_p}, with only the control of the first time step being utilized[Mac02, CB07]. Whereafter the horizon is shifted forward in time, one step, and the procedure repeats.

MPC relies on having a model of the system to be controlled, covering the entire prediction horizon; commonly obtained by extrapolating the discrete dynamics of the system to obtain predictions of the future state of the system. If N_{H_p} is the prediction horizon given in time steps, then it corresponds to the number of predicted time steps being considered.

One of MPC's many benefits is the ability to include constraints in the control formulation, both equality and inequality ones. The formulation of MPC is an optimization program, where the optimization variables are the control variables **u** used for minimizing a desired cost over the chosen prediction horizon, with

the following formulation:

$$J = \min_{\mathbf{u}} \sum_{k=0}^{N_{H_p}} l(\mathbf{x}_k, \mathbf{u}_k, \mathbf{w}_k) \tag{4.1}$$

$$s.t.$$

$$\mathbf{x}_{k+1} = \mathbf{f}(\mathbf{x}_k, \mathbf{u}_k, \mathbf{w}_k) \tag{4.2}$$

$$\mathbf{h}(\mathbf{x}_k, \mathbf{u}_k, \mathbf{w}_k) = \mathbf{0} \tag{4.3}$$

$$\mathbf{g}(\mathbf{x}_k, \mathbf{u}_k, \mathbf{w}_k) \leq \mathbf{0} \tag{4.4}$$

where $l(\cdot)$ is the cost at each time step, $f(\cdot)$ is the model dynamics, and $h(\cdot)$ and $g(\cdot)$ are the equality and inequality constraint functions respectively. The variables $\mathbf{x}_k$ are the predicted state at time k, while $\mathbf{w}_k$ is the system disturbances at time k. The state $\mathbf{x}_0$ is the current state of the system, and are commonly assumed to be known.

In MPC, the cost functions are commonly chosen to be either linear, quadratic, or a combination of the two, while the process- and constraint functions are usually formulated as linear functions. This is due to simpler computations of the optimal solution, but for most systems comes at the trade-off of simplifying the dynamics and constraint.

In order for us to find the optimal solution of the MPC, the MPC program has to have a solution also known as being feasible. The feasibility of an optimization program is purely determined by its constraint, both equality and inequality ones. A program is said to be infeasible (no solution) if two or more constraints overlap, such that the allowed set of solutions between the constraints are empty.

4.0.1   Optimality Conditions

The solution of the MPC program is found by solving the Karush-Kuhn-Tucker (KKT) optimality conditions [NW06]. If the process equation in (4.2) are substituted out, then the Lagrangian of the MPC program in (4.1)-(4.4) can be formulated as

$$L(\mathbf{u}, \boldsymbol{\lambda}, \boldsymbol{\mu}) = \sum_{k=0}^{N_{H_p}} l(\mathbf{x}_k, \mathbf{u}_k, \mathbf{w}_k) + \boldsymbol{\lambda}_k^T h(\mathbf{x}_k, \mathbf{u}_k, \mathbf{w}_k) + \boldsymbol{\mu}_k^T g(\mathbf{x}_k, \mathbf{u}_k, \mathbf{w}_k) \tag{4.5}$$

Where $\boldsymbol{\lambda}$ and $\boldsymbol{\mu}$ are the Lagrange multipliers over the whole horizon for the equality and inequality constraints respectively. In the Lagrangian given, we have omitted the recursive substitution of the dynamics and kept it as $\mathbf{x}_k$.

Using the same notation for the dynamics, the KKT conditions for an optimum solution is then given as

$$\nabla_{\mathbf{u}} L(\mathbf{u}, \boldsymbol{\lambda}, \boldsymbol{\mu}) = 0 \tag{4.6}$$

$$\nabla_{\boldsymbol{\lambda}_k} L(\mathbf{u}, \boldsymbol{\lambda}, \boldsymbol{\mu}) = \mathbf{h}(\mathbf{x}_k, \mathbf{u}_k, \mathbf{w}_k) = \mathbf{0} \tag{4.7}$$

$$\nabla_{\boldsymbol{\mu}_k} L(\mathbf{u}, \boldsymbol{\lambda}, \boldsymbol{\mu}) = \mathbf{g}(\mathbf{x}_k, \mathbf{u}_k, \mathbf{w}_k) \le \mathbf{0} \tag{4.8}$$

$$\mathbf{0} \le \boldsymbol{\lambda}_k, \boldsymbol{\mu}_k \tag{4.9}$$

$$\mu_{k,j} g_j(\mathbf{x}_k, \mathbf{u}_k, \mathbf{w}_k) = 0, \forall j, k \tag{4.10}$$

Where it can be seen that the derivatives of the Lagrangian with respect to the Lagrange multipliers are the initial constraints.

The KKT conditions are necessary conditions for an optimum solution, but it is not, in general, a sufficient condition for a solution to be optimal. One situation where the KKT conditions are also a sufficient condition is in convex programs, where the cost function and the inequality constraints are convex (def. 4.1) and the equality constraints are affine; then the Lagrangian in (4.5) is also convex, and the solutions to the KKT conditions are the global minimum of the program, [BV09]. Similar for maximization programs using the same Lagrangian, where the cost function has to be concave and the inequality constraints are convex.

DEFINITION 4.1 Convex: A set $S \in \mathbb{R}^n$ is a convex set if and only if that for any two points in the set, $x \in S$ and $y \in S$, the scaled sum, $\alpha x + (1 - \alpha)y \in S$ lies in the set for all $\alpha \in [0, 1]$. A function $f(x)$ is said to be a convex function if its domain S is a convex set, and that for any two arguments x and y lying in the domain, the following holds

$$f(\alpha x + (1 - \alpha)y) \le \alpha f(x) + (1 - \alpha)f(y), \quad \forall \alpha \in [0, 1] \tag{4.11}$$

Concave: a function g is said to be a concave function, if and only if its negative is convex: $-g(x)$ is a convex function.[NW06]

In the case where this does not apply, the second-order condition is needed to establish whether or not a solution is optimum. Let us denote the set of inequality constraints by $\mathcal{I}$ and the set of active constraints by $\mathcal{A}(x)$; the set of inequality constraints equal to zero and equality constraints at a given solution x. The second-order condition is that the second derivative of Lagrangian w.r.t. the control, also called the Hessian, for a given solution has to be semi-positive definite at least within the set $\mathcal{C}$:

$$\mathbf{s}^T \nabla_{\mathbf{u}, \mathbf{u}}^2 L(\mathbf{u}^*, \boldsymbol{\lambda}^*, \boldsymbol{\mu}^*) \mathbf{s} \ge 0 \tag{4.12}$$

where $\mathbf{s}$ is a vector in $\mathcal{C}$:

$$\mathbf{s} \in \mathcal{C}, \quad \mathcal{C} : \begin{cases} \nabla_{\mathbf{u}} \mathbf{h}_i(\mathbf{u}^*)^T \mathbf{s} = 0, \forall i \\ \nabla_{\mathbf{u}} \mathbf{g}_i(\mathbf{u}^*)^T \mathbf{s} = 0, \forall i \in \mathcal{A}(\mathbf{x}^*) \cap \mathcal{I} \text{ with } \mu_i^* \geq 0 \\ \nabla_{\mathbf{u}} \mathbf{g}_i(\mathbf{u}^*)^T \mathbf{s} \leq 0, \forall i \in \mathcal{A}(\mathbf{x}^*) \cap \mathcal{I} \text{ with } \mu_i^* = 0 \end{cases} \tag{4.13}$$

For the special case of quadratic/linear programs with linear equality constraints, and no inequality constraints:

$$f(u) = \frac{1}{2} \mathbf{u}^T H \mathbf{u} + \mathbf{G}^T \mathbf{u} \tag{4.14}$$

$$\mathbf{h}(u) = A\mathbf{u} - \mathbf{B} \tag{4.15}$$

The KKT conditions of the MPC solution can be stated as the KKT matrix:

$$\begin{bmatrix} H & A^T \\ A & 0 \end{bmatrix} \begin{bmatrix} \mathbf{u} \\ \boldsymbol{\lambda} \end{bmatrix} = \begin{bmatrix} -\mathbf{G} \\ \mathbf{B} \end{bmatrix} \tag{4.16}$$

$$\mathbf{0} \leq \boldsymbol{\lambda} \tag{4.17}$$

which is nonsingular, when A has full row rank, and either the Hessian is positive definite or the reduced Hessian $Z^T H Z$ is, where Z is the nonzero nullspace $AZ = 0$.

A reformulated version of the KKT matrix is used for solving programs with inequality constraints, e.g. the interior-point algorithm. For non-linear programs (non-quadratic), one approach to computing the solution is sequential quadratic programming; where the program is approximated as a QP, and iteratively the real solution is approached, by updating the approximation after each iteration.

4.1   Overflow Structure

In chapter 2, we discussed the sewer networks, and especially their weirs. The equation of weir flow in (2.6) was given for a rectangular weir, and would, in general, be even more nonlinear than is given here.

A common approach used in MPC design to simplifying the weir dynamics is to not consider the height above the weir crest, but instead consider the exceeding of the capacity of the tanks and pipes, in volume and flow respectively[GR94, MP05].

$$q_k^{cso} = \begin{cases} \max\left(\frac{V_k + \Delta T(q_k^{in} - q_k^{out}) - \overline{V}}{\Delta T}, 0 \right), & \text{Tank case} \\ \max\left(q_k^{in} - \overline{q}^{out}, 0 \right), & \text{Pipe case} \end{cases} \tag{4.18}$$

where tank case is based on the discrete mass balance discussed earlier in (3.7) and the assumption that all excessive volume at time k becomes weir flow at time k; an assumption which does not hold for the true description.

4.1.1 Mixed Integer approach

As discussed in section 2.3.2, the maximum function in the description above can be replaced with a logical variable[OM10]

$$q_k^{cso} = \begin{cases} \delta \frac{V_k + \Delta T(q_k^{in} - q_k^{out}) - \overline{V}}{\Delta T}, & \delta = 1 \Leftrightarrow V_k + \Delta T(q_k^{in} - q_k^{out}) \geq \overline{V} \\ \delta(q_k^{in} - \overline{q}^{out}), & \delta = 1 \Leftrightarrow q_k^{in} \geq \overline{q}^{out} \end{cases} \tag{4.19}$$

Where the logical equivalences to the right, defines the switching function $T(\cdot)$ of the weir, $\delta = 1 \Leftrightarrow T(\cdot) \geq 0$. The use of both logical (integer) variable and continuous variables are known as Mixed Integer (MI), and an MPC designed using MI is an MI-MPC. Computation of the solution of MI-MPCs can, in general, be thought of as a mix of search and optimization algorithms.

The above formulation of weirs for MI-MPC can be adjusted for similar mathematical structures, where the dynamics are piecewise functions of two pieces, such as maximum, minimum, or absolute functions. The MI description in (4.18) can be considered functional quadratic in the sense of multiplication of logical terms with the continuous functions corresponding to each piece.

If we consider the Mixed Logical Dynamical (MLD) approach introduced in [BM99a], then the description can be formulated as linear w.r.t. the logical variable. Let us consider the general variable z defined piecewise between the continuous functions $f(x)$ and $g(x)$, with the logical variable δ defining the switch based on the function $h(x)$

$$z = \delta f(x) + (1 - \delta)g(x) \tag{4.20}$$

$$\delta = 1 \Leftrightarrow h(x) \leq 0 \tag{4.21}$$

Then by utilizing the upper and lower bounds of the three functions, the "linearized" z can be formulated using six inequality constraints:

$$\underline{h}\delta \leq h(x) \leq \overline{h}(1 - \delta) \tag{4.22}$$

$$(\underline{g} - \overline{f})(1 - \delta) \leq z - f(x) \leq (\overline{g} - \underline{f})(1 - \delta) \tag{4.23}$$

$$(\underline{f} - \overline{g})\delta \leq z - g(x) \leq (\overline{f} - \underline{g})\delta \tag{4.24}$$

If any of the bounds on the functions are open, then a sufficiently large approximation of positive or negative infinity can be utilized.

4.1.2   Slack approach

Another approach to including weir flows in the MPC programs is through slack variables with an additional penalty cost to minimize[GR94, HF17]. The basic idea is to consider the weir flow q^{cso} an optimizable variable and excluding the discussed weir dynamics from the model. The new variable is then minimized through a penalty cost $l^{cso}(\cdot)$, designed to approximate the real behavior of the weir:

No weir flows, when capacity is not reached

and the assumption of all excessive volume becomes weir flow before the next sample.

The generalized formulation of MPC with approximated weir flow can be given by

$$J = \min_{\mathbf{u}, \mathbf{q}^{cso}} \sum_{k=0}^{N_{H_p}} l(\mathbf{x}_k, \mathbf{u}_k, \mathbf{w}_k, \mathbf{q}_k^{cso}) + l^{cso}(\mathbf{q}_k^{cso}) \tag{4.25}$$

$$s.t.$$

$$\mathbf{x}_{k+1} = \mathbf{f}(\mathbf{x}_k, \mathbf{u}_k, \mathbf{w}_k, \mathbf{q}_k^{cso}) \tag{4.26}$$

$$\mathbf{h}(\mathbf{x}_k, \mathbf{u}_k, \mathbf{w}_k, \mathbf{q}_k^{cso}) = \mathbf{0} \tag{4.27}$$

$$\mathbf{g}(\mathbf{x}_k, \mathbf{u}_k, \mathbf{w}_k, \mathbf{q}_k^{cso}) \leq \mathbf{0} \tag{4.28}$$

where the arguments of the functions in (4.1)-(4.4) are extended to include the weir flows.

The additional cost l^{cso} can be chosen in a lot of ways; [GR94] defined it as quadratic and linear sums of CSO volume of the system, both temporal and spatial, while [HF17] defined it as the linear sum of the accumulated CSO volume from each weir at each time step

$$V_{k,j}^{cso} = \Delta T \sum_{i=0}^{k} q_{i,j}^{cso} \tag{4.29}$$

where j indicates the spatial location of the accumulated CSO volume.

The definition used by [HF17] ensures that the optimization does not initiate a given CSO, mathematically, before the capacity of the given weir is reached; by the weight on the individual CSO being repeated at each later predicted accumulated volume. The approach also allows for spatially differentiated weighting

of CSO from each weir. Though the weightings of the different weirs have to follow some guidelines, see Paper A; for connected elements (tanks, pipes, etc.) there are not connected through a controller:

The weir upstream has to have a higher weighting than the downstream wear.

Preventing the generation of CSO upstream mathematically to avoid true CSO downstream, e.g. two tanks connected in a cascade, where the downstream is full and the upstream is half empty, and the flow between is passively driven by gravity; an optimization algorithm with even weighting might try an empty the upstream by CSO, to lessen the passive inflow to the downstream tank and therefore avoiding CSO there; the solution is mathematical as optimal as the physical CSO happening in the downstream tank.

For the case of the elements being connected through a controller, the controller acts as a savepoint for the MPC, disconnecting the CSOs upstream and downstream of the controller, see Paper G. This allows for more design-friendly weightings of the CSO.

4.2 Objectives in the Cost Function

In Chapter 2, we discussed the kind of control objectives often seen in the management of sewer networks, here we will see how these can be formulated into cost terms J_n for the minimization in the MPC.

The presented list of possible ways to implement the objectives is by no means complete, but a list of simple implementations of the objectives as costs. Each presented cost is a convex expression in line with the convex optimization discussed in section 4.0.1.

Reference objective Previously we discussed the objective of a given flow to either follow a reference or stay below it, if we instead of considering a flow in the objective, consider a feature $\mathbf{z}$ (flow, volume, etc.), then the cost term can be formulated as

$$J_n = ||\mathbf{z} - \mathbf{z}_{ref}||^2_{Q_{ref}}, \quad J_n = \mathbf{Q}_{ref}^T(\mathbf{z} - \mathbf{z}_{ref}) \qquad (4.30)$$

where to the left we have the quadratic cost of the objective of following a given reference $\mathbf{z}_{ref}$ with the weight Q_{ref} and to the right a linear cost of the objective of staying below a given reference with the weight $\mathbf{Q}_{ref}$.

By using this definition of reference objectives, some of the other objectives can be constructed using the same notation:

Minimum Volume: let $\mathbf{z}$ correspond to the volume of a given tank, then having a reference of zero would minimize the volume.

Maximum flow: let $\mathbf{z}$ correspond to a flow and the linear cost have a negative weight, then the flow is maximized.

Control usage: If $\mathbf{z}$ corresponds to a control flow, then the quadratic reference cost will penalize the usage of control deviating from the zero references. For non-negative controls, the linear cost can also be utilized.

Control change The simplest way to implement the objective of smooth control is by a quadratic cost on the change:

$$J_n = ||\Delta\mathbf{u}||^2_{Q_{\Delta u}} \tag{4.31}$$

where $Q_{\Delta u}$ is the matrix weight of the quadratic cost. There does also exist a linear version of the quadratic cost, formulated using slack variables $\mathbf{t}$, weights $\mathbf{Q}_t$, and extra inequality constraints:

$$J_n = \mathbf{Q}_t\mathbf{t} \tag{4.32}$$
$$-\mathbf{t} \leq \Delta\mathbf{u} \leq \mathbf{t} \tag{4.33}$$

CSO avoidance / minimization In the case of CSO avoidance, there is no term for the cost function. For the CSO minimization, it can be implemented both as a quadratic cost or as a linear cost, as we discussed above the slack approach.

$$J_n = ||\mathbf{q}^{cso}||^2_{Q_{cso}}, \quad J_n = \mathbf{Q}^T_{cso}\mathbf{q}^{cso} \tag{4.34}$$

where Q_{cso} is the matrix weight of the quadratic cost and $\mathbf{Q}_{cso}$ is the vector weight of the linear cost

4.3   Model Predictive Control Under Uncertainty

The discussion on MPC so far, have assumed the model and disturbances to be deterministic and known, a more realistic assumption is to include uncertainty in the MPC formulation. Over the years, MPC with handling of uncertainty has been extensively studied, and the resulting MPC methods can generally be divided into two classes; robust approaches[BM99b, MNSA03, KC16], and stochastic approaches[Mes16, KC16, GCGP09, ECK12, SN99]. Where robust MPC aims at finding solutions that hold for all realizations of the uncertainties,

and stochastic MPC aims to find solutions, which statistically covers a subset of the realizations, based on stochastic knowledge of the uncertainty.

Within both classes of MPC, there exist several different methods and variations of these, in this section we will discuss the following three of these methods and related theory to them:

- Tube-based MPC

- Scenario-Based MPC

- Chance-Constrained MPC

4.3.1   Tube-based MPC

The method known as tube-based MPC or Tube MPC (T-MPC) is from the class of robust MPCs. Robust MPCs, including T-MPC, are based on the assumption that any model and disturbance uncertainty is bounded by some known set $\mathcal{W}$[KC16], such that the uncertainties at time k are bounded by $w_k \in \mathcal{W}_k$. Let us define the set of uncertainties from two points in time as:

$$\mathcal{W}_{i:j} = \mathcal{W}_i \times \mathcal{W}_{i+1} \times \cdots \times \mathcal{W}_j, \quad i \leq j \tag{4.35}$$

where the set $\mathcal{W}_{0:N_{H_p}}$ from the current time to the end of the horizon, is the uncertainty set $\mathcal{W}$. The formulation of robust MPC is generally given in one of two versions [BM99b], one where the cost is based on the nominal value of the disturbances or one where the cost is given as a min-max problem as below; to optimize over the worst-case cost w.r.t. the disturbances.

$$J = \min_{\mathbf{u}} \max_{\mathbf{w} \in \mathcal{W}} \sum_{k=0}^{N_{H_p}} l(\mathbf{x}_k, \mathbf{u}_k, \mathbf{w}_k) \tag{4.36}$$

$$s.t.$$

$$\mathbf{x}_{k+1} = \mathbf{f}(\mathbf{x}_k, \mathbf{u}_k, \mathbf{w}_k) \tag{4.37}$$

$$\max_{\mathbf{w}_0 \times \cdots \times \mathbf{w}_k \in \mathcal{W}_{0:k}} \{\mathbf{g}(\mathbf{x}_k, \mathbf{u}_k, \mathbf{w}_k)\} \leq \mathbf{0} \tag{4.38}$$

where the equality constraints $\mathbf{h}(\cdot)$ either are not existing, formulated using the nominal disturbance or substituted into the cost and other constraints, by an invertion in some sense[NBP20]. The inequality constraints in (4.38) are usually interpreted as the maximization of the individual constraints:

$$\max_{\mathbf{w}_0 \times \cdots \times \mathbf{w}_k \in \mathcal{W}_{0:k}} \{g_i(\mathbf{x}_k, \mathbf{u}_k, \mathbf{w}_k)\} \leq 0 \tag{4.39}$$

in contrast to all constraints at once. Furthermore, it is also assumed that the
uncertainty lies in a convex polytopic set $\mathcal{W} = \{\mathbf{w} : V\mathbf{w} \leq \mathbf{v}\}$.

In T-MPC, as in other robust MPCs, the worst-case of the constraints are
considered; the constraints are formulated as deterministic constraints for the
nominal disturbance, with a tightening of the constraints, such that the solution
will allow the original constraint to hold, even for the worst realization of the
uncertainty. The approach used in T-MPC relies on defining tubes describing
the possible constraint realizations due to the uncertainty as a sequence of sets
corresponding to a given constraint across the prediction horizon. The sets in
the tubes are defined as robustly positively invariant sets (def. 4.2), such that
the desired properties of the MPC are true, such as recursive feasibility.

DEFINITION 4.2 (Robustly Positively Invariant set) a set $\mathcal{Z}$ is robustly posi-
tively invariant (RPI) under the dynamics $\mathbf{f}(\mathbf{z}, \mathbf{w})$ and constraints $\mathbf{g}(\mathbf{z}, \mathbf{w})$ if and
only if for all $\mathbf{w} \in \mathcal{W}$ and $\mathbf{z} \in \mathcal{Z}$, the constraints hold and the dynamics lie in
the set; $\mathbf{f}(\mathbf{z}, \mathbf{w}) \in \mathcal{Z}$, [KC16].

There exist many approaches to how exactly one computes both the RPI and
the constraints tightening depending on the kind of system considered [NBP20,
KC16]. Below is given a simple linear example of the approach of [NBP20].

EXAMPLE 1 *Let us consider the linear constraint $g_i(u, w) \leq H$ dependent on
the control $\boldsymbol{u}$ and the uncertain disturbance $\boldsymbol{w} \in \mathcal{W}$*

$$g_i(u, w) = \boldsymbol{F}^T \boldsymbol{u} + \boldsymbol{G}^T \boldsymbol{w} \leq H \tag{4.40}$$

The constraint's set of possible realizations can then be written as

$$\boldsymbol{F}^T \boldsymbol{u} \bigoplus \boldsymbol{G}^T \mathcal{W} \tag{4.41}$$

The tightening of the constraint can then be written as

$$\boldsymbol{F}^T \boldsymbol{u} \leq H - h_i \tag{4.42}$$

$$h_i = \max_{\boldsymbol{w} \in \mathcal{W}} \boldsymbol{G}^T \boldsymbol{w} \tag{4.43}$$

*where the computation of h_i reduces the constraint to a deterministic tightened
version of the constraint. One approach to solving (4.43) is using an uncertainty
description based on zonotopes[BR15].*

$$h_i = \boldsymbol{G}^T \boldsymbol{w}_0 + || \boldsymbol{G}^T \cdot diag(\overline{\Delta \boldsymbol{w}})||_1 \tag{4.44}$$

where the uncertainty is assumed bounded by $\boldsymbol{w} \in \boldsymbol{w}_0 \pm \overline{\Delta \boldsymbol{w}}$.

4.3.2   Scenario-based MPC

From the class of stochastic MPC, another approach to uncertainty in the MPC is the scenario-based MPC (SB-MPC), which is a statistical approximation of the robust MPC [GCGP09, CGP19]. It works by finding a solution of the MPC program, that holds for any realization of the disturbances, also called a scenario, within a given subset $\mathcal{W}_0$ of all possible realizations of the disturbances $\mathcal{W}$. The general scenario-based MPC is formulated as

$$J = \min_{\mathbf{u},\xi} \xi \tag{4.45}$$

$$s.t.$$

$$\sum_{k=0}^{N_{H_p}} l(\mathbf{x}_k, \mathbf{u}_k, \mathbf{w}_k) \leq \xi, \quad \forall \mathbf{w} \in \mathcal{W}_0 \tag{4.46}$$

$$\mathbf{x}_{k+1} = \mathbf{f}(\mathbf{x}_k, \mathbf{u}_k, \mathbf{w}_k), \quad \forall \mathbf{w} \in \mathcal{W}_0 \tag{4.47}$$

$$\mathbf{h}(\mathbf{x}_k, \mathbf{u}_k, \mathbf{w}_k) = \mathbf{0}, \quad \forall \mathbf{w} \in \mathcal{W}_0 \tag{4.48}$$

$$\mathbf{g}(\mathbf{x}_k, \mathbf{u}_k, \mathbf{w}_k) \leq \mathbf{0}, \quad \forall \mathbf{w} \in \mathcal{W}_0 \tag{4.49}$$

where cost constraint in (4.46) and the constraints are duplicated for each scenario in $\mathcal{W}_0$. If the cost constraint is independent of the uncertainty, then the cost function can be formulated as the cost constraint.

The theory used in SB-MPC relies on the scenarios in $\mathcal{W}$ being independently and randomly sampled. Under these assumptions, [GCGP09] introduced a formula for how many scenarios are needed for an approximation of a given quality:

$$N \geq \frac{2}{\epsilon}(ln(\frac{1}{\beta}) + d) \tag{4.50}$$

where N is the number of independent scenarios, ϵ is the violation parameter, β is the confidence parameter and d is the number of optimization variables in the MPC program. The confidence parameter β and violation parameter ϵ define the probability $1 - \beta$ that the solution of SB-MPC satisfies all constraint realizations except at most an ϵ-fraction of them.

While SB-MPC has the benefit of no assumption of distribution, and a formulation with the same order of non-linearity as the original MPC, it comes with the drawback of multiplying the program size; N copies of each constraint. If a large N is chosen, this can lead to increased computation time depending on the program. Let us consider (4.50) to see how large N should be; e.g. for a system with three optimization variables across the horizon, $d = 3$, if we choose a violation fraction $\epsilon = 0.1$ and a confidence of missing only one in a thousand,

$\beta = 10^{-3}$, then we can compute N:

$$\frac{2}{0.1}(ln(\frac{1}{10^{-3}}) + 3) = 60ln(10) + 60 \Rightarrow N \geq 199 \tag{4.51}$$

where it can be seen that even for a small program with a handful of variables, the size of N increases rapidly if the desired violation fraction is small. If we reverse the focus to the violation fraction and consider scenario sets of size 25 or 50, typical scenario forecast size from weather predictions[Ped18], then our violation fraction ϵ becomes 0.79 and 0.40 respectively. Both being larger and approaches one as the confidence and number of variables increases.

On this basis, it would only be sensible to utilize scenario-based MPC on sewer systems, if the given system were very limited in size w.r.t. optimization variables.

4.3.3   Chance Constrained Model Predictive Control

The last method, we will discuss is the Chance Constrained MPC (CC-MPC), also from the class of stochastic MPCs. In [SN99], the Chance Constrained approach to stochastic MPC was proposed, and have since then been well researched [KC16, Mes16]. While the T-MPC was based on knowing the boundary of the uncertainty, and the SB-MPC were based on access to enough independent random scenarios of the uncertainty; the CC-MPC is based on the assumption that we know the exact distribution of the constraints and cost, affected by the uncertainties. The knowledge is used to formulate a deterministic MPC, where the inequality constraints are tightened based on the probabilistic nature of the constraint, as opposed to the worst-case tightening in the case of T-MPC.

Often it is assumed that the distribution of the uncertainties is known and that the distribution of the constraints can be computed as needed. The general formulation of CC-MPC using this assumption is given by

$$J = \min_{\mathbf{u}} \sum_{k=0}^{N_{H_p}} E\{l(\mathbf{x}_k, \mathbf{u}_k, \mathbf{w}_k)\} \tag{4.52}$$

$s.t.$

$$\mathbf{x}_{k+1} = \mathbf{f}(\mathbf{x}_k, \mathbf{u}_k, \mathbf{w}_k) \tag{4.53}$$

$$E\{\mathbf{h}(\mathbf{x}_k, \mathbf{u}_k, \mathbf{w}_k)\} = \mathbf{h} \tag{4.54}$$

$$Pr\{g_j(\mathbf{x}_k, \mathbf{u}_k, \mathbf{w}_k) \leq \overline{\mathbf{g}}_j\} \geq \gamma_{j,k}, \quad \forall j \in [0, n_g] \tag{4.55}$$

$$w_{k,i} \sim F_{a_{k,i}}^{b_{k,i}}(\boldsymbol{\theta}_{k,i}) \tag{4.56}$$

where the cost and equality constraints are the expected values, and the inequality constraints are formulated as probabilistic constraints on each individual constraint. The probability constraints could also be formulated across several constraints, as a joint probability of all of the constraints being true.

In CC-MPC, the probabilistic formulation given above is rewritten such that it becomes deterministic. For the probabilistic constraint, we utilize the relation between probability and the CDF $\Phi_X(x)$ of a stochastic variable X in (4.57), to rewrite the constraint deterministically in terms of the quantile function of the constraint.

$$Pr\{g_j(\mathbf{x}_k, \mathbf{u}_k, \mathbf{w}_k) \leq 0\} = \Phi_{g_j(\mathbf{x}_k, \mathbf{u}_k, \mathbf{w}_k)}\{0\} \geq \gamma_{j,k} \tag{4.57}$$

$$\Phi^{-1}_{g_j(\mathbf{x}_k, \mathbf{u}_k, \mathbf{w}_k)}\{\gamma_{j,k}\} \leq 0 \tag{4.58}$$

The quantile function $\Phi_X^{-1}(x)$ is in general hard to compute, given that it might not be described by a well-researched quantile function, and due to its dependency on the optimization variable $\mathbf{u}$; making the quantile varying under the optimization. A common trick is to simplify the constraint, by splitting the constraint in a stochastic and deterministic part: $g(\mathbf{u}, \mathbf{w}) = g_{det}(\mathbf{u}) + g_{stoch}(\mathbf{u}, \mathbf{w})$. If the stochastic part, then becomes independent of the optimization, then the quantile becomes fixed for the given uncertainty, as would be the case of additive uncertainty.

$$\begin{aligned} Pr\{g(\mathbf{u}, \mathbf{w}) \leq 0\} &= Pr\{g_{stoch}(\mathbf{u}, \mathbf{w}) \leq -g_{det}(\mathbf{u})\} \\ &= \Phi_{g_{stoch}(\mathbf{u}, \mathbf{w})}\{-g_{det}(\mathbf{u})\} \end{aligned} \tag{4.59}$$

Another approach to ease the computation of the quantile function is through standardization of the constraint distribution and its quantile function. Depending on the constraint distribution, it might be possible with deterministic expression to formulate the quantile as a function of a quantile function with fixed distribution parameters. An example of a distribution with this property is the normal distribution, where the quantile function of the stochastic variable X is given by

$$\Phi_X^{-1}\{\gamma\} = E\{X\} + \sigma\{X\}\Phi^{-1}\{\gamma\} \tag{4.60}$$

where $\Phi^{-1}\{\gamma\}$ is the quantile function of the standard normal distribution $\mathcal{N}(0, 1)$. Both approaches can be used simultaneously.

Earlier in section 4.0.1, we discussed some benefits with quadratic and linear cost and constraints, in the case of CC-MPC this is even more true; given that both the expectation and variance functions for matrix/vector formulation have certain properties that lead to simpler computations of the cost and constraint

functions[Pou07]:

$$E\{A\mathbf{X}\} = AE\{\mathbf{X}\} \tag{4.61}$$

$$\sigma^2\{A\mathbf{X}\} = A\sigma^2\{\mathbf{X}\}A^T \tag{4.62}$$

$$tr\{\mathbf{X}^T A\mathbf{X}\} = tr\{A\mathbf{X}\mathbf{X}^T\} \tag{4.63}$$

$$E\{||\mathbf{X}||_A^2\} = E\{\mathbf{X}\}^T AE\{\mathbf{X}\} + tr\{A\sigma^2\{\mathbf{X}\}\} \tag{4.64}$$

The property given in (4.64) is especially useful for the cost in quadratic programs if the uncertainty in X is independent of the optimization; then the variance term becomes constant w.r.t. the optimization.

Similarly for linear cost and constraints are (4.61) practical to isolate the uncertain elements in the equations into the expectation of the uncertainties, which are fixed w.r.t. the optimization.

4.3.4   Estimation of Probability Distribution

So far we have discussed how CC-MPC is formulated and how it utilizes the knowledge of the distribution to formulate a deterministic MPC program. Here we will discuss how knowledge of the distributions can be obtained. The simplest way is of course that the knowledge is provided by some external source, otherwise, the distributions have to be estimated from available data about the uncertainty.

The simplest way of estimating a distribution from data is to evaluate the data against a standard distribution, through a goodness of fit test for the chosen standard distribution. With standard distribution, we mean any distribution described previously by research (and usually named). There exist several types of goodness of fit test[JFM11, Hay13], in the following paragraphs we will discuss a few of them, and what one needs to estimate the parameters of the distributions to compare with.

χ^2 **test:**   A goodness of fit χ^2-test is based on evaluating whether the data could belong to a given distribution, within a margin of error. It operates on the hypothesis that the data comes from a given distribution, and tests if this claim can be rejected, by comparing the test statistic with the critical point of a suitable χ^2 distribution. The test statistic is based on occurrences in intervals, where the intervals cover the span of the given distribution. There exist more than one type of χ^2 test, where the difference lies in the formulation of the test statistic. Below is the test statistic given for two common types.

α	0.20	0.10	0.05	0.02	0.01
d_α	1.07	1.22	1.36	1.52	1.63

Table 4.1: Values of the Kolomogorov-Smirnov critical point coefficient

Pearson's χ^2 test:

$$\chi^2 = \sum_{i=1}^{k} \frac{(O_i - E_i)^2}{E_i} \qquad (4.65)$$

likelihood ratio χ^2 test:

$$G^2 = 2 \sum_{i=1}^{k} O_i ln(\frac{O_i}{E_i}) \qquad (4.66)$$

where O_i is the number of occurrences within the ith interval and E_i is the expected number of occurrences in the ith interval. The number k is the number of intervals used, generally chosen so no occurrence is less than five.

if the test statistic χ^2 or G^2 are below the critical point $\chi^2_{\alpha,k-1}$, e.g. $\chi^2 \leq \chi^2_{\alpha,k-m}$, then the hypothesis of the data being from the given distribution is deemed plausible and accepted. m is the number of parameters estimated from the data to described the given distribution.

Kolmogorov-Smirnov Test for single populations   The Kolmogorov-Smirnov test is based on the empirical CDF $\Phi_{est}(x)$ and the largest difference between it and the CDF $\Phi_0(x)$ of a proposed distribution. The empirical CDF is defined using a data set of n samples as below, where the CDF value at x is defined as the number of samples below x

$$\Phi_{est}(x) = \frac{\#x_i \leq x}{n} \qquad (4.67)$$

The Kolmogorov-Smirnov test statistic M is computed as the largest difference between the CDFs defined as

$$M = \max_x |\Phi_{est}(x) - \Phi_0(x)| \qquad (4.68)$$

The hypothesis is rejected if M is large, which typically is formulated as

$$M \geq \frac{d_\alpha}{\sqrt{n}} \qquad (4.69)$$

where $\frac{d_\alpha}{\sqrt{n}}$ is the critical point of the test. In Table 4.1, the coefficient d_α is given for a selection of α values.

Anderson-Darling Test   Another test based on CDF is the Anderson-Darling test, where the data is sorted after size, such that $x_i \leq x_j$ and the test statistic A^2 is defined as

$$A^2 = -\frac{\sum\limits_{i=1}^{n}(2i-1)(ln(\Phi_0\{x_i\}) + ln(1 - \Phi_0\{x_{n+1-i}\})}{n} - n \qquad (4.70)$$

If the hypothesis is that the data follows a distribution F, then we reject the hypothesis if A^2 is larger than the critical point of the distribution F:

$$A^2 \geq F_\alpha \qquad (4.71)$$

Parameters   Whether the test is based on CDF or other formulations of the given distribution, the theoretical distributions depend on its parameters, which need to be chosen. The simplest scenario is when the proposed distribution includes values of the parameters and not only the distribution type; testing for a specific distribution such as the standard normal distribution $\mathcal{N}(0,1)$. In other cases, some or all of the parameters have to estimate from the data

EXAMPLE 2 *Let us consider a data set $X = \{x_1, x_2 \cdots x_n\}$ consisting of n samples, and the assumption that it follows a normal distribution with no prior assumption on the parameters. Then the parameters, mean μ and variance σ^2, has to be estimated from the data set:*

$$\mu_{est} = \sum_{i=1}^{n} \frac{x_i}{n} \qquad (4.72)$$

$$\sigma_{est}^2 = \sum_{i=1}^{n} \frac{(x_i - \mu_{est})^2}{n} \qquad (4.73)$$

providing a parameter set to define the distribution in the test.

Summary of Own Publications

In this chapter, we will discuss how the topics discussed in the previous chapters of this dissertation relate to the work of the ph.d. project; presented in the published/submitted papers used as the foundation of the dissertation.

In Table 5.1, we can see which papers relate to which of the discussed topics, while the more fundamental and informative topics are excluded from the table if no paper addresses the topic directly.

A more detailed discussion of the content and topics of each paper is given in the following sections.

5.1 Paper A

In this paper, we utilized a linear virtual tank model of the Barcelona case study through an implementation in MATLAB, to compare the CSO formulations of MI-MPC and slack approximation, see section 4.1. The MI-MPC was based on MLD formulations so that the MPC program was kept a QP program. The slack approach was similarly formulated as a comparable QP program. Both programs

Topic\Article:	pap A	pap B	pap C	pap D	pap E	pap F	pap G
virtual tanks	x	x	x	x	x	x	x
Hi-Fi simulation		x			x	x	
Design simulation	x		x	x			x
Barcelona	x		x				
Astlingen		x		x	x	x	
Aarhus							x
MI-MPC	x						
CSO Slacks	x	x		x	x	x	x
CSO avoid			x				
QP-MPC	x	x	x	x	x	x	
LP-MPC							x
CC-MPC			x	x	x	x	x
T-MPC						x	
Estimation							x
cost: Δu	x	x	x	x	x	x	
cost: u	x	x	x	x	x	x	x
cost: q^{cso}	x	x		x	x	x	x

Table 5.1: Overview of the Topics in each of the Papers: with x indicating paper includes topic given in that row

were given the same base cost, which the slack approach would extend. The comparison presented in this paper covered the operational and computational aspects of the two approaches to CSO formulation.

Given the simulation model were identical to the design model of the MI-MPC, the found CSO of MI-MPC would match the simulation per definition; from the simulations it was found that the slack approach likewise was able to predict the CSO of the simulation, therefore showing equal ability to predict the system. Operationally the added cost of the slack approach improves the CSO minimization in comparison to MI-MPC, but at the cost of worse performance on other cost criteria, where the MI-MPC performs better.

On the computational side, it was shown that the computation time of MI-MPC would increase drastically with increases in rain intensity or duration, while the slack approach was much less sensitive to the increases, computationally. The difference was shown for large rain events to generally be a factor of 500 times the computation time, for a horizon of 20 min by 5 min sampling. It was further compared the computation sensitivity to the horizon length, were again was shown that MI-MPC being more sensitive, with a drastic increase in computation time.

The slack approach used in this paper was based on the one of [HF17] with a quadratic term, and it was shown that it is applicable to CSO from pipes and not only tanks. The weighting rules for achieving physical behavior of the CSO, when using the slack approach were stated:

- the weight is on the accumulated CSO volume

- the weight on the CSO slack variable has to be relatively higher than any other costs

- the weight on CSO from upstream elements have to be higher than the downstream CSOs

5.2   Paper B

In this paper, we presented an implementation of the Astlingen system and the utility of MPC in comparison to other rule-based controllers, through simulations. My contributions were regarding the MPC, excluding the implementation of the system. The simulations were based on an SWMM model of Astlingen; a simulator solving the Saint-Venant equations[Ros17] discussed in section 2.1.

We showed that the MPC approach from paper A; a simple QP MPC using the slack approach, could achieve good operations on the nonlinear Astlingen system, and outperforming the tested rule-base controllers. Indicating the potential of using a simple advance controller instead of a simple rule-based controller.

5.3   Paper C

In this work, we considered the existence of uncertainty in the weather forecast and the implication on MPC performance. The performance was evaluated based on simulation of a simplified Barcelona model, without internal overflows. As part of the evaluation, we used the CC-MPC method, a method designed to handle uncertainty, as an alternative controller to the base MPC.

Both the base MPC and CC-MPC were designed as QP MPCs with CSO avoidance. The simulations were done with an MPC with perfect forecast as a comparison. The CC-MPC was given a distribution with the perfect forecast as the expected forecast, while the base MPC was given different realizations of

the forecast based on the same distribution. The evaluation of the performance focused on feasibility range and false CSO predictions.

It was found that both MPCs became more unfeasible as the rain events increased; MPC had fewer successful realizations and CC-MPC was restricted to lower confidence levels γ. This gives the CC-MPC a level of feasibility tuning, which the base MPC does not have. The MPC was found to produce solutions that caused CSO, though it should not, in contrast, the CC-MPC produced no such false positive predictions.

This paper represents the intermediate work and thoughts between paper A and B, and the methods and results of paper D.

5.4   Paper D

In this article, we presented the difficulties of applying CC-MPC to sewer networks, when aiming to minimize CSO and not avoid it. It was shown that the standard formulation used in paper C lead to insensible probabilistic constraints. On that basis, we proposed a different approach to the formulation of CC-MPC, when working with weirs; using the switch function $T(\cdot)$ in (4.19) to provide meaningful probabilistic constraints.

The proposed formulation is designed to include intrinsic feasibility, when the deterministic MPC has it, as well as including the usage of the slack approach:

$$E\{g_i(\mathbf{x}_k, \mathbf{u}_k, \mathbf{w}_k, \mathbf{q}_k^{cso}\} \leq 0 \tag{5.1}$$

$$\Phi_{T_i(\cdot)}^{-1}\{\gamma\} - c \leq 0 \tag{5.2}$$

$$0 \leq c \tag{5.3}$$

where g_i is the ith constraint at time k defining one of the overflows in $\mathbf{q}_k^{cso}$, T_i is the corresponding switching function of the defined overflow, and c is a slack variable providing intrinsic feasibility, with some associated penalty.

The formulation was tested successfully on a simulation of using the design model of the CC-MPC, inspired by the Astlingen network. Showing the proposed formulation works, w.r.t. overflow prediction, and expected performance, when compared to an MPC with perfect knowledge.

5.5 Paper E

In this work, the proposed formulation of CC-MPC from paper E was applied to the Astlingen simulation setup from paper B. The performance of CC-MPC was evaluated against a baseline of an MPC with perfect forecast. The evaluation focused on the sensitivity of the performance of CSO and flow to WTTP. The sensitivity was defined w.r.t. variation in the confidence level of the CC-MPC and different aspects of uncertainty, such as the bounds of the uncertainty, scaled biases and offset biases of the expected forecast.

It was found that for the Astlingen system, the CC-MPC and MPC were sensitive to overestimation biases of the forecast, while only MPC being sensitive to the corresponding underestimations. The CC-MPC's sensitivity towards the uncertainty bound appeared to be negligible.

5.6 Paper F

In this paper, we considered and compared the differences and similarities of robust and stochastic MPC, specifically tube-based MPC and CC-MPC. We compared the formulations and drawbacks of the two methods, specifically the uncertainty propagation and uncertainty handling in individual constraints. We found the propagation was the same, and while approaches to obtaining a deterministic constraint are different, both did so with constraint tightening; which for a linear case was found to have an inequality relation, for the uncertainty term $A\mathbf{Z}$ given as:

$$
\begin{aligned}
\Phi_{A\mathbf{Z}}^{-1}\{\gamma\} &\leq A\mathbf{Z}_0 + ||A \cdot diag(\overline{\Delta\mathbf{Z}})||_1 \\
\mathbf{Z} &= \mathbf{Z}_0 + \Delta\mathbf{Z}, \Delta\mathbf{Z} \in [-\overline{\Delta\mathbf{Z}}, \overline{\Delta\mathbf{Z}}]
\end{aligned}
\tag{5.4}
$$

The general drawbacks were found to be worst-case conservatism for the T-MPC and computation difficulties for CC-MPC; a simple formulation of T-MPC with chance-constrained bounds was proposed.

A comparison of performances was done using the Astlingen setup used in paper B and E. Like in paper E, we considered the sensitivity to the different aspects of the uncertainties. It was found that the T-MPC were less sensitive to the biases than the CC-MPC, with opposite relation to the uncertainty bounds. In general, it was found that CC-MPC would perform better w.r.t. CSO and WTTP flow.

5.7 Paper G

In this article, we proposed a framework for applying CC-MPC on general systems, through the use of ensembles; Ensemble-based CC-MPC. The difficulties in obtaining analytical quantile functions for the constraints for general distributions and/or nonlinear systems provided a limit to the application and usefulness of the CC-MPCs discussed in paper C,D,E, and F.

Therefore we proposed to propagate an ensemble of uncertainty scenarios, instead of propagating the distributions, and utilizing distribution estimation to obtain a distribution of the constraint. The estimation can be in terms of known distributions with known quantile functions, therefore providing the mathematical tools for the CC-MPC.

The framework was applied with good results on a linear design model of the Aarhus system, section 3.4.3, using the proposed CC-MPC formulation from paper D. The simulations were run with normal distributed uncertainty, and estimation checking the constraints against being normal or uniform distributed, using the Pearson's χ^2 test.

An update to the weighting rules of the CSO slack approach presented in paper A was introduced, such that the increase in upstream weightings can be reset if separated from the downstream by a controller.

Conclusion and future research

In this ph.d. project, the focus has been on the application of Model Predictive Control (MPC) to sewer networks, primarily w.r.t. the minimization of Combined Sewer Overflows (CSO) from weirs. The project has considered different types of existing approaches to formulate weirs in the MPC design; formulations based on either integer or slack variables. It was found that both formulations were adequate to represent the CSOs, with the difference being in the trade-off between computation-complexity and design freedom. The weighting rules of the slack approach were found to decrease the design freedom, while the computation time of the integer approach was seen to increase rapidly.

In the project, the presence of uncertainty has been considered w.r.t. the MPC performance and design, mainly focusing on forecast uncertainty. Several existing methods for including the uncertainty in the MPC design such as chance-constrained MPC (CC-MPC) were explored. It was seen how the MPC and CC-MPC operated to avoid CSO; given less feasible solution space for CC-MPC, but also avoiding the false-positive solutions of the MPC.

When considering the reduction of CSO, it was found that CC-MPC has issues of compatibility between the approach to uncertainty and weir formulation; the slack approach. A new formulation of CC-MPC was proposed; addressing and solving the issues of compatibility, with the addition of providing intrinsic

feasibility to the CC-MPC design, provided the deterministic MPC would have intrinsic feasibility.

The performance of the formulated CC-MPC was compared to the MPC's performance, both on design models and hifi models. It was found that in general, the CC-MPC would perform comparable to an MPC with known forecast, and better than those with biased forecasts.

A similar comparison was performed for the CC-MPC against Tube MPC, regarding performance and formulation. There found a mathematical relation between the conservatism of the two MPCs for linear constraints. Performance-wise, it was found that each had its own strengths, depending on the aspect and size of the uncertainty in the forecast.

The dependence of CC-MPC on the availability of the right stochastic knowledge has been considered. Based on the dependency and distribution estimation, a framework for CC-MPC using ensemble forecasts (ECC-MPC) were formulated. The ECC-MPC framework will allow for the complicated constraint distributions to be described in terms of known distributions; simplifying computations. The framework was tested against the formulated CC-MPC and they were found to perform comparable to each other.

6.1   Future research

In this dissertation and the ph.d. project, the research has generally been limited to linear design models and additive uncertainty terms. Real systems are generally nonlinear to some extent, with non-additive uncertainty relations existing. It would therefore be of interest to extend the research and methods presented in this dissertation to include such aspects. Among the possible topics there could be considered in future research are:

1. Further evaluation and testing of the performance of the ECC-MPC framework. Including simulations with HiFi models (nonlinear), as well as with non-normal distributed uncertainties, or using historical ensemble forecasts.

2. Applying the proposed MPC methods to nonlinear sewer networks, with a nonlinear design model for the MPC; in order to capture more of the system dynamics in the optimization. Allowing for evaluation of which nonlinearities are bests modeled as nonlinear or could be modeled as linear adequately for the desired management, with only negligible losses of

performances. A simple nonlinearity to introduce would be the tank out-flow, as given in (2.5). Sequential quadratic programming could be the solving method for such MPCs.

3. While uncertainty with additive relations to the optimization variables has certain nice properties, uncertainty with other relations such as multiplicative is just as present in real systems. How to expand the proposed methods to include other relations are therefore a topic of interest for future research. We have in Paper G briefly mentioned a scenario for which multiplicative relations should be applicable for the framework method; based on assuming a standardization of the quantile function similar to the normal distribution is reasonable. It would be interesting to see if other scenarios can provide quantile functions independent of the optimization; both for multiplicative relations as well as for other uncertainty relations.

4. A source of model uncertainty in MPC is the linearization or changes to the real system. An interesting research topic could therefore be coupling MPC with methods from adaptive control theory, such as extended Kalman filtering and system identification. A research topic could be how one would detect changes in the constraint limits, especially expansions.

Another interesting aspect of the research in MPC is the affect of the length of the prediction horizon. Given that longer horizons gives larger MPC programs, it also increases the risk of numerical issues to occur, e.g. combinations of very large and small values. The following topic could therefore be off interesst:

A Research into the use of several sample times across the prediction horizon, to increase its length without the consideral increase in MPC program. Such research would focus on the performance and applicability of the methods discussed in this dissertation.

Bibliography

[BD11]   David Butler and John W. Davies. *Urban Drainage*. Spon Press, 3rd edition, 2011.

[BM99a]   Alberto Bemporad and Manfred Morari. Control of systems integrating logic, dynamics, and constraint. *Automatica*, 35:407–427, 1999.

[BM99b]   Alberto Bemporad and Manfred Morari. *Robust model predictive control: A survey*, volume 245 of *Lecture Notes in Control and Information Sciences*, pages 207–226. Springer, London, 1999.

[BR15]   Matthias Beck and Sinai Robins. *Computing the Continous Discretely - Integer-Point Enumeration in Polyhedra*. Springer, Oct. 2015.

[BV09]   Stephen Boyd and Lieven Vandenberghe. *Convex Optimization*. Cambridge University Press, 7th edition, 2009.

[CB07]   E.F Camacho and C. Bordons. *Model Predictive Control*. Springer, 2nd edition edition, 2007.

[CGP19]   Marco C. Campi, Simone Garatti, and Maria Prandini. *Scenario Optimization for MPC*, pages 445–463. Springer International Publishing, Cham, 2019.

[CMM88]   Ven Te Chow, David R. Maidment, and Larry W. Mays. *Applied Hydrology*. McGraw-Hill, 1988.

[CQS$^+$04] Gabriela Cembrano, Joseba Quevedo, M. Salamero, Vicenç Puig, J. Figueras, and J. Marti. Optimal control of urban drainage systems. a case study. *Control Engineering Practice*, 12:1–9, 2004.

[DH20] Lars Haslev Drejer and Rasmus Halvgaard. Water smart cities milestone 5: Offline model predictive control (mpc) performance results for the marselisborg, aarhus case study. Technical report, DHI, April 2020.

[DHI17] DHI. Mouse pipe flow - reference manual. Technical report, DHI, 2017.

[Dre20] Lars Haslev Drejer, March 2020. Private Correnspondence.

[ECK12] Martin Evans, Mark Cannon, and Basil Kouvaritakis. Linear stochastic mpc under finitely supported multiplicative uncertainty. Proc. of the 2012 American Control Conference, June 2012.

[GBGE$^+$15] L. García, J. Barreiro-Gomez, E. Escobar, D. Téllez, N. Quijano, and Carlos Ocampo-Martinez. Modeling and real-time control of urban drainage systems: A review. *Advances in Water Resources*, 85:120–132, November 2015.

[GCGP09] S. Garatti, Marco C. Campi, Simone Garatti, and Maria Prandini. The scenario approach for systems and control design. *Annual Reviews in Control*, 33:149–157, October 2009.

[GGSvO14] Stefano Galelli, Albert Goedbloed, Dirk Schwanenberg, and Peter-Jules van Overloop. Optimal real-time operation of multipurpose urban reservoirs: Case study in singapore. *J. Water Resour. Plann. Manage.*, 140:511–523, 2014.

[GR94] M. S. Gelormino and N. L. Ricker. Model predictive control of a combined sewer system. *INT. J. CONTROL*, 59(3):793–816, 1994.

[Gre15] Ida Bülow Gregersen. *Past, present and future variations of extreme rainfall in Denmark*. PhD thesis, Technical University of Denmark, DTU Environment, Kgs. Lyngby, 2015.

[Hay13] Anthony Hayter. *Probability and Statistics for Engineers and Scientists*. Brooks/Cole Cengage Learning, 4th edition, 2013.

[HF17] Rasmus Halvgaard and Anne Kathrine Vinther Falk. Water system overflow modeling for model predictive control. In *Proceedings of the 12th IWA Specialised Conference on Instrumentation, Control and Automation*. Proceedings of the 12th IWA Spe-

cialised Conference on Instrumentation, Control and Automation, june 2017.

[HH15]   R. Horalek and J. Hlava. Multiple model predictive control of grid connected solid oxide fuel cell for extending cell life time. In *23rd Mediterranean Conference on Control and Automation*, pages 310–315, 2015.

[HJS08]   Elbert Hendricks, Ole Jannerup, and Paul Haase Sørensen. *Linear Systems Control*. Springer, 2008.

[JFM11]   Richard Johnson, John Freund, and Irwin Miller. *Miller and Freund's Probaility and Statistics for Engineers*. Pearson, 8th edition, 2011.

[JS09]   Ole Jannerup and Paul Haase Sørensen. *Reguleringsteknik*. Polyteknisk Forlag, 4th edition, 2009.

[KC16]   Basil Kouvaritakis and Mark Cannon. *Model Predictive Control - Classical, Robust and Stochastic*. Advances Textbooks in Control and Signal Processing. Springer, 2016.

[Kim13]   Sean Hay Kim*. Building demand-side control using thermal energy storage under uncertainty: An adaptive multiple model-based predictive control (mmpc) approach. *J. Building and Environment*, 67:111–128, 2013.

[LBM$^+$19] Nadia Schou Vorndran Lund, Morten Borup, Henrik Madsen, Ole Mark, Karsten Arnbjerg-Nielsen, and Peter Steen Mikkelsen. Integrated stormwater inflow control for sewers and green structures in urban landscapes. *Nature Sustainability*, 2:1003–1010, 2019.

[Lee11]   Jay H. Lee. Model predictive control: Review of the three decades of development. *International Journal of Control, Automation, and Systems*, 9(3):415–424, 2011.

[Mac02]   Jan Marian Maciejowski. *Predictive Control: with constraints*. Pearson, 2002.

[Mad07]   Henrik Madsen. *Time Series Analysis*. Chapman & Hall/CRC, 2007.

[Mes16]   Ali Mesbah. Stochastic model predictive control: An overview and perspectives for future research. *IEEE Control Systems Magazine*, pages 30–44, December 2016.

[MNSA03]   L. Magni, G. De Nicolao, R. Scattolini, and F. Allgöwer. Robust model predictive control for nonlinear discrete-time systems. *International Journal of Robust and Nonlinear Control*, 13(3-4):229–246, 2003.

[MP05]   Magdalene Marinaki and Markos Papageorgiou. *Optimal Real-time Control of Sewer Networks*. Advances in Industrial Control. Springer, 2005.

[NAP17]   Niels Woetmann Nielsen, Bjarne Amstrup, and Claus Petersen. Construction of a cloud burst index in numerical weather prediction. *DMI report 17-16*, page 17, 2017. Technical Report.

[NBP20]   M. Nassourou, J. Blesa, and V. Puig. Robust economic model predictive control based on a zonotope and local feedback controller for energy dispatch in smart-grids considering demand uncertainty. *Energies*, 13(3), 2020.

[NW06]   Jorge Nocedal and Stephen J. Wright. *Numerical Optimization*. Springer Series in Operations Research. Springer, 2nd edition, 2006.

[O'D09]   Aidan O'Dwyer. *Handbook of PI and PID Controller Tuning Rules*. Imperial College Press, 3rd edition, 2009.

[OM10]   Carlos Ocampo-Martinez. *Model Predictive Control of Wastewater Systems*. Advances in Industrial Control. Springer, 2010.

[PCR$^+$09]   Vicenç Puig, Gabriela Cembrano, J. Romera, Joseba Quevedo, B. Aznar, G. Ramón, and J. Cabot. Predictive optimal control of sewer networks using coral tool: application to riera blanca catchment in barcelona. *Water Science & Technology*, 60(4):869–874, 2009.

[Ped18]   Jonas Wied Pedersen, 2018. Private communication at Water Smart City workshop.

[Pou07]   Niels Kjølstad Poulsen. *Stokastisk Adaptiv Regulering - Stokastiske systemer, identifikation og regulering*. DTU Compute, Technical University of Denmark, 15th edition, 2007.

[Pro63]   A.I. Propoi. Use of lp methods for synthesizing sampled-data automatic systems. *Automatic Remote Control*, 24, 1963.

[QB03]   S. Joe Qin and Thomas A. Badgwell. A survey of industrial model predictive control technology. *Control Engineering Practice*, 11:733–764, 2003.

[Ros17]   Lewis A. Rossman. Storm water management model reference manual volume ii - hydraulics. Technical report, Nation Risk Management Laboratory, Office of Research and Development, U.S. Environmental Protection Agency, May 2017.

[RSvdGvO14] L. Raso, D. Schwanenberg, N.C. van de Giesen, and P.J. van Overloop. Short-term optimal operation of water systems using ensemble forecasts. *Advances in Water Resources*, 71:200–208, 2014.

[SCC$^+$03]   Manfred Schütze, Alberto Campisano, Hubert Colas, Peter Vanrolleghem, and Wolfgang Schilling. Real-time control of urban water system. In *Int. Conf. on Pumps, Electromechanical Devices and Systems Applied to Urban Water Management*, Valencia, Spain, April 2003.

[Sin88]   Vijay P. Singh. *Hydrologic Systems. Volume 1: Rainfall-runoff modelling.* Prentice Hall, 1988.

[SLPH18]   Manfred Schütze, Maja Lange, Michael Pabst, and Ulrich Haas. Astlingen - a benchmark for real time control (rtc). *Water Sci & Technol*, 2017(2):552–560, 2018.

[SN99]   Alexander T. Schwarm and Michael Nikolaou. Chance-constrained model predictive control. *AIChE Journal*, 45(8):1743–1748, August 1999.

[SSR14]   Lalu Seban, Narayan Sahoo, and B.K. Roy. Multiple model based predictive control of magnetic levitation system. In *Proc. Annual IEEE India Conference*, 2014.

APPENDIX A

Article A

The paper presented in this appendix was originally published in connection with a conference and an oral presentation of the content.

Information of the publication:

- Title: Model Predictive Control of Overflow in Sewer Networks - A comparison of two methods

- Conference: Systol 2019 - 4th International Conference on Control and Fault-Tolerant Systems.

- Date: September 18-20th, 2019

- place: Casablanca, Morocco

Model Predictive Control of Overflow in Sewer Networks
A comparison of two methods

Jan Lorenz Svensen[1], Hans Henrik Niemann[2] and Niels Kjølstad Poulsen[3]

Abstract— In this work, a comparison of two previous proposed methods for Model Predictive Control (MPC) of sewage systems are presented. The focus is on prediction of overflow from weirs and the computation time of the methods. The first method considered in this study is a mixed integer quadratic program MPC based on mixed linear dynamic formulations. The second method considered is a quadratic program MPC with optimizable overflows and accumulated overflow volume penalty. For the comparisons of the methods, a case study of the Barcelona sewer network is utilized. Our numerical experiments show that the predictions of the system's experienced overflow, performed by the quadratic program MPC are equivalent to the predictions of the mixed integer variant, but is computing faster and in general reduces the overflow volumes, due to the difference in the choice of control.

I. INTRODUCTION

Model Predictive Control (MPC) has been applied to dozens of work areas [5]-[8], urban drainage systems being one of them. In this work, two approaches to the modelling of design models for MPC in sewages system will be compared. One common way of simplifying the large sewage networks, are to model pipes, manholes, etc. of an area collectively as a virtual tank, such that only the volumetric storage dynamics are left [9]-[13]. The system is then only consisting of virtual tanks, real tanks and the connections between them. The only problem remaining for having a simple model of the system is to model the weir overflows occurring in the tanks and connections. These overflows depends on the amount of volume or flow above the weir limit of a given system part. This gives the overflows a binary nature; being zero below the weir limit and following a function above it. This binary nature has led previous work by Ocampo-Martinez [1] to apply Mixed Integer (MI) MPC to the system with good success. Another approach was given by Halvgaard and Falk [3] by expanding on Gelormino and Ricker's approach [4], where the overflow were modelled as a control variable to be optimized, allowing the MPC to be a quadratic program (QP), when using a linear model of the sewage network. For the comparison, the model of the Barcelona sewage system presented by Ocampo-Martinez will be utilized, shown in
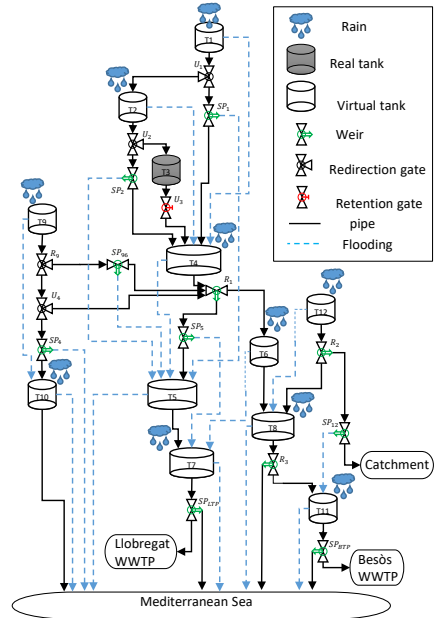
Fig. 1. A schematic of the Barcelona Sewage System model presented by Ocampo-Martinez [1], showing the interconnections between the different tanks and the environment. The controlled parts of the system is tagged with a U

Fig. 1. The focus in this paper is the two approaches' ability to predict the amount of overflow the sewer system experience, and what the benefits are using one approach over the other. The MPCs of the two approaches will be an MI QP MPC and a QP MPC.

A. Notation

The following notations are utilized in this paper. Bold font are used to indicate vectors, and the quadratic norm of $\mathbf{x}$ is given by $||\mathbf{x}||_A^2 = \mathbf{x}^T A \mathbf{x}$. The subscripts indicates either spatial placement or time in samples, while the superscripts noted with u and w indicates control and weir variables respectively. The inflow and outflow of a subpart of the system are noted with the superscript in and out respectively. Variables written with a q or V indicates flow or volume respectively. The sampling time is noted by ΔT and the min. and max. of a function f(x) are notated $\underline{f}$ and $\bar{f}$ respectively. The parameter β is the volume/flow conversion coefficient

introduced by Singh[14].

II. MODEL

Three models are needed for the comparison, a simulation model and two design models, one for each approach. The simulation model and the design model for the MI method are based on the MI model of the Barcelona sewage model introduced by Ocampo-Martinez [1]. The MI design model is the simulation model rewritten in a linear form, by utilizing the mixed logical dynamical (MLD) modelling framework, introduced by Bemporad and Morari[2]. Meaning that for the MI method, the design model and the simulation model are equivalent. The three models all consist of the same five type of subparts: manipulated/unmanipulated redirection gates, sewages pipes, virtual tanks, and real tanks with input gates. In the design model of the QP method, each subparts are described as a linear element without logical variables. By combining the subparts of each part of the system, the resulting design models of both methods have 12 state variables corresponding to the volume of the 12 tanks and 4 control variables representing the four manipulated gates in the system. In the MI design model, 32 logic variables δ are utilized to formulate the binary nature of 54 flow variables q, giving a total of 302 linear inequality constraints. While the QP design model only has 83 linear inequality constraints with 23 flow variables q^w describing the weir overflows. Among the subparts, overflow can occur in the virtual tanks and in the sewage pipes. In the following, a description of the virtual tank and the sewages pipe are given for the QP method. A comparison and description of all five subparts for both methods are given in appendix A.

A. Quadratic Program Overflow Model - Virtual Tank

The outflows of the tank are restricted linearly by the upper tank limit, while the overflow only occurs for volumes higher than the upper tank limit. By defining the effective volume of the virtual tank to be the tank volume minus the overflow volume, the outflow and the overflow of the tank can be written linearly, as seen in (1)-(4).

$$v_{k+1} = (1-\beta)(v_k - \Delta T q^w) + \Delta T q^{in} \quad (1)$$
$$q^{out} = \beta(v_k - \Delta T q^w) \quad (2)$$
$$0 \le v - \Delta T q^w \le \bar{v} \quad (3)$$
$$0 \le q^w \quad (4)$$

B. Quadratic Program Overflow Model - Sewages pipe

Overflows occurs, when the inflow surpasses the outflow limit. The pipe outflow can therefore be modelled as the inflow minus the overflow, with the outflow and weir overflow being constrained by thee physical limits as seen in (47)-(49).

$$q^{out} = q^{in} - q^w \quad (5)$$
$$0 \le q^{in} - q^w \le \bar{q}^{out} \quad (6)$$
$$0 \le q^w \quad (7)$$

III. COST FUNCTION

For finding the optimal solution for the system, when using the MI design model, we utilize the weight-based cost function given by (8) for a prediction horizon N.

$$J = \min_{\mathbf{q}^u, \boldsymbol{\delta}, \mathbf{q}^w} \sum_{k=0}^{N} \left(||\mathbf{z}_k - \mathbf{z}_k^{ref}||_Q^2 + ||\Delta\mathbf{q}_k^u||_R^2 \right) \quad (8)$$

The $\Delta\mathbf{q}_k^u$ are the changes in the control flows, and the output vector $\mathbf{z}_k$ and its reference vector $\mathbf{z}_k^{ref}$ contains four elements, corresponding to the following objectives:

- minimize the aggregated overflows from the virtual tanks and sewage pipes to the streets
- minimize the aggregated flow to the Mediterranean Sea from the sewage system
- maximize flow to Wastewater Treatment plant Llobregat
- maximize flow to Wastewater Treatment plant Besòs

The weights Q and R are diagonal matrices with the diagonal being (2.0, 1.0, 0.5, 0.5) and (0.01, 0.01, 0.01, 0.01) respectively, chosen such that the priority of the minimization is given to the weir overflow, flow to the sea, flow to treatment plants and the control change, in that order. The references of the flows towards the WWTPs are the maximum flow capacity of the corresponding pipes, while the references of the overflows are zero. The maximization of the flow to the WWTPs are defined as the minimization of the deviation from their maximum flow.

A. Linear Overflow Cost

The same cost function is utilized in the QP method, but with a linear term introduced in (9) by Halvgaard and Falk [3]. This term is added, because the QP method treats weir overflows as control variables, and the usage therefore needs to be penalized.

$$J = \min_{\mathbf{q}^u, \mathbf{q}^w} \sum_{k=0}^{N} \left(||\mathbf{z}_k - \mathbf{z}_k^{ref}||_Q^2 + ||\Delta\mathbf{q}_k^u||_R^2 + \mathbf{W}^T\mathbf{V}_k^w \right) \quad (9)$$

Halvgaard and Falk [3] introduced the extra term to penalize the accumulated overflow volume of each tank weir, but is here also used to penalize the accumulated overflow volume of pipe weirs. The accumulated overflow volume $\mathbf{V}_k^w$ of each weir at time k is given in (10), where $\mathbf{q}_i^w$ is a vector of overflows q_i^w from weirs at time i.

$$\mathbf{V}_k^w = \sum_{i=0}^{k} \Delta T \mathbf{q}_i^w \quad (10)$$

There are two guiding rules to the weighting of the extra term; firstly, the term should have a relatively high weight W, such that the cost of the extra term is significantly higher than the cost of the other terms in the cost function. Making the usage of the overflow undesirable if avoidable. The second rule, is that each wear's overflow volume are penalized differently to enforce physical overflows only; the reason is that if two components containing weirs are in a series, then the optimizer might start emptying the upstream component in order to prevent overflow downstream, even if the upstream

413

TABLE I
INDEPENDENT OVERFLOW VOLUME WEIGHTS

$q_{T_1}^w$	$q_{SP_1}^w$	$q_{T_2}^w$	$q_{SP_2}^w$	$q_{T_4}^w$	$q_{R_1}^w$
110	100	100	100	90	80
$q_{T_{12}}^w$	$q_{R_2}^w$	$q_{T_6}^w$	$q_{T_8}^w$	$q_{R_3}^w$	$q_{SP_{12}}^w$
80	60	60	50	20	20
$q_{T_{11}}^w$	q_{BTP}^w	$q_{SP_5}^w$	$q_{T_5}^w$	$q_{T_7}^w$	q_{LTP}^w
10	1	20	10	1	1
$q_{T_9}^w$	$q_{R_9}^w$	$q_{SP_{96}}^w$	$q_{SP_4}^w$	$q_{T_{10}}^w$	
110	100	90	20	1	

Fig. 2. Idealized Rain Pattern

Fig. 3. A representative selections of overflows predicted by QP MPC vs Overflows obtained in Simulation

Fig. 4. Difference between MIQP MPC and QP MPC's amount of flooded wastewater
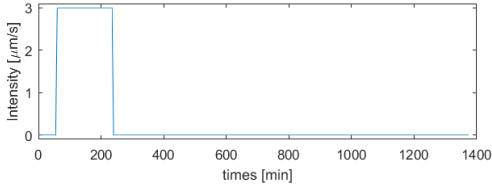
component is not full. This problem can be avoided by penalizing weir overflows from upstream components more than downstream components. The weights of the overflow volumes were chosen as 10^4 times an independent factor, shown for each weir in Table I. The subscripts indicates location in the system as displayed in Fig. 1.

IV. RESULTS

To compare the two methods, the results from simulations with rain events will be evaluated. For the simulations a sampling time ΔT of 5 min will be utilized[1] together with a prediction horizon of 20 min, chosen for its general low computation time. The rain events will be idealized rain patterns with the form of a step, as shown in Fig. 2 with a rain intensity of 3 $\mu m/s$, each rain pattern have an hour of dry weather before and a 19 hours of dry weather after the rain. The period of the rain in the simulations are varied with increments of a half hour from a half hour long to five hours long. The intensity of the rain in the simulations are varied with 2 $\mu m/s$ starting at 2 $\mu m/s$ ending with 14 $\mu m/s$. With the design model of the MI method being identical to the simulation model, the predictive overflows from the MI model are identical to the achieved overflow from the simulations, where the MI method were used as the controller. For the QP method, the design model deviates from the simulation model. In Fig. 3 selected weir flows are shown from a representative simulation controlled using the QP MPC, indicating the QP method succeeds to only predict overflows, which the system experience. In the next part of the result, we will focus on comparing the performance of the MPCs based on the objectives given in the cost functions, and a few other aspects.

A. Flooding

The flooding from the overflows of virtual tanks and pipes are the main terms of the cost function, especially in the
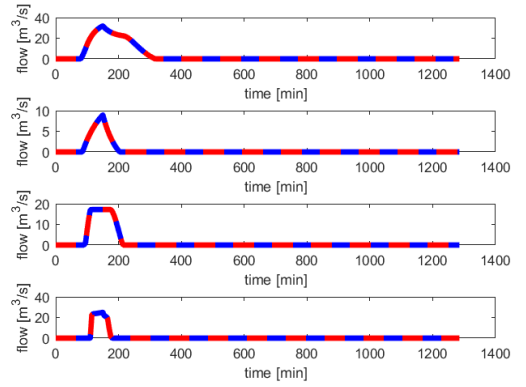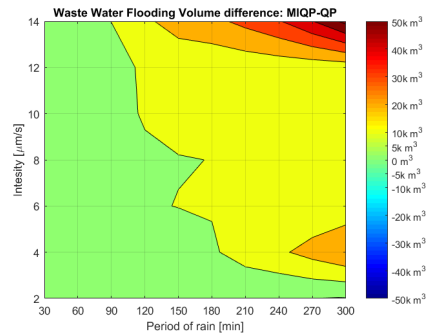
QP method. The total accumulated weir overflow volume of these terms are given in Fig. 4 for each simulation, as the difference between the results of the MI method and the QP method, with the latter subtracted. It can be seen that in general the MI method produces a higher weir overflow volume, corresponding to approximately 11k m^3 overflow volume on average. The percentage difference of overflow volume between specific rain events are on average 11.2% more overflow for the MI method.

B. Treated Waste Water

In the cost function the flow of wastewater to the systems two Treatment plants, Llobregat and Besós, were given as maximization objective. The results of the simulations tells that the QP method in general did worse than the MIQP MPC, with the average difference of amount of waste water being treated at the Llobregat and Besós plants being approximately 57 m^3 and 1.4k m^3 respectively. The difference of the combined treated wastewater is shown in Fig. 5 for the different intensities and period lengths. On average the percentage difference between the two methods are 3.7%, when considering treated wastewater volume of both plants.
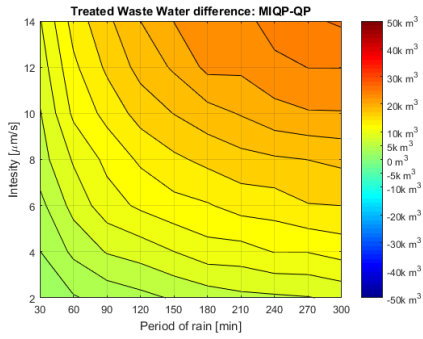
414

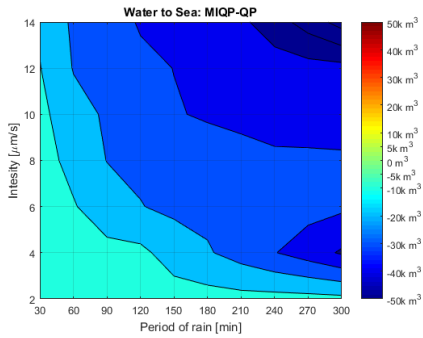Fig. 5. Difference between MIQP MPC and QP MPC's amount of treated wastewater

Fig. 7. Maximum Computational Time - QP MPC

Fig. 6. Difference between MIQP MPC and QP MPC's amount of sewage water directed to the sea

Fig. 8. Maximum Computational Time Ratio - MI/QP

C. Flow to Catchment and the Sea

The Barcelona sewages system also contain an outflow, which is not penalized in the cost function described earlier, the flow to a neighboring sewage catchment. This flow to the neighbor catchment were identical for both MPC methods. Given the flow is the result of an internal weir overflow; this indicates the QP methods ability to match the MI method prediction ability of the overflows of the system. The last flow contained in objectives of the cost function, is the flow to the Mediterranean Sea through the system (not flooding). The difference between the two methods can be seen in Fig. 6 given in accumulated volume, showing the QP method generally perform worse. The difference in volume were on average approximately 22.3k m^3 higher for the QP method than for the MI method; percentagewise the difference was on average 3.7% higher for the QP problem.

D. Computation Time

In the results so far, we have looked on the physical implications of the models and compared them; for the following results, the focus will be on the computational aspects of the methods. In Fig. 7, we see contour graphs of the maximum computation time of each optimization for the simulations with the QP method, and in Fig. 8, we see the ratio of the
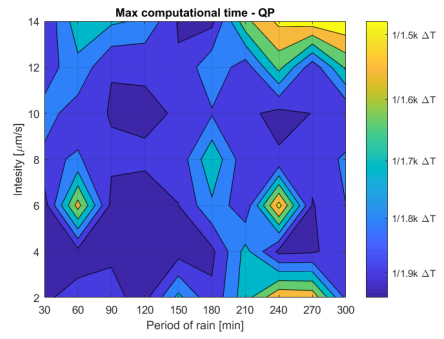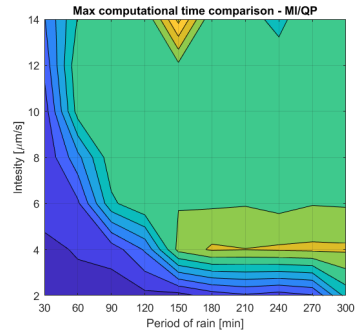
maximum computation time between the two methods. It can be seen that the computation time of the MI method for around half of the simulations takes 500 or more times longer to compute the solution, corresponding to at least a quarter of the sampling time of the computation. In the worst cases, the computation were more than 3000 times longer. While these high computation times occurs for less likely rain events, even the more likely events has computation times up to ten times as long. The computation time of the QP method were on the other hand very satisfying, with the worst cases being around one thousand five hundredth of the sampling time. For the MI method, the higher computation times occur as both the intensity and the period increased. The computation time peaks at rain events, generating the scenario of several tanks being full or almost full during the same horizon. Resulting in the logical variables oscillating between values depending on the control chosen, while the high and low intensity scenarios brings the system to its extreme, where the tanks are either full or relatively empty, making the logical variables settle independently of the control.

E. Horizon Length

The length of the prediction horizon affects the size of a MPC problem and therefore the computation time. In Fig. 9, the maximum computation time for both the QP and MI methods are shown as the prediction horizon increases for
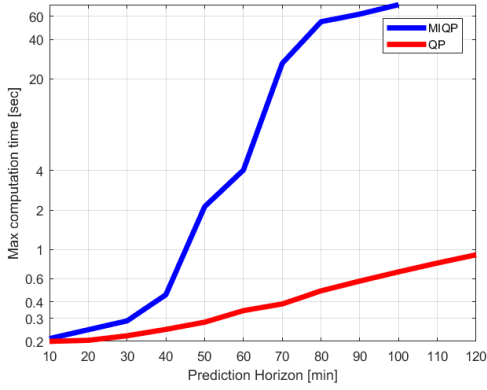
415

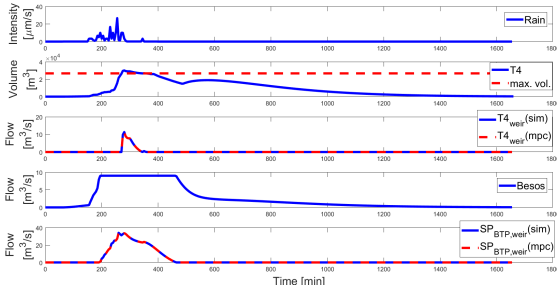Fig. 9. Maximum Computation time for prediction horizon length

Fig. 10. results of simulation with a historical rain event - QP MPC

a rain block of $2\ \mu m/s$ intensity and half hour duration; a rain pattern with no weir overflow. It can be seen that the computation time for the MI method increases dramatically in comparison to the QP problem, making MI method impractical for longer horizons with a sample times of five minutes. This is especially true in the context of weather, where a desired prediction horizon usually is not on the scale of a dozen minutes, but on the scale of at least a few hours.

F. Historical Rain

In Fig. 10 are shown the results of the QP method from a simulation with a historical rain event, recorded in Viby, Denmark on the 27th of August, 1992 by the Danish Spildevandskomité[15]. It can be seen that the overflow in the virtual tank 4 and the link towards Besós' first occurs, when the capacity limit has been reached, segmenting that the QP method succeeds in not violating the physical reality of weirs, despise using the overflows as optimization variables.

V. DISCUSSION

Based on the simulations it is clear that the QP method is an alternative to the MI method, as an approach for the design model of sewage systems with weir elements with regards to predicting the weir overflows. Furthermore the

QP method defined, has less constraints and variables to determine than the MIQP method, and no integer variables. The computational aspects tells it is possible to run the QP method with much longer prediction horizons than for the MI method. Some of the drawbacks of the use of the QP method includes; forced penalization of every overflow and not only unwanted overflow from weirs. With the weighting rules described in section III-A, the choosing of the weights of the cost function becomes more complex; with the weighting of the overflow terms, possible colliding with a desired prioritization of terms in the cost function. Another drawback is the weighting tends to large values, possible making the problem badly scaled. The extra term penalizing overflows in the cost function, is the reason for the disparity between the performances of the two methods, with overflows being more prioritized than treated wastewater and flow to the sea. The linear description of the gate elements does also come short in comparison to the MI description, given the control signal in the MI is corresponding to the actual position of the gate, and not the flow through the gate as in the QP method. The results of this study obtained were obtained using MATLAB R2017a with CVX v.2.1 and the Mosek 8.1 solver on a HP Elitebook Laptop with an Intel i7 processor.

VI. CONCLUSIONS

In this paper, two methods for handling weir overflow has been compared; Mixed Integer (MI) MPC and a QP MPC with a linear accumulated overflow volume cost term, run against a simulation model equivalent to the MI MPC design model. The results showed that the QP MPC were equivalent to the MI MPC, with regards to predicting the overflows occurring in the sewer system, while being significantly more efficient regarding computation times than the MI MPC. The performance of the QP MPC with regards to the MI MPC, showed a significant improvement, when considering the amount of flooding the system experienced. While the performance of the QP MPC were worse than the MI MPC with regards to maximizing the amount of wastewater being treated. The QP MPC could also be utilized with longer prediction horizons than the MI MPC, due to the computational improvement, giving it a wider practical utility.

APPENDIX

A. Sewage Model - Subparts

The five subparts of the sewage system model are discussed below, with a comparison between the model borrowed from Ocampo-Martinez[1] and the QP design model.

1) Virtual Tanks: For the MI model, the virtual tanks are described by (11)-(14), where both the outflow and the overflow depend on the logic variable δ, and the volume dynamics are a linear mass balance.

$$\delta = 1 \Leftrightarrow v \geq \bar{v} \tag{11}$$
$$q^w = \delta(v - \bar{v})/\Delta T \tag{12}$$
$$q^{out} = \delta\beta\bar{v} + (1 - \delta)\beta v \tag{13}$$
$$v_{k+1} = v_k + \Delta T(q^{in} - q^{out} - q^w) \tag{14}$$

The linear model in (15)-(18), is obtained by substitution in (13) and (14), with inequalities replacing the logics.

$$v_{k+1} = (1 - \beta)(v_k - \Delta T q^w) + \Delta T q^{in} \qquad (15)$$
$$q^{out} = \beta(v_k - \Delta T q^w) \qquad (16)$$
$$0 \leq v - \Delta T q^w \leq \bar{v} \qquad (17)$$
$$0 \leq q^w \qquad (18)$$

2) Real Tanks with Input Gates: These elements consist of a tank without a weir, where the inflow and outflow is controlled by a redirection and retention gate respectively. The inflow are in the MI model given by (19)-(24). For the QP model, the inequalities in (25)-(26) are a sufficient description of the controlled inflow.

$$\delta^1 = 1 \Leftrightarrow q^u \leq q^{in} \qquad (19)$$
$$q^{z1} = \delta^1 q^u + (1 - \delta^1)q^{in} \qquad (20)$$
$$\delta^2 = 1 \Leftrightarrow q^{z1} \leq \bar{q}^u \qquad (21)$$
$$q^{z2} = \delta^2 q^{z1} + (1 - \delta^2)\bar{q}^u \qquad (22)$$
$$\delta^5 = 1 \Leftrightarrow \bar{v} - v \leq \Delta T(q^{z2} - q^{out,tank}) \qquad (23)$$
$$q^{in,tank} = \delta^5 \left(\frac{\bar{v} - v}{\Delta T} + q^{out,tank} \right) + (1 - \delta^5)q^{z2} \qquad (24)$$
$$0 \leq q^{u,in} \leq q^{in} \qquad (25)$$
$$q^{u,in} \leq \bar{q}^{u,in} \qquad (26)$$

In a similar way does (27)-(28) describe the tank outflow for the MI model, while (31)-(32) describes the linear model.

$$\delta^3 = 1 \Leftrightarrow q^{out} \leq \bar{q}^{out} \qquad (27)$$
$$q^{z3} = \delta^3 q^{out} + (1 - \delta_3)\bar{q}^{out} \qquad (28)$$
$$\delta^4 = 1 \Leftrightarrow q^z(3) \leq \beta v \qquad (29)$$
$$q^{out,tank} = \delta^4 q^{z3} + (1 - \delta^4)\beta v \qquad (30)$$
$$0 \leq q^{u,out} \leq \bar{q}^{u,out} \qquad (31)$$
$$q^{u,out} \leq \beta v \qquad (32)$$

The tank dynamics and gate outflow of the two models are similar, with the QP model including the limits on the tank volume as inequality constraints.

$$v_{k+1} = v_k + \Delta T(q^{in,tank} - q^{out,tank}) \qquad (33)$$
$$q^{out} = q^{in} - q^{in,tank} \qquad (34)$$
$$0 \leq v_k \leq \bar{v} \qquad (35)$$

3) Manipulated Redirection Gates: The inflow are divided in two outflows. In the MI model, the control flow q^u is the max. flow for a given gate position. The MI model is seen in (36)-(40), with the flows written by logic terms.

$$\delta^1 = 1 \Leftrightarrow q^{in} \leq q^u \qquad (36)$$
$$\delta^2 = 1 \Leftrightarrow q^u \leq \bar{q}^u \qquad (37)$$
$$q^{z1} = \delta^1 q^{in} + (1 - \delta^1)q_u \qquad (38)$$
$$q^{out,con} = \delta^2 q^{z1} + (1 - \delta^2)\bar{q}^u \qquad (39)$$
$$q^{out,res} = q^{in} - q^{out,con} \qquad (40)$$

In the linear model, the control flow q^u is the actual flow through the gate, disallowing still standing gates when inflow

drops. As seen in (41)-(43), the logic description has been replaced with the inequalities of the physical limits.

$$q_{out} = q_{in} - q_u \qquad (41)$$
$$0 \leq q_u \leq q_{in} \qquad (42)$$
$$q_u \leq \bar{q}_u \qquad (43)$$

4) Sewage Pipes & Unmanipulated Redirection Gates: Mathematically the unmanipulated redirection gates are identical to the sewage pipes. The MI description of both is given in (44)-(46), with logic describing the outflow and overflow.

$$\delta = 1 \Leftrightarrow q^{in} \geq \bar{q}^{out} \qquad (44)$$
$$q^{out} = \delta \bar{q}^{out} + (1 - \delta)q^{in} \qquad (45)$$
$$q^w = \delta(q^{in} - \bar{q}^{out}) \qquad (46)$$

The linear model in (47)-(49), is obtained by substituting q^w out of the outflow description, and adding the physical constraints of the weir flow and the outflow.

$$q^{out} = q^{in} - q^w \qquad (47)$$
$$0 \leq q^{in} - q^w \leq \bar{q}^{out} \qquad (48)$$
$$0 \leq q^w \qquad (49)$$

REFERENCES

[1] C. Ocampo-Martinez, *Model Predictive Control of Wastewater Systems*, ser. Advances in Industrial Control. Springer, 2010.
[2] A. Bemporad and M. Morari, "Control of systems integrating logic, dynamics, and constraint," *Automatica*, vol. 35, pp. 407–427, 1999.
[3] R. Halvgaard and A. K. V. Falk, "Water system overflow modeling for model predictive control," in *Proceedings of the 12th IWA Specialised Conference on Instrumentation, Control and Automation*. IWA, 2017.
[4] M. S. Gelormino and N. L. Ricker, "Model predictive control of a combined sewer system," *INT. J. CONTROL*, vol. 59, no. 3, pp. 793–816, 1994.
[5] R. Horalek and J. Hlava, "Multiple model predictive control of grid connected solid oxide fuel cell for extending cell life time," in *23rd Mediterranean Conference on Control and Automation*, 2015, pp. 310–315.
[6] J. H. Lee, "Model predictive control: Review of the three decades of development," *International Journal of Control, Automation, and Systems*, vol. 9, no. 3, pp. 415–424, 2011.
[7] S. J. Qin and T. A. Badgwell, "A survey of industrial model predictive control technology," *Control Engineering Practice*, vol. 11, pp. 733–764, 2003.
[8] R. R. Negenborn, B. D. Schutter, and H. Hellendoorn, "Multi-agent model predictive control for transportation networks: Serial versus parallel schemes," in *IEEE Int. Conference on Networking, Sensing and Control*, 2006, pp. 296–301.
[9] M. Marinaki and M. Papageorgiou, *Optimal Real-time Control of Sewer Networks*, ser. Advances in Industrial Control. Springer, 2005.
[10] G. G. Patry, "A linear programming model for the control of combined sewer systems with off-line storage facilities," *Canadian Water Resources Journal*, vol. 8, no. 1, pp. 83–105, 1983.
[11] L. Raso, D. Schwanenberg, N. van de Giesen, and P. van Overloop, "Short-term optimal operation of water systems using ensemble forecasts," *Advances in Water Resources*, vol. 71, pp. 200–208, 2014.
[12] G. Cembrano, J. Quevedo, M. Salamero, V. Puig, J. Figueras, and J. Marti, "Optimal control of urban drainage systems. acase study," *Control Engineering Practice*, vol. 12, pp. 1–9, 2004.
[13] L. Garcia, J. Barreiro, E. Escobar, N. Q. F. Tellez, and C. Ocampo-Martinez, "Modelling and real-time control fo urban drainage systems: A review," *Advances in Waterb Resources*, vol. 85, pp. 120–132, 2015.
[14] V. P. Singh, *Hydrologic Systems. Volume 1: Rainfall-runoff modelling*. Prentice Hall, 1988.
[15] DHI, 2018, private communication.

APPENDIX B

Article B

The paper presented in this appendix was originally published in a journal.

Information of the publication:

An MPC-Enabled SWMM Implementation of the Astlingen RTC Benchmarking Network

Congcong Sun [1,*], Jan Lorenz Svensen [2], Morten Borup [3], Vicenç Puig [1], Gabriela Cembrano [1,4] and Luca Vezzaro [3]

[1]   Advanced Control Systems Group at the Institut de Robòtica i Informàtica Industrial (CSIC-UPC), Llorens i Artigas, 4-6, 08028 Barcelona, Spain; vpuig@iri.upc.edu (V.P.); gcembrano@externalpartner.com (G.C.)
[2]   Department of Applied Mathematics and Computer Science (DTU Compute), Technical University of Denmark, 2800 Kongens Lyngby, Denmark; jlsv@dtu.dk
[3]   Department of Environmental Engineering (DTU Environment), Technical University of Denmark, 2800 Kongens Lyngby, Denmark; morb@env.dtu.dk (M.B.); luve@env.dtu.dk (L.V.)
[4]   CETaqua, Water Technology Centre, 08904 Barcelona, Spain
*   Correspondence: csun@iri.upc.edu; Tel.: +34-644041855

Abstract: The advanced control of urban drainage systems (UDS) has great potential in reducing pollution to the receiving waters by optimizing the operations of UDS infrastructural elements. Existing controls vary in complexity, including local and global strategies, Real-Time Control (RTC) and Model Predictive Control (MPC). Their results are, however, site-specific, hindering a direct comparison of their performance. Therefore, the working group 'Integral Real-Time Control' of the German Water Association (DWA) developed the Astlingen benchmark network, which has been implemented in conceptual hydrological models and applied to compare RTC strategies. However, the level of detail of such implementations is insufficient for testing more complex MPC strategies. In order to provide a benchmark for MPC, this paper presents: (1) The implementation of the conceptual Astlingen system in an open-source hydrodynamic model (EPA-SWMM), and (2) the application of an MPC strategy to the developed SWMM model. The MPC strategy was tested against traditional and well-established local and global RTC approaches, demonstrating how the proposed benchmark system can be used to test and compare complex control strategies.

Keywords: Astlingen benchmark network; SWMM model; model predictive control; real-time control

1. Introduction

Real-time operations of urban drainage systems (UDS) have proven to be an efficient and cost-effective management strategy for reducing pollution to the aquatic environment without having to invest in expensive infrastructural expansions [1–6]. Applied approaches include Real-Time Control (RTC), such as rule-based control (RBC) [7,8], and Model Predictive Control (MPC) [9–11]. However, RTC and MPC performances are site-specific and also depend on the rainfall characteristics, hindering cross-validation of control algorithms across systems and research groups. There is therefore the need for a common method for comparing RTC and MPC approaches in order to support further advancements and widespread application of these technologies in both academia and practice [12]. Under this necessity, the working group 'Integral Real-Time Control' of the German Water Association (DWA) has constructed the Astlingen example network [5], which serves as a benchmark complementing the German DWA-M180 document on planning of RTC systems [6]. The purpose of a benchmarking model was to encourage as many experts (researchers, practitioners) as possible to use and compare performance of different control methodologies under the same test bed. Therefore, the Astlingen benchmark model should preferably also be implemented in a free, widely used open-source software.

Currently available implementations of the Astlingen network are based on simple hydrological models. For example, the hydrological module of the Simba# simulator has previously been used to demonstrate the base case (BC) of locally controlled throttle settings, as well as the global rule-based equal-filling-degree (EFD) approach [13]. MPC has been widely investigated for UDS optimization solutions [1,3,4,7,9–11,14–17], but it is difficult to find a contribution with clear definition of the internal MPC model, as well as the core implementation principles [11]. Therefore, the extension of the benchmark model for MPC application and testing can support the development of these techniques. Furthermore, testing MPC often requires more complex description of the hydraulic processes taking place in the network (e.g., backwater effects). Therefore, simple conceptual hydrological models might be inadequate.

This paper presents an implementation of the Astlingen case based on a hydrodynamic Storm Water Management Model (SWMM). EPA-SWMM 5.1.013 [18] is a free, open-source software that is widely used in both academia and practice, thereby making the Astlingen benchmark case available to a wider audience. The SWMM model was calibrated to emulate the results from the Simba# model implementation, which was used as reference in this paper [5,19]. The SWMM implementation was combined with an MPC strategy to provide an example of a detailed description of the methods and core principles of an MPC application for UDS control. The MPC controller was defined by two aspects: The internal model and the control design. The internal model used a simplified discrete model of the Astlingen system, while the control design defined the behavior of the system and the length of each prediction. The MPC optimization was defined by the conceptual network of Astlingen, while the effects of the generated control setpoints were simulated in the SWMM model. In order to integrate the optimization and simulation process, a closed-loop RTC scheme wrapped in PySWMM (a Python-based SWMM Software) was also provided. A one-year simulation was used to evaluate the MPC approach, which was compared against two control scenarios: Base case (BC) and EFD.

To facilitate the wide usage of the results from this article for benchmarking, teaching, research and development, all the data, models, and codes used for the examples can be freely accessed on https://github.com/open-toolbox/SWMM-Astlingen.

2. SWMM Model and Rule-based Control

2.1. The Astlingen Benchmark System

The Astlingen benchmark system [5,18] is a hypothetical case area including both combined and separated sewer systems. The schematic representation of the Astlingen network is presented in Figure 1 (adapted from [5]). Rainfall spatial heterogeneity is included using four rainfall gauges, connected to 10 subcatchments (SC). The system includes six storage tanks (where Tank 1 and 5 are not controlled) with a total storage volume of 5900 m^3. There are 10 combined sewer overflows (CSO): One for each storage basin (CSO1-6) and four at junction nodes (CSO7-10). Flow routing and transport across the network are represented by time delays (ranging from a minimal 5-minute to a maximal 20-minute). The documentation provided by the working group 'Integral Real-Time Control' of the German Water Association (DWA) also includes additional information on the network layout, overflow structures, as well as 10-year rainfall data [20]. These are provided as four rainfall series based on measurements provided by the Erftverband water utility (Germany) with a five-minute time resolution [19,20]. The average annual rainfall at these four rainfall stations amounts to 705 mm, 723 mm, 699 mm, and 711 mm, respectively, and an overview of the first year rainfall of data is shown in Figure S1(Supplementary Materials). Two receiving bodies are defined for the CSOs, which are the Main River and the smaller but more sensitive Park Creek.
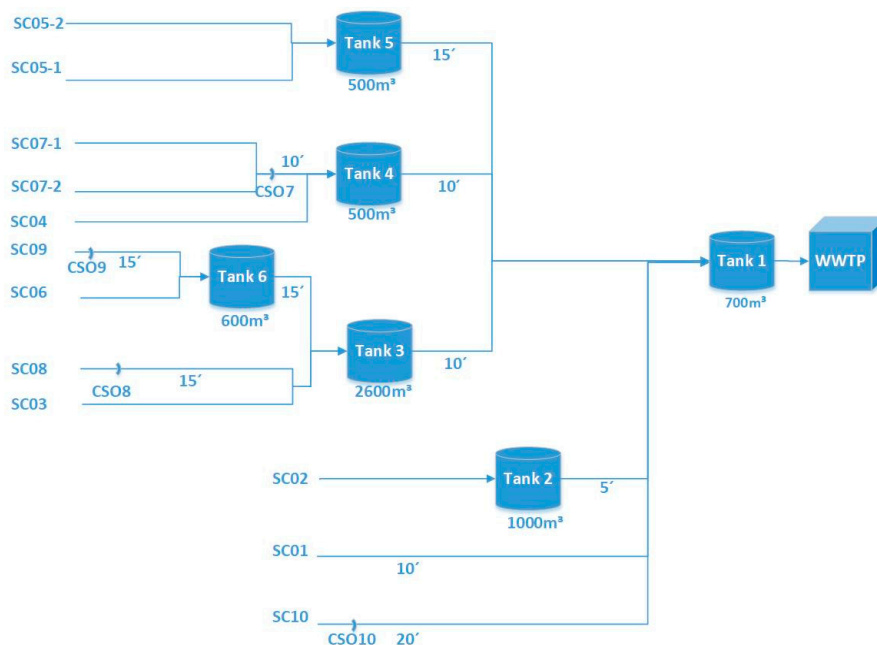
Figure 1. Scheme of Astlingen Sewer Network (adapted from [5]), showing the location of the 10 subcatchments (SC) and combined sewer overflow (CSO) structures, along with the six basins (with respective storage volumes). Transport times are long the network are expressed in minutes.

2.2. Model building

The SWMM model was built to emulate the results from the implementation in Simba# presented in [5], which was used as reference. Implementing the Astlingen benchmark network in the detailed hydrodynamic SWMM model requires a series of assumptions, since the original system has been described with a level of details suitable for a simple hydrological model. These assumptions include the definition of physical details of the system, such as system setup and geometric elements between tanks. The criteria used to build the SWMM model and to define its elements were:

- The deviation between the outputs provided by SWMM and Simba# models should be less than 10%. This comparison was based on a one-year simulation with both models.
- The number of additional elements added to the detailed model should be kept to a minimum.

The detailed SWMM model was developed by following a three-step procedure: (1) Rainfall-Runoff Calibration, to estimate the subcatchments parameters; (2) Base Case Calibration, to configure and estimate the parameters of the new elements added in the detailed models; (3) EFD Verification, to ensure that the detailed model achieve the same results as the conceptual when applied for testing control strategies.

2.2.1. Rainfall-Runoff Calibration

In the conceptual Simba# model of Astlingen, rainfall-runoff flows are calculated using Linear Reservoir Models with the parameters $n = 3$ (number of tanks) and k = 5 minutes (reservoir constant).

SWMM conceptualizes a subcatchment as a rectangular surface with uniform slope S (-) and width W (m), draining to a single outlet channel. The relative runoff flow Q [m/s] from this subcatchment was computed using the Manning equation expressed as (see [21] for further details):

$$Q = \frac{1}{Ae} W S^{1/2} d^{5/3} \tag{1}$$

where $A\ [m^2]$ is the impervious area, e (s/m$^{1/3}$) is the impervious area roughness, d (m) is the net depth excess ponds atop the subcatchment surface. Considering that A for a subcatchment is a constant defined in the conceptual model, the parameters to be estimated are W, S, and e. These were estimated by a trial and error procedure, comparing the simulated runoff from SWMM against the one from Simba#. The parameters were calibrated until a Nash–Sutcliffe Efficiency [22] above 0.65 was reached, and the parameter set which generate the best fitting was used (Table 1). An example of the simulated runoff from the 10 subcatchments is shown in Figure S2 (Supplementary Materials).

Table 1. SWMM rainfall-runoff parameters estimated for the 10 subcatchments in Astlingen.

Subcatchment	A (ha)	W (m)	S (-)	e (s/m$^{1/3}$)
SC01	33.00	2400	0.80	0.009
SC02	22.75	1500	0.80	0.009
SC03	18.00	2000	0.50	0.007
SC04	6.90	200	0.70	0.009
SC05	15.60	1000	0.50	0.007
SC06	32.55	985	0.50	0.010
SC07	4.75	360	0.51	0.020
SC08	28.00	1950	0.45	0.010
SC09	6.90	650	0.40	0.016
SC10	11.75	650	0.50	0.008

2.2.2. Base Case Calibration

The BC scenario is based on local controls which uses constant nominal throttle flow settings. Six orifices are used to control the emptying of each storage tanks, which are the only controllable elements in the Astlingen network. These directly affect the CSO volumes from the overflow structures located at basins (CSO1-6), and indirectly the volumes discharged at the junction nodes (CSO7-10). The latter are also affected by the characteristics of the upstream network (e.g., flow input and the routing abilities). Therefore, the throttle settings, as well as the physical characteristics of the nodes, orifices, and related pipes, were estimated by comparing the CSO volumes simulated by the two models. Similar to the Rainfall-Runoff Calibration, the parameters were estimated using a trial and error procedure until deviation between SWMM and Simba# output was below 10%.

2.2.3. Equal-Filling Degree Verification

The EFD approach is a simple illustrative example of a global RBC strategy, which compares the filling degree of the storage tanks in the network and sets the throttle flows emptying the tanks accordingly, aiming at establishing an equal filling degree in all the tanks [23]. EFD is among the control algorithms implemented in the conceptual Simba# model, where additional aspects of sensor and control delays, rainfall predictions, etc., are deliberately not considered. The EFD was also implemented in the SWMM implementation of Astlingen in order to verify its applicability for testing control strategies and to compare the estimated improvements in CSO volumes against those estimated by the Simba# implementation.

To implement EFD in the SWMM model, the control editor embedded in EPA-SWMM was used with the defined rules of comparing filling degrees for the Tank 2, 3, 4, and 6. If the water levels at these tanks were all lower than the threshold value of 20%, the nominal throttle flows values defined for the BC were used. Otherwise, the minimal possible flows were used to increase the storage in tanks with low filling, while the maximum possible flows were used for emptying tanks with high filling.

3. Model Predictive Control

MPC consists of receding horizon optimizations based on predictions from an internal model of the system to be controlled and a control design. The internal model is usually a simplified discrete

representation of the internal dynamics of the system to be controlled. The control design defines the desired behavior of the controlled system, the optimal behavior, and the length of each prediction.

The MPC in this contribution utilizes a simplified conceptual model of Astlingen as its internal model, with the assumption of perfect forecast, generated by precomputed simulations. The MPC sampling time was 5 min, with prediction and control horizons chosen of 100 min. The MPC was implemented in MATLAB, which communicated to the detailed SWMM model through PySWMM. In order to integrate the optimization and simulation processes, a closed-loop scheme of MPC and SWMM was used (Figure 2). At each time step, the MPC optimizer (quadratic program solver from Mosek's Matlab toolbox) generated optimal control actions and sent them as setpoints to the simulator, which fine-tuned them, computed the effects of these control actions, and updated state measurements, which were used to initialize a new optimization in the following time step. A similar scheme can be used for other RTC approaches.
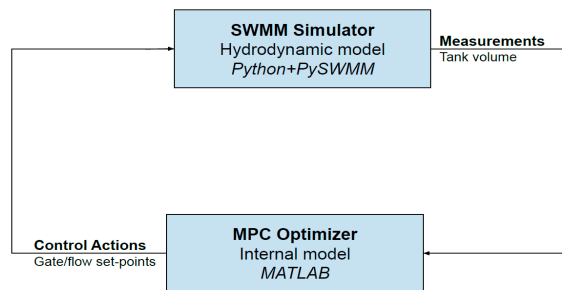
Figure 2. The closed-loop Real-Time Control (RTC) scheme.

3.1. Internal model

The internal MPC model includes the elements of the Astlingen system described in Figure 1, and it was built by utilizing a modular approach of well-defined sewer structures. These modules included a linear reservoir tank with a passive outflow, linear reservoir tank with a controlled outflow, and pipe with delays. The approach used for modelling weir overflow in this paper was an approximation approach through a penalty [24]. The CSOs were treated as optimization variables with a heavy cost for minimizing their use.

3.1.1. Linear Reservoir Tank—Passive outflow

The module describing the linear reservoirs or tanks at the *k-th* time step was based on water volume-balance:

$$V_{k+1} = (1 - \Delta T \beta)V_k + \Delta T\left(q_k^{in} - q_k^w\right) \tag{2}$$

$$q_k^{out} = \beta V_k \tag{3}$$

In the case of a tank with a passive outflow, the tank volume vector is defined by the current volume $V_k \in \mathbb{R}^{n_p}$ (m^3), the total inflow $q_k^{in} \in \mathbb{R}^{n_f}$ to the tank (m^3/s), and the weir overflow of the tank $q_k^w \in \mathbb{R}^{n_p}$ (m^3/s), where ΔT is the sampling time (s), n_p, n_f are the numbers of the tanks and pipes (-), respectively. This relation is given by the process in Equation (2). The tank outflow in Equation (3) is a linear approximation, defined by the volume-flow coefficient $\beta = \frac{\overline{q}^{out}}{\overline{V}}$ [25].

$$0 \leq (1 - \Delta T \beta)V_k + \Delta T\left(q_k^{in} - q_k^w\right) \leq \overline{V} \tag{4}$$

$$0 \leq q_k^w \tag{5}$$

The module was further defined by the constraints on the volume and the overflow given in Equations (4) and (5), where the vector $\overline{V}$ represents maximal storage capacities of the tanks. This module was used to describe Tank 1 and 5, whose emptying orifices were passive and uncontrollable.

3.1.2. Linear Reservoir Tank—Controlled outflow

The module for the linear reservoirs with a controlled outflow was formulated in a similar manner to the passive outflow variant.

$$V_{k+1} = V_k + \Delta T\left(q_k^{in} - q_k^u - q_k^w\right) \tag{6}$$

$$q_k^{out} = q_k^u \tag{7}$$

The difference in the formulations is that the volume now also depends on the control flow q_k^u, and the outflow is the control flow as seen in Equations (6) and (7).

$$0 \le V_k + \Delta T\left(q_k^{in} - q_k^u - q_k^w\right) \le \overline{V} \tag{8}$$

$$0 \le q_k^u \le \beta V_k \tag{9}$$

$$q_k^u \le \overline{q}^u \tag{10}$$

$$0 \le q_k^w \tag{11}$$

The constraints of this module cover the limits to the tank volume, as well as the limits to the control flow, as seen in Equations (8)–(11). The controlled outflow in the Astlingen model were all orifice-based, and were therefore dependent on the volume of the tank. For the module, this resulted in two upper constraints for the control flow, one being the linear volume-flow relation discussed previously and the second being the physical limit of the outflow pipe.

3.1.3. Pipe with Delays

The interconnection between the tanks in the Astlingen model consist of pipes. Depending on the length of the pipes, the time it takes to flow from one tank to arrive in another tank might exceed the sampling time of the model ΔT. For these pipes, we introduced a delay module corresponding to one sampling time ΔT.

$$\eta_{k+1,i} = q_{k,i}^{in} \tag{12}$$

$$q_{k,i}^{out} = \eta_{k,i} \tag{13}$$

The outflow of the module is then equal to the delay flow η, as seen in Equations (12) and (13), and the delay between tanks can be constructed as a cascade of delay modules, e.g., a 15-min delay would correspond to three delay states in succession.

Based on the different modules, it was possible to generate the entire model by connecting the right inflows and outflows together from each module. The inflow to each subpart can be seen in Table 2, where the *i-th* runoff inflow is noted by $w_{k,i}$, and the *i-th* tank is noted by T_i. The delay flow to the *i-th* tank is given as $\eta_{i:j}$, where j is the total remaining delay in minutes to the tank. The outflow of subpart z is written as $q_{k,z}^{out}$.

Table 2. Inflows to the different elements of the systems.

Subpart	Inflow
T_1	$q_{k,\eta_{1:5}}^{out}$
T_2	$w_{k,2}$
T_3	$w_{k,3} + q_{k,\eta_{3:5}}^{out}$
T_4	$w_{k,4}$
T_5	$w_{k,5}$
T_6	$w_{k,6}$
$\eta_{1:5}$	$q_{k,T_2}^{u} + q_{k,\eta_{1:10}}^{out}$
$\eta_{1:10}$	$w_{k,1} + q_{k,T_3}^{u} + q_{k,T_4}^{u} + q_{k,\eta_{1:15}}^{out}$
$\eta_{1:15}$	q_{k,T_5}^{out}
$\eta_{3:5}$	$q_{k,\eta_{3:10}}^{out}$
$\eta_{3:10}$	$q_{k,\eta_{3:15}}^{out}$
$\eta_{3:15}$	q_{k,T_6}^{u}

3.2. Control Design

The design of the MPC [26] utilized in this work was based on the model discussed above. The operational objectives for the system utilized in the MPC design in this work were:

- Maximizing flow to the WWTP (q_{k,T_1}^{out});
- Minimizing CSO flow to the river/creek;
- Minimizing roughness of control.

The first objective can be achieved by a linear negative cost on the outflow of Tank 1, while the second objective can be formulated as a linear positive cost on the total overflow of the system. These objectives are collectively written as vector z_k. The third objective of control roughness aims for smooth control and can be written as a quadratic cost on the change in control flow. Due to the overflow being modelled by an approximation approach, a fourth objective of minimizing the accumulated overflow volume V_k^w was needed.

$$J = \min_{q^u, q^w} \sum_{k=0}^{Hp} \|\Delta q_k^u\|_R^2 + Q^T z_k + W^T V_k^w \tag{14}$$

$$z = \Phi_{Con} q^u + \Psi V_0 + \Theta w + \Gamma q^w \tag{15}$$

$$V_k^w = \sum_{i=0}^{k} \Delta T q_i^w \tag{16}$$

$$\Omega_{Con} q^u + \Omega_{vol} V_0 + \Omega_{rain} w + \Omega_{weir} q^w \leq \Omega \tag{17}$$

By utilizing the internal model over the prediction horizon Hp, the cost function of the MPC can be written as in Equation (14), where $\|X\|_R^2$ is the weighted quadratic norm $X^T R X$, while the predicted objectives z and overflow volumes, given by Equations (15) and (16), were derived from the internal model and propagation through the predicted volumes and delays. The constraints of the internal model can similarly be collected into a single matrix inequality given by Equation (17). The matrices Ψ, Φ, Θ, and Γ define the influence of the initial volume, the predicted control q^u, inflow w, and CSO q^w on the objectives, respectively. The weighting of the different objectives in the cost function was done in accordance with the approximation approach [27]. The fourth objective (minimizing accumulated CSO volume) has to have a high cost relative to all other objectives, and upstream CSOs (discharging to the more sensitive creek) have higher cost than downstream. The priority of the different objectives was given in the following order from highest to lowest priority:

1.　Minimization of accumulated CSO volume (16);
2.　Minimization of CSO to the river/creek;
3.　Maximizing flow to the WWTP;
4.　Minimizing roughness of control.

The weighs for the accumulated overflow volume from each tank are given in Table 3, while the weights of the remaining objectives are:

- 2 for the flow to the river/creek
- −1 for the flow to the WWTP
- 0.01 for the roughness of the control.

Table 3. Cost function weighting of accumulated overflow volum W, showing a higher cost for upstream tank modules discharging to the sensitive creek.

Tank 1	Tank 2	Tank 3	Tank 4	Tank 5	Tank 6
1000	5000	5000	5000	5000	10,000

These weights indicate that the avoidance of the flow to the river and creek is prioritized twice as high as increasing flow to the WWTP. The weight on the roughness indicates the desire for the control to be smooth, but not a general priority. As seen from Table 3, the priority of the accumulated overflow can be inferred to be significantly higher than the other objectives, given the weights and the overflow volume/flow relation given by Equation (16).

4. Results

4.1. Detailed Model of Astlingen

4.1.1. SWMM Implementation

The implementation of the Astlingen benchmark network in the detailed hydrodynamic SWMM model is shown in Figure 3. The SWMM model and the reformatted rainfall series, as well as the defined EFD control rules, can be downloaded through https://github.com/open-toolbox/SWMM-Astlingen and applied directly through EPA-SWMM with different RTC approaches configured by interested practitioners.
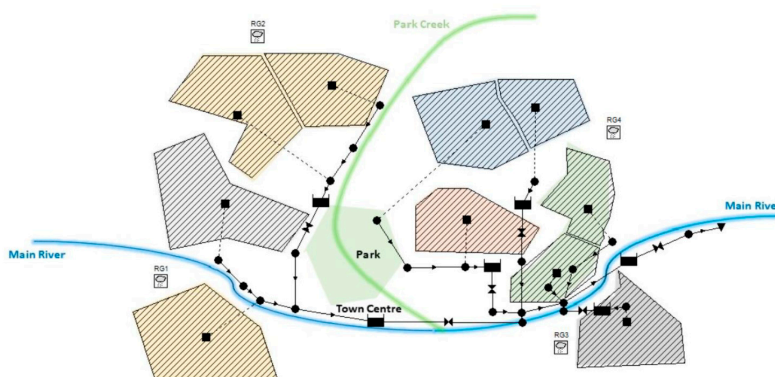
Figure 3. Layout of the detailed SWMM model of Astlingen benchmark network.

4.1.2. Base Case Scenario

As described in the Section 2.2.2, the BC scenario was used to compare the results from the detailed SWMM model against the reference conceptual model in Simba#. Table 4 compares the throttle flows and CSO volumes from the two models for a one-year simulation. These results show that the deviations between the models were less than 4.5%, i.e., below the 10% criteria defined in calibration. This shows how the proposed SWMM model satisfactory emulated the reference Simba# implementation, i.e., results from the detail models can directly be compared against those provide by the authors of [5].

Table 4. Simulated throttle flow (reported as maximum values) and CSO volumes for BC scenario.

	Throttle Flow (L/s)		CSO Volume(m^3)	
	SWMM	**Simba#**	**SWMM**	**Simba#**
Tank1/CSO1	271	271	79,459	77,339
Tank2/CSO2	33	32	32,875	31,605
Tank3/CSO3	124	124	27,600	26,029
Tank4/CSO4	28	28	11,157	10,058
Tank5/CSO5	39	39	15,460	14,053
Tank6/CSO6	75	76	69,593	66,095
CSO7	85	86	3972	3920
CSO8	487	485	15,902	15,862
CSO9	127	129	3972	3951
CSO10	202	203	4741	4711
TOTAL			264,731	253,623
Max Deviation	<4.5%		<4.5%	

4.1.3. Equal-Filling Degree Control

The improvements in terms of CSO volumes obtained after the application of the EFD rule-based control were compared against the results obtained in the BC scenario. Table 5 presents the results of the two scenarios for both the detailed and the conceptual Astlingen models. The reduction in CSO volume for the EFD scenario simulated by the SWMM model was 6.4%, compared to the 8.3% reduction estimated using the reference Simba# model. Considering the differences in the model structures and level of details of the two models, the estimated CSO reduction can be considered as similar, i.e., the SWMM model can be considered as equivalent to the reference Simba# model for evaluating the performance of control strategies.

Table 5. Simulated CSO volumes (m^3) for different control scenarios (EFD and BC) obtained by the detailed (SWMM) and conceptual (Simba#) models.

|	Detailed (SWMM)		Conceptual (Simba#)	
	EFD	**BC**	**EFD**	**BC**
Tank1/CSO1	99,721	79,459	71,302	77,339
Tank2/CSO2	24,882	32,875	26,371	31,605
Tank3/CSO3	26,229	27,600	34,743	26,029
Tank4/CSO4	9356	11,157	8886	10,058
Tank5/CSO5	15,460	15,460	14,053	14,053
Tank6/CSO6	43,552	69,593	49,557	66,095
CSO7	3972	3972	3920	3920
CSO8	15,903	15,902	15,862	15,862
CSO9	3972	3972	3951	3951
CSO10	4751	4741	4711	4711
TOTAL	**247,788**	**264,731**	**232,320**	**253,623**
CSO Reduced by EFD	**6.4%**		**8.3%**	

4.2. Model Predictive Control

4.2.1. CSO Volume

The simulated CSO volumes resulting from the application of MPC to the SWMM implementation of Astlingen are shown in Table 6, along with the percentage volume reduction compared to volumes for the BC and EFD scenarios. Compared to the BC and EFD scenarios, the MPC discharged significant less CSO volumes to the river and creek for most of the storage tanks (up to over 50% reduction for single discharge points). Considering that the MPC scenario led to an increase of discharges from some CSO structures, the overall improvement was around 7% and 13% against EFD and BC, respectively. It can be seen that the discharges from the passive parts of the system (CSO7-10, Tank1 and 5) increased with around 1%–2% as a result of control choices and due to backwater flows. The MPC successfully managed to achieve a major CSO reduction for the most sensitive part of the system (creek). These results are further illustrated by Figure 4, where the CSO volumes are subdivided according to the receiving water body.

Table 6. Simulated CSO volumes (m^3) for the Model Predictive Control (MPC) scenario, and percentage difference from the BC and Equal-Filling Degree Verification (EFD) scenarios. Positive variations denote reductions in CSO volume, while negative values denote increases in discharges.

Tank & CSO	MPC (m^3)	EFD (%)	BC (%)
Tank 1	93251	6.49	−17.36
Tank 2	15484	37.77	52.90
Tank 3	34017	−29.69	−23.25
Tank 4	4814	48.55	56.85
Tank 5	15147	2.02	2.02
Tank 6	37950	12.86	45.47
CSO 7	4016	−1.11	−1.11
CSO 8	16207	−1.91	−1.92
CSO 9	4030	−1.46	−1.46
CSO 10	4838	−1.83	−2.05
River	183754	6.39	1.84
Creek	45996	10.68	40.68
Total	229750	7.28%	13.21%
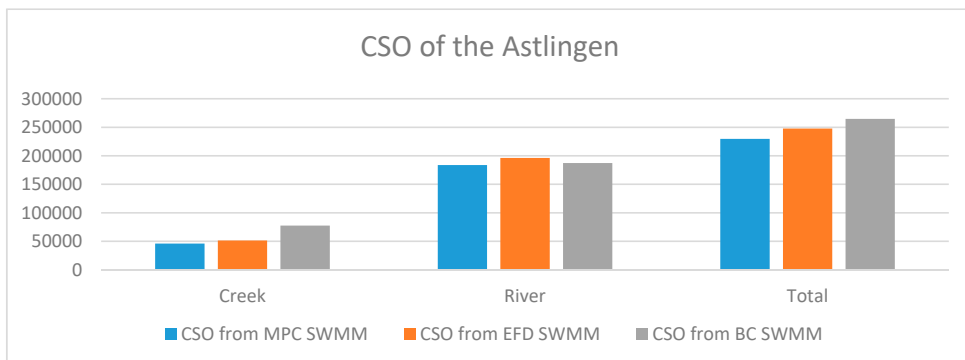
Figure 4. Comparison of CSO volumes for the MPC, EFD, and BC scenarios subdivided by the receiving water body.

4.2.2. CSO Events

The simulated number of CSO events and days with recorded CSOs for the MPC scenario are shown in Table 7, together with results from the BC and EFD scenarios. Since some CSO events took place over midnight, there was a discrepancy between these two values. Overall, the MPC and EFD scenarios produced less CSO events, but more days with CSOs than in the BC scenario. This suggests that both the control strategies stored water in the system more efficiently, and that they caused longer (but smaller) CSO events. Also, coupled rain events can be lumped into a single event due to the increased storage and longer emptying of the tanks. Indeed, CSO events were defined based on the physical characteristics of the system, i.e., a six-hour threshold was used to distinguish them. Considering that the total storage volume in the system was 5900 m^3 and that the system can be emptied with a maximal rate of 0.271 m^3/s [5], it took roughly six hours to empty the system in the BC scenario. This emptying time was clearly increased by the control algorithms in the EFD and MPC scenarios.

Table 7. Simulated CSO events for the MPC, EFD, and BC scenarios.

CSO Events	MPC	EFD	BC
Number	58	58	61
Days	70	65	62

5. Conclusions

This paper presents a hydrodynamic model of the Astlingen benchmark network in the open-source software SWMM, enabling a more widespread usage of Astlingen for benchmarking complex control strategies. The development of this detailed model provides a unified test-bed, which allows the interested researchers and engineers to use and compare performance of different control methodologies. This will also solve practical difficulties confronted by researchers or interested engineers to share models and data of real-life urban drainage systems for RTC implementations.

The detailed hydrodynamic model was developed to emulate the reference the conceptual model using a three-step procedure and two model development criteria. The performance of the SWMM model was evaluated against the reference model by comparing a local throttle control (Base Case) and a global RTC approach (EFD rule-based strategy). The developed model and data are freely available on a public repository and they can be downloaded and applied directly through EPA-SWMM with different RTC approaches configured by interested practitioners.

The potential of the detailed SWMM model of the Astlingen benchmark network for testing complex control algorithms was demonstrated by applying an MPC strategy. This was described with clear internal model and core principle definitions. The MPC utilizes the conceptual model of Astlingen to generate optimal control actions, while the detailed SWMM model was used for the fine-tuning of the control setpoints. In order to integrate the optimization and simulation processes, a closed-loop scheme of MPC and SWMM was used. This configuration can be used in other cases other than Astlingen, and with any other complex control algorithm (RTC and MPC).

The flexibility of the proposed implementation of the Astlingen benchmark model was shown for different control strategies, with different level of complexity, ranging from simple local controls (BC), global RTC (EFD), and complex MPC strategies. Researchers and practitioners therefore now have a new useful case for testing and comparing different control strategies.

inspiring discussions and comments. G.C. and V.P. supervised the MPC applications with revising the MPC results. L.V. is the one who proposed this topic, defined the problem, and contributed with regular supervisions and efficient coordination. All the co-authors contributed in the manuscript review. All authors have read and agreed to the published version of the manuscript.

References

1. Schütze, M.; Campisano, A.; Colas, H.; Schilling, W.; Vanrolleghem, P. Real time control of urban wastewater systems—Where do we stand today? *J. Hydrol.* **2004**, *299*, 335–348. [CrossRef]
2. García, L.; Barreiro-Gomez, J.; Escobar, E.; Téllez, D.; Quijano, N.; Ocampo-Martinez, C. Modeling and real-time control of urban drainage systems: A review. *Adv. Water Resour.* **2015**, *85*, 120–132. [CrossRef]
3. Sun, C.C.; Cembrano, G.; Puig, V.; Meseguer, J. Cyber-physical systems for real-time management in the urban water cycle. In Proceedings of the 4th International Workshop on Cyber-Physical Systems for Smart Water Networks, Porto, Portugal, 10–13 April 2018; pp. 5–8.
4. Cembrano, G.; Quevedo, J.; Salamero, M.; Puig, V.; Figueras, J.; Martí, J. Optimal control of urban drainage systems. A case study. *J. Contr. Engin. Pract.* **2004**, *12*, 1–9. [CrossRef]
5. Schütze, M.; Lange, M.; Pabst, M.; Haas, U. Astlingen—A benchmark for real time control (RTC). *Water Sci. Technol.* **2017**, *2*, 552–560. [CrossRef] [PubMed]
6. DWA 2005 Framework for Planning of Real Time Control of Sewer Networks. Guideline DWA-M 180E, German Association for Water, Wastewater and Waste, DWA, December 2005. Available online: https://webshop.dwa.de/de/guideline-dwa-m-180-december-2005.html (accessed on 1 October 2019).
7. Meneses, E.J.; Gaussens, M.; Jakobsen, C.; Mikkelsen, P.S.; Grum, M.; Vezzaro, L. Coordinating rule-based and system-wide model predictive control strategies to reduce storage expansion of combined urban drainage systems: The case study of Lundtofte, Denmark. *Water* **2018**, *20*, 76. [CrossRef]
8. Klepiszewski, K.; Schmitt, T. Comparison of conventional rule based flow control with control processes based on fuzzy logic in a combined sewer system. *Water Sci. Technol.* **2002**, *46*, 77–84. [CrossRef] [PubMed]
9. Sun, C.C.; Joseph, B.; Maruejouls, T.; Cembrano, G.; Muñoz, E.; Meseguer, J.; Montserrat, A.; Sampe, S.; Puig, V.; Litrico, X. Efficient integrated model predictive control of urban drainage systems using simplified conceptual quality models. In Proceedings of the 14th IWA/IAHR International Conference on Urban Drainage, Prague, Czech Republic, 10–15 September 2017; pp. 1848–1855.
10. Sun, C.C.; Joseph, B.; Cembrano, G.; Puig, V.; Meseguer, J. Advanced integrated real-time control of combined urban drainage systems using MPC: Badalona case study. In Proceedings of the 13th International Conference on Hydroinformatics, Palermo, Italy, 1–5 July 2018; pp. 2033–2041.
11. Lund, N.S.V.; Falk, A.K.V.; Borup, M.; Madsen, H.; Mikkelsen, P.S. Model predictive control of urban drainage systems: A review and perspective towards smart real-time water management. *Crit. Rev. Environ. Sci. Technol.* **2018**, *48*, 279–339. [CrossRef]
12. Borsanyi, P.; Benedetti, L.; Dirckx, G.; De Keyser, W.; Muschalla, D.; Solvi, A.M.; Vandenberghe, V.; Weyand, M.; Vanrolleghem, P.A. Modelling real-time control options on virtual sewer systems. *J. Environ. Eng. Sci.* **2008**, *7*, 395–410. [CrossRef]
13. 10ifak 2018: Simba# 3.0—Manual, ifak Institute for Automation and Communication, Magdeburg, 39106, Germany, 2018. Available online: https://nextcloud.ifak.eu/s/simba3?path=%2FFlyer#pdfviewer (accessed on 1 October 2019).
14. Sun, C.C.; Joseph, B.; Maruejouls, T.; Cembrano, G.; Meseguer, J.; Puig, V.; Litrico, X. Real-time control-oriented quality modelling in combined urban drainage networks. In Proceedings of the 20th IFAC World Congress, Toulouse, France, 9–14 July 2017; pp. 3941–3946.

15. Sun, C.C.; Joseph, B.; Maruejouls, T.; Cembrano, G.; Muñoz, E.; Meseguer, J.; Montserrat, A.; Sampe, S.; Puig, V.; Litrico, X. Conceptual quality modelling and integrated control of combined urban drainage system. In Proceedings of the 12th IWA Conference on Instrumentation, Control and Automation, Quebec City, Canada, 11–16 June 2017; pp. 141–148.

16. Fu, G.; Khu, S.; Butler, D. Optimal distribution and control of storage tank to mitigate the impact of new developments on receiving water quality. *J. Environ. Engine.* **2010**, *136*, 335–342. [CrossRef]

17. Sun, C.C.; Puig, V.; Cembrano, G. Real-Time Control of Urban Water Cycle under Cyber-Physical Systems Framework. *Water* **2020**, *12*, 406. [CrossRef]

18. Rossman, L. *Storm Water Management Model Users' Manual Version 5.1*; Environmental Protection Agency: Washington, DC, USA, 2015.

19. DWA 2018 Abflusssteuerung in Kanalnetzen—Anwendungsbeispiel. DWA-Themenband T1/2018, German Association for Water, Wastewater and Waste, DWA, November 2018. Available online: https://www.ifak.eu/de/bibcite/reference/5042 (accessed on 1 October 2019).

20. Müller, T.; Schütze, M.; Bárdossy, A. Temporal asymmetry in precipitation time series and its influence on flow simulations in combined sewer systems. *Adv. Water Resour.* **2017**, *107*, 56–64. [CrossRef]

21. Rossman, L.A.; Huber, W.C. Storm Water Management Model Reference Manual Volume 1—Hydrology, EPA, www2.epa.gov/water-research, January 2016. Available online: https://cfpub.epa.gov/si/si_public_record_report.cfm?Lab=NRMRL&dirEntryId=309346 (accessed on 1 October 2019).

22. Nash, J.E.; Sutcliffe, J.V. River flow forecasting through conceptual models part I-A discussion of principles. *J. Hydrol.* **1970**, *10*, 282–290. [CrossRef]

23. Halvgaard, R.; Falk, A.K.V. Water system overflow modelling for model predictive control. In Proceedings of the 12th IWA Specialized Conference on Instrumentation, Control and Automation, Quebec City, Canada, 11–16 June 2017; pp. 1–4.

24. Dirckx, G.; Van Assel, J.; Weemaes, M. Real Time Control from Desk Study to Full Implementation. In Proceedings of the 13th International Conference on Urban Drainage, Kuching, Malaysia, 7–12 September 2014.

25. Singh, V.P. *Hydrologic Systems. Volume 1: Rainfall-Runoff Modelling*; Prentice Hall: Bergen, NJ, USA, 1988.

26. Maciejowski, J.M. *Predictive Control: With Constraints*; Prentice Hall: Bergen, NJ, USA, 2002.

27. Svensen, J.L.; Niemann, H.H.; Poulsen, N.K. Model Predictive Control of overflow in sewer networks. In Proceedings of the 4th International Conference on Control and Fault-tolerant Systems, Casablanca, Morocco, 18–20 September 2019.

Appendix C

Article C

The paper presented in this appendix is a non-published article. It was intended for the water-orientated Conference Novatech 2022.

Information of the publication:

- Title: Stochastic Model Predictive Control and Sewer Networks

- Unpublished

- Date: January, 2020

Stochastic Model Predictive Control and Sewer Networks

Jan Lorenz Svensen[1], Hans Henrik Nieman[2], Anne Katrine Vinther Falk[3] and Niels Kjølstad Poulsen[4]

Abstract— **In this work, an evaluation of Chance-Constrained Model Predictive Control (CC-MPC) in sewer systems over the use of the classical deterministic Model Predictive Control (MPC) is presented. The focus of this evaluation is on the avoidance of weir overflow when uncertainty is present. Furthermore, the design formulation of CC-MPC is presented with a comparison to the design of MPC. For the evaluation, a simplified model of the Barcelona sewer network case study is utilized. Our comparison shows that for sewer systems with uncertain inflows, a CC-MPC allows for better statistical guarantees for avoiding weir overflow, than relying on a deterministic MPC. A simple back-up strategy in case of infeasible optimization program was also apparent for the CC-MPC based on the results of the analysis.**

I. INTRODUCTION

For the last few decades, the usage of Model Predictive Control (MPC) in sewer systems has been researched[1]-[6]. While the previous research has primarily focused on deterministic scenarios, known systems and inflows, we will in this work focus on the uncertainty there in reality does exist in sewer systems and how it can be handled. Some of the uncertainties there exist with regard to controlling and observing sewer systems includes model and inflow deviations from the expected. The uncertainty of the inflow is especially important for the MPC, given its reliance on the predicted forecast of the inflow. Therefore the type of uncertainty considered in this work will be limited to the uncertainty of the inflow.

While the deterministic MPC previously considered in research, is not directly designed to handle uncertainties in the optimization, stochastic formulations of MPC do exist[7]-[11]. These stochastic MPCs are designed to handle uncertainties to some degree, and by different approaches depending on the type of stochastic MPC chosen. These approaches have wide ranges; some approaches might consider a statistic-based robust method through finite realizations of the uncertainties[10], while others might consider expectation or probabilistic constraints to handle the uncertainties[11], some with additive uncertanties[8] others

[1]Jan Lorenz Svensen is with the Department of Applied Mathematics and Computer Science, Technical University of Denmark, 2800 Kgs. Lyngby, Denmark jlsv@dtu.dk
[2]Hans Henrik Niemann with the Department of Electrical Engineering, Technical University of Denmark, 2800 Kgs. Lyngby, Denmark hhn@elektro.dtu.dk
[3]Anne Katrine Vinther Falk with the DHI Denmark, 2970 Hørsholm, Denmark akf@dhigroup.com
[4]Niels Kjølstad Poulsen is with the Department of Applied Mathematics and Computer Science, Technical University of Denmark, 2800 Kgs. Lyngby, Denmark nkpo@dtu.dk
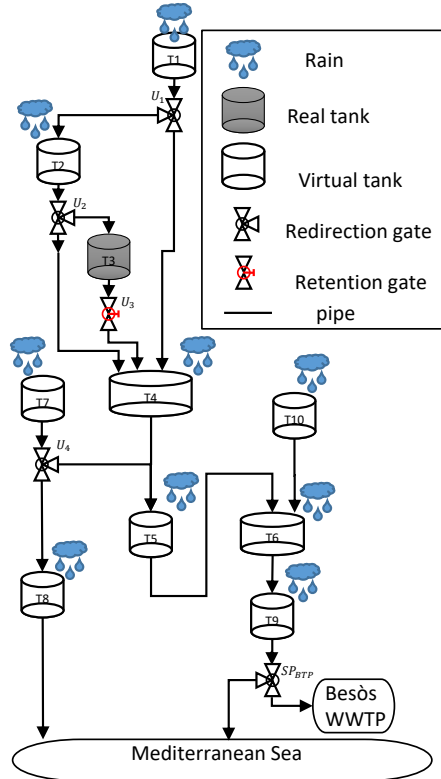
Fig. 1. A schematic of the simplified model inspired by the Barcelona Sewage System model presented by Ocampo-Martinez [2], showing the interconnections between the different tanks and the environment. The controlled parts of the system are tagged with a U

with multiplicative uncertanties[9]. In this work, we investigate a probabilistic method known as Chance-Constrained MPC (CC-MPC), previously applied to drinking water networks[8].

For an evaluation and comparison of both the deterministic and the stochastic MPCs' performance, the results of simulations are utilized. The evaluation will primarily focus on their performance in avoiding weir overflows from occurring. In the evaluations, a model inspired by the Barcelona Case study[2] is utilized. The model, seen in Fig. 1, is a simplified version of its inspiration formulated as a linear model.

In this paper, the following notations are employed. Bold font is used to write vectors, while the quadratic norm of $\mathbf{x}$ is written as $||\mathbf{x}||_A^2 = \mathbf{x}^T A \mathbf{x}$, while a generic set of function varibales are indicated by the bullet •. The functions $E(x)$, $Pr(X \leq x)$ and $\Phi_F(x)$ indicate the expectation of x, the probability of X less than x, and the cumulative density function(CDF) of a given distribution F respectively. The notation $X \sim F$ indicates that X is following a given distribution F, While distributions written as F_a^b indicate bounds on the distribution, a for the lower and b for the upper bound. Distributions written without parameters are standardized distributions, e.q. normal distribution with zero mean and unit variance. The variables written as μ_x and σ_x^2 are the mean and variance of a variable x. The min. and max. of a function $f(x)$ is denoted by $\underline{f}$ and $\bar{f}$ respectively. The superscripts indicate the nature of the parameter with the following meanings: u means a controlled variable, w means it relates to a weir, ref means it is a reference, and in and out denotes inflow and outflow respectively. The subscript k indicates the sample time, while the sampling time of the system is written as ΔT. A variable noted by a V or q is representing a volume or a flow respectively.

II. MODELS

Two models are utilized for the evaluation, one for the simulation and one for the control design. The models are based on the Barcelona sewage system model[2] but reduced such that the system only contains ten tanks, and only has weirs in the virtual tank elements. Given that the aim for the controllers is to avoid weir overflows, the weirs are not included in the model for the MPC. The simplified models can be described as a combination of a few components, assembled as in Fig. 1. The main component is the virtual tank, given by (1) and (2). For the simulation model, the weir overflow is given by (3), while it is zero in the control model. The control model also includes boundaries on the tank volume given in (4)

$$V_{k+1} = V_k + \Delta T(q_k^{in} - q_k^{out} - q_k^w) \tag{1}$$
$$q_k^{out} = \beta(V_k - \Delta T q_k^w) \tag{2}$$
$$q_k^w = \max\left(0, \frac{V_k - \bar{V}}{\Delta T}\right) \tag{3}$$
$$0 \leq V_k \leq \bar{V} \tag{4}$$

Where β is the volume/flow cofficient[12] of the tank outflow. The system also contains a real tank, where the difference from the virtual tank is that the weir overflow q_k^w is zero for both models. Another difference is that the outflow q^{out} is controlled by a retention gate $q^{u,out}$. In the control model, the controlled outflow is constrained by:

$$0 \leq q^{u,out} \leq \bar{q}^{u,out} \tag{5}$$
$$q^{u,out} \leq \beta V_k \tag{6}$$

The last component is the redirection gate, which is given by (7). The control flow q^u of the redirection gate reduces the outflow and is constrained in the control model by (8)-(9).

$$q_k^{out} = q_k^{in} - q_k^u \tag{7}$$
$$0 \leq q_k^u \leq q_k^{in} \tag{8}$$
$$q_k^u \leq \bar{q}^u \tag{9}$$

III. MPC DESIGN

The classical MPC is a deterministic controller and is designed based on the assumption of the ideal scenario; where we would have perfect knowledge about the rain inflow to the sewer systems. In MPC, an optimization program is solved at each time instance k in conjuction with the prediction horizon receeding. The formulation of the optimization program consists of two parts; a cost function and a constraint set, which together form the program. In this paper, we will formulate the program of the MPC as a quadratic program of the minimization variant. A quadratic program means the terms of the cost function can only be quadratic or linear, and that the constraints are all linear. The cost function utilized in this work is given by (10) and aims at minimizing the cost terms.

$$J = \min_u \sum_{k=0}^N ||(\mathbf{z}_k - \mathbf{z}_k^{ref})||_Q^2 + ||\Delta \mathbf{q}_k^u||_R^2 \tag{10}$$

The terms of the cost functions consist of a penalty on the change of controlled flow $\Delta\mathbf{q}_k^u$ for each time step k, similarly, it contains a penalty for deviations of the output $\mathbf{z}_k$ from the desired output reference $\mathbf{z}_k^{ref}$. The output vector z_k consists of two elements, corresponding to the objectives given below:

- maximize flow to the Besós Wastewater Treatment Plant
- minimize the aggregated flow to the Mediterranean Sea

The priority of the different terms in the cost function was mostly put on the flow to the sea followed by the flow to the treatment plant, with least priority given to the change in control flow. The weight matrices Q and R were on this basis chosen to be diagonal matrices, with the Q matrix having the weights of each objective being 0.5 and 1.0 respectively, while the R matrix was chosen to 0.01 uniformly in the diagonal.

The constraint set of the MPC is obtained by combining each component of the control model according to Fig. 1, resulting in a constraint set on the form given below for each time step k.

$$\mathbf{V}_{k+1} = A\mathbf{V}_k + B\mathbf{q}_k^u + G\mathbf{q}_k^{rain} \tag{11}$$
$$\mathbf{z}_k = C\mathbf{V}_k + D\mathbf{q}_k^u + F\mathbf{q}_k^{rain} \tag{12}$$
$$\Delta\mathbf{q}_k^u = \mathbf{q}_k^u - \mathbf{q}_{k-1}^u \tag{13}$$
$$M\mathbf{q}_k^u + P\mathbf{V}_k + S\mathbf{q}_k^{rain} \leq \mathbf{K} \tag{14}$$

Which consists of the three linear equality constraints in (11)-(13) represents the tank volume process equation, the output equation, and the change of control flow definition respectively. The inequality constraint in (14) describes the boundaries of the specific variables and combinations of them. The variable $\mathbf{q}_k^{rain}$ is the external inflows into the sewer system, such as rain and dry weather flows.

A. Stochastic MPC - Chance Constrained MPC

In stochastic MPC, the system is not assumed to be deterministic as before. Instead are knowledge about the uncertainty of the inflow taken into account during the optimization. The usage of the knowledge of uncertainty requires that the MPC formulation is changed to accommodate the information. While there exist many different approaches to stochastic MPC, we will focus only on the Chance-Constrained (CC) method here. The CC-MPC method was chosen for the statistical guarantees it provides, as well as its simplicity and similarity to MPC under specific assumptions on the uncertainties. In CC-MPC and other stochastic MPCs, one change from MPC is the cost function. Before we minimized the actual cost of the system, but with the introduction of uncertainty, we will instead gain the optimum, by minimizing the expected cost of the system as seen in (15). This allows for the cost function to be formulated by the same terms as we utilized in the MPC earlier.

$$J = \min_u E\left\{ \sum_{k=0}^{N} ||(\mathbf{z}_k - \mathbf{z}_k^{ref})||_Q^2 + ||\Delta \mathbf{q}_k^u||_R^2 \right\} \quad (15)$$

By reformulation of the cost function into sums of expectations, the only non-constant quadratic term present is the left-hand side of (16). While the right-hand side rewrites it to a quadratic term and a trace term of the variance of the output.

$$E(\mathbf{z}_k^T Q \mathbf{z}_k) = E(\mathbf{z}_k)^T Q E(\mathbf{z}_k) + tr(Q \sigma_{\mathbf{z}_k}^2) \quad (16)$$

In addition to the reformulation of the cost function, the constraint set also needs to be reformulated. For CC-MPC, this is done in different ways for equality constraints and inequality constraints. The equality constraints are handled by taking the expectation of the constraints, similar to the cost function.

For the inequality constraints, a different approach is utilized. Here the deterministic constraints are handled on single constraints basis. Each constraint is rewritten as a probabilistic constraint as seen in (17), which is a constraint on the probability of the deterministic constraint being true. The probability guaranty γ ensures that the deterministic constraint is fulfilled for any rain inflow realization within the most likely $\gamma 100\%$ realizations of the inflow. In (17), the original inequality constraint is split in a stochastic part f_{stoch} and in a deterministic part f_{det}.

$$Pr(f_{stoch} \leq f_{det}) \geq \gamma \quad (17)$$

For CC-MPC, the stochastic part of the probabilistic constraint is assumed to follow a known distribution F, as given in (18).

$$f_{stoch} \sim F(\bullet) \quad (18)$$

Given that the probability function of constraint corresponds to the CDF of the deterministic part $\Phi_{F(\bullet)}(f_{det})$, the constraint can be rewritten using the quantile function of the distribution corresponding to γ, as below.

$$f_{det} \geq \Phi_{F(\bullet)}^{-1}(\gamma) \quad (19)$$

Given that the quantile function above is depending on the parameters of the distribution, which likely are varying with the system, the constraint can be simplified by reformulation utilizing the CDF of a standardized distribution of F. In (20), the standardized reformulation of distributions defined purely by their mean μ_f and their variance σ_f^2 is given, such as the normal distribution. For the remainder of this discussion, we will assume f_{stoch} follows such a type of distribution, see (21).

$$\Phi_F\left(\frac{f_{det} - \mu_f}{\sigma_f} \right) \geq \gamma \quad (20)$$

$$f_{stoch} \sim F(\mu_f, \sigma_f^2) \quad (21)$$

With the constraint being formulated with a standardized CDF, the quantile function Φ_F^{-1} of the standardized distribution F can again be applied to reformulate the constraints as (22), where only deterministic formulations are remaining. The usage of quantile functions is a potential drawback of CC-MPC, given that it requires that the quantile function of the given distribution to exist explicitly, or that the specific quantile corresponding to γ is accessible for the computation.

$$f_{det} \geq \mu_f + \sigma_f \Phi_F^{-1}(\gamma) \quad (22)$$

Doing the above reformulation for each inequality constraint and taking the expectation of the cost function and equality constraints, allows for the uncertainty to be removed from the formulation of the optimization problem. The inclusion of additional functions such as trace, mean and variance in the formulation, does potentially increase the complexity of the optimization. If some assumption on the uncertainty does hold, which is discussed below, the increased complexity can be avoided. Similarly discussed below is the case, when the distribution of the uncertainty was bounded by an interval.

1) CDF of Truncated Distribution: In some cases, the stochastic uncertainty is upper and/or lower bounded. Such a stochastic variable is said to follow a truncated distribution, as seen in (23) for the variable X following a distribution F truncated between a and b. An illustration of the difference between an unbounded distribution and a truncated variant is given in Fig. 2.

$$X \sim F_a^b(\mu_x, \sigma_x^2) \Rightarrow a \leq X \leq b \quad (23)$$

The CDF of a truncated distribution is given by (24). Where it can be seen to be formulated by the standardized unbounded distribution F. It can be observed that choosing either a or b to be infinity, indicating no bound, would remove the corresponding term in the CDF by either becoming 0 or 1 respectively or if both are chosen, becoming the standard distribution.

$$\Phi_{F_a^b(\mu_x, \sigma_x^2)}(x) = \frac{\Phi_F\left(\frac{x - \mu_x}{\sigma_x}\right) - \Phi_F\left(\frac{a - \mu_x}{\sigma_x}\right)}{\Phi_F\left(\frac{b - \mu_x}{\sigma_x}\right) - \Phi_F\left(\frac{a - \mu_x}{\sigma_x}\right)} \quad (24)$$
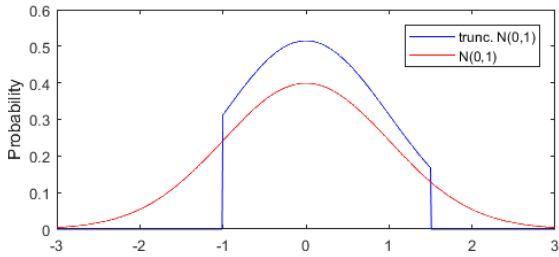
Fig. 2. An illustration of a standard normal distribution, and a truncated standard normal distribution, truncated to within -1 and 1.5

Fig. 3. An example of actual rain inflow and a predicted rain inflow realization, shown for a step of $0.7\ \mu m/s$ with a duration of 90 minutes

By rearranging and substitution of the truncated CDF, a bounded version of the probability constraint in (20) can be formulated as (25).

$$\Phi_F(\frac{x - \mu_x}{\sigma_x}) \geq \gamma\Phi_F(\frac{b - \mu_x}{\sigma_x}) + (1 - \gamma)\Phi_F(\frac{a - \mu_x}{\sigma_x})\ \ (25)$$

By applying the quantile function reformulation, the deterministic description of the probabilistic constraint with a bounded distribution can be formulated.

2) Assumptions on Uncertainty: The CC-MPC is mathematically similar to MPC but does contain a few extra function terms in its formulation, such as the trace function, the quantile function and variances. All of these functions may potentially add to the computational difficulties for solving the optimization. However, if the following two assumptions hold, then the CC-MPC holds the same computational complexity as the deterministic MPC during the optimization.

The first assumption is on the independency of the uncertainty in the system, as stated:

- the uncertain inflow of time k is independent of the uncertainty of the tank volume at time k, $\mathbf{V}_k \perp \mathbf{q}_k^{rain}$

This allows the variance $\sigma_{\mathbf{z}_k}^2$ in (16) to be rewritten as below, given that the covariance terms become zero.

$$\sigma_{\mathbf{z}_k}^2 = C\sigma_{\mathbf{V}_k}^2 C^T + F\sigma_{\mathbf{q}_k^{rain}}^2 F^T \qquad (26)$$

The variance of the tank volume can with the same argumentation, be rewritten until it is only dependent on the initial variance of the volume and the variance of all inflows up until time $k - 1$. This rewritten of the variance, leads to the trace term in (16) becomes constant during an optimization. This reduces the cost function and the equality constraints to a deterministic formulation, where the variables correspond to the expected value instead of the actual value.

The second assumption is that the stochastic part of the constraints f_{stoch} is independent of the optimization variables. This means that under an optimization, the mean and variance of the stochastic part is constant, resulting in the right-hand side of both (22) and (25) to also be constant. The resulting constraints have the same non-linearity as their MPC counterpart.
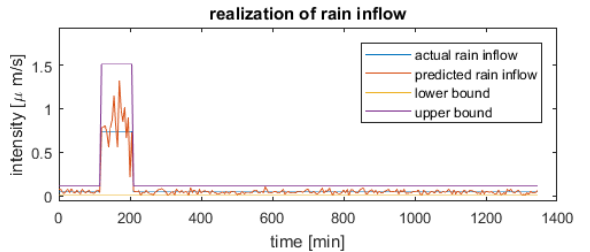
IV. RESULTS & DISCUSSION

In this section, the results of simulations with the different MPCs are discussed and compared. The MPC methods utilized are standard deterministic MPCs with perfect and imperfect predictions of the rain inflow, and CC-MPCs with different probability guarantees γ. For the MPCs, with imperfect predictions, 10 random realizations of the rain inflow were utilized for each simulation scenario, such that the realizations would be representative of the uncertainty. The probability guarantees γ of the CC-MPC was utilized with all inequality constraints having the same probability with the following values being used: 95%, 90%, 80%, 70%, and 60%.

In the simulations, the rain inflow utilized were step inflows, which had varying rain durations and intensities. The rain steps utilized all had a dry weather period before and after the step with a duration of two and nineteen hours respectively. During the dry weather periods, the inflow to the sewers would be $0.04\ \mu m/s$. The duration of the rain steps was varied with half-hour increments, starting at half an hour and ending at five-hour durations, while the intensity was varied from $0.1\mu m/s$ to $11\mu m/s$, with increments of $0.1\mu m/s$. The inflow predictions utilized by the MPCs discussed above were generated as a truncated normal-distributed inflow with the mean being equal to the actual inflow, and the standard deviation σ being $0.01\ \mu m/s$ with a third of the actual inflow added to it. The lower bound on the truncated distribution was chosen to be zero, given that rain inflows are not negative. The upper bound was chosen to be three σ above the expected inflow, corresponding to 99.7% of rain inflow realizations for normal-distributed uncertainty. In Fig. 3, an example of the rain inflow is shown together with one realizations of the predicted rain inflow with its lower and upper bounds.

In the comparison, the MPC with perfect prediction will be utilized as a benchmark for the other MPCs. The focus of the comparisons is the avoidance of weir overflow generations. Given that the MPCs are designed to avoid overflows, there are only two scenarios for which an overflow would occur. The first scenario is the case for which an overflow is unavoidable, regardless of the control chosen; in other words, the optimization problem has become infeasible. The problem could have been infeasible from the start of the

simulation (e.g. too heavy rain) or the previous choice of control has led it to be infeasible, due to uncertainty. In such cases, the controller relies on either previous computed predictions or other back-up procedures, such as less strict uncertainty handling. The second scenario is the case for which the MPC finds a feasible solution, but due to the uncertainties, the computed control leads to the generation of overflows. The feasible solution of this case is a false positive solution, in the sense that they are solution expected to be feasible, but are not. In the following sections, we will focus on each of these cases, but the scenario used for the comparison will only include those for which the MPC with perfect knowledge is feasible.

A. Feasibility of Predictions

For the first case, the feasibility of the MPCs are the focus. In Fig. 4, we can observe the feasibility of the deterministic MPC with imperfect knowledge. Given that the blue line indicates the feasibility limit of the MPC with perfect knowledge, we can infer about the likelihood of the imperfect MPC being infeasible. We can observe that the closer the scenario is to the feasibility limits, the more of the ten realizations becomes infeasible. It is clear that for the scenarios with long duration goes directly from all realizations are feasible to all are infeasible. While the scenarios with short durations slowly lose realizations to infeasibility as the intensity increases. Given that higher intensity in these simulations means higher variance, these results are in agreement with expectations of stochastic realizations of the uncertainty.

In Fig. 5, the feasibility lines for the considered CC-MPCs are shown. It can clearly be seen that the CC-MPC with $\gamma = 95\%$, stops being feasible significantly lower than the remainder of the CC-MPC or the perfect MPC. As the value of γ decreases the feasibility lines close in on the MPC feasibility line. While higher values of γ have more rain realizations covered by the solution, a slight decrease in value can restore feasibility, if the desired γ would lead to infeasibility. This allows for a simple, but effective back-up strategy for CC-MPC; if the problem is infeasible, reduce the probability guarantee γ until a feasible solution is found.

When we compare the CC-MPC feasibility lines with the colored feasibility points of the realizations of the imperfect MPC, we can observe that for a coverage of for example $\gamma = 80\%$, the corresponding simulations with imperfect MPC have an infeasibility rate of around 4 out of 10. Giving approximately 40% of rain realization not to be covered by the MPC, with additional scenarios below also having a higher chance of experiencing infeasibility. The discrepancy between the two types of MPCis most apparent, when the variance is higher, making the infeasibility tendencies converge as duration increases. This means that it is more likely that the use of CC-MPC will conserve feasibility, than by relying on a given rain prediction and a deterministic MPC.
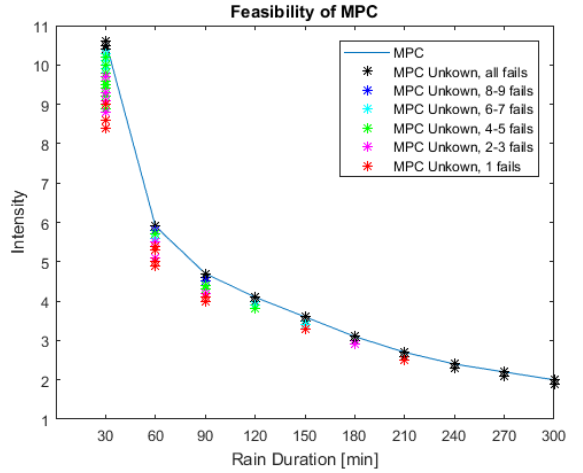
Fig. 4. Feasibility of MPC with imperfect knowledge
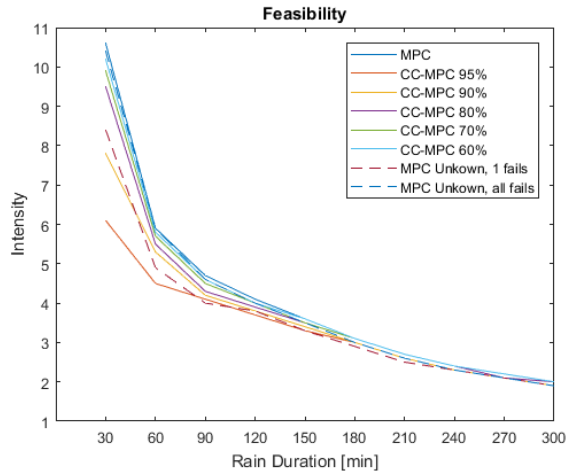
Fig. 5. Feasibility of all three types of MPC

B. False Positive Predictions

We will now focus on the case of false positive predictions, where the computed feasible predictions are in fact infeasible when implemented by the control. The occurrence of unpredicted weir overflows produced by the MPC with imperfect knowledge and by the CC-MPC can be seen in Fig. 6 and Fig. 7 respectively. The red line in the figures is the feasibility line of the given MPC design. It can be observed that while the CC-MPC does not produce any false positive prediction of overflows, the basic MPC does. We can further observe that the false positive overflow occur when the rain intensity gets closers to the feasibility line in the graph. It can further be seen that they only occur for longer rain durations, possible due to the increase in variance for the higher intensities at
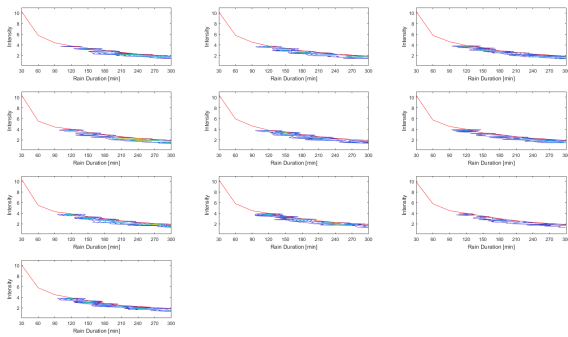
Fig. 6. Weir overflow of MPC with imperfect knowledge, False positive predictions
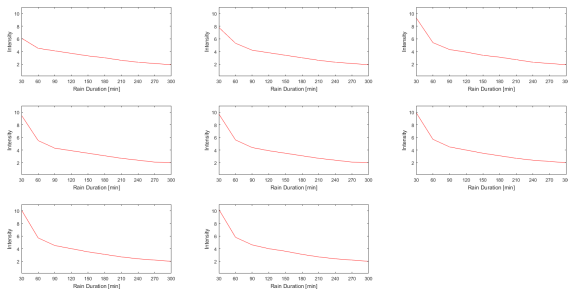
Fig. 7. Weir overflow of Chance-Constrained MPC, False positive predictions

the lower durations; simply making the MPC infeasible. As is evident from the feasibility discussion of Fig. 4, showing how many realizations becoming infeasible at each scenario.

C. Thoughts on different stochastic inflows

In the previous sections, we have focused on stochastic forecasted rain inflows for which the actual inflow was equal to the expected inflow of the system, which is not generally the case. A simple deviation from this simple rain inflow is to assume the actual rain inflow has some bias, a sort of offset from the expected inflow of the system. When the bias makes the expected inflow larger than the actual inflow, it generally would lead to fewer overflows generated by both the MPC with imperfect knowledge and the CC-MPC, as long as the MPC's still is feasible. While a bias which makes the expected inflow lower than the actual inflow, generally would lead to more overflows and false positive predictions, due to the system being filled faster than expected. In the case of imperfect MPC, such bias would simply skew the probability of a given realization, therefore still leaving the feasibility of the MPC to chance. For the CC-MPC, a bias from the expected overflow would be accounted for by the constraint-restriction introduce by the probability guarantee γ, as long as the actual inflow does not correspond to a rain realization outside the covered realizations.

The rain considered in this work has been a simple step up and down; in reality, rains are a lot more varying and fluctuating in intensity. This means real rain has several spikes, and in general, an appearance closer to the uncertain predictions used earlier than actual steps. On the other hand, given that MPC is a discrete method, any fluctuating rain can be described as a series of sample-length steps. This means that as long as the description of the stochastic distribution of the rain is known, then the CC-MPC can operate as seen if the actual rain lies within the bounds of a feasible probability guarantee γ.

V. CONCLUSIONS

In this paper, we have considered the utilization of the deterministic MPC and the stochastic Chance-Constrained MPC (CC-MPC) in a sewage system with uncertain predictions of the rain inflow. From the results of the simulations, it was shown that CC-MPC was less prone to false positive predictions about feasibility and could keep the system feasible for a larger portion of possible rain realizations in comparison to the deterministic MPC. The CC-MPC being a more optimization-complex MPC type was shown to have the same complexity as the deterministic MPC, under the right assumptions on the uncertainty. In addition, the CC-MPC also had a clear and simple back-up procedure in case of infeasibility during computation, by slacking the desired probabilistic guarantees.

REFERENCES

[1] M. S. Gelormino and N. L. Ricker, "Model predictive control of a combined sewer system," *INT. J. CONTROL*, vol. 59, no. 3, pp. 793–816, 1994.

[2] C. Ocampo-Martinez, *Model Predictive Control of Wastewater Systems*, ser. Advances in Industrial Control. Springer, 2010.

[3] N. S. V. Lund, A. K. V. Falk, M. Borup, H. Madsen, and P. S. Mikkelsen, "Model predictive control of urban drainage systems: A review and perspective towards smart real-time water management," *Critical Reviews in Environmental Science and Technology*, vol. 48, no. 3, pp. 279–339, 2018.

[4] S. J. Qin and T. A. Badgwell, "A survey of industrial model predictive control technology," *Control Engineering Practice*, vol. 11, pp. 733–764, 2003.

[5] L. Garcia, J. Barreiro, E. Escobar, N. Q. F. Tellez, and C. Ocampo-Martinez, "Modelling and real-time control fo urban drainage systems: A review," *Advances in Water Resources*, vol. 85, pp. 120–132, 2015.

[6] M. Marinaki and M. Papageorgiou, *Optimal Real-time Control of Sewer Networks*, ser. Advances in Industrial Control. Springer, 2005.

[7] A. Mesbah, "Stochastic model predictive control: An overview and perspectives for future research," *IEEE Control Systems Magazine*, pp. 30–44, December 2016.

[8] J. M. Grosso, C. Ocampo-Martinez, V. Puig, and B. Joseph-Duran, "Chance-constrained model predictive control for drinking waternetworks," *Journal of Process Control*, vol. 24, pp. 504–516, February 2014.

[9] M. Evans, M. Cannon, and B. Kouvaritakis, "Linear stochastic mpc under finitely supported multiplicative uncertainty," in *Proc. of the 2012 American Control Conference*, June 2012.

[10] M. C. Campi, S. Garatti, and M. Prandini, "The scenario approach for systems and control design," *Annual Reviews in Control*, vol. 33, pp. 149–157, October 2009.

[11] B. Kouvaritakis and M. Cannon, *Model Predictive Control - Classical, Robust and Stochastic*, ser. Advances Textbooks in Control and Signal Processing. Springer, 2016.

[12] V. P. Singh, *Hydrologic Systems. Volume 1: Rainfall-runoff modelling*. Prentice Hall, 1988.

APPENDIX D

Article D

The paper presented in this appendix was originally submitted to a journal.

Information of the publication:

- Title: Chance-Constrained Model Predictive Control - A reformulated approach suitable for sewer networks

- Journal: *Submitted* to Advanced Control for Applications

- Date: July, 2020

Chance-Constrained Model Predictive Control
A reformulated approach suitable for sewer networks

Jan Lorenz Svensen*[1] | Hans Henrik Niemann[2] | Anne Katrine Vinther Falk[3] | Niels Kjølstad Poulsen[1]

[1]Department of Applied Mathematics and Computer Science, Technical University of Denmark, 2800 Kongens Lyngby, Denmark

[2]Department of Electrical Engineering, Technical University of Denmark, 2800 Kongens Lyngby, Denmark

[3]Emerging Technologies, DHI A/S, Agern Allé 5, 2970 Hørsholm, Denmark

Correspondence
*Jan Lorenz Svensen, Department of Applied Mathematics and Computer Science, Technical University of Denmark, Asmussens Allé 303B, 2800 Kgs. Lyngby, Denmark. Email: jlsv@dtu.dk

Present Address
Asmussens Allé 303B, 2800 Kgs. Lyngby, Denmark.

Abstract

In this work, a revised formulation of Chance-Constrained (CC) Model Predictive Control (MPC) is presented. The focus of this work is on the mathematical formulation of the revised CC-MPC, and the reason behind the need for its revision. The revised formulation is given in the context of sewer systems, and their weir overflow structures. A linear sewer model of the Astlingen Benchmark sewer model is utilized to illustrate the application of the formulation, both mathematically and performance-wise through simulations. Based on the simulations, a comparison of performance is done between the revised CC-MPC and a comparable deterministic MPC, with a focus on overflow avoidance, computation time, and operational behavior. The simulations show similar performance for overflow avoidance for both types of MPC, while the computation time increases slightly for the CC-MPC, together with operational behaviors getting limited.

KEYWORDS:
stochastic MPC; Combined Sewer Overflow; chance-constrained; Astlingen sewer network

1 | INTRODUCTION

With the increase in heavy rains in the recent decade[1], the operation of sewer systems has become more important. In sewage systems[2], there are several objectives for the ideal system operation; control of the flow to the wastewater treatment plant (WWTP), and the avoidance of weir overflows are among some of them. In the previous decades, Model Predictive Control (MPC) has been applied to sewage systems with fair results[3]-[8] aiming for the ideal operation. However, the structure of sewage systems is always changing leading to model uncertainties, and the systems being intrinsically driven by rain and dry weather inflows, creating a dependency on the quality of the predictions of those inflows. With the classical MPC being a deterministic method, the presence of uncertainty has not in general been included in the research on MPC for sewer networks.

While the classical MPC is deterministic, MPC methods for handling uncertainty has been developed in the past decades[9]-[13], but not applied to sewer systems. Collectively these methods are referred to as Stochastic Model Predictive Control (SMPC) and include a wealth of methods. The methods range from finite scenario-based robust approaches[12] to methods based on the probability of constraints being true[10,11,13], among other methods[9]. In this work, we will focus on the method known as chance-constrained MPC (CC-MPC), which previously has been applied to other systems, such as drinking water systems[10] with good results. The CC-MPC method utilizes an optimization based on the expected cost of the system, together with probabilistic formulations of the constraints. The probabilistic formulations are introduced in order to tighten the constraints so that the performance resulting from the controller are feasible within the real constraints with a given probability.

While CC-MPC and other similar SMPC methods can utilize information of the uncertainty to generate constraint tightenings for more robust performances, it does not come without drawbacks. Given that tighter constraints mean the workspace of the controller gets smaller and in worst-case results loss of feasibility for the CC-MPC. This can happen if the uncertainty is too large or if the desired probability for the constraints to hold are too high, resulting in overlapping constraints and infeasibility.

Another important aspect of MPC design for sewer networks, besides feasibility, is how the overflows from weirs are integrated into the design formulation. Weirs are physical structures with a binary nature of either overflowing or not, giving two different dynamics of the systems to include in the MPC design. Weir overflows are usually integrated by one of three approaches: 1) they are ignored in the formulation and their occurrence means an infeasible scenario. 2) They are integrated into the constraints but excluded from the dynamics. And 3) they are integrated into the dynamics and propagates through the MPC formulation. In this paper, we will consider the third formulation of the weir overflows, however, the CC-MPC mentioned earlier is not suitable for this formulation, due to the overflows being defined by the original constraints (without tightening). The inclusion of overflow into the dynamics leads to another issue with the formulation of CC-MPC. With the inclusion, the constraints defining the weir elements become intrinsically feasible through the presence of overflow. This results in the probabilistic formulations of the CC-MPC method becomes insensible with probabilities larger or equal to one.

To deal with the above drawbacks of CC-MPC applied to sewer networks, we will in this paper outline and apply a revised formulation of the CC-MPC applicable for sewer networks with weir structures. The reformulation will aim to introduce sensible probabilistic constraints, suitability for the inclusion of weir structures in dynamics, as well as the preservation of the original feasibility of the system.

For the application of the revised CC-MPC formulation will utilize a model of the Astlingen benchmark Network [14], displayed in Fig. 2. Furthermore, will the focus of this paper will be given on the revised CC-MPC's performance in view of the classical deterministic MPC's performance when using the third approach to overflow integration.

In the following sections, we will first present the general MPC program for systems with overflows, and then we will discuss and formulate the revised CC-MPC formulation. The paper will end with an applied example and evaluation of the formulated method.

1.1 | Notation

In this paper, the following notation is utilized. Bold font is utilized to indicate vectors, while a bullet • represents a subset or set of a function's variables. For a stochastic variable X, the expectation and variance are denoted $E\{X\}$ and σ_X^2 respectively, while $Pr\{X \leq x\}$ and $\Phi(x)$ is the probability function and cumulative distribution function (CDF) respectively for a given value x. The notation $X \sim F$ indicates that X is following a given distribution F. The weighted quadratic norm of x is denoted by $||\mathbf{x}||_A^2 = \mathbf{x}^T A \mathbf{x}$, while the minimum and maximum of a given function $f(x)$ are denoted $\underline{f}$ and $\overline{f}$ respectively. The notation ΔT and the subscript k indicate the sampling time and the sample number respectively. Variables written with the letters V and q are used to indicate volume and flow respectively. The superscripts in, out, u, and w indicate the inflow, outflow, control flow, and weir overflow respectively.
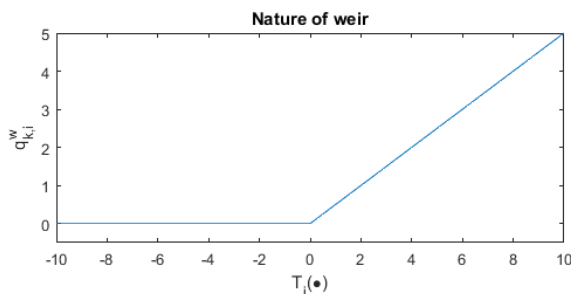
FIGURE 1 An illustration of the nature of weirs where the weir flow $q_{k,i}^w$ is zero when the switching function $T(\bullet)$ is negative, and following a given non-negative weir function $t_w(T)$, when the switching function is positive.

2 | STOCHASTIC MPC WITH WEIR ELEMENTS

Systems with weirs or weir-like structures, such as sewer systems, have a binary nature originating from the weirs. The binary natures are shown in Fig. 1 for a linear weir function $t_w(T)$. The binary nature can easily be observed, by noting that the flow is zero when the switching function $T_i(\bullet)$ is negative, and otherwise follows some given function depending on the switching function. The general deterministic formulation of MPC for systems with weirs can be formulated as below.

$$J = \min_{\mathbf{u}} f(\mathbf{x}, \mathbf{u}, \mathbf{z}^{ref}, \mathbf{w}, \mathbf{q}^w) \tag{1}$$

$$\mathbf{x}_{k+1} = h_{proc}(\mathbf{x}_k, \mathbf{u}_k, \mathbf{w}_k, \mathbf{q}_k^w), \quad \mathbf{x}_0 = \mathbf{x}_{ini} \tag{2}$$

$$q_{k,i}^w = \begin{cases} t_{w,i}(T_i(\bullet)), & T_i(\bullet) \geq 0 \\ 0 \end{cases} \quad \forall i \in \{1 : N_w\} \tag{3}$$

$$\mathbf{h}(\mathbf{x}_k, \mathbf{w}_k, \mathbf{u}_k, \mathbf{q}_k^w) = 0 \tag{4}$$

$$\mathbf{g}(\mathbf{x}_k, \mathbf{w}_k, \mathbf{u}_k, \mathbf{q}_k^w) \leq \bar{\mathbf{g}} \tag{5}$$

Where $\mathbf{x}$ corresponds to the system states, the control of the system is $\mathbf{u}$, $\mathbf{w}$ is the rain inflow into the system, and the weir flow $q_{k,i}^w$ corresponds to the ith weir element out of N_w at time k, and is always non-negative, while $\mathbf{x}_{ini}$ is the system's initial condition.

As mentioned earlier, we will in this work consider the stochastic MPC method CC-MPC. Using the CC-MPC method to handle uncertainty, the cost function in (1) and the equality constraints in (4) are rewritten as the expectation of the given function. The inequality constraints in (5) are reformulated as the probability of the constraints holds true with a given probability. The process equation (2) and weir definition (3) can be substituted into the cost function and constraints so that the only state the system is explicitly depending on is the initial state $\mathbf{x}_0$. Due to the presence of weirs with (3), the resulting probability functions become meaningless as will be shown later. Therefore, we will reformulate the CC-MPC formulation, such that the inclusion of weir structures gives a sensible expression of the probabilistic formulation.

2.1 | Revised CC-MPC Formulation

In our revised formulation of CC-MPC, we will formulate how to include weir structures in the probabilistic formulation, but we will also consider the feasibility of the program, as well as overflow determination. In the formulation of the cost function and the equality constraints, the approach utilized in standard CC-MPC can be reused as given below.

$$J = \min_{\mathbf{u}} E\{f(\mathbf{x}_0, \mathbf{u}, \mathbf{z}^{ref}, \mathbf{w}, \mathbf{q}^w)\} \tag{6}$$

$$0 = E\{h(\mathbf{x}_0, \mathbf{u}, \mathbf{w}, \mathbf{q}^w)\} \tag{7}$$

Where $\mathbf{q}^w$ is written for clarity of the presence of weirs. The formulation of the probability constraints in CC-MPC can cover sets of constraints or individual constraints. We consider the latter in this work, where the approach to the reformulation of the inequality constraints depends on the specific constraint. If the constraint does not contain a weir element, meaning that no weir overflow is defined by this particular constraint, then the direct probabilistic approach from CC-MPC can be utilized to handle the uncertainty. Below is shown the probabilistic rewriting of the ith inequality constraint (8), into the quantile function-based constraint (10), with arrows indicating the order of steps in the process.

$$g_i(\bullet) \leq \bar{g}_i \tag{8}$$

$$\rightarrow \quad Pr\{g_i(\bullet) \leq \bar{g}_i\} \geq \alpha \tag{9}$$

$$\rightarrow \quad \Phi_{g_i(\bullet)}^{-1}(\alpha) \leq \bar{g}_i \tag{10}$$

The above quantile function is based on the distribution of the constraint. Given the optimization variables are contained in the quantile, this is difficult to solve optimization-wise. Utilizing standardization of the constraint distribution, this can be simplified as shown in (11), where the distribution is assumed defined purely by its expectation and variance. Such distributions include the normal distribution; therefore, we will utilize this assumption in the rest of this discussion of the reformulation of the CC-MPC.

$$E\{g_i(\bullet)\} \leq \bar{g}_i - \sigma_{g_i(\bullet)}\Phi^{-1}(\alpha) \tag{11}$$

If the constraint does define a weir overflow, then the direct probabilistic approach results in a meaningless probability. This is due to the weir element making the constraint intrinsically feasible, by counteracting the breaching of the constraint, as

demonstrated below:

$$g_i(\bullet, q_{k,i}^w) \leq \bar{g}_i, \quad q_{k,i}^w = 0 \tag{12}$$

$$g_i(\bullet, q_{k,i}^w) = \bar{g}_i, \quad q_{k,i}^w > 0 \tag{13}$$

$$\rightarrow Pr\{g_i(\bullet, q_{k,i}^w) \leq \bar{g}_i\} = 1 \tag{14}$$

where regardless of which parameters $\bullet$ the constraint depends on, the weir overflow will be depending on the same parameters so that the constraint holds.

For this reason, including the above constraint in the optimization formulation is redundant. In order for achieving a statistical bound on the overflow generation, we instead turn to the probability of keeping the weir overflow $q_{k,i}^w$ non-positive, where we can see this is related to its switching function $T(\bullet)$, as shown below.

$$Pr\{q_{k,i}^w \leq 0\} = Pr\{T_i(\bullet) \leq 0\} \geq \gamma \tag{15}$$

$$\rightarrow \quad E\{T_i(\bullet)\} \leq -\sigma_{T_i(\bullet)}\Phi^{-1}(\gamma) \tag{16}$$

This allows us to formulate probabilistic constraints for both constraints with or without weir elements, as were shown in (16) and (11).

2.2 | Feasibility

In the above, we only considered handling the uncertainty such that a given solution would be feasible in the real system with known probability. This leads to probabilistic restrictions on the inequality constraints, but these restrictions will also lead to more rain scenarios causing infeasibility during computations. By utilizing slack variables with a suitable cost term in the cost function, we can restore the original feasibility of the constraints by the following approach, while keeping the probabilistic restrictions, when possible.

$$E\{g_i(\bullet)\} \leq \bar{g}_i + s_k - \sigma_{g_i(\bullet)}\Phi^{-1}(\alpha) \tag{17}$$

$$E\{T_i(\bullet)\} \leq c_k - \sigma_{T_i(\bullet)}\Phi^{-1}(\gamma) \tag{18}$$

$$0 \leq s_k, c_k \tag{19}$$

Where the constraints without weirs are given by (17) and the weir defining constraints is given by (18). For the constraint without weirs, an extra constraint is necessary to represent the original constraint of the system:

$$s_k - \sigma_{g_i(\bullet)}\Phi^{-1}(\alpha) \leq 0 \tag{20}$$

Using the above versions of the constraints, the formulation of the optimization program for feasible CC-MPC can be written as the following:

$$J = \min_{\mathbf{u},\mathbf{c},\mathbf{s}} E\{f(\mathbf{x}_0, \mathbf{u}, \mathbf{z}^{ref}, \mathbf{w}, \mathbf{q})\} + l(\mathbf{c}, \mathbf{s}) \tag{21}$$

$$0 = E\{h(\mathbf{x}_0, \mathbf{u}_k, \mathbf{w}_k, \mathbf{q}_k^w)\} \tag{22}$$

$$E\{g_i(\bullet)\} \leq \bar{g}_i + s_k - \sigma_{g_i(\bullet)}\Phi^{-1}(\alpha) \tag{23}$$

$$E\{T_i(\bullet)\} \leq c_k - \sigma_{T_i(\bullet)}\Phi^{-1}(\gamma) \tag{24}$$

$$s_k \leq \sigma_{g_i(\bullet)}\Phi^{-1}(\alpha) \tag{25}$$

$$0 \leq s_k, c_k \tag{26}$$

where the additional function $l(c, s)$ in the cost functions is the cost term of the slack variables, penalizing their usage.

2.3 | Overflow Approximation

So far, we have been considering an optimization formulation with a dynamic description of the weir overflows included in it. Given the nature of weir overflows being binary as seen in (3) and therefore not being convex, the inclusion of the dynamic can lead the optimization program to be computational heavy. One approach to deal with this is to treat the weir overflows as additional optimization variables and penalize their utilization[5]. Given that overflows cannot be negative, a constraint for this needs to be added. Another aspect is the determination of the value of the overflow for approximation; Given that we are

minimizing the overflow, we need a constraint telling us the minimum size of the overflow. A fitting constraint for this is the original constraint containing the overflow, due to it being its very definition. We can utilize the expectation of this constraint, to achieve a description of the overflow size and still taken care of the uncertainty. Based on the added constraint shown below, our approximated overflow can be considered the expected overflow of the system in some sense.

$$E\{g_i(\bullet, \mathbf{q}^w)\} \le \bar{g}_i \tag{27}$$

$$0 \le q_k^w \tag{28}$$

With the approximation approach we have utilized, we can formulate the optimization program as below. The cost function now includes a penalty term on the overflow variables. This term is a penalty on the accumulated overflow volumes at each sample in the predictions.

$$J = \min_{\mathbf{u,c,s,q}^w} E\{f(\mathbf{x}_0, \mathbf{u}, \mathbf{z}^{ref}, \mathbf{w}, \mathbf{q})\} + l(\mathbf{c}, \mathbf{s}) + \sum_{k=0}^{N} \mathbf{M}_k^T \mathbf{q}_k^w \tag{29}$$

$$0 = E\{h(\mathbf{x}_0, \mathbf{u}_k, \mathbf{w}_k, \mathbf{q}_k^w)\} \tag{30}$$

$$E\{g_i(\bullet)\} \le \bar{g}_i + s_k - \sigma_{g_i(\bullet)}\Phi^{-1}(\alpha) \tag{31}$$

$$E\{T_i(\bullet)\} \le c_k - \sigma_{T_i(\bullet)}\Phi^{-1}(\gamma) \tag{32}$$

$$s_k \le \sigma_{g_i(\bullet)}\Phi^{-1}(\alpha) \tag{33}$$

$$E\{g_i(\bullet, q_k^w)\} \le \bar{g}_i \tag{34}$$

$$0 \le s_k, c_k, q_k^w \tag{35}$$

3 | MODEL & COST

In this section, we will outline an example of the application of the revised CC-MPC formulation. For clarity, we will first outline the design model of the deterministic MPC followed by the stochastic counterpart. The system considered is a linear model of the Astlingen sewer network [14] illustrated in Fig. 2. The Astlingen system consists of 10 catchment areas connected to a system of 6 controllable tanks and 4 independent weirs, all capable of flooding the nearby river by overflows. For the cost function of the MPC given below, we will utilize a mix of linear and quadratic cost terms, including the overflow approximation approach, discussed previously [5][15].

$$J = \min_{\mathbf{u,q}^w} \sum_{k=0}^{N} ||\Delta \mathbf{u}_k||_R^2 + \mathbf{Q}^T \mathbf{z}_k + \mathbf{W}^T \mathbf{V}_k^w \tag{36}$$

$$\mathbf{V}_k^w = \sum_{i=0}^{k} \mathbf{q}_i^w \tag{37}$$

where the cost is minimized over an N step prediction horizon on the system, with a quadratic penalty of the control change $\Delta \mathbf{u}$ and a linear cost on the output objective $\mathbf{z}$. The output objectives correspond to the following objectives:

- maximizing flow to WWTP

- minimizing flow to the environment

The third term $\mathbf{W}^T \mathbf{V}_k^w$ is a linear penalty on the accumulated overflow volume at time k.

The system can be considered to consist of tanks, pipes with weirs, and delay pipe elements. If the sizes of the delays are in multiples of the sampling time, then they can be considered a cascade of delays of the size of the sampling time, $D_{k,i}$. The dynamics of the tanks and delays are described by the following equations:

$$V_{k+1,i} = V_{k,i} + \Delta T(q_{k,i}^{in} - q_{k,i}^{out,V} - q_{k,i}^w) \tag{38}$$

$$D_{k+1,i} = q_{k,i}^{in} \tag{39}$$
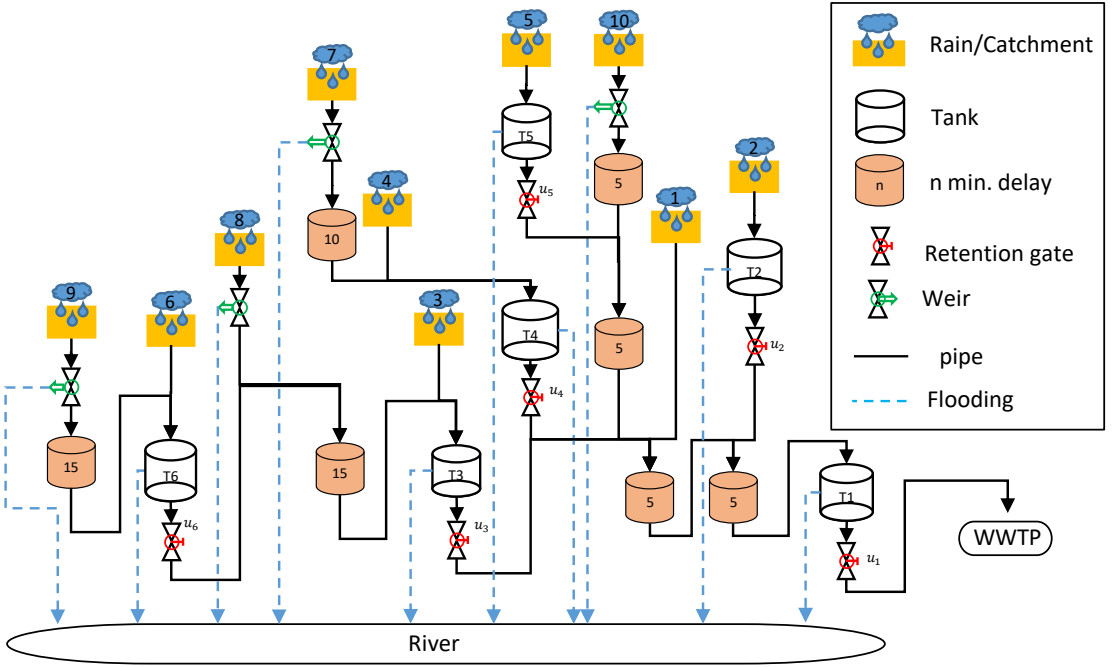
FIGURE 2 A schematic of the system model based on a linear version of the Astlingen Benchmark Network [14]. It shows the interconnections between tanks, pipes, and the environment. The parts tagged with a u_i is controllable.

The outflows of each element are described by the equations below, where V, P, and D indicate the type of element; tank volume, pipe flow, and delay flow respectively.

$$q_{k,i}^{out,V} = u_{k,i} \tag{40}$$

$$q_{k,i}^{out,P} = q_{k,i}^{in} - q_{k,i}^{w} \tag{41}$$

$$q_{k,i}^{out,D} = D_{k,i} \tag{42}$$

The inflow $q_{k,i}^{in}$ of the ith element, given below, are dependent on the connections of the elements in the system as shown in Table 1. Where the ith tank is denoted by Ti, pipe i from catchment i by pi and the n minute delay to tank i is given by Ti:n.

$$q_{k,i}^{in} = w_{k,i} + \sum_{j\in\mathcal{U}_i} u_{k,j} + \sum_{j\in\mathcal{Q}_i^V} q_{k,j}^{out,V} + \sum_{j\in\mathcal{Q}_i^P} q_{k,j}^{out,P} + \sum_{j\in\mathcal{Q}_i^D} q_{k,j}^{out,D} \tag{43}$$

Where the j denotes the flows of the subsets $\mathcal{U}_i, \mathcal{Q}_i^V, \mathcal{Q}_i^P, \mathcal{Q}_i^D$ of all control flows, tank outflows, pipe outflows, and delay outflows respectively. The variable $w_{k,i}$ indicates the rain inflow to the system part.

The inequality constraints are formulated below, where the upper and lower limits of the tank volumes, the pipe outflow, control flow, and the weir overflows are stated for time k. The constraints are based on the individual elements i of the system. Not all of the constraints are applicable for all types of elements, e.g. (44) are only applicable for tanks.

$$0 \leq V_{k,i} - \Delta T q_{k,i}^{w} \leq \bar{V}_i \tag{44}$$

$$0 \leq q_{k,i}^{out,P} \leq \bar{q}_i^{out,P} \tag{45}$$

$$0 \leq q_{k,i}^{out,V} \leq \beta_i V_{k,i} \tag{46}$$

$$0 \leq u_{k,i} \leq \bar{u}_i \tag{47}$$

$$0 \leq q_{k,i}^{w} \tag{48}$$

TABLE 1 Inflows to the different elements of the systems

Element	Inflow
T1	$q_{k,T1:5}^{out,D}$
T2	$w_{k,2}$
T3	$w_{k,3} + q_{k,T3:5}^{out,D}$
T4	$w_{k,4} + q_{k,T4:5}^{out,D}$
T5	$w_{k,5}$
T6	$w_{k,6} + q_{k,T6:5}^{out,D}$
T3:5	$q_{k,T3:10}^{out,D}$
T3:10	$q_{k,T3:15}^{out,D}$
T3:15	$q_{k,6}^{u} + q_{k,p8}^{out,P}$
T4:5	$q_{k,T4:10}^{out,D}$
T4:10	$q_{k,p7}^{out,P}$

Element	Inflow
p7	$w_{k,7}$
p8	$w_{k,8}$
p9	$w_{k,9}$
p10	$w_{k,10}$
T1:5	$q_{k,2}^{u} + q_{k,T1:10}^{out,D}$
T1:10	$w_{k,1} + q_{k,3}^{u} + q_{k,4}^{u} + q_{k,T1:15}^{out,D}$
T1:15	$q_{k,5}^{u} + q_{k,T1:20}^{out,D}$
T1:20	$q_{k,p10}^{out,P}$
T6:5	$q_{k,T6:10}^{out,D}$
T6:10	$q_{k,T6:15}^{out,D}$
T6:15	$q_{k,p9}^{out,P}$

Where β is the volume-flow coefficient [16]. The upper constraints of the tank volumes and pipe outflows are the definitions of the occurrence of overflow. With the corresponding switching function given by (49).

$$T_i(\bullet) = \begin{cases} V_{k,i} - \bar{V}_i & \text{(Tank)} \\ q_{k,i}^{in} - \bar{q}_i^{out,P} & \text{(Pipe)} \end{cases} \tag{49}$$

3.1 | Stochastic Model

The revised formulation of CC-MPC with overflow handling presented earlier can now be applied to the system described above. The cost function of the revised CC-MPC can then be written as:

$$J = \min_{\mathbf{u},\mathbf{c},\mathbf{s},\mathbf{q}^w} \sum_{k=0}^{N} E\{||\Delta\mathbf{u}_k||_R^2 + \mathbf{Q}^T\mathbf{z}_k + \mathbf{W}^T\mathbf{V}_k^w\} + \mathbf{W}_c^T\mathbf{c} + \mathbf{W}_s^T\mathbf{s} \tag{50}$$

Both the rewritten cost function and the later inequality constraints depend on the expectation of the system's subpart equations. Where the expected tank volume, delay flow, element inflow, tank outflow, pipe outflow, and delay outflow are given by (51)-(56) respectively.

$$E\{V_{k+1,i}\} = E\{V_{k,i}\} + \Delta T(E\{q_{k,i}^{in}\} - E\{q_{k,i}^{out,V}\}) - q_{k,i}^{w} \tag{51}$$

$$E\{D_{k+1,i}\} = E\{q_{k,i}^{in}\} \tag{52}$$

$$E\{q_{k,i}^{in}\} = E\{w_{k,i}\} + \sum_{j\in\mathcal{U}_i} u_{k,j} + \sum_{j\in\mathcal{Q}_i^V} E\{q_{k,j}^{out,V}\} + \sum_{j\in\mathcal{Q}_i^P} E\{q_{k,j}^{out,P}\} + \sum_{j\in\mathcal{Q}_i^D} E\{q_{k,j}^{out,D}\} \tag{53}$$

$$E\{q_{k,i}^{out,V}\} = u_{k,i} \tag{54}$$

$$E\{q_{k,i}^{out,P}\} = E\{q_{k,i}^{in}\} - q_{k,i}^{w} \tag{55}$$

$$E\{q_{k,i}^{out,D}\} = E\{D_{k,i}\} \tag{56}$$

In the following paragraphs, the formulation of each inequality constraint is given in the context of the corresponding subpart. The resulting formulation of the lower constraint of the tank volume is given by:

$$\sigma_{V_{k,i}}\Phi^{-1}(\alpha_j) - s_{j,k} \leq E\{V_{k,i}\} - \Delta T q_{k,i}^{w} \tag{57}$$

$$0 \leq s_{j,k} \leq \sigma_{V_{k,i}}\Phi^{-1}(\alpha_j) \tag{58}$$

where j indicates the specific constraint. The probabilistic formulation of the upper constraint of the tank volume is then defined by the switching function (49) as written in (59). The constraint for overflow approximation is given by (60).

$$E\{V_{k,i}\} \le \bar{V}_i - \sigma_{V_{k,i}}\Phi^{-1}(\gamma) + c_k \tag{59}$$

$$E\{V_{k,i}\} - \Delta T q_{k,i}^w \le \bar{V}_i \tag{60}$$

$$0 \le c_k \tag{61}$$

From (54), we know that the tank outflows are controlled and therefore deterministic, this gives us that the lower limit is the same as in (46). For the upper limit, the probabilistic formulation is given by (62) and (63).

$$u_{k,i} \le \beta E\{V_{k,i}\} - \beta\sigma_{V_i}\phi^{-1}(\alpha_j) + s_{j,k} \tag{62}$$

$$0 \le s_{j,k} \le \beta\sigma_{V_i}\phi^{-1}(\alpha) \tag{63}$$

The limits on the pipes with weirs are given by (64) and (65) for the lower limit, and by (66)-(68) for the upper limit.

$$\sigma_{q_{k,i}^{out,P}}\Phi^{-1}(\alpha_j) - s_{j,k} \le E\{q_{k,i}^{out,P}\} \tag{64}$$

$$0 \le s_{j,k} \le \sigma_{q_{k,i}^{out,P}}\Phi^{-1}(\alpha) \tag{65}$$

$$E\{q_{k,i}^{in}\} - q_{k,i}^w \le \bar{q}_i^{out,P} \tag{66}$$

$$E\{q_{k,i}^{in}\} \le \bar{q}_i^{out,P} + c_{j,k} - \sigma_{q_{k,i}^{in}}\Phi^{-1}(\gamma_j) \tag{67}$$

$$0 \le c_{j,k} \tag{68}$$

Given that there is, per definition, no uncertainty in optimization variables, the constraints on the control and weir overflow are deterministic and are therefore the same as in (47) and (48).

3.2 | Benefits and costs

The utilization of the approximation method discussed above has some significant drawbacks as previously discussed in [15]. The main drawbacks are the loss of design freedoms in the weighting of the cost function. These come from the extra weights on the aggregated overflow volume has to be relatively higher than the main terms of the cost functions, and have hierarchically weightings depending on their relative placement in the systems.

These design restrictions on the weightings limit the flexibility of the control with regards to the planning of overflow countermeasures. While the revised CC-MPC does not change these drawbacks, it might give a possible remedy for the hierarchical weightings requirement. If a given weir overflow in the system is more attractive to society than weir overflow further down the system (e.g. downstream is a bathing area). Then by having a higher probability guarantee (α, γ in (11), (16), and section 3.1) on the downstream part than on the specific upstream overflow, the downstream constraints will be less likely to cause an overflow, if it is possible to avoid.

The revised CC-MPC formulation has the drawbacks of introducing more optimization variables and inequality constraints, even without the weir overflow approximation. These drawbacks arise from the conserved feasibility through the slack variables and the constraints on these for elements without weirs. The revised CC-MPC also has the clear benefits of conserving feasibility but more importantly giving statistical constraints on overflow generation, similar to the CC-MPC formulation for systems without internal overflow description.

3.3 | Variance of Constraints

Given the assumption of the variance of the probabilistic constraints exist, and that the probabilistic constraints are scalar, the variance of each constraint is also scalar. We can utilize this feature to derive a computationally simple method for computing

TABLE 2 Cost function weighting of accumulated overflow volume **W**, showing a higher cost for upstream elements.

T1	T2	T3	T4	T5	T6	p7	p8	p9	p10
1000	5000	5000	5000	5000	10000	10000	10000	15000	5000

the variance for the constraints. Firstly, we need to define the variance of each constraint.

$$\sigma_{V_{k,i}}^2 = \sigma_{V_{k-1,i}}^2 + \Delta T^2 \sigma_{q_{k-1,i}^{in}}^2 \tag{69}$$

$$\sigma_{D_{k,i}}^2 = \sigma_{q_{k-1,i}^{in}}^2 \tag{70}$$

$$\sigma_{q_{k,i}^{out,P}}^2 = \sigma_{q_{k,i}^{in}}^2 \tag{71}$$

$$\sigma_{q_{k,i}^{out,D}}^2 = \sigma_{D_{k,i}}^2 \tag{72}$$

$$\sigma_{q_{k,i}^{in}}^2 = \sigma_{w_{k,i}}^2 + \sum_{j \in Q_i^P} \sigma_{q_{k,j}^{out,P}}^2 + \sum_{j \in Q_i^D} \sigma_{q_{k,j}^{out,D}}^2 \tag{73}$$

where each source of uncertainty is assumed to be independent both temporally and spatially. This gives equations for the variances, which is a linear model of the initial state variance and the rain inflow variances as shown in (74). Utilizing this, all of the constraints discussed above can be combined into a matrix inequality covering the entire prediction horizon as shown in (75)-(77).

$$\boldsymbol{\sigma}^2 = \Theta \sigma_{\mathbf{V}_0}^2 + \Gamma \sigma_{\mathbf{w}}^2 \tag{74}$$

$$\Omega_u U + \Omega_{q^w} q^w \leq \Omega_{const} + \Omega_s S + \Omega_c C + \Omega_I \sigma_{Diag} \Phi^{-1}(\gamma) \tag{75}$$

$$\Omega_{const} = \Omega + \Omega_x E\{\mathbf{x}_0\} + \Omega_w E\{\mathbf{W}\} \tag{76}$$

$$\sigma_{Diag} = \sqrt{diag(\boldsymbol{\sigma}^2)} \in \mathcal{R}^{nxn} \tag{77}$$

4 | RESULTS & DISCUSSION

In the previous sections, we have introduced the revised CC-MPC formulation, in this section; we will focus on analyzing the difference between the performance of the revised CC-MPC and the classical deterministic MPC applied to the Astlingen model introduced earlier. In the simulations, the examples of the MPC designs given in section 3 are used with a prediction horizon of a 100 min., where the weights of each objective in the cost function have the following values; 2 for minimizing flow to nature, -1 for maximizing flow to WTTP, and 0.01 for the change in control flow. The higher the absolute weight is the higher the priority, while a negative weight indicates maximization, instead of minimization in the objective. The weighting of the accumulated overflow volume is given in table 2, where it can be seen the weights vary accordingly to the placements of the overflows in the system, as described in [15]. The usages of the slack variables are weighted uniformly with 100.

Several scenarios with varying parameters have been run during the simulations. The profiles for the rain inflows in simulations were all step rains, where the rain intensity was varied from 0.5 to 6 $\mu m/s$, and the rain duration varying from a half-hour to five hours, with 0.5 $\mu m/s$ and half-hour intervals. For the revised CC-MPC, the probability guaranty was equal across all constraints and was varied between scenarios, with values of 90%, 80%, and 70% respectively. The deterministic MPC is assumed to have perfect forecasts of the rain inflow, while the revised CC-MPCs are operating with uncertainties following a truncated Gaussian distribution, with the expectation being the actual rain inflow. The size of the uncertainty for the CC-MPC (the standard variation σ), was chosen as a third of the expectation plus a constant deviation of $0.01\mu m/s$, to avoid zero uncertainty. The truncated distribution of the uncertainty was assumed to be non-negative and below three σ above the expectation, resulting in all realizations of the inflows to be within two times the expected non-zero value. A realization of a rain scenario can be seen in Fig. 3, with the actual rain and bounds on the uncertainty, included.

max computation time difference [seconds]
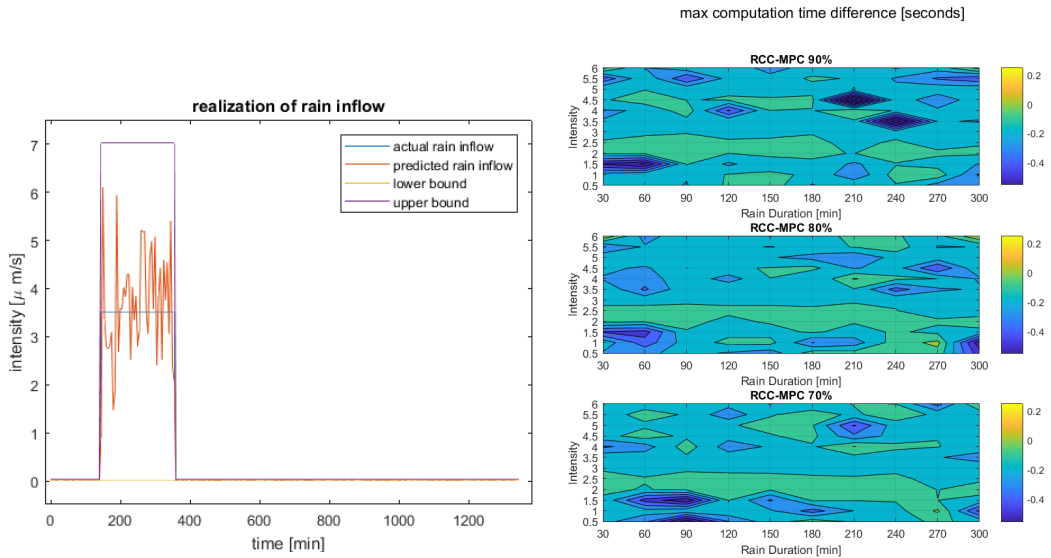
FIGURE 3 Realization of the rain forecast of a rain scenario with 3.5 $\mu m/s$ intensity and a three and a half-hour rain duration. Showing the uncertain prediction around the actual inflow.

FIGURE 4 The difference of Maximum computation time during each rain scenario simulation of the perfect MPC and the revised CC-MPC computed as MPC - revised CC-MPC

4.1 | Computation Time

From Fig. 4, we can observe the difference in the maximum computation time between the deterministic MPC and the revised CC-MPC with the three chosen probability guarantees. It can be observed that in general, the revised CC-MPCs are around 0.1 seconds slower than the deterministic MPC, while occasional computations performer faster or slower for both types of controllers due to numerical variations.

4.2 | Weir Overflow

In this part, we focus on the results of the simulation to do with weir overflows. In fig. 5, one of the simulations results is shown, showing the overflow over time for both the MPC with perfect forecast and the revised CC-MPC with 90% probability bound on the constraints. We can observe that the experienced overflow of the system is identical between the two controllers. This is further supported by the percental difference between the controllers for each rain scenario, shown in Fig. 7. Here we can see that in general, the difference is approximately zero, but also that a few scenarios have larger differences. These differences are due to the conservatism of the CC-MPC when the end of the rain cannot be seen within the prediction horizon, giving the CC-MPC a better start position than the MPC for the next time step. The total volume of weir overflow of the deterministic MPC can be seen in Fig. 6. By comparison to the percental differences before, we can see that the larger differences occurred, when the overflow volume is small for the MPC, making small divergences big in percentages.

4.3 | WWTP

In this part, we focus on the results of the simulation to do with the amount of water sent to the wastewater treatment plant of the system. In Fig. 8 and Fig. 9, we can observe the volumetric difference and the percentage difference in wastewater sent to the treatment plant respectively.

We can see from the volume difference, that the deterministic MPC has an outflow, which is generally larger than the outflows of the revised CC-MPC, by somewhat constant volume bias around 120 m^3 depending on the probability bound. We can observe
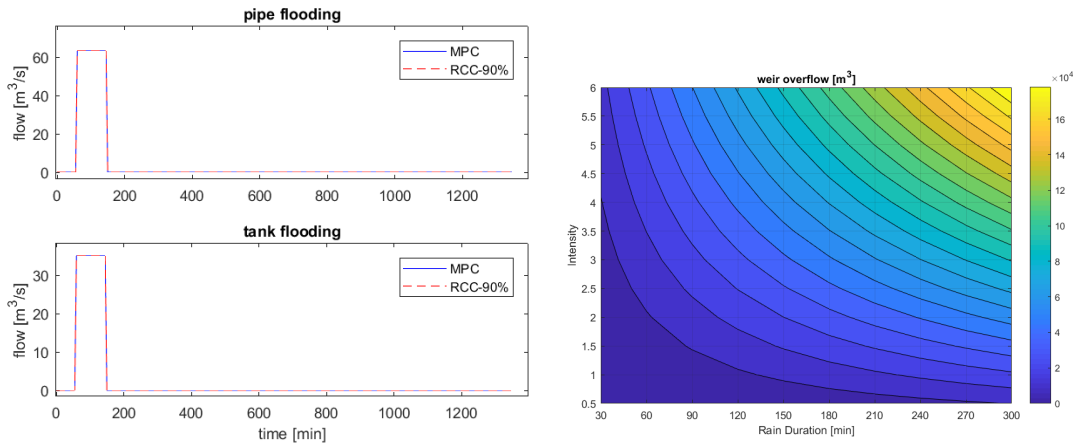
FIGURE 5 The total temporal overflow of a representative simulation

FIGURE 6 Total overflow volume of MPC with perfect knowledge

from the percentage difference that while the bias is constant, the percentage difference primarily decreases with the duration of the rain, and not with the intensity of the rain. We can further see that the decrease in percentage difference corresponds to the increase in the outflow, depicted for the deterministic MPC in Fig. 10

4.4 | Scenario example

In this section, we will focus on a representative simulation and the operational behavior across the system. The corresponding realization of the rain and the total overflow historic were already shown earlier in Fig. 3 and Fig. 5. From Fig. 11, we can observe the computational difference given as the cost difference. Here we can observe that the cost of the revised CC-MPC is always higher than for the deterministic MPC, with revised CC-MPC having a constant additional cost. It can also be observed that the revised CC-MPC with the highest probability bound has the highest cost, as one would expect.

The tank operational behavior of the system can be observed in Fig. 12, with the tank outflow controllers displayed in Fig. 13. From the tank volumes, we can once again see that the different MPCs agree on the optimal amount of volume exceeding the tanks. We can also observe that the revised CC-MPCs find a steady-state volume, which is higher than the steady-state volume of the deterministic MPC. This can further be observed by the control flows, where we can see that the control flows of both the deterministic MPC and the revised CC-MPC with 90% probability bound stay below the individual physical control constraint bounds of the control flows. We can see that the deterministic MPC, in general, operates slightly higher than the revised CC-MPC, and as expected can operate on the constraint bound. While the graph only depicts individual physical control constraint bounds, it is still interesting to note how far the steady-state operation of the revised CC-MPC is operating from the constraint bounds, due to the stochastic restraints. It can also be noted that the difference in operation between the two MPCs, first occurs after the rain has ended and not before, where rain was forecasted to happen. This indicates the difference is due to cost priority of the steady-state operation.

5 | CONCLUSIONS

In this paper, we have presented a revised formulation of Chance-Constrained MPC (CC-MPC) inspired for application in sewer networks. The main aspect of the reformulation focuses on preserving feasibility and introducing overflow handling of binary structures. The mathematical formulation and reasoning behind the revised CC-MPC has been stated and applied to a model of the Astlingen sewer system for testing the method. A comparison of the performance of the revised CC-MPC and deterministic MPC was based on simulations with idealized step rain inflows as the perturbation of the Astlingen system. From the results of

weir overflow: CC-MPC - MPC % difference
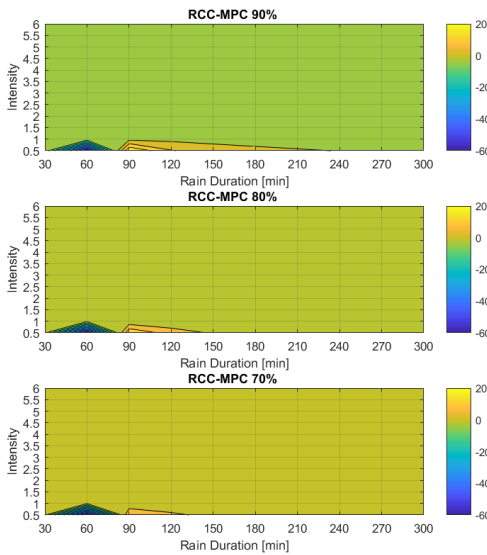
WWTP: CC-MPC - MPC difference
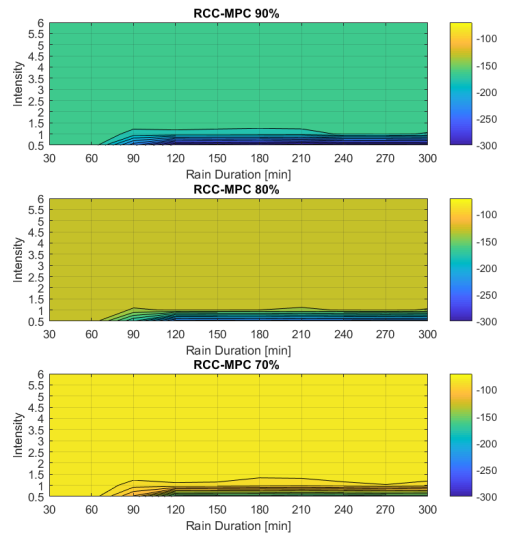
FIGURE 7 Percentage difference in total overflow expe-rience, between revised CC-MPC and MPC with perfect knowledge

FIGURE 8 The difference in wastewater volume sent to the treatment plants, between the revised CC-MPC and the MPC with perfect knowledge

WWTP: CC-MPC - MPC % difference
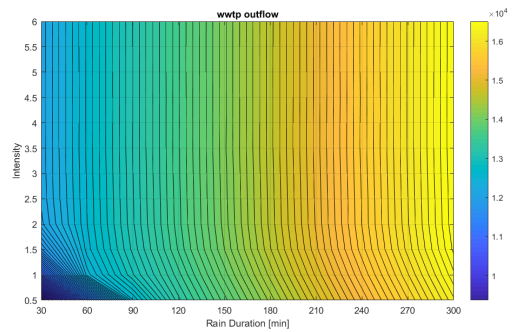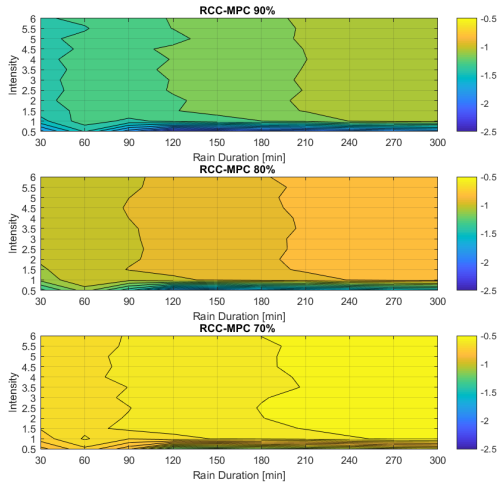
FIGURE 9 The percentage difference in wastewater volume sent to the treatment plants, between the revised CC-MPC and the MPC with perfect knowledge

FIGURE 10 The total outflow volume of the deterministic MPC with perfect knowledge.
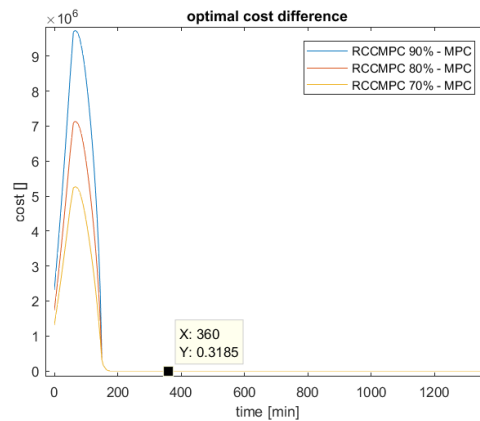
FIGURE 11 The difference in optimal cost function value between the revised CC-MPC and the MPC with perfect knowledge

the simulations, it was shown that the weir overflow avoidance of the revised formulation provides similar results as the MPC with perfect forecast. Indicating the revised CC-MPC as an alternative to MPC, when a perfect forecast is not achievable. The results also showed a trade-off with regards to the worst-case computation time, which in general increased slightly.

References

1. Gregersen IB. *Past, present and future variations of extreme rainfall in Denmark*. PhD thesis. Technical University of Denmark, DTU Environment, Kgs. Lyngby; 2015.

2. Butler D, Davies JW. *Urban Drainage*. Spon Press. third ed. 2011.

3. Gelormino MS, Ricker NL. Model Predictive Control of a Combined Sewer System. *INT. J. CONTROL* 1994; 59(3): 793-816.

4. Ocampo-Martinez C. *Model Predictive Control of Wastewater Systems*. Advances in Industrial ControlSpringer . 2010.

5. Halvgaard R, Falk AKV. Water system overflow modeling for Model Predictive Control. In: Proceedings of the 12th IWA Specialised Conference on Instrumentation, Control and Automation. ; 2017.

6. Lund NSV, Falk AKV, Borup M, Madsen H, Mikkelsen PS. Model predictive control of urban drainage systems: A review and perspective towards smart real-time water management. *Critical Reviews in Environmental Science and Technology* 2018; 48(3): 279-339. doi: 10.1080/10643389.2018.1455484

7. Qin SJ, Badgwell TA. A survey of industrial model predictive control technology. *Control Engineering Practice* 2003; 11: 733-764.

8. Marinaki M, Papageorgiou M. *Optimal Real-time Control of Sewer Networks*. Advances in Industrial ControlSpringer . 2005.

9. Mesbah A. Stochastic Model Predictive Control: An overview and Perspectives for Future Research. *IEEE Control Systems Magazine* 2016: 30-44. doi: 10.1109/MCS.2016.2602087

10. Grosso JM, Ocampo-Martinez C, Puig V, Joseph-Duran B. Chance-constrained model predictive control for drinking waternetworks. *Journal of Process Control* 2014; 24: 504-516.

11. Evans M, Cannon M, Kouvaritakis B. Linear Stochastic MPC under finitely supported multiplicative uncertainty. In: Proc. of the 2012 American Control Conference. ; 2012: 442âĂŞ447.
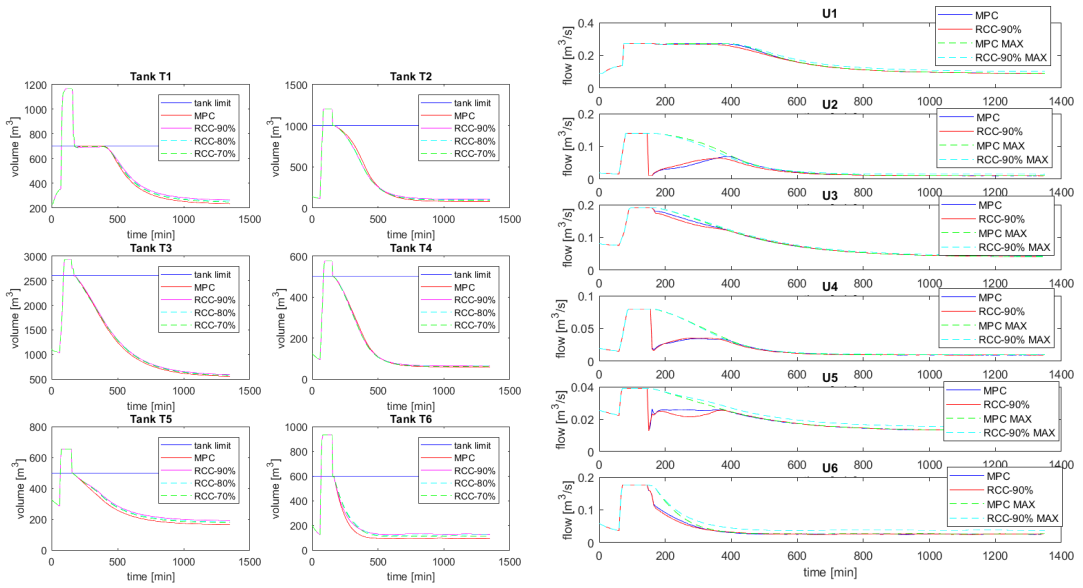
FIGURE 12 The volume historic of all six tanks for the deterministic MPC and the three revised CC-MPCs, with the addition of the physical tank limits. The blue lines indicate the tank limits, the red lines are the volume of the deterministic MPC, while the purple, green and cyan lines are the volume of the three revised CC-MPCs.

FIGURE 13 The control flow histories with the individual upper constraints marked for both the deterministic MPC and the revised CC-MPC with 90% probability bound. The blue the red line are the actual control flows of the MPC and revised CC-MPC respectively, while the green and cyan lines are the respective individual upper bounds.

12. Garatti S, Campi MC, Garatti S, Prandini M. The scenario approach for systems and control design. *Annual Reviews in Control* 2009; 33: 149-157.

13. Kouvaritakis B, Cannon M. *Model Predictive Control - Classical, Robust and Stochastic*. Advances Textbooks in Control and Signal ProcessingSpringer . 2016

14. Schütze M, Lange M, Pabst M, Haas U. Astlingen - a benchmark for real time control (RTC). *Water Sci & Technol* 2018; 2017(2): 552-560.

15. Svensen JL, Niemann HH, Poulsen NK. Model Predictive Control of Overflow in Sewer Networks: A comparison of two methods. In: Proc. of the 4th Int. Conf. on Control and Fault-Toleran Systems (SysTol). IEEE; 2019; Cassablanca, Morocco: 412-417.

16. Singh VP. *Hydrologic Systems. Volume 1: Rainfall-runoff modelling*. Prentice Hall . 1988.

APPENDIX E

Article E

The paper presented in this appendix was originally submitted to a journal.

Information of the publication:

- Title: Chance-constrained Stochastic MPC of Astlingen Urban Drainage Benchmark Network

- Journal: *Submitted* to Control Engineering Practice

- Date: August, 2020

Chance-constrained Stochastic MPC of Astlingen Urban Drainage Benchmark Network*

Jan Lorenz Svensen^{a,*}, Congcong Sun^b, Gabriela Cembrano^{b,c}, Vicenç Puig^b

^{a}*Department of Applied Mathematics and Computer Science, Technical University of Denmark, Richard Petersens Plads 324, 2800 Kongens Lyngby, Denmark*
^{b}*Advanced Control Systems Group, the Institut de Robòtica i Informtica Industrial (CSIC-UPC), Llorens i Artigas, 4-6, 08028 Barcelona, Spain*
^{c}*CETaqua, Water Technology Centre, Barcelona, 08904, Spain*

Abstract

In urban drainage systems (UDS), a proven method for reducing the combined sewer overflow (CSO) pollution is real-time control (RTC) based on model predictive control (MPC). MPC methodologies for RTC of UDSs in the literature rely on the computation of the optimal control strategies based on deterministic rain forecast. However, in reality, uncertainties exist in rainfall forecasts which affect severely accuracy of computing the optimal control strategies. Under this context, this work aims to focus on the uncertainty associated with the rainfall forecasting and its effects. One option is to use stochastic information about the rain events in the controller; in the case of using MPC methods, the class called stochastic MPC is available, including several approaches such as the chance-constrained MPC method. In this study, we apply stochastic MPC to the UDS using the chance-constrained method. Moreover, we also compare the operational behavior of both the classical MPC with perfect forecast and the chance-constrained MPC based on different stochastic scenarios of the rain forecast. The application and comparison have been based on simulations using a SWMM model of the Astlingen urban drainage benchmark network.

Keywords: Astlingen benchmark network, CSO, Stochastic MPC, Chance-Constrained, Real-Time Control,

1. Introduction

Regarding the state-of-the-art during the last couple of decades, Model Predictive Control (MPC) [1] has been proved beneficial for the optimal op-

eration of urban drainage systems (UDS)[2]-[10]. Those studies use different types of modeling and optimization techniques to compute the best control actions, based on models and forecasts, which are subject to uncertainty. However, up to now, most of the MPC applications of UDS are based on deterministic rain forecasts without considering uncertainties, which may risk in introducing sub-optimal or undesired behaviors to the MPC solutions [2]-[16]. For a more realistic scenario, uncertainty has to be considered as a part of the UDS. The way how the uncertainty is treated by the control, becomes an important design decision: using a stochastic approach, or robustly operating on worst-case assumptions.

*Corresponding Author
Email addresses: `jlsv@dtu.dk` (Jan Lorenz Svensen), `congcong@upc.edu` (Congcong Sun), `gabriela.cembrano@upc.edu` (Gabriela Cembrano), `vicenc.puig@upc.edu` (Vicenç Puig)

While the basic formulation of MPC is deterministic, how to handle uncertainty in MPC has been researched for many years [17]-[27]. This has resulted in several different methods for handling uncertainty divided into two categories; the group of the methods known collectively as robust MPC[24]-[27], and the group of methods known as stochastic MPC[17]-[24]. The first group essentially considers the worst-case scenario and operates conservatively so that the solution is optimal for all possible realizations of the uncertainty. The second group addresses the uncertainty by using knowledge about the uncertainty, such as its distribution to only take the statistical likely scenarios into account for the control.

In this work, we will focus on a method from the group of stochastic methods known as chance-constrained MPC (CC-MPC)[17]-[20] to operate the UDS in order to reduce pollution to the receiving waters through minimization of the combined sewer overflows (CSO). Given that the CSOs are purely dependent on the volumes and flows of the system; the overflow constraints are intrinsically feasible and probabilistic insensitive, when CC-MPC is applied directly. We will therefore use the revised CC-MPC formulation[17] in this work.

In our previous work[4], an MPC methodology was implemented and tested on a SWMM model of the Astlingen urban drainage benchmark network [28], where the goal was to minimize the CSOs volume of the system, while maximizing the amount of treated wastewater by the wastewater treatment plant (WWTP). We obtained good results from this, in comparison with other real-time control strategies. In this paper, we return to the Astlingen urban drainage system for applying stochastic MPC using chance-constrained method regarding the uncertainty of rainfall forecast, and comparing the performance of CC-MPC with uncertain forecasts against the performance of the deterministic MPC with a perfect forecast. The key performance indexes considered are the CSO volume, and the volume received by the WWTP.

In this paper, the following mathematical notations are used. $\overline{f}$ indicates the maximum of a given function $f(x)$, β represents the volume-flow coefficient[29], and bold font is used to indicate vectors. The formulation $\|\mathbf{x}\|_A^2 = \mathbf{x}^T A \mathbf{x}$ is the weighted quadratic norm of x. The superscript u indicates control variables, superscript w indicates CSO elements, and the superscripts in and out indicate inflow and outflow related flow, respectively. The letters V and q indicate variables of volume and flow respectively, while the variables written with w are inflows from catchments. The notation ΔT and the subscript k represent the sampling time of the system and the sample number respectively.

2. Internal model of the Astlingen Benchmark Network

The Astlingen urban drainage network consists of six tanks and a single outflow towards a WWTP (see Figure 1). In between and upstream of the tanks there are pipes of varying lengths, causing flow delays in the system. The system also consists of four pipes with CSO capabilities. The control variables of the system are the outflow of tanks 2, 3, 4, and 6. The desired operation of the system is to have the least amount of CSO as possible, and secondly having the largest amount of wastewater being sent to the WWTP. For designing an MPC controller for the system, an internal model describing the dynamics and constraints of this system is required, typically a simplified model of the system capturing the main dynamic behaviours is used.

From Figure 1, it is clear that the system can be deduced to be uncontrollable (passive) in the sections upstream the tanks; therefore, the internal model will be limited to only covering the tanks of the system. The internal model is constructed with the same modular approach as used in previous works[4]. In the internal model, the CSO are treated as optimization variables through a penalty approach[2]. The elements of the internal model consist of the following parts: linear reservoir tanks and pipes with delays that are described below.

In CC-MPC, the internal model of the deterministic MPC mentioned above is extended with a process equation of the variance of the dynamics, while the dynamics are replaced with the ex-

pectation of the dynamics. The constraints are reformulated either as the expectation of the constraint or as a probabilistic version of the constraints. The prior is in general used for equality constraints, while the latter is used for inequality constraints.

In this work, the run-off flows (w, covering runoff and passive flows) generated by forecasted rainfalls are the disturbance, involving uncertainty. We will assume this uncertainty to follow a normal distribution, which is commonly used to interpret fluctuations in measured or forcasted variables[30, 31]. Then, for uncertainties following a normal distribution, the probabilistic constraints can be written deterministically as shown in (1), using the expectation $E\{x\}$ and standard deviation $\sigma\{x\}$ of the stochastic variable X, as well as the quantile function $\Phi^{-1}(x)$ of the standard normal distribution on the desired probability confidence level γ

$$Pr(X \leq x) \geq \Leftrightarrow x \geq E\{X\} + \sigma\{X\}\Phi^{-1}(\gamma) \quad (1)$$

Furthermore, the only sources of uncertainty considered in the formulation of the internal model for the CC-MPC are the initial states of the system and the inflow from the run-off sources such as catchments. It is further assumed that the different sources of uncertainties are independently distributed, in both spatial and temporal sense.

2.1. Linear Reservoir Tank - passive outflow

The linear reservoir model has either a passive outflow or a controlled outflow and is based on mass-balance to describe the dynamics of tank volume. The volume of the tank V_k is driven by the inflow q_k^{in} and the weir overflow q_k^w. In the case of passive outflows, the outflow is controlled by gravity, and is assumed linear with a volume-flow coefficient[29] defined as $\beta = \overline{q}^{out}/\overline{V}$.

For the passive outflow case, the volume update and the outflow are defined by:

$$V_{k+1} = (1 - \Delta T\beta)V_k + \Delta T(q_k^{in} - q_k^w) \quad (2)$$
$$q_k^{out} = \beta V_k \quad (3)$$

The constraints of the reservoir are based on the physical constraints with the tank limits given by

$$0 \leq (1 - \Delta T\beta)V_k + \Delta T(q_k^{in} - q_k^w) \leq \overline{V} \quad (4)$$
$$0 \leq q_k^w \quad (5)$$
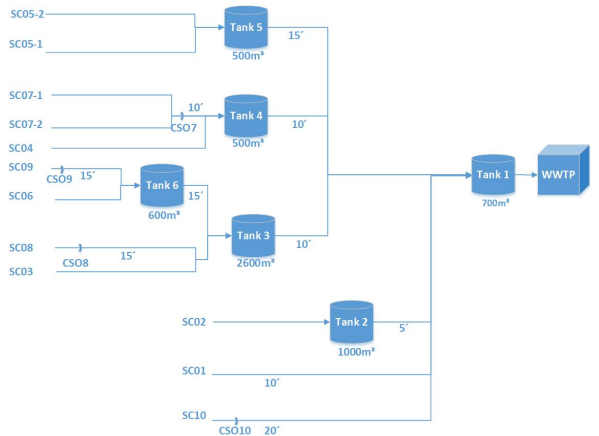
Figure 1: A scheme of the Astlingen Benchmark Network[28] showing the interconnections between tanks, pipes and the WWTP, with CSOs coming from the six tanks and the four pipes noted CSO7 to CSO10. The delay between tanks and/or pipes are noted by x' in minutes.

2.1.1. CC-MPC formulation

Utilizing the revised CC-MPC formulation[17] mentioned earlier, the passive reservoir model can be reformulated, such that the volume update and the outflow are defined by their expectation and variance given by

$$E\{V_{k+1}\} = (1 - \Delta T\beta)E\{V_k\} + \Delta T(E\{q_k^{in}\} - q_k^w) \quad (6)$$
$$E\{q_k^{out}\} = \beta E\{V_k\} \quad (7)$$
$$\sigma^2\{V_{k+1}\} = (1 - \Delta T\beta)^2\sigma^2\{V_k\} + \Delta T^2\sigma^2\{q_k^{in}\} \quad (8)$$
$$\sigma^2\{q_k^{out}\} = \beta^2\sigma^2\{V_k\} \quad (9)$$

The stochastic interpretation of the physical constraints is given by (10)-(14), utilizing slack variables for guaranteeing feasibility[17].

The stochastic constraint for the lower limit of the tank is given by (10), while the upper limit is given by (11) and (12). The first one is a stochastic constraint for avoiding weir overflow q_k^w, while the latter is an expectation constraint defining the

3

expected overflow

$$\sigma\{(1 - \Delta T\beta)V_k + \Delta Tq_k^{in}\}\Phi^{-1}(\gamma) - s_k \leq$$
$$(1 - \Delta T\beta)E\{V_k\} + \Delta T(E\{q_k^{in}\} - q_k^w) \tag{10}$$

$$(1 - \Delta T\beta)E\{V_k\} + \Delta TE\{q_k^{in}\} \leq$$
$$\overline{V} - \sigma\{(1 - \Delta T\beta)V_k + \Delta Tq_k^{in}\}\Phi^{-1}(\gamma) + c_k \tag{11}$$

$$(1 - \Delta T\beta)E\{V_k\} + \Delta T(E\{q_k^{in}\} - q_k^w) \leq \overline{V} \tag{12}$$

$$s_k \leq \sigma\{(1 - \Delta T\beta)V_k + \Delta Tq_k^{in}\}\Phi^{-1}(\gamma) \tag{13}$$

$$0 \leq q_k^w, s_k, c_k \tag{14}$$

The limits on the slack variables s_k, c_k are given by (13) and (14). For the control of the Astlingen model, Tank 1 and Tank 5 are considered tanks with passive outflow.

2.2. Linear Reservoir Tank - Controlled outflow

For a linear reservoir tank with controlled outflow, the volume is driven by the inflow q_k^{in}, the control flow q_k^u and the weir overflow q_k^w. The volume update and outflow are defined by

$$V_{k+1} = V_k + \Delta T(q_k^{in} - q_k^u - q_k^w) \tag{15}$$

$$q_k^{out} = q_k^u \tag{16}$$

and the physical limits on the tanks and control are given by

$$0 \leq V_k + \Delta T(q_k^{in} - q_k^u - q_k^w) \leq \overline{V} \tag{17}$$

The limits of the control including two upper limits of the control flow are defined as

$$0 \leq q_k^u \leq \overline{q}^u \tag{18}$$

$$q_k^u \leq \beta V_k \tag{19}$$

$$0 \leq q_k^w \tag{20}$$

where the first one establishes the physical limit of the outflow pipe, and the other one a linear Bernoulli expression given by the volume-flow coefficient β.

2.2.1. CC-MPC formulation

The controlled reservoir model can be formulated for CC-MPC as below, considering that the volume update and outflow are defined by the expectation and variance

$$E\{V_{k+1}\} = E\{V_k\} + \Delta T(E\{q_k^{in}\} - q_k^u - q_k^w) \tag{21}$$

$$E\{q_k^{out}\} = q_k^u \tag{22}$$

$$\sigma^2\{V_{k+1}\} = \sigma^2\{V_k\} + \Delta T^2\sigma^2\{q_k^{in}\} \tag{23}$$

$$\sigma^2\{q_k^{out}\} = 0 \tag{24}$$

Note that the outflow variance is zero, due to the control.

According to the reformulation[17], the stochastic version of the physical constraints is given by

$$0 \leq E\{V_k\} + \Delta T(E\{q_k^{in}\} - q_k^u - q_k^w) \tag{25}$$

$$E\{V_k\} + \Delta T(E\{q_k^{in}\} - q_k^u) \leq$$
$$\overline{V} - \sigma\{V_k + \Delta Tq_k^{in}\}\Phi^{-1)}(\gamma) + c_k \tag{26}$$

$$E\{V_k\} + \Delta T(E\{q_k^{in}\} - q_k^u - q_k^w) \leq \overline{V} \tag{27}$$

$$0 \leq q_k^u \leq q^u \tag{28}$$

$$q_k^u \leq \beta E\{V_k\} - \beta\sigma\{V_k\}\Phi^{-1}(\gamma) + s_k \tag{29}$$

$$s_k \leq \beta\sigma\{V_k\}\Phi^{-1}(\gamma) \tag{30}$$

$$0 \leq q_k^w, c_k, s_k \tag{31}$$

where the slack variables are limited by (30) and (31). The constraints (25)-(27) define the upper and lower limits of the tank, in a similar way as (10)-(12). The control limits are defined by (28) and (29).

2.2.2. Decoupling of slack variables

In (25), the lower limit of the tank is given as expectation constraint, while in (10) it was expressed in a probabilistic manner. The change is due to the interconnections of the slack variables of the upper and lower constraints as follows

$$s_k \leq c_k + \overline{V} - \Delta Tq_k^w \tag{32}$$

where the upper slack is forced to be active if the lower slack is too large.

This can lead to an undesired trade-off during optimization when the uncertainty term is too

4

large. This can be solved by a rescaling of the optimization weights or by reformulating the probability constraint. The latter was used here. The probability of the tank volume being above zero (33) can be rewritten

$$Pr(0 \leq V_k + \Delta T(q_k^{in} - q_k^u - q_k^w))$$
$$= Pr(\Delta T q_k^u \leq V_k + \Delta T(q_k^{in} - q_k^w)) \geq \gamma \quad (33)$$

by considering that the tank volume V_k are always below the upper tank limit, given that any volume above it would have turned into an overflow. This leads to the volume only decreases, when the control flow is used, i.e.

$$V_k \leq V_k + \Delta T(q_k^{in} - q_k^w) \quad (34)$$

From here, we can replace (33) with a stricter and simpler probability as follows

$$Pr(0 \leq V_k + \Delta T(q_k^{in} - q_k^u - q_k^w))$$
$$\geq Pr(\Delta T q_k^u \leq V_k) \geq \gamma \quad (35)$$

By multiplying with the volume-flow coefficient β and assuming that $\beta \Delta T \leq 1$, the probability constraint can be rewritten even stricter. The assumption is fair, given that if the opposite is true, then the volume can become negative. The resulting probability constraint

$$Pr(\beta \Delta T q_k^u \leq \beta V_k) \geq Pr(q_k^u \leq \beta V_k) \geq \gamma \quad (36)$$

can be recognized as (29), the stochastic version of one of the upper control limits. This indicates that if (29) holds so does (36), and therefore (33) would be a duplicate. For this reason, (33) can be replaced with the expectation constraint given in (25), for the inclusion of the lower limit of the tank.

2.3. Pipe with delays

In the Astlingen network [28], the tanks and upstream catchments are connected through pipes. The presence of these pipes introduces delays in the flows to the tanks from the upstream parts of the system. The importance of these delays depend on the chosen sampling time. Delays η of exactly one sampling can be described by

$$\eta_{k+1,i} = q_{k,i}^{in} \quad (37)$$
$$q_{k,i}^{out} = \eta_{k,i} \quad (38)$$

Subpart	Inflow	Subpart	Inflow
T_1	$q_{k,\eta_{1:5}}^{out}$	$\eta_{1:5}$	$q_{k,T_2}^{out} + q_{k,\eta_{1:10}}^{out}$
T_2	$w_{k,2}$	$\eta_{1:10}$	$w_{k,1} + q_{k,T_2}^{out} + q_{k,T_4}^{out} + q_{k,\eta_{1:15}}^{out}$
T_3	$w_{k,3} + q_{k,\eta_{3:5}}^{out}$	$\eta_{1:15}$	q_{k,T_5}^{out}
T_4	$w_{k,4}$	$\eta_{3:5}$	$q_{k,\eta_{3:10}}^{out}$
T_5	$w_{k,5}$	$\eta_{3:10}$	$q_{k,\eta_{3:15}}^{out}$
T_6	$w_{k,6}$	$\eta_{3:15}$	q_{k,T_6}^{out}

Table 1: Inflows to the different elements of the systems

where delays of multiple sampling times, can be constructed as a cascade of single delays

2.3.1. CC-MPC formulation

For the CC-MPC, the delay equations are replaced by their expectations

$$E\{\eta_{k+1,i}\} = E\{q_{k,i}^{in}\} \quad (39)$$
$$E\{q_{k,i}^{out}\} = E\{\eta_{k,i}\} \quad (40)$$

In addition, the variance of the delay equations are given by

$$\sigma^2\{\eta_{k+1,i}\} = \sigma^2\{q_{k,i}^{in}\} \quad (41)$$
$$\sigma^2\{q_{k,i}^{out}\} = \sigma^2\{\eta_{k,i}\} \quad (42)$$

2.4. Constructing the model

The MPC model of Astlingen network can now be constructed considering the interconnection of the tanks and delays presented in Figure 1 and using the models discussed above. The inflow of each considered subpart of the network are summarized in Table 1. The i-th tank and the delay flow to it are noted by T_i and $\eta_{i:j}$ respectively, with j being the remaining delay in minutes to the tank. The outflow of subpart z is written as $q_{k,z}^{out}$, and the i-th run-off inflow to the system is given by $w_{k,i}$.

3. MPC design

The design of controllers used in this work for both MPC and CC-MPC are based on the models discussed above and the minimization of a cost that considers the following operational objectives for the network:

- Maximizing flow to the WWTP

- Minimizing flow to the river/creek

- Minimizing roughness of control

5

The first objective can be achieved by a linear negative cost on the outflow of tank 1, while the second objective can be formulated as a linear positive cost on the total overflow of the system; these objectives are collectively written as $\mathbf{z}_k$, with the weight $\mathbf{Q}$. The third objective can be written as a quadratic cost on the change in control flow Δq_k^u, with the diagonal weight R. Due to the overflow being modeled by a penalty approach, a fourth objective of minimizing the accumulated overflow volume $\mathbf{V}_k^w$ is introduced, with the weight $\mathbf{W}$.

$$J = \min_{\mathbf{q}^u, \mathbf{q}^w} \Sigma_{k=0}^N \|\Delta \mathbf{q}_k^u\|_R^2 + \mathbf{Q}^T \mathbf{z}_k + \mathbf{W}^T \mathbf{V}_k^w \quad (43)$$

subject to

$$\mathbf{z} = \Phi_{Con} \mathbf{q}^u + \Psi \mathbf{V}_0 + \Theta \mathbf{w} + \Gamma \mathbf{q}^w \quad (44)$$
$$\mathbf{V}_k^w = \Sigma_{i=0}^k \Delta T \mathbf{q}_i^w \quad (45)$$

By using the MPC model over the prediction horizon N, the cost function of the MPC can be written as in (43), while the predicted objectives $\mathbf{z}$ and accumulated overflow volumes, given by (44) and (45), are derived by substitution of the predicted volumes and delays. The constraints of the MPC model can similarly be collected into a single matrix inequality given by

$$\Omega_{Con} \mathbf{q}^u + \Omega_{vol} \mathbf{V}_0 + \Omega_{rain} \mathbf{w} + \Omega_{weir} \mathbf{q}^w \leq \mathbf{\Omega} \quad (46)$$

where the subscripts of the Ω matrix terms relates to the corresponding terms: *Con* for the control term, *vol* for the initial volume term, *rain* for the external inflows term, and *weir* for the term describing the CSOs of the system.

The design of the CC-MPC can similarly be derived using the corresponding model presented above. The cost of the resulting optimization program, appear as the expectation of (43) with the added linear cost term of the minimization of the slack variables $\mathbf{c}$ and $\mathbf{s}$ with weights $\mathbf{W}_c$ and $\mathbf{W}_s$.

$$J = \min_{\mathbf{q}^u, \mathbf{q}^w, \mathbf{c}, \mathbf{s}} E\{\Sigma_{k=0}^N \|\Delta \mathbf{q}_k^u\|_R^2 + \mathbf{Q}^T \mathbf{z}_k \\ + \mathbf{W}^T \mathbf{V}_k^w\} + \mathbf{W}_c^T \mathbf{c} + \mathbf{W}_s^T \mathbf{s} \quad (47)$$

The expected objectives are given by

$$E\{\mathbf{z}\} = \Phi_{Con} \mathbf{q}^u + \Psi E\{\mathbf{V}_0\} + \Theta E\{\mathbf{w}\} + \Gamma \mathbf{q}^w \quad (48)$$

T1	T2	T3	T4	T5	T6
1000	5000	5000	5000	5000	10000

Table 2: Cost function weighting of accumulated overflow volume $\mathbf{W}$, showing a higher cost for upstream elements.

while the accumulated overflow volume is unchanged from (45).

The matrix inequality of the collected probabilistic constraints are given by

$$\Omega_{Con} \mathbf{q}^u + \Omega_{vol} E\{\mathbf{V}_0\} + \Omega_{rain} E\{\mathbf{w}\} + \Omega_{weir} \mathbf{q}^w \leq \\ \mathbf{\Omega} - \sigma\{\Omega_{vol} \mathbf{V}_0 + \Omega_{rain} \mathbf{w}\} \Phi^{-1}(\gamma) + \Omega_s \mathbf{s} + \Omega_c \mathbf{c} \quad (49)$$

and the variance term

$$\sigma^2 \{\Omega_{vol} \mathbf{V}_0 + \Omega_{rain} \mathbf{w}\} = \Xi_{vol} \sigma^2 \{\mathbf{V}_0\} + \Xi_{rain} \sigma^2 \{\mathbf{w}\} \quad (50)$$

The weighting of the different objectives in the cost functions is done in accordance with the penalty approach[2, 3]. The priority of the different objectives is given in the following order from highest to lowest priority:

1. Minimization of accumulated overflow volume $\mathbf{V}_k^w$
2. Minimization of flow to the river/creek
3. Maximizing flow to the WWTP
4. Minimizing roughness of control

The weightings used in this work are for the accumulated overflow volume given in Table 2 for each tank weir. The weights of the remaining objectives are 2 for the flow to the river/creek, -1 for the flow to the WWTP, 0.01 for the roughness of the control, and in the CC-MPC case 10 for the usage of the slack variables. The weights indicate that the avoidance of the flow to the river is prioritized twice as high as increasing flow to the WWTP. The weight on the roughness indicates the desire for the control to be smooth, but not a general priority. As seen from the table, the priority of the accumulated overflow is significantly higher than the other objectives.

4. Results

The CC-MPC discussed above has been applied to the SWMM model of the Astlingen benchmark network. In order to test the strength of

the CC-MPC, different types of uncertainty have been applied. Four different scenarios have been tested with the first being variations in the probability confidence level γ, changing from 60% to 100%. The remaining three scenarios are related with the uncertainty itself and how the MPC relies on its forecast information, where one scenario varies the size of the bound of the uncertainty and the last two varies the expected values of the inflow predictions deviation from the actual inflow, through scaled and offset biases. During each test, only one parameter has been changed. In the baseline test case, the CC-MPC has been designed using a 90% probability confidence level, a 50% uncertainty bound, 0% scaled bias and zero offset bias. In all the simulations, the uncertainty has been assumed that it follows a truncated normal distribution, where the lower bound is zero and the upper bound is three standard deviations above the expected disturbance.

4.1. CC-MPC with Various Probability Confidence Levels γ

The results in terms of CSO volume from varying the probability confidence level can be observed in Table 3, and in Table 4 for the volume of treated water in WWTP. From these tables, we can see the distribution of CSO through the system. Both the CSO and WWTP volume of the CC-MPCs are comparatively close to the results of the deterministic MPC, regardless of the chosen probability guaranty. Similar conclusions can be obtained from Figure 2, which presents volume dynamics for the tanks with controllable orifices (Tank 2, Tank 3, Tank 4, Tank 6) under CC-MPCs with probability confidence levels in the range from 60% to 100%. In Figure 2, there are small deviations for the tank volumes resulting from CC-MPCs with different probability confidence levels. However, a slightly trend can be observed such that the smaller the probability confidence levels, the larger volumes at the peak points, which may reach the maximal storage more easily and generate more CSOs for the corresponding tanks. This figure only presents simulation results for day 10 and day 11 in order to provide a clearer view.
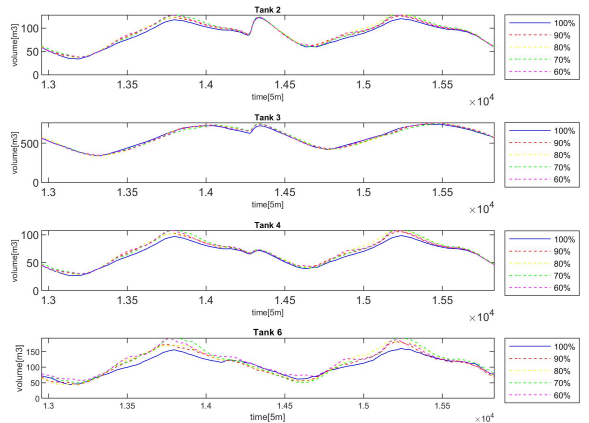
Figure 2: The volumes for the tanks with controllable orifices (Tank 2, Tank 3, Tank 4, Tank 6) for the CC-MPCs with probability confidence levels γ of 100-60%.

4.2. CC-MPC with Various Uncertainty Bounds

The uncertainty bound describes the interval the uncertainty can take. For these simulations, a constant lower bound of zero is used; while the upper bound is defined as a percentage p of the actual inflow above the expected rain inflow, see (51). The standard deviation of the uncertainty is assumed a third of the actual rain inflow times the percentage p, while the expectation is assumed equal to the actual rain. For normal distributions, this leads to the bound to be defined as

$$bound = [0, E\{q\} + p\mu] \tag{51}$$

corresponding to the 99.7% confidence interval of a corresponding unbounded distribution, if expectation matches the actual inflow. The CC-MPC is tested with percentage p bounds of 25%, 50% and 75%. From Tables 5 and 6, we can observe the resulting CSO volume and WWTP volume, respectively. It can be observed that the deviations from the results of the deterministic MPC are negligible of up to a few hundred cubic meters. Figure 3 provides detailed dynamic evolution for the tank volumes of CC-MPC with uncertainty bounds of 25%, 50% and 75%, confirming conclusions obtained from Table 5 showing that the deviations brought by CC-MPCs are negligible. On another hand, it can be observed from Figure 3 that, the larger the uncertainty bound is, the

Tank & Pipes	MPC	CC-MPC 100%	CC-MPC 90%	CC-MPC 80%	CC-MPC 70%	CC-MPC 60%
T1	93251	93713	92927	93015	93114	93229
T2	15484	15683	15544	15543	15543	15543
T3	34017	34174	34313	34214	34427	34248
T4	4814	4823	4814	4814	4814	4815
T5	15147	15147	15147	15147	15147	15147
T6	37950	37723	37946	37939	37980	37870
P7	4016	4016	4015	4016	4016	4016
P8	16207	16207	16191	16203	16203	16199
P9	4030	4030	4029	4029	4029	4029
P10	4838	4838	4842	4839	4839	4840
River	183754	184585	183778	183774	184086	184020
Creek	45996	45769	45990	45984	46025	45915
Total	229750	230353	229768	229758	230111	229935
R. %		-0.4522%	-0.0131%	-0.0109%	-0.1807%	-0.1448%
C. %		0.4935%	0.0130%	0.0261%	-0.0630%	0.1761%
Tot. %		-0.2625%	-0.0078%	-0.0035%	-0.1571%	-0.0805%

Table 3: Overflow results of the SWMM simulations with different controllers: MPC, and CC-MPC with the probability guarantees of 100-60%

	MPC	CC-MPC 100%	CC-MPC 90%	CC-MPC 80%	CC-MPC 70%	CC-MPC 60%
WWTP Vol.	3772057	3771560	3772159	3772088	3771889	3771795
Imp. %		-0.0132%	0.0027%	0.0008%	-0.0045%	-0.0069%

Table 4: Treated Wastewater results of the SWMM simulations with different controllers: MPC, and CC-MPC with the probability guarantees of 100-60%

smaller the tank volume is, which may cause less CSOs to the corresponding tank. This is because the larger uncertainty bounds make the CC-MPC generate more conservative orifice operations with the function of preventing CSOs. This conclusion is also in agreement with the basic deviations trends for the tanks CSO comparisons in Table 5.

4.3. CC-MPC with Various Scaled Biases

In this section, the percentage bound on the uncertainty are kept constant, 50%, instead the expected inflow is introduced as a scaled version of the actual rain inflow, given by

$$E\{q\} = aq^{actual} \qquad (52)$$

Both the CC-MPC and the MPC are tested with 20% and 10% underestimated inflow, perfect forecast, and 10% and 20% overestimated inflow. The results can be seen in Table 7 and 8, for the CSO

Tank & Pipes	MPC	CC-MPC 25%	CC-MPC 50%	CC-MPC 75%
T1	93251	93067	92927	92795
T2	15484	15543	15544	15544
T3	34017	34267	34313	34067
T4	4814	4814	4814	4814
T5	15147	15147	15147	15147
T6	37950	37939	37946	37673
P7	4016	4016	4015	4016
P8	16207	16203	16191	16207
P9	4030	4029	4029	4030
P10	4838	4839	4842	4838
River	183754	183879	183778	183412
Creek	45996	45984	45990	45718
Total	229750	229864	229768	229130
R. %		-0.0680%	-0.0131%	0.1861%
C. %		0.0261%	0.0130%	0.6044%
Tot. %		-0.0496%	-0.0078%	0.2699%

Table 5: Overflow results of the SWMM simulations with different controllers: MPC and CC-MPC with the uncertainty bound of 25-75%.

Figure 4: The volumes for the controllable tanks under CC-MPC with different scaled bias.

	MPC	CC-MPC 25%	CC-MPC 50%	CC-MPC 75%
WWTP Vol.	3772057	3772086	3772159	3772676
Imp. %		0.0008%	0.0027%	0.0164%

Table 6: Treated Wastewater results of the SWMM simulations with different controllers: MPC, and CC-MPC with the uncertainty bound of 25-75%.

Figure 3: The volumes for the tanks with controllable orifices (Tank 2, Tank 3, Tank 4, Tank 6) for the CC-MPC with the uncertainty bound of 25-75%

volume and the WWTP volume, respectively. We can observe that if the expected inflow is overestimated then both types of MPC perform relatively worse as the overestimation increases with respect to CSO volume, and slight improvement of WWTP volume. When the inflow is underestimated, then the MPC performs significantly worse than the MPC with perfect forecast, when regarding CSO but only slightly better for the WWTP volume. For the CC-MPC, both the total CSO and WWTP results are relatively close to the MPC with perfect forecast, but with the drawback of the distribution of the CSOs being significantly worse for the creek. Figure 4 gives detail volume comparisons for the controllable tanks under CC-MPC with different scaled bias through a two-day simulation (day 10 and day 11). The dynamics of Figure 4 confirm that CC-MPC with an underestimated inflow performs significantly worse than that the CC-MPC with overestimated inflows. The explanation for this conclusion is also due to less conservative generated by the underestimated inflows. Moreover, the larger scales tend to have more differences in terms of tank volumes.

4.4. CC-MPC with Various with Offset Biases

In this section, the bias is changed from a scaling to an offset, see (53). Both the CC-MPC and

Tank & Pipes	MPC -20%	CC-MPC -20%	MPC -10%	CC-MPC -10%	MPC 0%	CC-MPC 0%	MPC 10%	CC-MPC 10%	MPC 20%	CC-MPC 20%
T1	96776	90004	95187	91355	93251	92927	94419	94728	96383	96615
T2	16727	16801	15957	16023	15484	15544	15384	15383	15317	15316
T3	33182	33298	33842	33857	34017	34313	34239	34065	33928	34304
T4	5938	5960	5191	5206	4814	4814	4730	4729	4714	4713
T5	15147	15147	15147	15147	15147	15147	15147	15147	15147	15147
T6	39252	39082	38341	38296	37950	37946	37790	37770	37908	37836
P7	4015	4015	4016	4015	4016	4015	4015	4016	4015	4015
P8	16195	16190	16208	16195	16207	16191	16188	16203	16188	16191
P9	4029	4029	4030	4029	4030	4029	4028	4029	4028	4029
P10	4841	4843	4837	4841	4838	4842	4843	4839	4843	4842
River	188805	182242	186369	182623	183754	183778	184949	185094	186519	187129
Creek	47297	47126	46387	46341	45996	45990	45834	45815	45952	45880
Total	236102	229368	232756	228964	229750	229768	230782	230909	232470	233008
R. %	-2.7488	0.8228	-1.4231	0.6155		-0.0131	-0.6503	-0.7292	-1.5047	-1.8367
C. %	-2.8285	-2.4567	-0.8501	-0.7501		0.0130	0.3522	0.3935	0.0957	0.2522
Tot. %	-2.7647	0.1663	-1.3084	0.3421		-0.0078	-0.4492	-0.5045	-1.1839	-1.4181

Table 7: Overflow results of the SWMM simulations with different controllers: MPC and CC-MPC under different scaled bias.

	MPC -20%	CC-MPC -20%	MPC -10%	CC-MPC -10%	MPC 0%	CC-MPC 0%	MPC 10%	CC-MPC 10%	MPC 20%	CC-MPC 20%
WWTP Vol.	3765554	3772166	3769365	3772992	3772057	3772159	3771015	3770672	3769214	3768942
Imp. %	-0.1724	0.0029	-0.0714	0.0248		0.0027	-0.0276	-0.0367	-0.0754	-0.0826

Table 8: Treated Wastewater results of the SWMM simulations with different controllers: MPC, and CC-MPC under different scaled bias.

the MPC are tested with zero offset and three positive offsets. The sizes of the offsets are the annual mean inflow (0.02) times the factors of 1 and 0.25, and 10 times the dry-weather inflow (0.1)

$$E\{q\} = q^{actual} + b \qquad (53)$$

The results of both MPC types can be seen in Table 9 and 10 for the CSO and WWTP volume, respectively. We can observe that for both non-zero offsets, the CSO is significantly worse, with the offset of 0.1 being even worse. The results of the WWTP volume are also worse than the MPC with perfect forecast. Figure 5 gives more information about the performance of CC-MPC under different offsets. The differences in tank volume among CC-MPC using different offsets are compared. As always, the more volume in the tank indicates an increased chance of having more CSOs. From Figure 5, we can conclude that CC-MPC with 0.1 offset have more tank volume than that the offsets, which means, CC-MPC with 0.1 offset behaves worse than that of MPC. However, the CC-MPC with 0.005 and 0.02 did not show a clear trend.

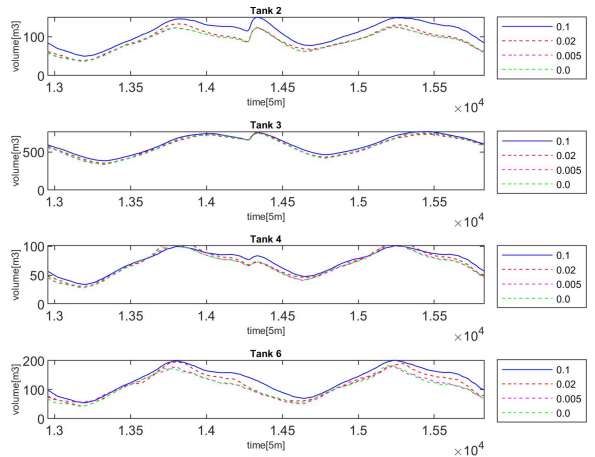From the above results, we can infer that the

Figure 5: The volumes for the controllable tanks under CC-MPC using different offsets.

Tank & Pipes	MPC	CC-MPC 0	MPC 0.005	CC-MPC 0.005	MPC 0.02	CC-MPC 0.02	MPC 0.1	CC-MPC 0.1
T1	93251	92927	93655	93856	96472	96590	131407	130211
T2	15484	15544	15387	15450	15453	15452	15847	15511
T3	34017	34313	33975	34322	34086	34485	36811	36548
T4	4814	4814	4728	4728	4639	4644	4465	4465
T5	15147	15147	15147	15147	15147	15147	15147	15147
T6	37950	37946	37916	37961	37877	37780	37907	37763
P7	4016	4015	4015	4015	4015	4016	4016	4016
P8	16207	16191	16188	16193	16188	16203	16203	16203
P9	4030	4029	4028	4029	4028	4029	4029	4029
P10	4838	4842	4843	4842	4843	4839	4839	4839
River	183754	183778	183922	184536	186828	187360	224718	222925
Creek	45996	45990	45959	46005	45920	45825	45952	45808
Total	229750	229768	229881	230541	232748	233185	270670	268733
R. %		-0.0131	-0.0914	-0.4256	-1.6729	-1.9624	-22.2928	-21.3171
C. %		0.0130	0.0804	-0.0196	0.1652	0.3718	0.0957	0.4087
Tot. %		-0.0078	-0.0570	-0.3443	-1.3049	-1.4951	-17.8107	-16.9676

Table 9: Overflow results of the SWMM simulations with different controllers: MPC and CC-MPC under different off-set biases.

	MPC	CC-MPC 0	MPC 0.005	CC-MPC 0.005	MPC 0.02	CC-MPC 0.02	MPC 0.1	CC-MPC 0.1
WWTP Vol.	3772057	3772159	3771978	3771575	3768823	3768643	3731689	3733651
Imp. %		0.0027	-0.0021	0.0001	-0.0857	-0.0905	-1.0702	-1.0182

Table 10: Treated Wastewater results of the SWMM simulations with different controllers: MPC, and CC-MPC under different off-set biases.

CC-MPC is capable of handling different type of uncertainties, and for those type of uncertainties, it performs similarly to the deterministic MPC. We can further see that the CC-MPC, while not performing that well with constant offset biases, these biases were also outside the uncertainty bound, practically making the CC-MPC as blind as the deterministic MPC. In real-world scenarios, the uncertainty of the inflow is not exactly as the one used here. Instead the uncertainty bound would vary across the prediction horizon, as would do the biases of the expected inflow.

5. Conclusion

A stochastic MPC has been applied to a hydrodynamic SWMM model of the Astlingen urban drainage benchmark network, using a chance-constraint formulation of MPC. A comparison study of the application of both CC-MPC and MPC has been done for several scenarios and types of uncertainties in forecasts, involving both biases in the forecast to different sizes of the uncertainty. Based on the simulations, we can conclude that only the uncertainty regarding biases has an effect on the performance of CC-MPC. Furthermore, it could be observed that the performance of both type of MPC considered deteriorate similarly with respect to CSO volume, when the forecast overestimates the rain inflow. However, when the forecast underestimates the rain inflow, then the CC-MPC performs similarly to the ideal case, while the performances of deterministic MPC deteriorates.

References

[1] J. M. Maciejowski, Predictive Control: with constraints, Pearson, 2002.

[2] R. Halvgaard, A. K. V. Falk, Water system overflow modeling for model predictive control, in: Proceedings of the 12th IWA Specialised Conference on Instrumentation, Control and Automation, Proceedings of the 12th IWA Specialised Conference on Instrumentation, Control and Automation, 2017.

[3] J. L. Svensen, H. H. Niemann, N. K. Poulsen, Model predictive control of overflow in sewer networks: A comparison of two methods, in: Proc. of the 4th Int. Conf. on Control and Fault-Toleran Systems, Proc. of the 4th Int. Conf. on Control and Fault-Toleran Systems, 2019, pp. 412–417.

[4] C. Sun, J. L. Svensen, M. Borup, V. Puig, G. Cembrano, L. Vezzaro, An mpc enabled swmm implementation of the astlingen rtc benchmaking network, Water 12 (1034) (2020).

[5] M. S. Gelormino, N. L. Ricker, Model predictive control of a combined sewer system, INT. J. CONTROL 59 (3) (1994) 793–816.

[6] C. Sun, B. Joseph, T. Maruejouls, G. Cembrano, E. Muñoz, J. Meseguer, A. Montserrat, S. Sampe, V. Puig, X. Litrico, Efficient integrated model predictive control of urban drainage systems using simplified conceptual quality models, 14th IWA/IAHR International Conference on Urban Drainage, Prague, 2017, pp. 1848–1855.

[7] C. Sun, B. Joseph, G. Cembrano, V. Puig, J. Meseguer, Advanced integrated real-time control of combined urban drainage systems using mpc: Badalona case study, 13th International Conference on Hydroinformatic, Palermo, 2018, pp. 2033–2041.

[8] C. Ocampo-Martinez, Model Predictive Control of Wastewater Systems, Advances in Industrial Control, Springer, 2010.

[9] M. Marinaki, M. Papageorgiou, Optimal Real-time Control of Sewer Networks, Advances in Industrial Control, Springer, 2005.

[10] L. Cen, Y. Xi, Aggregation-based model predictive control of urban combined sewer networks, in: Proc. of the 7th Asian Control Conference, Proc. of the 7th Asian Control Conference, 2009.

[11] C. Sun, G. Cembrano, V. Puig, J. Meseguer, Cyberphysical systems for real-time management in the urban water cycle, in: Proceedings of the 4th International Workshop on Cyber-Physical Systems for Smart Water Networks, 2018, pp. 3–5.

[12] C. Sun, B. Joseph-Duran, T. Maruejouls, G. Cembrano, J. Meseguer, V. Puig, X. Litrico, Real-time control-oriented quality modelling in combined urban drainage networks, in: Proceedings of the IFAC 2017 World Congress, 2017, pp. 4002–4007.

[13] C. Sun, V. Puig, G. Cembrano, Real-time control of urban water cycle under cyber-physical systems framework, Water 12 (406) (2020).

[14] B. Joseph-Duran, J. Meseguer, G. Cembrano, T. Maruejouls, Closed-loop simulation of real-time controllers for urban drainage systems using high resolution hydraulic simulators, in: Proceedings of the 14th IWA/IAHR International Conference on Urban Drainage, 2017.

[15] G. Cembrano, J. Quevedo, M. Salamero, V. Puig, J. Figueras, J. Marti, Optimal control of urban drainage systems. acase study, Control Engineering Practice 12 (2004) 1–9.

[16] P. Overloop, Model Predictive Control on Open Water Systems, Delft University Press: Delft, 2006.

[17] J. L. Svensen, H. H. Niemann, A. K. V. Falk, N. K. Poulsen, Chance-constrained model predictive control - a reformulated approach suitable for sewer networks, Advanced Control of Applications, Submitted.

[18] J. M. Grosso, C. Ocampo-Martinez, V. Puig, B. Joseph-Duran, Chance-constrained model predictive control for drinking waternetworks, Journal of Process Control 24 (2014) 504–516.

[19] H. Arellano-Garcia, G. Wozny, Chance constrained water quality management model for reservoir systems: I. strict monotonicity, Comput. Chem. Eng. 33 (10) (2009) 15681583.

[20] A. Dhar, B. Datta, Chance constrained water quality management model for reservoir systems, ISH J. Hydraul. Eng. 12 (3) (2006) 39–48.

[21] M. Evans, M. Cannon, B. Kouvaritakis, Linear stochastic mpc under finitely supported multiplicative uncertainty, Proc. of the 2012 American Control Conference, 2012.

[22] S. Garatti, M. C. Campi, S. Garatti, M. Prandini, The scenario approach for systems and control design, Annual Reviews in Control 33 (2009) 149–157.

[23] A. Mesbah, Stochastic model predictive control: An overview and perspectives for future research, IEEE Control Systems Magazine (2016) 30–44doi:10.1109/MCS.2016.2602087.

[24] B. Kouvaritakis, M. Cannon, Model Predictive Control - Classical, Robust and Stochastic, Advances Textbooks in Control and Signal Processing, Springer, 2016. doi:10.1007/978-3-319-24853-0.

[25] Z. Wan, M. V. Kothare, Robust output feedback model predictive control using o-line linear matrix inequalities, Journal of Process Control 12 (7) (2002) 763–774.

[26] L. Magni, G. D. Nicolao, R. Scattolini, F. Allgöwer, Robust model predictive control for nonlinear discrete-time systems, International Journal of Robust and Nonlinear Control 13 (3-4) (2003) 229246.

[27] Z. Q. Sun, L. Dai, K. Liu, Y. Q. Xia, K. H. Johansson, Robust mpc for tracking constrained unicycle robots with additive disturbances, Automatica 90 (2018) 172–184.

[28] M. Schütze, M. Lange, M. Pabst, U. Haas, Astlingen - a benchmark for real time control (rtc), Water Sci & Technol 2017 (2) (2018) 552–560.

[29] V. P. Singh, Hydrologic Systems. Volume 1: Rainfall-runoff modelling, Prentice Hall, 1988.

[30] P. Karantonis, C. Weber, Use of iso measurement uncertainty guidelines to determine uncertainties in noise & vibration predictions and design risks, in: Proceedings of ACOUSTICS, Proceedings of ACOUSTICS, Brisbane, Australia, 2016, pp. 1–9.

[31] P. Scott, UNCERTAINTY IN MEASUREMENT: NOISE AND HOW TO DEAL WITH IT, 2003. URL http://physics.ucsc.edu/~drip/133/ch2.pdf

Article F

The paper presented in this appendix was originally submitted to a journal.

Information of the publication:

Towards Robust & Stochastic MPC: a comparison of Tube-Based and Chance Constrained MPC methods*

Jan Lorenz Svensen[a,*], Congcong Sun[b], Gabriela Cembrano[b,c], Vicenç Puig[b]

[a]*Department of Applied Mathematics and Computer Science, Technical University of Denmark, Richard Petersens Plads 324, 2800 Kongens Lyngby, Denmark*
[b]*Advanced Control Systems Group, the Institut de Robòtica i Informtica Industrial (CSIC-UPC), Llorens i Artigas, 4-6, 08028 Barcelona, Spain*
[c]*CETaqua, Water Technology Centre, Barcelona, 08904, Spain*

Abstract

Model Predictive Control (MPC) has become a mature approach being researched and applied in many different domains, such as the field of urban drainage considered as application case study in this paper. Within the MPC applications, an important aspect to deal with is the presence of uncertainty in models and/or disturbances. Two families of MPC exist, the robust MPCs and stochastic MPCs, which considers the uncertainties during the optimization process, each with their own approach to model uncertainty. These two families of approaches to handle uncertainty have both similarities and differences depending on which specific methods are considered. But, how different and similar the families really are, is still a question to be addressed. Under this consideration, in this paper, we discuss the two MPC families through comparing tube-based and chance constrained MPC approaches because of some similiraties in the way of dealing with uncertainty bounds. The analysis has been done by comparing their general mathematical methods, with a focus on their constraint formulations for specific methods. Afterwards, the performance has been compared through optimising the combined sewer overflow problems in urban drainage systems using the Astlingen model. The obtained results confirm great similarity in their general formulations and concepts, with some differences in the involved mathematical computations. Furthermore, the performance comparison results indicates which MPC method best suited for different type of considered uncertainty.

Keywords: Robust MPC, tube-based, Stochastic MPC, chance constrained, Astlingen sewer network

1. Introduction

Model Predictive Control (MPC) has, since its conception[1], been proved as an effective method for multivariable constrained control problems, due to its capacity of handling multi-input and multi-output control systems under certain performances and operational objectives. In this time, MPC has been matured to a well-researched field of study, covering from the original linear-quadratic problems to nonlinear and mixed-integer problems[1]-[35]. A research field within MPC is the handling of the presence of uncertainty in the controlled

system[18]-[35]. Depending on the approach to handle uncertainty, the MPC reasearch can be grouped into two general families of methods; the robust MPCs and the stochastic MPCs.

The robust MPCs utilize knowledge about the set that bounds the uncertainty realizations, and consider the worst-case of the constraints and occasionally the cost function[21, 28]-[35]. There are plenty of methods on how to design robust MPC. The easiest way relies on exploiting the inherent robustness of MPC, where the open-loop control action is determined without explicitly considering uncertainties affecting the system [4, 5]. However, due to the possible reduction of the control performance and to guarantee the feasibiliy and closed-loop stability, feedback control can be designed to explicitly consider uncertainty[30, 31]. With this aim, min-max MPC is a standard approach to include robustness in MPC. But, it typically leads to quite conservative results because it considers all possible (worst-case) disturbance realizations[35] and the computational load is, in general, also intractable[32]. In contrast to these approaches, a type of MPC design, which can deal with robustness with conservatism and reasonable computational load is required. The tube-based MPC (T-MPC)[21, 28, 29] which bounds the uncertainty deviation through a sequence of invariant sets (so called tubes) in the state space can meet these requirements[33, 34]. This is the main motivation of considering T-MPC in this paper.

On the other hand, considering the fact that system uncertainties usually have probabilistic characteristics, stochastic MPC which takes into account the probabilistic nature of the uncertainties in the controller design[20] is helpful. Stochastic MPC utilizes the knowledge about the stochastic distribution of the uncertainty to ensure the computed control satisfies the constraints for the most likely realizations [20]-[27]. Stochastic MPC includes many approaches, from the scenario-based MPC[27] approximating the robust approach to the chance constrained MPC (CC-MPC), whose probabilistic constraint tightenings consider violation probability under a chosen confidence level. Given that the CC-MPC approach has been used successfully in different domains with promising results[18, 24]-[26], it will therefore be the stochastic approach considered in this paper.

The T- and CC-MPC present some similiraties in their handling of the uncertainty. Both consider the uncertainty restricted to some set of values, but requiring different type of knowledge (interval vs probabilistic distribution). The question is then how different and similar the approaches really are? This paper contributes to discuss this question through comparisons of the two methods, the T- and CC-MPC, theoretically and practically:

1. A general comparison of their mathematical formulations is provided to show what are their strengths and weakness, respectively.

2. A comparison of the constraint formulations is provided, in the context of two specific methods; discussing how uncertainty propagates and is included in the constraints, and how the methods relates to each other.

3. A mathematical comparison of a proposed chanced-constrained T-MPC method with T-MPC and CC-MPC is presented.

4. A performance comparison of the two specific MPC methods in solving the combined sewer overflow (CSO) problems in an urban drainage system is included. A well-known benchmark, the Astlingen urban drainage network, is used as case study[17, 36], simulated using a SWMM[1] simulator.

5. A comparative discussion is also given to clarify which MPC approach is best suited under different type of considered uncertainty.

1.1. Nomenclature

In this paper, the following notations are used. Vectors are denoted by bold font, while the dimension of a function or variable $\mathbf{f}$ is given by n_f. The minimum and maximum of a given function $f(x)$ are noted by $\underline{f}$ and $\overline{f}$ respectively, while the sampling time and sample number is denoted by ΔT and the subscript k, respectively. A stochastic variable X following a distribution F is written by $X \sim F$, while its expectation is given by

---

[1]EPA's Storm Water Manegement Model

$E\{X\}$. The probablity function for the value of x is denoted by $Pr\{X \leq x\}$, likewise the cumulative distribution function (CDF) is given by $\Phi_X\{x\}$.

2. Tube-based MPC and Chance Constrained MPC - generic formulation

Before considering the general aspects of T-MPC and CC-MPC, let us begin with defining a generic formulation of MPC for the deterministic case. MPC consists of a minimization of a cost l (typically, linear or quadratic) defined over the prediction horizon H_p subject to the constraints consisting of a process function $\mathbf{f} : \mathbb{R}^{n_x+n_u+n_w} \rightarrow \mathbb{R}^{n_x}$ and an inquality constraint function $\mathbf{g} : \mathbb{R}^{n_x+n_u+n_w} \rightarrow \mathbb{R}^{n_g}$, as given by

$$J = \min_{\mathbf{u}} l(\mathbf{x}, \mathbf{u}, \mathbf{w}) \tag{1}$$

$s.t.$

$$\mathbf{x}_{i+1|k} = \mathbf{f}(\mathbf{x}_{i|k}, \mathbf{u}_{i|k}, \mathbf{w}_{i|k}) \tag{2}$$
$$\mathbf{g}(\mathbf{x}_{i|k}, \mathbf{u}_{i|k}, \mathbf{w}_{i|k}) \leq \overline{\mathbf{g}}, \quad \forall i \leq H_p \tag{3}$$

where $\mathbf{x}$ is the predicted states, $\mathbf{u}$ is the manipulated control, and $\mathbf{w}$ is the disturbance across the prediction horizon from time k, while $\mathbf{x}_{0|k}$ is the known initial state at time k.

In its general formulation, T-MPC is similar to other robust MPC methods and formulated as seen in (4) or (5). For robust MPCs, the uncertainty in the disturbances $\mathbf{w}$ is only considered to be bounded within a known set $\mathcal{W} \subseteq \mathbb{R}^{n_w \times H_p}$, considering the worst-case effect on the systems. The given formulations is for two approaches to uncertainties in the cost function, worst-case(left) and nominal (right)[21]. The cost in the prior case is defined by the maximization of the cost with respect to the disturbance $\mathbf{w}$. In the latter case, the nominal cost is intepreted as the cost based on the expected disturbance and the nominal states x_{nom}

$$J = \min_{\mathbf{u}} \max_{\mathbf{w} \in \mathcal{W}} l(\mathbf{x}, \mathbf{u}, \mathbf{w}) \tag{4}$$

$s.t.$

$$\mathbf{x}_{i+1|k} = \mathbf{f}(\mathbf{x}_{i|k}, \mathbf{u}_{i|k}, \mathbf{w}_{i|k})$$
$$\max_{\mathbf{w}_{0|k},\dots\mathbf{w}_{i|k} \in \mathcal{W}_{0|k} \times \dots \times \mathcal{W}_{i|k}} \mathbf{g}(\mathbf{x}_{i|k}, \mathbf{u}_{i|k}, \mathbf{w}_{i|k}) \leq \overline{\mathbf{g}}$$

$$J = \min_{\mathbf{u}} l(\mathbf{x}_{nom}, \mathbf{u}, E\{\mathbf{w}\}) \tag{5}$$

$s.t.$

$$\mathbf{x}_{i+1|k} = \mathbf{f}(\mathbf{x}_{i|k}, \mathbf{u}_{i|k}, \mathbf{w}_{i|k})$$
$$\max_{\mathbf{w}_{0|k},\dots\mathbf{w}_{i|k} \in \mathcal{W}_{0|k} \times \dots \times \mathcal{W}_{i|k}} \mathbf{g}(\mathbf{x}_{i|k}, \mathbf{u}_{i|k}, \mathbf{w}_{i|k}) \leq \overline{\mathbf{g}}$$

where the maximization of the constraints, can be intepreted both as a n_g maximizations of the individual constraints or as maximizations over several constraints. The set $\mathcal{W}$ bounding the disturbance $\mathbf{w}$ is a tube consisting of temporal sets $\mathcal{W}_{i|k}$ following:

$$\mathcal{W}_{i|k} = \{\mathbf{w}_{i|k} : \underline{\mathbf{w}}_{i|k} \leq \mathbf{w}_{i|k} \leq \overline{\mathbf{w}}_{i|k}\} \subseteq \mathbb{R}^{n_w} \tag{6}$$

each corresponding to the disturbances $\mathbf{w}_{i|k}$ at the i-th prediction.

On the other hand, where the robust MPCs were reliant on knowing the workspace of disturbances, the CC-MPC approach is based on stochastic knowledge of the uncertainty $\mathbf{w}$ that assumes a known probability distribution, $\mathbf{w} \sim F$. In the formulation of CC-MPC, the cost function is typically given as the expected cost[21, 24], while the constraint set is expressed as probabilistic constraints, as given below

$$J = \min_{\mathbf{u}} \mathbb{E}\{l(\mathbf{x}, \mathbf{u}, \mathbf{w})\} \tag{7}$$

$s.t.$

$$\mathbf{x}_{i+1|k} = \mathbf{f}(\mathbf{x}_{i|k}, \mathbf{u}_{i|k}, \mathbf{w}_{i|k}) \tag{8}$$
$$Pr\{\mathbf{g}(\mathbf{x}_{i|k}, \mathbf{u}_{i|k}, \mathbf{w}_{i|k}) \leq \overline{\mathbf{g}}\} \geq \gamma \tag{9}$$
$$\Longleftrightarrow \Phi^{-1}_{\mathbf{g}(\mathbf{x}_{i|k}, \mathbf{u}_{i|k}, \mathbf{w}_{i|k})}\{\gamma\} \leq \overline{\mathbf{g}} \tag{10}$$

where γ is the chosen confidence level, defining how robust the solution should be with respect to the stochastic nature of the disturbances. Typically, the probabilistic constraints are defined in terms of their quantile function as is shown in (10). As with the maximization constraints before, the probabilistic constraints can be intepreted as probabilities on the individual constraints or as joint probability on the group of constraints.

From the general formulations given above, the different ways to treat uncertainty in both MPC approaches can clearly be seen. In case of the T-MPC, each possible realization of the disturbances is considered, resulting in very conservative solutions (worst-case). For most cases,

this also makes the T-MPC very dependent on the existence of finite bounds on the uncertainty set. This dependency can be illustrated as the disturbance term either having a natural bound independent of the disturbance as e.g. a periodic behavior modelled as $sin(w)$ as seen in (11), or being unbounded in nature such as e.g. a linear model, where the bound is needed to do maximization.

$$\max_{w} sin(w) = 1 \qquad (11)$$

In constrast, the CC-MPC fundamentally relies on the assumption of the distribution of the disturbances being a known quantity. For most scenarios of constraint functions and uncertainty distributions, the probabilistic constraints increase the computational difficulties of the optimization, through the computation of the distributions of the constraints, and their's corresponding quantile functions.

Regarding the cost formulations, it can be seen that their complexity compared to each other, depends on the order of the cost $l(\cdot)$. For example, if the cost is linear, then the nominal and expected are identical, while for quadratic they are equivalent, if the variance is independet of optimization, and likewise for more nonlinear costs the expectation becomes more complex, which is similar for maximization.

These drawbacks can also be interpreted as benefits of the tube-based MPC that involves simpler computations without requiring the propagation of distributions. However, the CC-MPC presents the benefits of handling unbounded uncertainties and having a tunable degree of conservatism, through the chosen confidence level γ of the probabilistic constraint.

The T-MPC's reliance on the entire bounding set of the disturbances, can in stochastic terms of the CC-MPC be intepredet as assuming a uniform distribution of the disturbances within its boundaries, where all realization is just as likely and important for consideration. In the context of a probilistic constraint, this would correspond to a confidense level γ of 1.

3. Tube-based MPC and Chance Constrained MPC - Constraints Comparison

From the discussion of the general formulation given above, it is clear that the uncertainty is treated differently in the two different types of MPC. In order to understand how differently the treatment of the uncertainty really is, a mathematical comparison of the constraint formulation is discussed in this section. For simplicity, we will consider a linear system with additive uncertainty as given below, and we will consider the maximization and probabilistic constraints being defined in the form of individual scalar constraints

$$f(\mathbf{x}_{i|k}, \mathbf{u}_{i|k}, \mathbf{w}_{i|k}) = A\mathbf{x}_{i|k} + B\mathbf{u}_{i|k} + G\mathbf{w}_{i|k} \quad (12)$$

$$\begin{aligned} g_j(\mathbf{x}_{i|k}, \mathbf{u}_{i|k}, \mathbf{w}_{i|k}) = \boldsymbol{\Psi}_{i,j}\mathbf{x}_{i|k} + \boldsymbol{\Gamma}_{i,j}\mathbf{u}_{i|k} \\ + \boldsymbol{\Theta}_{i,j}\mathbf{w}(i|k) \le \phi_{i,j} \end{aligned} \quad (13)$$

where

$$A \in \mathbb{R}^{n_x \times n_x}, B \in \mathbb{R}^{n_x \times n_u}, G \in \mathbb{R}^{n_x \times n_d} \qquad (14)$$

and

$$\boldsymbol{\Psi}_{i,j} \in \mathbb{R}^{1 \times n_x}, \boldsymbol{\Gamma}_{i,j} \in \mathbb{R}^{1 \times n_u}, \boldsymbol{\Theta}_{i,j} \in \mathbb{R}^{1 \times n_d}, \phi_{i,j} \in \mathbb{R} \qquad (15)$$

The i-th step prediction of the system states is given by (12), while the j-th scalar constraint at the i-th step is given by (13). By propagation of (12), the i-th predicted states can be formulated in terms of the initial states, as follows

$$\mathbf{x}_{i|k} = A^i\mathbf{x}_{0|k} + \sum_{j=0}^{i-1} A^{i-1-j}B\mathbf{u}_{j|k} + \sum_{j=0}^{i-1} A^{i-1-j}G\mathbf{w}_{j|k} \qquad (16)$$

And through substitution of (16) into (13), the propagated version of the j-th constraint becomes

$$\boldsymbol{\Psi}_{i,j}A^i\mathbf{x}_{0|k} + \boldsymbol{\Psi}_{i,j} \sum_{j=0}^{i-1} A^{i-1-j}B\mathbf{u}_{j|k} + \boldsymbol{\Gamma}_{i,j}\mathbf{u}_{i|k}$$

$$+ \boldsymbol{\Psi}_{i,j} \sum_{j=0}^{i-1} A^{i-1-j}G\mathbf{w}_{j|k} + \boldsymbol{\Theta}_{i,j}\mathbf{w}_{i|k} \le \phi_{i,j}$$

$$(17)$$

From the constraint given by (17), we can formulate a compact notation of the predicted disturbances and control variables as follows

$$\mathbf{W}_{i|k} = [\mathbf{w}_{0|k}^T \quad \mathbf{w}_{1|k}^T \quad \dots \quad \mathbf{w}_{i|k}^T]^T \qquad (18)$$
$$\mathbf{U}_{i|k} = [\mathbf{u}_{0|k}^T \quad \mathbf{u}_{1|k}^T \quad \dots \quad \mathbf{u}_{i|k}^T]^T \qquad (19)$$

and with the corresponding constraint terms being

$$\tilde{\boldsymbol{\Theta}}_{i,j} = [\boldsymbol{\Psi}_{i,j}A^{i-1}G \quad \boldsymbol{\Psi}_{i,j}A^{i-2}G \dots \boldsymbol{\Psi}_{i,j}G \quad \boldsymbol{\Theta}_{i,j}] \qquad (20)$$

$$\tilde{\boldsymbol{\Gamma}}_{i,j} = [\boldsymbol{\Psi}_{i,j}A^{i-1}B \quad \boldsymbol{\Psi}_{i,j}A^{i-2}B \dots \boldsymbol{\Psi}_{i,j}B \quad \boldsymbol{\Gamma}_{i,j}] \qquad (21)$$

The j-th constraint can then be stated in the following compact notation for the i-th prediction

$$\boldsymbol{\Psi}_{i,j}A^i\mathbf{x}_{0|k} + \tilde{\boldsymbol{\Gamma}}_{i,j}\mathbf{U}_{i|k} + \tilde{\boldsymbol{\Theta}}_{i,j}\mathbf{W}_{i|k} \leq \phi_{i,j} \qquad (22)$$

3.1. Tube-Based MPC

For T-MPC, there are many approaches on how to define the tube approach used in solving the maximization of the constraints[21]. For the comparison given here, we will use a tube approach[29] based on zonotopes[37]. We will consider the initial state $\mathbf{x}_{0|k}$ and the disturbances $\mathbf{W}_{i|k}$ of the system as the uncertain terms in the constraints. Let us define them in terms of an expected known part $(\tilde{\mathbf{x}}_{0|k}, \tilde{\mathbf{W}}_{i|k})$ and a unknown uncertain part $(\Delta\mathbf{x}_{0|k}, \Delta\mathbf{W}_{i|k})$. The unkown part is assumed symmetrically bounded, and the expected part is defined as the mean of the bounds on the uncertainty, as seen in (23) and (24), such that the bounding set of the unknown part corresponds to a translation of the original bounding set. We can collect these terms in a general uncertainty $\mathbf{Z}_{i|k}$ for the i-th prediction, and formulate it as a zonotope as shown in (25)

$$\mathbf{W}_{i|k} = \tilde{\mathbf{W}}_{i|k} + \Delta\mathbf{W}_{i|k}, \quad \tilde{\mathbf{W}}_{i|k} = \frac{1}{2}(\overline{\mathbf{W}}_{i|k} + \underline{\mathbf{W}}_{i|k}),$$
$$\Delta\mathbf{W}_{i|k} \in [-\overline{\Delta\mathbf{W}}_{i|k}, \overline{\Delta\mathbf{W}}_{i|k}] \qquad (23)$$

$$\mathbf{x}_{0|k} = \tilde{\mathbf{x}}_{0|k} + \Delta\mathbf{x}_{0|k}, \quad \tilde{\mathbf{x}}_{0|k} = \frac{1}{2}(\overline{\mathbf{x}}_{0|k} + \underline{\mathbf{x}}_{0|k}),$$
$$\Delta\mathbf{x}_{0|k} \in [-\overline{\Delta\mathbf{x}}_{0|k}, \overline{\Delta\mathbf{x}}_{0|k}] \qquad (24)$$

$$\mathbf{Z}_{i|k} = [\mathbf{x}_{0|k}^T, \mathbf{W}_{i|k}^T]^T, \quad \Delta\mathbf{Z}_{i|k} \in \mathbf{0} \oplus H_{z,i}\mathbf{z}_{d,i} \qquad (25)$$

where: $H_{z,i}$ is a diagonal matrix defined as

$$H_{z,i} = diag(\overline{\Delta\mathbf{x}}_{0|k}, \overline{\Delta\mathbf{w}}_{0|k}, \dots, \overline{\Delta\mathbf{w}}_{i|k}) \qquad (26)$$

and

$$\mathbf{z}_{d,i} \in \mathcal{B}^{n_x + (i+1) \times n_d} \qquad (27)$$

where $\mathcal{B} = [-1, 1]$, $\oplus$ denotes the Minkowski sum and the $\mathbf{0}$-vector is the center of the zonotope. With the uncertainty zonotope $\Delta\mathbf{Z}_{i|k}$ and expected part $\tilde{\mathbf{Z}}_{i|k}$ defined, the j-th constraint can be written in terms of the uncertainty $\mathbf{Z}_{i|k}$

$$[\boldsymbol{\Psi}_{i,j}A^i \quad \tilde{\boldsymbol{\Theta}}_{i,j}]\tilde{\mathbf{Z}}_{i|k} + [\boldsymbol{\Psi}_{i,j}A^i \quad \tilde{\boldsymbol{\Theta}}_{i,j}]\Delta\mathbf{Z}_{i|k}$$
$$+ \tilde{\boldsymbol{\Gamma}}_{i,j}\mathbf{U}_{i|k} \leq \phi_{i,j} \qquad (28)$$

The propagated uncertainty in the constraint can then be formulated as a zonotope $\Delta_{i,j}$ with the below definition and reformulated constraint

$$\Delta_{i,j} = \mathbf{0} \oplus [\boldsymbol{\Psi}_{i,j}A^i \quad \tilde{\boldsymbol{\Theta}}_{i,j}]H_{z,i}\mathbf{z}_{d,i} \qquad (29)$$
$$[\boldsymbol{\Psi}_{i,j}A^i \quad \tilde{\boldsymbol{\Theta}}_{i,j}]\tilde{\mathbf{Z}}_{i|k} + \tilde{\boldsymbol{\Gamma}}_{i,j}\mathbf{U}_{i|k} \leq \phi_{i,j} - \Delta_{i,j} \qquad (30)$$

With the zonotopes of the constraints defined, the constriction of the T-MPC constraints can be formulated. Using the 1-norm to compute the interval hull of the zonotope[29], the largest possible value of $\Delta_{i,j}$ can be found, as follows

$$\Delta_{i,j} = \|[\boldsymbol{\Psi}_{i,j}A^i \quad \tilde{\boldsymbol{\Theta}}_{i,j}]H_{z,i}\|_1 \quad i \geq 0 \qquad (31)$$

3.2. Chance Constrained MPC

Following the CC-MPC definition in (7)-(10), the j-th constraint of the i-th prediction is given below as the probability of the constraint being true

$$Pr\{\boldsymbol{\Psi}_{i,j}\mathbf{x}_{i|k} + \boldsymbol{\Gamma}_{i,j}\mathbf{u}_{i|k} + \boldsymbol{\Theta}_{i,j}\mathbf{w}_{i|k} \leq \phi_{i,j}\} \geq \gamma_{i,j} \qquad (32)$$

Similarly, to the T-MPC, the constraint can be rewritten using the proposed propagation in (16). If we use the same notation as in (16)-(21), the constraint can be rewritten as

$$Pr\{\boldsymbol{\Psi}_{i,j}A^{i-1}\mathbf{x}_{0|k} + \tilde{\boldsymbol{\Gamma}}_{i,j}\mathbf{U}_{i|k} + \tilde{\boldsymbol{\Theta}}_{i,j}\mathbf{W}_{i|k} \leq \phi_{i,j}\} \geq \gamma_{i,j} \qquad (33)$$

or in terms of the uncertainty $\mathbf{Z}_{i|k}$

$$Pr\{[\boldsymbol{\Psi}_{i,j}A^{i-1} \quad \tilde{\boldsymbol{\Theta}}_{i,j}]\mathbf{Z}_{i|k} \leq \phi_{i,j} - \tilde{\boldsymbol{\Gamma}}_{i,j}\mathbf{U}_{i|k}\} \geq \gamma_{i,j} \qquad (34)$$

In CC-MPC, as mentioned, it is assumed that the uncertainties follow some stochastic distribution F, defined by the parameters $\boldsymbol{\theta}$, in the intervals between $\mathbf{a}$ and $\mathbf{b}$

$$\mathbf{Z}_{i|k} \sim F_{\mathbf{a}}^{\mathbf{b}}(\boldsymbol{\theta}), \quad \mathbf{a} \leq \mathbf{b} \qquad (35)$$

where the interval of the distribution can be open or not ($\mathbf{a}$ and/or $\mathbf{b}$ or neither are infinite). From (34), we can reformulate the probabilistic constraint in a deterministic way by using the quantile function

$$\tilde{\boldsymbol{\Gamma}}_{i,j}\mathbf{U}_{i|k} \leq \phi_{i,j} - \Phi^{-1}_{[\boldsymbol{\Psi}_{i,j}A^{i-1} \quad \tilde{\boldsymbol{\Theta}}_{i,j}]\mathbf{z}_{i|k}}\{\gamma_{i,j}\} \quad (36)$$

where the quantile function can be considered to be constricting the constraint.

As discussed earlier, the approach used in T-MPC assumes the disturbances are uniformly distributed within the intervals between $\mathbf{a}$ and $\mathbf{b}$, as

$$\begin{aligned}
\mathbf{Z}_{i|k} &\sim \mathcal{U}(\mathbf{a},\mathbf{b}), \\
(\mathbf{a},\mathbf{b}) &= (\tilde{\mathbf{Z}}_{i|k} - \overline{\Delta \mathbf{Z}}_{i|k}, \tilde{\mathbf{Z}}_{i|k} + \overline{\Delta \mathbf{Z}}_{i|k})
\end{aligned} \qquad (37)$$

Based on the above analysis of the constraint formulations, we can formulate a relation between the constraint constrictions of the two types of MPCs, as given by Theorem 1

Theorem 1. *For the zonotope-based T-MPC, let us consider the expected part $\tilde{\boldsymbol{Z}}_{i|k}$ of the disturbance as part of the constraint constriction for the T-MPC, and the constraint's distribution used by the CC-MPC to be upper bounded, then the constraint constriction of the two MPCs is related by*

$$\begin{aligned}
&\Phi^{-1}_{[\boldsymbol{\Psi}_{i,j}A^{i-1} \quad \tilde{\boldsymbol{\Theta}}_{i,j}]\boldsymbol{Z}_{i|k}}\{\gamma_{i,j}\} \leq [\boldsymbol{\Psi}_{i,j}A^{i-1} \quad \tilde{\boldsymbol{\Theta}}_{i,j}]\tilde{\boldsymbol{Z}}_{i|k} \\
&+ \|[\boldsymbol{\Psi}_{i,j}A^{i-1} \quad \tilde{\boldsymbol{\Theta}}_{i,j}]H_{z,i}\|_1 \quad \forall \gamma_{i,j} \in [0,1] \quad (38)
\end{aligned}$$

with the two sides being identical at $\gamma_{i,j} = 1$.

Proof 1. *Considering the fact that for any upper bounded stochastic variable X of some distribution F_a^b, the quantile with a lower confidence level γ_1 is smaller that the quantile with a higher confidence level γ_2, it naturally follows that a confidence level of 1 corresponds to the upper bound of*

the variable.

$$X \sim F_a^b(\boldsymbol{\theta}), \quad a \leq X \leq b \qquad (39)$$
$$\begin{aligned}
\Phi_X^{-1}\{\gamma_1\} \leq &\Phi_X^{-1}\{\gamma_2\} \leq \Phi_X^{-1}\{1\} = b, \\
&0 \leq \gamma_1 \leq \gamma_2 \leq 1
\end{aligned} \qquad (40)$$

Given that the constraintment of the right hand side of (38) corresponds to the upper bound of the constraint's uncertainty, the right hand side are therefore, equal or larger than the quantile function of any distribution for the given variable.

Although the approaches for handling uncertainty appear very different at first glance as we discussed in Section 2, the propagation of the uncertainty through the system is the same for both types of MPCs. Moreover, we have realized that the T-MPC's approach corresponds to a general assumption of a bounded uniform distribution, while the CC-MPC assumes the exact distribution to be known. This difference in assumptions leads to both the more conservative constriction of the tube-based MPC, but also the more computationally complex optimization of the CC-MPC, depending on the exact distribution.

4. Tube-based MPC with Chance Constrained bounds

For any given constraint set and uncertainty distribution, bounded or not, it would be beneficial if the chosen MPC could be simple to compute, while also providing less conservative solutions than worst-case. As discussed earlier, the T-MPC is simpler to compute but has the main issue of being worst-case conservative and not being defined for unbounded uncertainties, while the CC-MPC quickly becomes hard to compute, but handles unbounded distributions at an arbitary level of conservatism.

Combining the T-MPC with the probabilistic approach of CC-MPC can be done in several ways[28] to deal with the issues of both MPC types. A simple approach to formulating a probabilistic bounded T-MPC is defining the utilized bounds ($\underline{\mathbf{w}},\overline{\mathbf{w}}$) on the uncertainty as scalar or joint

probabilities of the disturbances with a chosen criterion γ, by assuming a distribution for each disturbance $w_i \sim F_i$ (uniform, normal, etc.)

$$Pr\{\mathbf{w} \geq \overline{\mathbf{w}}\} \geq \gamma \tag{41}$$

$$Pr\{\underline{\mathbf{w}} \leq \mathbf{w}\} \geq \gamma \tag{42}$$

This provides the minimum upper bound and the maximum lower bound needed to cover the disturbances with probability γ:

$$\overline{\mathbf{w}} \geq \Phi_{\mathbf{w}}^{-1}\{\gamma\} \tag{43}$$

$$\underline{\mathbf{w}} \leq -\Phi_{-\mathbf{w}}^{-1}\{\gamma\} \tag{44}$$

This approach allows for the knowledge of the uncertainty distribution to be incorporated, but it can also be used with only knowledge of bounds through an assumption of uniform distribution. Furthermore, it does not propagate the distribution through the dynamics to the constraint, therefore keeping the computation of the optimum as simple as the T-MPC discussed earlier. The general formulation of the chance constrained bounded robust MPC approach can then be written as below for the worst-case cost

$$J = \min_{\mathbf{u}} \max_{\mathbf{w}} l(\mathbf{x}, \mathbf{u}, \mathbf{w}) \tag{45}$$

$$s.t.$$

$$\mathbf{x}_{i+1|k} = \mathbf{f}(\mathbf{x}_{i|k}, \mathbf{u}_{i|k}, \mathbf{w}_{i|k}) \tag{46}$$

$$\max_{\mathbf{w}} \mathbf{g}(\mathbf{u}, \mathbf{w}) \leq \bar{\mathbf{g}} \tag{47}$$

$$-\Phi_{-\mathbf{w}}^{-1}\{\gamma\} \leq \mathbf{w} \leq \Phi_{\mathbf{w}}^{-1}\{\gamma\} \tag{48}$$

The solution of the CC bound T-MPC is less conservative than the original T-MPC when the original maximization of the constraint corresponds to a disturbance $\mathbf{w}$ outside the stochastic bounds; otherwise, the solution is the same as the original T-MPC. In comparison to the CC-MPC, the formulation only utilizes the knowledge of the distribution on the bounds, while the CC-MPC covers the entire spectrum of the constraints. This leads to simpler computations in comparison to the CC-MPC.

With regards to the conservatism and CC-MPC, it is generally hard to predict which method is most conservative; due to the dependency of the quantile function on the constraint function. Under some conditions, it is given that the CC-MPC is the least conservative for the chosen probability criterion. For example, if the constriction of the CC-MPC corresponds to the constraint with a disturbance realization $\mathbf{w}^{\Phi}$; lying in the uncertainty set defined by (48) as given below, then it is clear that the CC bound T-MPC has considered the given realization, and therefore is more or equally conservative

$$\Phi_{\mathbf{g}(\mathbf{u},\mathbf{w})}^{-1}\{\gamma\} \equiv \mathbf{g}(\mathbf{u}, \mathbf{w}^{\Phi}) \tag{49}$$

$$-\Phi_{-\mathbf{w}}^{-1} \leq \mathbf{w}^{\Phi} \leq \Phi_{\mathbf{w}}^{-1} \tag{50}$$

For some constraint functions, this can be shown to be true in general. An example of such is given below for joint probabilities, and the set of invertible constraint functions (linear and nonlinear).

Example 1. *Consider the set of fully invertible constraint functions $\mathbf{g}(\mathbf{u}, \mathbf{w}) \in \mathbb{R}^n$ on the domain of $\mathbf{w} \in \mathbb{W}^m$ as described by*

$$\mathbf{g}(\mathbf{u}, \mathbf{w}) = \mathbf{y} \tag{51}$$

$$\mathbf{g}^{-1}(\mathbf{u}, \mathbf{g}(\mathbf{u}, \mathbf{w})) = \mathbf{w} \in \mathbb{W}^w, \forall \mathbf{u} \in \mathbb{U} \tag{52}$$

$$\mathbf{g}(\mathbf{u}, \mathbf{g}^{-1}(\mathbf{u}, \mathbf{y})) = \mathbf{y}, \forall \mathbf{u} \in \mathbb{U} \tag{53}$$

with the relations to inequalities and inversion given by

$$\mathbf{g}(\mathbf{u}, \mathbf{w}) \leq \bar{\mathbf{g}} \Leftrightarrow a_1 \mathbf{w} \leq a_2 \mathbf{g}^{-1}(\mathbf{u}, \bar{\mathbf{g}}), \exists \mathbf{u} \in \mathbb{U} \tag{54}$$

$$a_{1,i,j}, a_{2,i,j} = \begin{cases} 0 & i \neq j \\ 1 \\ -1 \end{cases} \tag{55}$$

where the parameters $a_{k,i,j}$ depend on the specific constraint function, and are introduced to preserve the used inequality notation.

Let us define the probability constraint of the CC-MPC as a joint probability across the constraints, and reformulate it accordingly to (54):

$$Pr\{\mathbf{g}(\mathbf{u}, \mathbf{w}) \leq \bar{\mathbf{g}}\} = Pr\{a_1 \mathbf{w} \leq a_2 \mathbf{g}^{-1}(\mathbf{u}, \bar{\mathbf{g}})\} \geq \gamma \tag{56}$$

and formulated using the appropriate quantile function for the joint probability as

$$a_2 \mathbf{g}^{-1}(\mathbf{u}, \bar{\mathbf{g}}) \geq \Phi_{a_1 \mathbf{w}}^{-1}\{\gamma\} \tag{57}$$

Given that $a_1^2 = I$, we can inject a_1^2 into the right-hand side of (57), obtaining the same form as in (54). We can now reverse the invertion of the inequality constraint from (56)

$$a_1(a_1 \Phi_{a_1 w}^{-1}\{\gamma\}) \leq a_2 \boldsymbol{g}^{-1}(\boldsymbol{u}, \overline{\boldsymbol{g}})$$
$$\Longleftrightarrow \boldsymbol{g}(\boldsymbol{u}, a_1 \Phi_{a_1 w}^{-1}\{\gamma\}) \leq \overline{\boldsymbol{g}} \qquad (58)$$

Depending on whether the elements of a_1 is positive or negative, we can see that the obtained constraints corresponds to a disturbance realization $\boldsymbol{w}^\Phi$ equal to the upper or lower bounds of the disturbance workspace in the probabilistic T-MPC (47)-(48). This case correponds to an example in which (49)-(50) are true.

The formulation of the constriction of CC-MPC given in (58) can in general be considered to be utilized in standard CC-MPC, as a way to ease the computation of the quantile function of joint probabilities, when the constraint function is invertible.

5. Performance Comparison: Simulation Setup

In the previous sections, we have compared and discussed the mathematical differences and similarities of T-MPC and CC-MPC, even considering possible combinations of the two methods approaches to uncertainty, for fixing drawbacks. While these discussions have all been theoretical, we will in the next few sections focus on a more practical oriented performance comparison, based on simulations. In particular, the T-MPC approach and CC-MPC, discussed in Section 3, will be compared to the performance achieved by means of an appropriate standard MPC without uncertainty (perfect MPC).

5.1. Urban Drainage

Urban drainage system is a critical infrastructure in modern cities, which carries wastewater and rainwater to be treated in the wastewater treatment plant (WWTP) before releasing them into the natural environment. However, when the combined water is out of the capacity of the system during storm weather, CSO occurs and
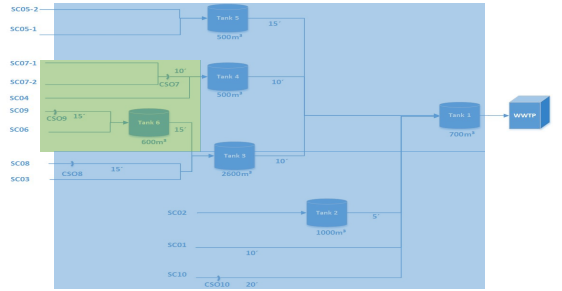

Figure 1: A schematic of the Astlingen system[36] showing the interconnections between tanks, CSO pipes and the WWTP, as well as pipe delays x' in minutes. The CSOs the creek receives comes from the green section, while the river receives CSO from the blue section.

brings serious pollution to the water ecosystem. MPC has been used as an important type of control approach to optimize CSO and protect the environment[38].

5.2. Case Study System

As application case study, we will utilize the Astlingen urban drainage system [36] in a setup of pySWMM and Matlab, where the controller is defined in Matlab, while the simulator is given in SWMM with connection to Matlab through the pySWMM Python package [17]. The Astlingen is a combined sewer network, carrying wastewater and rain together to a wastewater treatment plant (WWTP) as seen in Figure 1. It contains weir structures where CSOs may occur, located in water detentions (tank 1-6) and diversion structures (CSO 7-10). The system consists of two receiving bodies for CSO, a creek and a river, where the latter is the preferred receiver. It is also driven by the unknown rain inflow as disturbances.

For the design of the MPCs, the linear model of the Astlingen discussed in [18] is used. Furthermore, the uncertainty utilized in the simulations are normal distributed; the quantile functions of the constraints can therefore be written as

$$\Phi_{g_j(u,w)}^{-1}\{\gamma\} = E\{g_j(\mathbf{x}_{i|k}, \mathbf{u}_{i|k}, \mathbf{w}_{i|k})\}$$
$$+\sigma\{g_j(\mathbf{x}_{i|k}, \mathbf{u}_{i|k}, \mathbf{w}_{i|k})\}\Phi^{-1}\{\gamma\} \qquad (59)$$

where $\Phi^{-1}\{\gamma\}$ is the quantile of the standard normal distribution.

5.3. Constraint Formulation

When CC-MPC is applied directly, the presence of uncertainty in urban drainage systems gives issues with CSO definition and feasibility as discussed in [18,19], for the given case considering the needed revision of CC-MPC formulation. These issues are identical for both T-MPC and CC-MPC given they originates from the presence of the constraint constrictions. We can, therefore, use the same revision as was introduced for the CC-MPC on the T-MPC. As a simple example from the considered case study system, let us consider the constraints of a tank with controlled output

$$V_{i+1|k} = V_{i|k} + \Delta T(q_{i|k}^{in} - q_{i|k}^{u} - q_{i|k}^{CSO}) \quad (60)$$

$$0 \leq V_{i|k} + \Delta T(q_{i|k}^{in} - q_{i|k}^{u} - q_{i|k}^{CSO}) \leq \overline{V} \quad (61)$$

where the upper constraint defines the CSO of the tank, $q_{i|k}^{CSO}$ for the i-th prediction.

If we consider the volume $V_{i|k}$ and inflow $q_{i|k}^{in}$ to be uncertain, and the controlled outflow $q_{i|k}^{u}$ and CSO flow $q_{i|k}^{CSO}$ to be optimization variables, then the robust constraints become

$$\max(-V_{i|k} - \Delta T q_{i|k}^{in}) \leq -\Delta T(q_{i|k}^{u} + q_{i|k}^{CSO}) \quad (62)$$

$$\max(V_{i|k} + \Delta T q_{i|k}^{in}) - \Delta T(q_{i|k}^{u} + q_{i|k}^{CSO}) \leq \overline{V} \quad (63)$$

for the direct application of T-MPC. If we introduce the mentioned revisions from [19], then (63) can be divided into

$$\mathbb{E}\{V_{i|k} + \Delta T q_{i|k}^{in}\} - \Delta T(q_{i|k}^{u} + q_{i|k}^{CSO}) \leq \overline{V} \quad (64)$$

$$\max(V_{i|k} + \Delta T q_{i|k}^{in}) - \Delta T q_{i|k}^{u} - c_{i|k} \leq \overline{V} \quad (65)$$

The first being a constraint defining the CSO flows, based on some expected value of the uncertainty, while the latter formulates the robustness of avoiding CSO. The robust constraint introduces an unbound slack variable c for guaranteeing feasibility. For the lower constraint in (62), the revised version can be obtained by introducing a bounded slack variable s for the feasibility issue

$$\max(-V_{i|k} - \Delta T q_{i|k}^{in}) - s_{i|k} \leq -\Delta T(q_{i|k}^{u} + q_{i|k}^{CSO}) \quad (66)$$

$$s_{i|k} \leq \|\Delta V_{i|k} + \Delta T \Delta q_{i|k}^{in} k\|_1 \quad (67)$$

$$0 \leq s_{i|k}, c_{i|k} \quad (68)$$

where the upper bound on the slack variable s is set to equal to the constriction as discussed in (31)

For the simulations of T-MPC, the expected value in (64) is defined as the mean of the bounds of the uncertainty.

5.4. Cost formulation

In the simulations, the different MPCs will operate on the same basis cost function, with the only difference being the cost of slacks introduced by the revisions, discussed above. The cost function is the quadratic-linear program described in [18],where the CSO flows are detimined by the approximation through penalty costs[12, 14, 15] and only considering the inflow uncertainties. The terms in cost function are a quadratic cost given on the change of control flow. While linear cost is used for maximizing outflow to WWTP and minimizing CSO flow, with the latter ones giving higher priority. For the T-MPC, the outflow term of the cost is formulated as the maximum cost, while for the CC-MPC it is the expected cost.

6. Performance Comparison: Simulation Results

The simulations were performed using a one-year dataset. In the simulations, a prediction horizon of a 100 min was utilized with a sampling time of 5 min for all MPC types. In the simulations, the CC-MPC is utilized with a confidence level γ of 90% for all probabilistic constraints.

In each set of simulations, a single parameter was changed in order to compare the sensitivity between the controllers towards the given parameter, performance-wise. The parameters considered are the bound on the uncertainty, scaling bias of the expected disturbance and offset bias of the expected disturbance. For each parameter, a base value was chosen to be utilized in the simulation, when the parameter was not varied. The base values were chosen as 50% for the bound on uncertainty, 0% for the scaling bias and zero for the offset bias.

9

Table 1: Overflow results of the SWMM simulations with different Controllers: MPC and CC- and tube-based MPC with the uncertainty bound of 25-75%.

Tank & Pipes	MPC	CC-MPC 25%	T-MPC 25%	CC-MPC 50%	T-MPC 50%	CC-MPC 75%	T-MPC 75%
T1	93251	93067	85742	92927	89509	92795	92766
T2	15484	15543	18999	15544	17526	15544	16350
T3	34017	34267	32602	34313	33693	34067	34699
T4	4814	4814	7642	4814	6595	4814	5478
T5	15147	15147	15147	15147	15147	15147	15147
T6	37950	37939	41585	37946	39733	37673	38489
P7	4016	4016	4016	4015	4016	4016	4015
P8	16207	16203	16203	16191	16199	16207	16190
P9	4030	4029	4029	4029	4029	4030	4029
P10	4838	4839	4839	4842	4840	4838	4843
River	183754	183879	181174	183778	183509	183412	185473
Creek	45996	45984	49630	45990	47778	45718	46532
Total	229750	229864	230804	229768	231287	229130	232005
R. %		0.0680%	-1.4041%	0.0131%	-0.1333%	-0.1861%	0.9355%
C. %		-0.0261%	7.9007%	-0.0130%	3.8742%	-0.6044%	1.1653%
Tot. %		0.0496%	0.4588%	0.0078%	0.6690%	-0.2699%	0.9815%

Table 2: Treated Wastewater results of the SWMM simulations with different Controllers: MPC, and CC- and tube-based MPC with the uncertainty bound of 25-75%.

	MPC	CC-MPC 25%	T-MPC 25%	CC-MPC 50%	T-MPC 50%	CC-MPC 75%	T-MPC 75%
WWTP Vol.	3772057	3772086	3771026	3772159	3770439	3772676	3769809
Imp. %		0.0008%	-0.0273%	0.0027%	-0.0429%	0.0164%	-0.0596%
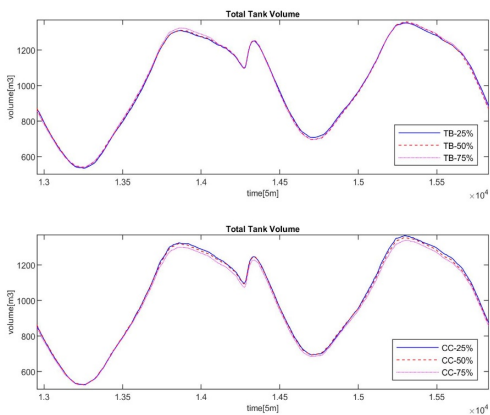
Figure 2: The total volume evolutions under T-MPC and CC-MPC with the uncertainty bounds of 25-75%.

6.1. Uncertainty Bound

The first parameter in the comparison is the bound on the uncertainty of the inflow disturbance q. The bound is defined by (69), where the disturbance is assumed to be non-negative and below three standard deviation σ above the expected inflow

$$\text{bound} = [0, \mathbb{E}\{q\} + 3\sigma] \tag{69}$$

In the simulations, the size of the standard deviation was varied so that the upper bound would correspond to 25%, 50% and 75% above the expected value. The results of simulations with each of the controller types with the three uncertainty bounds can be observed in Table 1 for CSO results and in Table 2 for treated wastewater volume results. In Table 1, we can see the total CSO

volume for each tank and pipe weirs, the CSO volume to the receiving bodies, the river and the creek, and as well as the total CSO volume for the system. Moreover, the percentage changes from the perfect MPC to the last three volumes are also given. In Table 2, the total amount of treated wastewater and the percental change is provided. From these comparisons, it can be observed that the CC-MPC performs slightly better than the T-MPC in the total CSO volume. Moreover, we can also conclude from Table 1 that the T-MPC perform worse as the uncertainty bound increases, while the CC-MPC works better with the increase in uncertainty bounds. Figure 2 also confirms this conclusion, wherethe total volume evolutions for all the tanks under MPCs with different uncertainty bounds are provided (in order to have clear evolution, only the day 10 and day 11 are presented). In this figure, the increasing uncertainty bounds for the CC-MPC, seems to result in less tank volumes, which indicate less possible CSOs. The T-MPC seems affected slightly by the changes of uncertainty bounds in the limits of the tank volume. The difference in how the MPC approaches are affected by the increase in uncertainty bound, is consistent and can be explained by their formulation; the CC-MPC becomes more strict or conservative. While the T-MPC expect more inflow (higher bound mean), as well as trying to be more strict, resulting in both increased and decreased local volumes internally in the system, and an increase in the entire system. With regard to the treated wastewater, we can see that both controllers are in general indifferent to the change of uncertainty bound.

6.2. Scaled Bias

The second compared parameter is the scaling bias of the expected disturbance in comparison to the actual disturbance, as given by (70). The factor a corresponds to a scaling bias k, by $a = 1 + k/100$. Therefore, the negative scaling biases indicates an underestimation of the actual disturbance and an overestimation for positive scaling biases
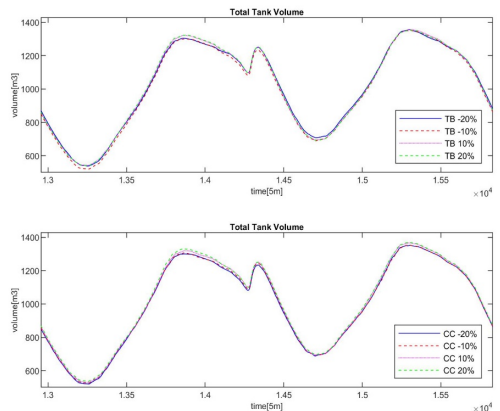
$$\mathbb{E}\{q\} = aq^{actual} \qquad (70)$$

Figure 3: The total volume evaluations for the tanks under T-MPC and CC-MPC with different scale bias.

When running the simulations, the following scaling biases have been utilized: 0%, ±10% and ±20%. The results of CSO volume and amount of treated wastewater can be seen in Table 3 and Table 4, respectively. It is clear that for both the T-MPC and the CC-MPC, the CSO performances are deteriorating as the scaling bias increases. Furthermore, it can also be seen, that the T-MPC perform slightly worse than both the perfect and CC-MPC. For the T-MPC, we again observe a deterioration of the distribution of the CSO, which is not seen for the CC-MPC. Figure 3 illustrates the conclusions graphically, where the total tank volume evolution for day 10 and day 11 are compared among MPC approaches with different scaled bias values. MPCs with 20% have larger tank volumes, which indicates more CSO may occur in the future. Actually, the figures appear very similar, but there is slight trend showing that the increase of scaled bias slightly increase the tank volumes, which indicates more potential CSO.

When considering the treated wastewater, the improvements and deteriorations become close to negligible for both controllers, but with the notion that they all perform worse as the bias increases toward positive.

11

Table 3: Overflow results of the SWMM simulations with different Controllers: MPC and CC- and tube-based MPC with scaled uncertainty bias of -20-20%.

Tank & Pipes	MPC	Type	-20%	-10%	0%	10%	20%
T1	93251	CC-MPC	90004	91355	92927	94728	96615
		T-MPC	86457	87834	89509	90712	92138
T2	15484	CC-MPC	16801	16023	15544	15383	15316
		T-MPC	18718	18166	17526	17041	16565
T3	34017	CC-MPC	33298	33857	34313	34065	34304
		T-MPC	32706	33102	33693	34413	34488
T4	4814	CC-MPC	5960	5206	4814	4729	4713
		T-MPC	7457	7010	6595	6078	5704
T5	15147	CC-MPC	15147	15147	15147	15147	15147
		T-MPC	15147	15147	15147	15147	15147
T6	37950	CC-MPC	39082	38296	37946	37770	37836
		T-MPC	41132	40350	39733	39101	38755
P7	4016	CC-MPC	4015	4015	4015	4016	4015
		T-MPC	4016	4016	4016	4015	4015
P8	16207	CC-MPC	16190	16195	16191	16203	16191
		T-MPC	16203	16203	16199	16191	16192
P9	4030	CC-MPC	4029	4029	4029	4029	4029
		T-MPC	4029	4029	4029	4029	4029
P10	4838	CC-MPC	4843	4841	4842	4839	4842
		T-MPC	4839	4839	4840	4842	4842
River	183754	CC-MPC	182242	182623	183778	185094	187129
		T-MPC	181526	182301	183509	184423	185076
Creek	45996	CC-MPC	47126	46341	45990	45815	45880
		T-MPC	49177	48395	47778	47144	46799
Total	229750	CC-MPC	229368	228964	229768	230909	233008
		T-MPC	230704	230696	231287	231567	231875
R.%		CC-MPC	-0.8228%	-0.6155%	0.0131%	0.7292%	1.8367%
		T-MPC	-1.2125%	-0.7907%	-0.1333%	0.3641%	0.7194%
C. %		CC-MPC	2.4567%	0.7501%	-0.0130%	-0.3935%	-0.2522%
		T-MPC	6.9158%	5.2157%	3.8742%	2.4959%	1.7458%
Tot. %		CC-MPC	-0.1663%	-0.3421%	0.0078%	0.5045%	1.4181%
		T-MPC	0.4152%	0.4118%	0.6690%	0.7909%	0.9249%

Table 4: Treated Wastewater results of the SWMM simulations with different Controllers: MPC, and CC- and tube-based MPC with scaled uncertainty bias of -20-20%.

	MPC	Type	-20%	-10%	0%	10%	20%
WWTP Vol.	3772057	CC-MPC	3772166	3772992	3772159	3770672	3768942
		T-MPC	3771113	3770657	3770439	3770220	3769903
Imp. %		CC-MPC	0.0029%	0.0248%	0.0027%	-0.0367%	-0.0826%
		T-MPC	-0.0250%	-0.0371%	-0.0429%	-0.0487%	-0.0571%

6.3. Offset Bias

The final parameter in the comparison is the offset bias given by (71), where the offset b skews the expected disturbance away from the actual disturbance. For the simulations, the following constant offsets have been used as illustrative values; zero, one fourth, one and five times the average inflow disturbance

$$\mathbb{E}\{q\} = q^{actual} + b \qquad (71)$$

In Table 6, we can observe the results of treated wastewater showing that the T-MPC is less sensitive to increases in offset biases than the CC-MPC. It can also be observed that for lower offsets, the deviation from the results of the perfect MPC are negligible, but that the CC-MPC has less deviation, in comparison to the T-MPC.

The results of CSO volume are shown in Table 5, where we can again observe that the sensitivity to increase in offset, is significantly lower for T-MPC than the CC-MPC. It can also be seen that the performance of the CC-MPC is significantly deteriorated for the higher offsets, but only slightly affected for lower offsets, while the T-MPC have performances that are significantly less affected for higher offsets, and only slightly worse for lower offsets. It can further be observed, that for both types of MPCs the distribution of the CSO improves as the offset increases, but with deteriorating performances as a result. For the T-MPC, the CSO distribution through the system is in general performing significantly worse than for the CC-MPC. Figure 4 gives additional graphically information about the CSO performance of CC-MPC under different offsets through comparing the differences in tank volume among CC-MPC using different offsets. As explained previously, the more volume in the tank indicates the more chance of having more CSOs. From Figure 4, we can conclude that the CC-MPC with 0.1 offset have more tank volume than those of CC-MPC with different offsets, which means, the CC-MPC with 0.1 offset behaves worse than the other CC-MPCs, as one would expect. While for the T-MPC, the T-MPC with less offset has more tank volume, which indicates more possible
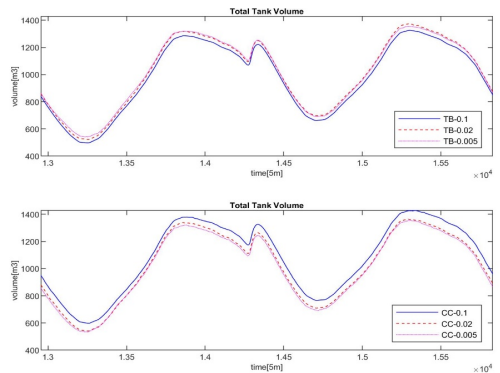

Figure 4: The total tank volumes under T-MPC and CC-MPC with different offset bias.

CSOs. This is in despite of the higher offset CSO results from the table, shows the opposite situation. The difference in volume and CSO behavior is due to the overestimated inflow making the T-MPC stricter resulting in lower dry-weather tank volume, but also overreacting towards CSO avoidance of the upstream tanks, disregarding CSO volume minimization over CSO distribution.

6.4. Chance Constrained or Tube-Based MPC

From the analysis of the performance comparisons above, we can evaluate when and where each method is most applicable, based on one's confidence in the knowledge of the disturbance. It can be concluded that for the compared methods, the T-MPC works better for achieving a performance insensitive to bias uncertainty, while the CC-MPC is more insensitive with the size of the uncertainty bound. If the preference is given to the performance (CSO / treated wastewater), then, in general, the CC-MPC works better with the exception of a few cases of extreme uncertainty. The difference in performances between CC-MPC and T-MPC is usually around a thousand cubic meters, corresponding to around 0.3% difference with respect to the perfect MPC for CSO performance.

Table 5: Overflow results of the SWMM simulations with different Controllers: MPC and CC- and tube-based MPC with offset uncertainty bias.

Tank & Pipes	MPC	Type	0	0.005	0.02	0.1
T1	93251	CC-MPC	92927	93856	96590	130211
		T-MPC	89509	90134	92357	97668
T2	15484	CC-MPC	15544	15450	15452	15511
		T-MPC	17526	17103	16417	15514
T3	34017	CC-MPC	34313	34322	34485	36548
		T-MPC	33693	33865	34071	35306
T4	4814	CC-MPC	4814	4728	4644	4465
		T-MPC	6595	6151	5131	4567
T5	15147	CC-MPC	15147	15147	15147	15147
		T-MPC	15147	15147	15147	15147
T6	37950	CC-MPC	37946	37961	37780	37763
		T-MPC	39733	39645	39062	37608
P7	4016	CC-MPC	4015	4015	4016	4016
		T-MPC	4016	4015	4015	4016
P8	16207	CC-MPC	16191	16193	16203	16203
		T-MPC	16199	16196	16195	16203
P9	4030	CC-MPC	4029	4029	4029	4029
		T-MPC	4029	4029	4029	4029
P10	4838	CC-MPC	4842	4842	4839	4839
		T-MPC	4840	4841	4841	4839
River	183754	CC-MPC	183778	184536	187360	222925
		T-MPC	183509	183437	184158	189244
Creek	45996	CC-MPC	45990	46005	45825	45808
		T-MPC	47778	47689	47106	45653
Total	229750	CC-MPC	229768	230541	233185	268733
		T-MPC	231287	231126	231264	234897
R.%		CC-MPC	0.0131%	0.4256%	1.9624%	21.3171%
		T-MPC	-0.1333%	-0.1725%	0.2199%	2.9877 %
C. %		CC-MPC	-0.0130%	0.0196%	-0.3718%	-0.4087%
		T-MPC	3.8742%	3.6808%	2.4133%	-0.7457%
Tot. %		CC-MPC	0.0078%	0.3443%	1.4951%	16.9676%
		T-MPC	0.6690%	0.5989%	0.6590%	2.2403%

Table 6: Treated Wastewater results of the SWMM simulations with different Controllers: MPC, and CC- and tube-based MPC with offset uncertainty bias.

	MPC	Type	0	0.005	0.02	0.1
WWTP Vol.	3772057	CC-MPC	3772159	3771978	3768643	3733651
		T-MPC	3770439	3770306	3770471	3767206
Imp. %		CC-MPC	0.0027%	-0.0021%	-0.0905%	-1.0182%
		T-MPC	-0.0429%	-0.0464%	-0.0420%	-0.1286%

7. Conclusion

In this paper, the tube-based MPC (T-MPC) from the robust MPC family and the chance constrained MPC (CC-MPC) for the stochastic MPC family have been compared mathematically, showing how similar and different they are in concepts, and displaying how the assumptions on uncertainty affect the constriction of the constraints for the two types of MPC. The drawbacks of each method were also discussed and used as inspiration for formulating a T-MPC with chance constrained bounded uncertainty. Moreover, we have also compared the performances of both MPC types, on a case study of an urban drainage control problem, using simulations on a SWMM model of the Astlingen benchmark network. The following conclusions of the analysis can be summarized:

1. T-MPC is computational simpler, while the solutions are worst-case conservative and in general requiring bounded disturbances.

2. CC-MPC is in general computationally difficult, but provide solutions of tuneable conservativism and are applicable for bounded and unbounded disturbances

3. CC-MPC assumes the exact distribution is known, while T-MPC only assumes uncertainty bounds are known; which is equivalent to the assumption of uniform distribution

4. An inequality relation between constraint constriction of T-MPC and CC-MPC have been derived; showing that the T-MPC constriction is always stricter than the CC-MPC constriction.

5. The proposed chance constrained bound T-MPC is less conservative than the original T-MPC, while being computational simpler than the CC-MPC.

6. Performance-wise, we can conclude that when uncertainty biases are low or the uncertainty interval are high, the CC-MPC performs better, while the performance of T-MPC is more insensitive to biases.

References

[1] A. Propoi, Use of lp methods for synthesizing sampled-data automatic systems, Automatic Remote Control 24 (1963).

[2] J. M. Maciejowski, Predictive Control: with constraints, Pearson, 2002.

[3] E. Camacho, C. Bordons, Model Predictive Control, 2nd Edition, Springer, 2007.

[4] P. O. M. Scokaert, J. B. Rawlings, Stability of model predictive control under perturbations, Proceedings of the IFAC Symposium on Nonlinear Control Systems Design, 1995, pp. 1317–1322.

[5] D. L. Marruedo, T. Alamo, E. F. Camacho, Stability analysis of systems with bounded additive uncertainties based on invariant sets: Stability and feasibility of mpc, Proceedings of American Control Conference, 2002, pp. 364–369.

[6] C. Sun, M. Morley, D. Savic, V. Puig, G. Cembrano, Z. Zhang, Combining model predictive control with constraint-satisfaction formulation for the operative pumping control in water networks, Proceedings of the 13th Computing and Control for the Water Industry Conference, Leicester, 2015, pp. 963–972.

[7] C. Sun, V. Puig, G. Cembrano, Multi-layer model predictive control of regional water networks: Application to the catalunya case study, 52nd IEEE Conference on Decision and Control, Florence, 2013, pp. 7095–7100.

[8] C. Sun, V. Puig, G. Cembrano, Two-layer scheduling scheme for pump stations, 2014 IEEE Conference on Control Applications, Antibes, 2014, pp. 1741–1746.

[9] L. Cen, Y. Xi, Aggregation-based model predictive control of urban combined sewer networks, in: Proc. of the 7th Asian Control Conference, Proc. of the 7th Asian Control Conference, 2009.

[10] M. Marinaki, M. Papageorgiou, Optimal Real-time Control of Sewer Networks, Advances in Industrial Control, Springer, 2005.

[11] C. Ocampo-Martinez, Model Predictive Control of Wastewater Systems, Advances in Industrial Control, Springer, 2010.

[12] M. S. Gelormino, N. L. Ricker, Model predictive control of a combined sewer system, INT. J. CONTROL 59 (3) (1994) 793–816.

[13] C. Sun, B. Joseph, T. Maruejouls, G. Cembrano, E. Muñoz, J. Meseguer, A. Montserrat, S. Sampe, V. Puig, X. Litrico, Efficient integrated model predictive control of urban drainage systems using simplified conceptual quality models, 14th IWA/IAHR International Conference on Urban Drainage, Prague, 2017, pp. 1848–1855.

[14] R. Halvgaard, A. K. V. Falk, Water system overflow modeling for model predictive control, in: Proceedings of the 12th IWA Specialised Conference on Instrumentation, Control and Automation, Proceedings

of the 12th IWA Specialised Conference on Instrumentation, Control and Automation, 2017.

[15] J. L. Svensen, H. H. Niemann, N. K. Poulsen, Model predictive control of overflow in sewer networks: A comparison of two methods, in: Proc. of the 4th Int. Conf. on Control and Fault-Toleran Systems, Proc. of the 4th Int. Conf. on Control and Fault-Toleran Systems, 2019, pp. 412–417.

[16] C. Sun, B. Joseph, G. Cembrano, V. Puig, J. Meseguer, Advanced integrated real-time control of combined urban drainage systems using mpc: Badalona case study, 13th International Conference on Hydroinformatic, Palermo, 2018, pp. 2033–2041.

[17] C. Sun, J. L. Svensen, M. Borup, V. Puig, G. Cembrano, L. Vezzaro, An mpc enabled swmm implementation of the astlingen rtc benchmaking network, Water 12 (1034) (2020).

[18] J. L. Svensen, C. Sun, G. Cembrano, V. Puig, Chance-constrained stochastic mpc of astlingen urban drainage benchmark network, Control Engineering PracticeSubmitted (August 2020).

[19] J. L. Svensen, H. H. Niemann, A. K. V. Falk, N. K. Poulsen, Chance-constrained model predictive control - a reformulated approach suitable for sewer networks, Advanced Control of Applications, Submitted (July 2020).

[20] A. Mesbah, Stochastic model predictive control: An overview and perspectives for future research, IEEE Control Systems Magazine (2016) 30–44doi:10.1109/MCS.2016.2602087.

[21] B. Kouvaritakis, M. Cannon, Model Predictive Control - Classical, Robust and Stochastic, Advances Textbooks in Control and Signal Processing, Springer, 2016. doi:10.1007/978-3-319-24853-0.

[22] A. T. Schwarm, M. Nikolaou, Chance-constrained model predictive control, AIChE Journal 45 (8) (1999) 1743–1748.

[23] M. Evans, M. Cannon, B. Kouvaritakis, Linear stochastic mpc under finitely supported multiplicative uncertainty, Proc. of the 2012 American Control Conference, 2012.

[24] J. M. Grosso, C. Ocampo-Martinez, V. Puig, B. Joseph-Duran, Chance-constrained model predictive control for drinking waternetworks, Journal of Process Control 24 (2014) 504–516.

[25] H. Arellano-Garcia, G. Wozny, Chance constrained water quality management model for reservoir systems: I. strict monotonicity, Comput. Chem. Eng. 33 (10) (2009) 1568–1583.

[26] A. Dhar, B. Datta, Chance constrained water quality management model for reservoir systems, ISH J. Hydraul. Eng. 12 (3) (2006) 39–48.

[27] S. Garatti, M. C. Campi, S. Garatti, M. Prandini, The scenario approach for systems and control design, Annual Reviews in Control 33 (2009) 149–157.

[28] A. D. Bonzanini, T. L. M. Santos, A. Mesbah, Tube-based stochastic nonlinear model predictive control: A comparative study on constraint tightening, Vol. 52, 12th IFAC Symposium on Dynamics and Control of Process Systems, including Biosystems DYCOPS 2019, Florianopolos, Brazil, 2019, pp. 598–603.

[29] M. Nassourou, J. Blesa, V. Puig, Robust economic model predictive control based on a zonotope and local feedback controller for energy dispatch in smart-grids considering demand uncertainty, Energies 13 (3) (2020).

[30] Z. Wan, M. V. Kothare, Robust output feedback model predictive control using off-line linear matrix inequalities, Journal of Process Control 12 (7) (2002) 763–774.

[31] L. Magni, G. D. Nicolao, R. Scattolini, F. Allgöwer, Robust model predictive control for nonlinear discrete-time systems, International Journal of Robust and Nonlinear Control 13 (3-4) (2003) 229–246.

[32] Z. Q. Sun, L. Dai, K. Liu, Y. Q. Xia, K. H. Johansson, Robust mpc for tracking constrained unicycle robots with additive disturbances, Automatica 90 (2018) 172–184.

[33] K. Hariprasad, S. Bhartiya, A computationally efficient robust tube based mpc for linear switched systems, Nonlinear Analysis: Hybrid System 19 (2006) 60–76.

[34] W. W. Qin, J. Y. Liu, X. X. Hu, B. He, G. Liu, Tube-based active robust mpc for uncertain constrained linear systems with time delays, IEEE Access 7 (2019) 125552–125561.

[35] D. Limón, T. Alamo, F. Salas, E. F. Camacho, Input to state stability of min-max mp controllers for nonlinear systems, Automatica 42 (5) (2006) 797–803.

[36] M. Schütze, M. Lange, M. Pabst, U. Haas, Astlingen - a benchmark for real time control (rtc), Water Sci & Technol 2017 (2) (2018) 552–560.

[37] M. Beck, S. Robins, Computing the Continous Discretely - Integer-Point Enumeration in Polyhedra, Springer, 2015.

[38] C. Sun, L. Romero, B. Joseph-Duran, J. Meseguer, E. Craviotto, R. Guasch, M. Martinez, V. Puig, G. Cembrano, Integrated pollution-based real-time control of sanitation systems, Journal of Environmental Management 269 (110798) (September 2020).

APPENDIX G

Article G

The paper presented in this appendix was originally submitted to a journal.

Information of the publication:

- Title: Sewer Orientated Framework for Ensemble-based Chance-Constrained MPC
- Journal: *Submitted* to Advanced Control for Applications
- Date: October, 2020

Sewer Orientated Framework for Ensemble-based Chance-Constrained MPC

Jan Lorenz Svensen*[1] | Hans Henrik Niemann[2] | Anne Katrine Vinther Falk[3] | Niels Kjølstad Poulsen[1]

[1]Department of Applied Mathematics and Computer Science, Technical University of Denmark, 2800 Kongens Lyngby, Denmark

[2]Department of Electrical Engineering, Technical University of Denmark, 2800 Kongens Lyngby, Denmark

[3]DHI Denmark, 2970 Hørsholm, Denmark

Correspondence
*Jan Lorenz Svensen, Department of Applied Mathematics and Computer Science, Technical University of Denmark, Asmussens Allé 303B, 2800 Kgs. Lyngby, Denmark. Email: jlsv@dtu.dk

Present Address
Asmussens Allé 303B, 2800 Kgs. Lyngby, Denmark.

Abstract

In this work, we present a framework for ensemble-based (E) chance-constrained (CC) model predictive control (MPC) in sewer systems. The framework considers the availability of ensemble forecasts and the difficulties with propagation of distributions; through distribution estimation. Utilizing a case study of the sewer network of the city of Aarhus in Denmark, the performance of the ECC-MPC framework is evaluated through simulations. The evaluations were based on linear models of the case study and compare the ECC-MPC performance with the performance of CC-MPC. Based on the simulations, it was found that the ECC-MPC performed comparable to the performance of the CC-MPC, not only in the context of overflow and outflow but also with respect to behavior in response to changes in different aspects of forecast uncertainties. Regarding the aspects, it was found that expectation offset biases in the forecast were affecting the performance of the CC- and ECC-MPC the most. While other aspects only had a reduced effect on the performances, within the ranges tested. With the comparable performances, it was found that ECC-MPC would work as an alternative approach to CC-MPC.

KEYWORDS:
stochastic MPC; Combined Sewer Overflow; chance-constrained; Ensemble; Sewer system

1 | INTRODUCTION

In the last few decades, research into Model Predictive Control (MPC) has been applied many types of systems with promising results [1,2]. One application is sewer systems [3–7], which will be the focus of this work. In sewer systems, MPC have been applied for its predictive abilities, to include the information from rain forecasts into the control.

For MPC applied to sewer systems, the used models are usually simplified to consist of networks of interconnected virtual tanks; lumped models of volume capacity representing segments of the overall system's network of pipes and tanks. The performance of MPC is depending on the accuracy of the used model and the forecasted disturbances to the system; the model and forecast uncertainty. In the case of sewer systems, model uncertainty comes from the simplified model not perfectly describing the real system, while forecast uncertainty originates in the rain forecast of the inflows to the system.

Within the MPC research there are many approaches on how to handle the presence of uncertainty [8–15]; from the robust MPC methods aiming for the worst-case scenario, to the stochastic MPC methods aiming for statistic coverage of the uncertainty.

For this work, we will consider the CC-MPC from the group of stochastic MPC methods as the approach to handling uncertainty. The choice of CC-MPC are due to rain forecasts can be considered stochatstic disturbances, describing the likelihood of
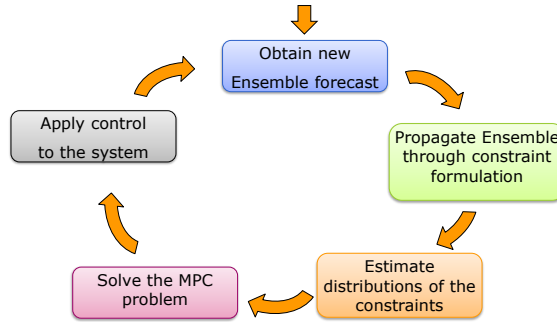
FIGURE 1 Conceptual framework layout of Ensemble-based CC-MPC.

different inflow scenarios. The CC-MPC method relies on knowing the stochastic distribution of the uncertainties of each constraint and formulating the inequality constraints as probabilistic constraints. The knowledge about the constraint distributions is used to obtain deterministic versions of the probability constraints, utilizing the quantile functions of the constraint distributions.

The reliance on knowing distributions and quantile functions gives the CC-MPC method some drawbacks, given that constraint distributions are obtained from knowledge of the distributions of the model and forecast uncertainties across the prediction horizon of the CC-MPC. For most types of systems and uncertainty distributions, propagation of a distribution throughout the system would change the initial type of distribution, e.q. adding together the squares of different types of distribution. The quantile function of the resulting constraint distribution might then become impractical to compute. Exceptions to such distribution changes include linear systems with additive uncertainty with a normal distribution.

In the context of sewer systems, the usage of CC-MPC is further complicated by the rain forecasts rarely being provided as a distribution. It is more commonly provided as a fixed-sized ensemble of statistical scenarios of the rain's temporal and spatial development, from where the distribution has to be determined.

The main contribution of this work are the suggestion of a framework for applying CC-MPC to the general sewer system. The proposed framework aims to handle the issues with the propagation and lack of available initial distribution, through estimation of the constraint distributions based on propagated ensemble forecasts, as illustrated in Fig. 1.

A performance evaluation of the proposed framework of ensemble-based CC-MPC (ECC-MPC) is given, based on simulations of the Aarhus case study [16] from Denmark. The evaluation is done by comparison to a CC-MPC with known quantile functions (propagated distribution). The Aarhus case study is discussed through a design model for MPC; autogenerated from a MIKE URBAN Hi-Fi model by DHI [16,17].

For the performance evaluation, we will consider a linear system model, where only forecast uncertainty is included. The uncertainties in the evaluation will be normal distributed with varying bounds and biases between simulations. Given that sewer systems experience combined sewer overflows (CSO) from their weir structures, the CC-MPC formulations utilized in this work are based on our previous proposed revised formulation [10].

In the following section, we will first present a brief formulation of the MPC and CC-MPC used in the work, followed by the formulation and a diskussion of the suggested ECC-MPC framework. In the third section, we discuss the design models of the Aarhus case study. In the fourth section, we discuss the simulations of ECC-MPC and CC-MPC, and the results of the performance comparison. We end the paper with a conclusion of the paper's results.

1.1 | Notation

The notations utilized in this paper are as follows; the superscripts *in*, *out*, *u* and *cso* indicate the inflow, outflow, control flow, and weir overflow respectively, while the subscript k indicates the sample number and ΔT notes the sampling time. A bullet • represents a subset or set of a function's variables, while Bold font indicates vectors and $\overline{f}$ notes the maximum of a given function $f(x)$. For a stochastic variable X, the notation $X \sim F$ indicates that X is following a distribution F. While $E\{X\}$ and σ_X^2 note the expectation and variance of X respectively, and $Pr\{X \leq y\}$ and $\Phi_X(y)$ are the probability function and cumulative distribution function (CDF) of X respectively for a given value y.

2 | MPC AND THE FRAMEWORK

The general formulation of MPC for systems with overflows, such as sewer systems can be written as

$$J = \min_{\mathbf{u}} f(\mathbf{x}, \mathbf{u}, \mathbf{z}^{ref}, \mathbf{w}, \mathbf{q}^{cso}) \tag{1}$$

$$\mathbf{x}_{k+1} = h_{proc}(\mathbf{x}_k, \mathbf{u}_k, \mathbf{w}_k, \mathbf{q}_k^{cso}) \quad \forall k > 0 \tag{2}$$

$$q_{k,i}^w = \begin{cases} t_{w,i}(T_i(\bullet)), & T_i(\bullet) \geq 0 \\ 0 \end{cases} \quad \forall i \in \{1 : N_w\} \tag{3}$$

$$\mathbf{h}_k(\mathbf{x}_k, \mathbf{w}_k, \mathbf{u}_k, \mathbf{q}_k^{cso}) = \mathbf{0} \quad \forall k \geq 0 \tag{4}$$

$$\mathbf{g}_k(\mathbf{x}_k, \mathbf{w}_k, \mathbf{u}_k, \mathbf{q}_k^{cso}) \leq \bar{\mathbf{g}}_k \quad \forall k \geq 0 \tag{5}$$

Where $\mathbf{x}$, $\mathbf{u}$, and $\mathbf{w}$ corresponds to the states of the system, the control of the system, and the inflow disturbances into the system, fx. rain. The overflows are given by $\mathbf{q}^w$ and defined by some function $t_{w,i}$ and the switching function T_i, where each ith overflow corresponds to the overflow structure of the system.

The above formulation can be simplified by approximating the overflows $\mathbf{q}^w$ as optimization variables through a minimization cost [3][6][18]. Thus increasing the number of variables in the formulation, and removing the logical part given in (3); resulting in a program that is simpler to compute, perhaps even convex. If the process equation of (2) is further substituted into the constraints of (4) and (5), the simplified program can be written as

$$J = \min_{\mathbf{u}, \mathbf{q}^w} f_q(\mathbf{x}_0, \mathbf{u}, \mathbf{z}^{ref}, \mathbf{w}, \mathbf{q}^{cso}) \tag{6}$$

$$\tilde{\mathbf{h}}_k(\mathbf{x}_0, \mathbf{w}, \mathbf{u}, \mathbf{q}^{cso}) = \mathbf{0} \quad \forall k \geq 0 \tag{7}$$

$$\tilde{\mathbf{g}}_k(\mathbf{x}_0, \mathbf{w}, \mathbf{u}, \mathbf{q}^{cso}) \leq \bar{\mathbf{g}}_k \quad \forall k \geq 0 \tag{8}$$

$$\mathbf{0} \leq \mathbf{q}^{cso} \tag{9}$$

where the cost function f_q contains the initial cost function f and the substituted process, plus an additional cost for the approximation by minimization. While $\tilde{\mathbf{h}}_k$ and $\tilde{\mathbf{g}}_k$ are the equality and inequality constraints with substituted process equation.

In the case of the CC-MPC, the revised formulation addresses the oddity of a probabilistic constraint on an intrinsical feasible constraint [10], with the formulation given by (10)-(16).

$$J = \min_{\mathbf{u}, \mathbf{q}^w} E\{f_q(\mathbf{x}_0, \mathbf{u}, \mathbf{z}^{ref}, \mathbf{w}, \mathbf{q}^{cso})\} + f_s(\mathbf{s}, \mathbf{c}) \tag{10}$$

$$E\{\tilde{\mathbf{h}}_k(\mathbf{x}_0, \mathbf{w}, \mathbf{u}, \mathbf{q}^{cso})\} = \mathbf{0} \quad \forall k \geq 0 \tag{11}$$

$$\Phi^{-1}_{\tilde{g}_{k,i}(\mathbf{x}_0, \mathbf{w}, \mathbf{u}, \mathbf{q}^w)}(\gamma_i) \leq \bar{g}_{k,i} + s_{k,i} \quad \forall k \geq 0, \forall i \notin \mathcal{N}^w \tag{12}$$

$$E\{\tilde{g}_{k,i}(\mathbf{x}_0, \mathbf{w}, \mathbf{u}, \mathbf{q}^{cso})\} \leq \bar{g}_{k,i} \quad \forall k \geq 0, \forall i \in \mathcal{N}^{cso} \tag{13}$$

$$\Phi^{-1}_{\tilde{T}_i(\mathbf{x}_0, \mathbf{w}, \mathbf{u}, \mathbf{q}^{cso}_{\neq i})}(\gamma_i) \leq 0 + c_{k,i} \quad \forall k \geq 0, \forall i \in \mathcal{N}^{cso} \tag{14}$$

$$0 \leq s_{k,i} \leq \Phi^{-1}_{\tilde{g}_{k,i}(\mathbf{x}_0, \mathbf{w}, \mathbf{u}, \mathbf{q}^{cso})}(\gamma_i) - E\{\tilde{g}_{k,i}(\mathbf{x}_0, \mathbf{w}, \mathbf{u}, \mathbf{q}^{cso})\} \tag{15}$$

$$\mathbf{0} \leq \mathbf{q}^{cso}, \mathbf{c} \tag{16}$$

where $\mathcal{N}^{cso}$ is the set of constraints defining an overflow in the system, and the added slack variables $\mathbf{s}$ and $\mathbf{c}$ preserves the feasibility of the original MPC with regards to expectation, see (15), but ensures the probability constraint holds if possible through minimization of an added cost f_s. The set $\mathcal{N}^w$ is utilized to determine which constraints can be formulated as a probability constraint directly (12) or are formulated as an expectation constraint (13). Wherefore the latter case has the addition of a probability constraint (14) based on the process substituted switching function $\tilde{T}_i$ corresponding to the overflow defined by the given constraint.

For some distributions such as the normal distribution, the quantile function of the constraints can be standardized as below

$$\Phi^{-1}_{\tilde{g}(\mathbf{x}_0, \mathbf{w}, \mathbf{u}, \mathbf{q}^{cso})}(\gamma) = E\{\tilde{g}(\mathbf{x}_0, \mathbf{w}, \mathbf{u}, \mathbf{q}^{cso})\} + \sigma\{\tilde{g}(\mathbf{x}_0, \mathbf{w}, \mathbf{u}, \mathbf{q}^{cso})\}\Phi^{-1}(\gamma) \tag{17}$$

Allowing for simplification of the optimization program into a deterministic formulation. For example, when considering additive uncertainty, the variance-quantile function term of the right-hand-side in (17) becomes constant with respect to the optimization variables. Later, in the performance evaluation, we will utilize this to construct a CC-MPC with known quantile function.

2.1 | Framework for probabilistic constraints

The formulation of CC-MPC given above relies on knowing the expectations and γ-quantiles of the constraints; which in general can be difficult to have knowledge about. In the case of uncertainties with a constant nature, such as a fixed distribution; the expectations and quantile functions of the constraints could be determined once and for all, therefore providing the needed knowledge for the CC-MPC. An example of this could be some types of model uncertainties affecting the constraints.

If one can not be certain of the nature of the uncertainties are unchanged, then even knowing the exact distribution of the uncertainties might not be of much use. Given that the propagation of uncertainty throughout the constraints might very well change the distribution to a different type of distribution. One for which the quantile functions might not be well-defined or easy to determine. For examples when the constraint distribution results in a mix of different types of distributions.

Therefore it might be more effective to determine the constraint distribution through an estimation, based on propagating scenarios of the uncertainty rather than distribution formulas. Where the scenarios describe both temporal and spatial aspects of the uncertainties. If the distribution of the uncertainty is known, then an ensemble of such scenarios can be generated for the propagation. This further means that the knowledge of the distribution of the uncertainty is no longer a necessity if an ensemble of uncertainty scenarios is available from another source.

In general, the propagation of the uncertainty ensemble $\mathbf{w}^E$ is given by (18), where an ensemble of n scenarios are given for m sources of uncertainties w, and mapped to an ensemble of n scenarios of the ith constraint as a function of deterministic parameters and variables

$$\mathbf{w}^E \in \mathcal{R}^{m \times n} \rightarrow g_i(\mathbf{x}_0, \mathbf{w}^E, \mathbf{u}, \mathbf{q}^{cso}) = g_i^E(\mathbf{x}_0, \mathbf{u}, \mathbf{q}^{cso}) \in \mathcal{R}^{1 \times n} \tag{18}$$

Given that the constraint ensemble is a function of the optimization variables, the ensemble suffers the same computational issues that the standard CC-MPC has with the quantile functions for general constraint functions: the distribution depends on the optimization.

Under the right conditions for the relationship between uncertainty and variables, these issues disappear with regards to certain stochastic properties of the constraints. To start with, if the relationship is multiplicable then it follows from lemma 1, that the expectation and variance of the constraint are deterministic. Similarly, if the relationship is additive, then from lemma 2, it follows that the quantile function of the constraint is deterministic in addition to the expectation and variance of the constraint.

Lemma 1 (Multiplicative properties). If the scalar constraint function is given by (19) and w is following some distribution $\mathcal{F}$

$$g(\mathbf{u}, \mathbf{w}) = \sum_{i=0}^{N} g_{1,i}(\mathbf{w}) g_{2,i}(\mathbf{u}), \quad \mathbf{w} \sim \mathcal{F}, g_{i,j}(\mathbf{x}) : \mathcal{R}^{n_x \times 1} \rightarrow \mathcal{R}, \forall i, j \tag{19}$$

Then it follows that the expectation is given by

$$E\{g(\mathbf{u}, \mathbf{w})\} = \sum_{i=0}^{N} E\{g_{1,i}(\mathbf{w})\} g_{2,i}(\mathbf{u}) \tag{20}$$

$$\sigma^2\{g(\mathbf{u}, \mathbf{w})\} = \sum_{i=0}^{N} \sum_{j=0}^{N} \sigma^2\{g_{1,i}(\mathbf{w}), g_{1,j}(\mathbf{w})\} g_{2,i}^2(\mathbf{u}) g_{2,j}^2(\mathbf{u}) \tag{21}$$

Lemma 2 (Additive properties). If the scalar constraint function is given by (22) and w is following some distribution $\mathcal{F}$

$$g(\mathbf{u}, \mathbf{w}) = g_1(\mathbf{w}) + g_2(\mathbf{u}), \quad \mathbf{w} \sim \mathcal{F}, g_{i,j}(\mathbf{x}) : \mathcal{R}^{n_x \times 1} \rightarrow \mathcal{R}, \forall i, j \tag{22}$$

Then it follows that the quantile function, expectation, and variance is given by

$$\Phi_{g(\mathbf{u}, \mathbf{w})}^{-1}\{\gamma\} = \Phi_{g_1(w)}^{-1}\{\gamma\} + g_2(\mathbf{u}) \tag{23}$$

$$E\{g(\mathbf{u}, \mathbf{w})\} = E\{g_1(w)\} + g_2(\mathbf{u}) \tag{24}$$

$$\sigma^2\{g(\mathbf{u}, \mathbf{w})\} = \sigma^2\{g_1(w)\} \tag{25}$$

The lemmas above are also applicable to the constraint ensemble, in the sense that the estimation of the constraint distribution with respect to certain stochastic properties only needs to consider the constraint part g_1 that includes the uncertainties. This can simplify the estimation and the following MPC program, by the formulation becoming deterministic.

For this reason, the definition of our framework will assume the uncertainty to be additive, such that the estimated quantile function is independent of the optimization variables. The procedure of the ECC-MPC framework can be summarized as the following steps:

- Obtain an Ensemble forecast, $\mathbf{w}^E$

- Propagate the Ensemble to the constraints, $\mathbf{g}^E$

- Estimate the constraint distributions, $\Phi^{-1}_{g_i(\mathbf{u},\mathbf{w})}$

- Solve the CC-MPC

- Apply control solution

- Repeat

The procedure is also illustrated in Fig.1. The second step in the procedure provides us with the ensemble of constraint scenarios we need for the third step, by taking each forecast scenario in the ensemble and propagate it through the entire system description. With the constraint ensemble ready, the distributions of the constraints can be estimated. There are many ways to do such estimation, one of them is a Pearson's χ^2 goodness of fit test; that allows one to estimate the constraint distribution in terms of well-known distributions such as normal, uniform, gamma, and others. This method has the benefit of estimating the constraint distribution as the best fitting distribution with a known quantile function, ready to be applied to the constraint formulation. In the simulations, presented later in this work, this approach to the estimation of the constraint distributions is utilized.

2.1.1 | Benefits and limitations

The ECC-MPC framework described above has both benefits and limitations to its usage. The framework has the benefits of not being reliant on either the presence of ensemble forecast data from external sources or forecast distributions, but being usable when either one is available. With regard to the stochastical nature of the uncertainty, the framework only assumes the expectation and quantile functions can be estimated. This means the framework is benefiting from not depending on assumptions such as the uncertainties being independently distributed; in order to simplify the propagation throughout the system and its cross-correlations.

Given the ECC-MPC framework is based on an estimation approach, the choice of approach is a limiting factor in the quality of the estimation, and therefore in the resulting controller. This also means the computation time of the framework is reliant on the choice of estimation approach, while the traditional CC-MPC method does not rely on estimations, which can increase computation time. Furthermore, if one relies on externally sourced ensemble forecasts then the size of the ensemble is also a limiting factor of the estimation. Another limiting aspect of the estimations is the necessity of the constraint ensembles being independent of each other, in order for the estimation to be statistically valid. This means the ensembles of the ensemble forecast also has to be independently generated, regardless of their origin.

As mentioned earlier the ECC-MPC framework assumes the uncertainties and optimization variables to have an additive relationship. This limits the types of systems it can be applied to, excluding relationships such as multiplicative, logarithmic, and others. For the multiplicative case, the framework could be used if the standardization shown in (17) is reasonable to assume, utilizing lemma 1 to achieve a deterministic constraint.

2.1.2 | Thoughts on other MPC-types

The ECC-MPC framework can easily be redesigned for other types of MPCs, by changing the distribution estimation step. If the desired controller is a tube-based controller from the class of robust MPCs, then the estimation step could either be changed to only estimating the indirectly assumed uniform distribution of the constraints, or directly utilizing the worst-case from the available constraint scenarios; obtained from the propagation of the ensembles. similarly, other types of MPC could refit the estimation step to suit the type of data they rely on.

3 | AARHUS SEWER SYSTEM AND MPC DESIGN

As mentioned earlier, the system utilized in the performance evaluation later in this work is based on the Marselisborg sewer system, specifically the segment of the system covering the city of Aarhus. Aarhus is a city covering an area of $91 km^2$ with a population of 280534 in 2020 [19]. Given that a sewer system is a network of pipes and tanks described by the Saint-Venant
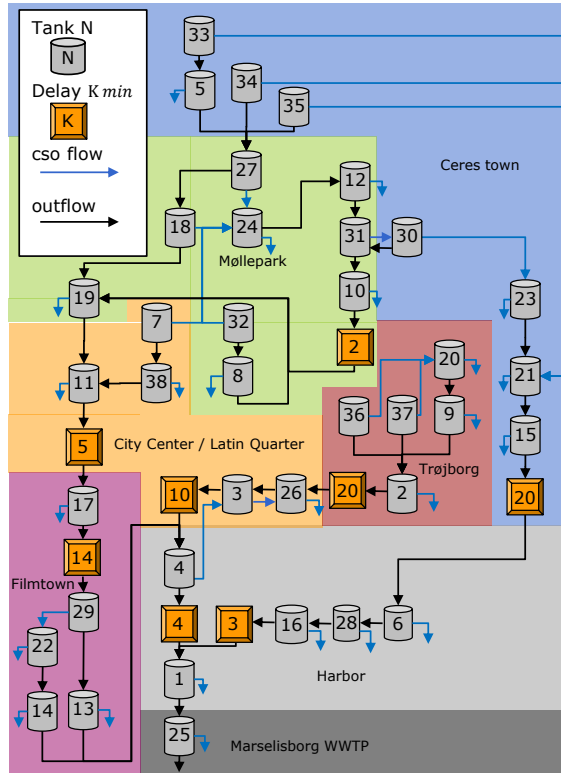
FIGURE 2 A schematic of the Aarhus sewer system model based on an autogenerated virtual tank description. The colored segments correspond to different quarters of the city, with their names written in the segments. The apparent layout differentiates from the real geography of the city.

equations [20,21], a simpler description is usually preferred for the MPC design; such as virtual tank models. In such models, complete sections of the system are lumped together and described by their combined volume storage capacity and their interactions with other sections [22,4]. A virtual tank model description of the Aarhus sewer system can be seen in Fig. 2. The shown description was autogenerated by DHI from a high fidelity MIKE URBAN model [16] and translated to a design of deterministic MPC. One of the design criteria in the autogeneration among others; is that each section has a controlled outflow, and is extended from there until another section is reached.

In this work, we will utilize this design of the deterministic MPC to formulate our CC- and ECC-MPC, and as a baseline in the later performance evaluation. The design is based on a modular approach, such that each module corresponds to one of the tanks in Fig. 2, and connected likewise so. The dynamics of the tanks utilized in the model are given by

$$V_{k+1} = AV_k + Bq_k = V_k + \Delta T q_k \tag{26}$$

where q_k is the sum of flows in and out of the tank, at time k. In the design of MPC, a prediction horizon H_p is chosen as a set number of samples to predict into the future of the system. The dynamics above can be reformulated to cover the entire

prediction horizon as given below

$$\mathbf{V} = \mathbf{M}_0 V_0 + M\mathbf{q}, \quad \mathbf{V} = [V_1, V_2, \dots, V_{H_p}]^T, \quad \mathbf{q} = [q_0, q_1, q_2, \dots, q_{H_p-1}]^T \tag{27}$$

$$M = \begin{bmatrix} B & 0 & \dots \\ AB & B & 0 & \dots \\ \vdots & \vdots & \ddots & \ddots \\ A^{H_p-1}B & A^{H_p-2}B & \dots & B \end{bmatrix} = \Delta T \begin{bmatrix} 1 & 0 & \dots \\ 1 & 1 & 0 & \dots \\ \vdots & \vdots & \ddots & \ddots \\ 1 & 1 & \dots & 1 \end{bmatrix} \in \mathcal{R}^{H_p x H_p}, \quad \mathbf{M}_0 = \begin{bmatrix} A \\ A^2 \\ \vdots \\ A^{H_p} \end{bmatrix} = \begin{bmatrix} 1 \\ 1 \\ \vdots \\ 1 \end{bmatrix} \in \mathcal{R}^{H_p x 1} \tag{28}$$

The inflows and outflows of the tanks can be quantified as the controlled output q^{out}, CSO q^{cso}, internal inflow q^{in} and disturbance inflow q^{din}. This gives the following predictive dynamics

$$\mathbf{V} = \mathbf{M}_0 V_0 + M\mathbf{q}^{in} + M\mathbf{q}^{din} - M\mathbf{q}^{out} - M\mathbf{q}^{cso} \tag{29}$$

In the MPC design, the CSO is treated as an optimization variable[3,6,18], by a minimization cost on accumulated CSO volume $\mathbf{V}_k^{cso}$, defined as

$$\mathbf{V}_k^{cso} = \sum_{i=0}^{k} \Delta T \mathbf{q}_i^{cso} \Rightarrow \quad \mathbf{V}^{cso} = M\mathbf{q}^{cso} \tag{30}$$

The cost function of the MPC design can be defined as the sum of cost functions $J_{D,i}$ from each module as seen in the left equation of (31), with minimization with respect to $\mathbf{q}^{out}$ and $\mathbf{q}^{cso}$. Similarly, the right equation shows the cost function of the CC- and ECC-MPC and the module costs $J_{CC,i}$; with the slack variables $\mathbf{c}$ and $\mathbf{s}$ discussed earlier as optimization variables.

$$J = \min_{\mathbf{u},\mathbf{q}^w} \sum_{i=1}^{N_s} J_{D,i}, \quad J = \min_{\mathbf{u},\mathbf{q}^w,\mathbf{c},\mathbf{s}} \sum_{i=1}^{N_s} J_{CC,i} \tag{31}$$

The different modules in the model have different physical meanings and are therefore formulated differently. Each module can be classified as one of five types of tanks; regular tanks, dynamic tanks, and backflow tanks, as well as a strict control version of the regular and backflow tanks. For the deterministic MPC, the modular cost function can be generalized as in (32) with linear costs on the outflow and accumulated CSO volume.

$$J_{D,i} = \boldsymbol{\rho}_{Q,i}^T \mathbf{q}_i^{out} + \frac{\boldsymbol{\rho}_{C,i}^T}{H_p} M \mathbf{q}_i^{cso} \tag{32}$$

Where $\boldsymbol{\rho}_Q$ and $\boldsymbol{\rho}_C$ are uniform weight vectors on the cost terms. A few modules diverge from the above cost and will be discussed later. In the case of the CC- and ECC-MPC, the cost function is an extended version of the deterministic case as seen in (33), and is utilized both for the ECC-MPC and the distribution-based CC-MPC.

$$J_{CC,i} = \boldsymbol{\rho}_{Q,i}^T \mathbf{q}_i^{out} + \frac{\boldsymbol{\rho}_{C,i}^T}{H_p} M \mathbf{q}_i^{cso} + \boldsymbol{\rho}_S^T (\mathbf{s}_i + \mathbf{c}_i) \tag{33}$$

The added cost $\boldsymbol{\rho}_S$ on the slack variables is the same for all slack variables across all modules, with a value of a 100. The cost on the outflow and CSO for each module can be observed in Table 1. The table also shows the maximum volume and outflow of each tank as well as their module type. It can be seen that the tanks with larger volumes ($300 + m^3$) have a slight cost for maximizing the outflow, while small tanks aim at minimizing its usage. By comparison to Fig. 2, it can be seen that CSO connecting to external receivers are weighted higher (5000+), while internal CSOs have lower weights (200-), in order to avoid pollution outside the sewer system.

For the formulation of the modules in the paragraphs below, a few definitions are suitable. In (34), a variable $\mathbf{d}_i$ is given representing the disturbance and initial volume terms of the predictive dynamics for the ith tank, together with its ensemble counterpart $\mathbf{d}_i^E$.

$$\mathbf{d}_i = \begin{bmatrix} M_0 & M \end{bmatrix} \begin{bmatrix} V_{0,i} \\ \mathbf{q}_i^{din} \end{bmatrix}, \quad \mathbf{d}_i^E = \begin{bmatrix} M_0 & M \end{bmatrix} \begin{bmatrix} V_{0,i}^E \\ \mathbf{q}_i^{din,E} \end{bmatrix} \tag{34}$$

The ith switching function discussed earlier in (3) is given by (35) over the prediction horizon H_p, as the volume above the ith tank's limit.

$$\mathbf{T}_i = \mathbf{M}_0 V_{0,i} + M\mathbf{q}_i^{in} + M\mathbf{q}_i^{din} - M\mathbf{q}_i^{out} - M_I \mathbf{q}_i^{cso} - \overline{\mathbf{V}}_i, \quad M_I = M - \Delta T I_{H_p} \tag{35}$$

where I_{H_p} is the identity matrix of size H_p, making the kth prediction of the CSO term independent of the kth CSO. For the CC-MPC based on distribution knowledge, we assume it follows a standardizable distribution as in (17) and that the different

Tank	type	$\overline{V}[m^3]$	$\overline{q}[\frac{m^3}{s}]$	ρ_Q	ρ_C	Tank	type	$\overline{V}[m^3]$	$\overline{q}[\frac{m^3}{s}]$	ρ_Q	ρ_C
1	regular sc	300	1.50	-0.01	5000	20	regular	13001	0.22	-0.01	5000
2	regular sc	20	0.60	10^{-4}	5000	21	regular	10001	0.40	-0.01	5000
3	backflow sc	350	1.00	-0.01	200	22	regular	3501	0.18	-0.01	5000
4	backflow sc	844	1.80	-0.01	200	23	regular sc	90	1.20	10^{-4}	5000
5	dynamic	200	0.50	10^{-4}	5000	24	regular	3001	0.09	-0.01	15000
6	regular sc	200	0.80	10^{-4}	5000	25	regular	6699	1.50	-0.01	5000
7	regular	100	0.10	10^{-4}	0.02	26	dynamic	3503	0.10	-0.01	10000
8	dynamic	10	0.04	10^{-4}	5000	27	regular	200	0.20	10^{-4}	0.02
9	regular	10	1.00	10^{-4}	5000	28	regular	60	0.70	10^{-4}	5000
10	regular	10	0.20	10^{-4}	5000	29	regular	100	0.20	10^{-4}	0.02
11	regular	150	0.35	10^{-4}	5000	30	regular	85	0.10	10^{-4}	200
12	regular	10	0.10	10^{-4}	5000	31	backflow	200	0.20	10^{-4}	20
13	regular sc	10	0.80	10^{-4}	5000	32	dynamic	100	0.04	10^{-4}	200
14	regular	10	0.20	10^{-4}	5000	33	dynamic	32	0.50	10^{-4}	200
15	regular	10	0.40	10^{-4}	5000	34	dynamic	25	0.50	10^{-4}	200
16	regular	10	0.70	10^{-4}	5000	35	dynamic	12	0.50	10^{-4}	200
17	regular sc	70	0.80	10^{-4}	5000	36	regular	80	0.30	10^{-4}	200
18	regular sc	50	0.15	10^{-4}	200	37	regular	90	0.40	10^{-4}	200
19	regular sc	85	0.98	10^{-4}	5000	38	regular	10	0.10	10^{-4}	5000

TABLE 1 The system data of the Aarhus network[17]

uncertainties are independent. Under these assumptions, the predicted variance $\boldsymbol{\sigma}_i$ of the ith module is given by

$$\boldsymbol{\sigma}_i = \sqrt{M_0^2 \sigma_{V_{0,i}}^2 + M^2 \boldsymbol{\sigma}_{q_i^{din}}^2} \tag{36}$$

where both the squares and root are to be understood as element operations.

3.1 | Modules - regular and backflow type

For the ith module belonging to either the regular or backflow type, the definition is identical with the difference lying in connections between tanks. For the deterministic MPC, the module is defined by the constraints given by (37)-(39), describing the volume, outflow, and CSO limitations.

$$0 \le \mathbf{V}_i \le \overline{\mathbf{V}}_i \tag{37}$$

$$0 \le \mathbf{q}_i^{out} \le \overline{\mathbf{q}}_i^{out} \tag{38}$$

$$0 \le \mathbf{q}_i^{cso} \tag{39}$$

For the distribution-based CC-MPC, the constraints in (40)-(44) define the module as according to section 2, with the volume and switching function being substituted by (29) and (35) respectively.

$$0 + \boldsymbol{\sigma}_i \Phi^{-1}(\gamma_i) - \mathbf{s}_i \le E\{\mathbf{d}_i\} + M\mathbf{q}_i^{in} - M\mathbf{q}_i^{out} - M\mathbf{q}_i^{cso} \le \overline{\mathbf{V}}_i \tag{40}$$

$$0 \le \mathbf{q}_i^{out} \le \overline{\mathbf{q}}_i^{out} \tag{41}$$

$$0 \le \mathbf{q}_i^{cso}, \mathbf{c}_i \tag{42}$$

$$E\{\mathbf{d}_i\} + M\mathbf{q}_i^{in} - M\mathbf{q}_i^{out} - M_I\mathbf{q}_i^{cso} \le \overline{\mathbf{V}}_i - \boldsymbol{\sigma}_i \Phi^{-1}(\gamma_i) + \mathbf{c}_i \tag{43}$$

$$0 \le \mathbf{s}_i \le \boldsymbol{\sigma}_i \Phi^{-1}(\gamma_i) \tag{44}$$

For the ECC-MPC, the definition is given by (45)-(49), where the quantile terms $\mathbf{\Phi}_{\pm\mathbf{d}^E}^{-1}$ needs to be estimated.

$$0 + \Phi_{-d_i^E}^{-1}(\gamma_i) - \mathbf{s}_i \leq M\mathbf{q}_i^{in} - M\mathbf{q}_i^{out} - M\mathbf{q}_i^{cso} \leq \overline{\mathbf{V}}_i - E\{\mathbf{d}_i^E\} \tag{45}$$

$$0 \leq \mathbf{q}_i^{out} \leq \overline{\mathbf{q}}_i^{out} \tag{46}$$

$$0 \leq \mathbf{q}_i^{cso}, \mathbf{c}_i \tag{47}$$

$$M\mathbf{q}_i^{in} - M\mathbf{q}_i^{out} - M_I\mathbf{q}_i^{cso} \leq \overline{\mathbf{V}}_i - \mathbf{\Phi}_{\mathbf{d}_i^E}^{-1}(\gamma_i) + c_i \tag{48}$$

$$0 \leq \mathbf{s}_i \leq \mathbf{\Phi}_{-\mathbf{d}_i^E}^{-1}(\gamma_i) - E\{-\mathbf{d}_i^E\} \tag{49}$$

3.2 | Modules - strict control regular and backflow type

The strict control versions of the regular and backflow modules are using the same formulation as their counterpart, but includes extra constraints on the controlled outflow of the tank, as seen in (50). These added limitations relate the outflow to the volume of the tank by the volume-flow coefficient β [23]. The lower constraint is scaled by the parameter $a_{sc,i}$, limiting how far the outflow can be from the physical limit.

$$a_{sc,i}\beta_i\mathbf{V}_i \leq \mathbf{q}_i^{out} \leq \beta_i\mathbf{V}_i \tag{50}$$

For regular modules with strict control, the value of $a_{sc,i}$ is 0.8, while it is 0.95 for the corresponding backflow modules.

For the definition of the modules with respect to the CC- and ECC-MPC, the added constraints introduce two new slack variables, with more cost terms added to the base module cost from (33), as seen in (51).

$$J_{CC,i} = J_{CC,i}^{base} + \boldsymbol{\rho}_S^T(\mathbf{s}_{1,i} + \mathbf{s}_{2,i}) \tag{51}$$

The module definition of the distribution-based CC-MPC is similar to above, the same formulation as the non-strict counterpart with the added constraints given by (52)-(54)

$$a_{sc,i}\beta_i E\{\mathbf{V}_i\} + a_{sc,i}\beta_i\boldsymbol{\sigma}_i\Phi^{-1}(\gamma_i) - \mathbf{s}_{1,i} \leq \mathbf{q}_i^{out} \leq \beta_i E\{\mathbf{V}_i\} - \beta_i\boldsymbol{\sigma}_i\Phi^{-1}(\gamma_i) + \mathbf{s}_{2,i} \tag{52}$$

$$0 \leq \mathbf{s}_{2,i} \leq \beta_i\boldsymbol{\sigma}_i\Phi^{-1}(\gamma_i) \tag{53}$$

$$0 \leq \mathbf{s}_{1,i} \leq a_{sc,i}\beta_i\boldsymbol{\sigma}_i\Phi^{-1}(\gamma_i) \tag{54}$$

From the constraints in (55)-(57), the additional constraints to defined the module for ECC-MPC are given, with the quantile function being dependent on scaled ensembles of $\mathbf{d}^E$.

$$a_{sc,i}\beta_i M(\mathbf{q}_i^{in} - \mathbf{q}_i^{out} - \mathbf{q}_i^{cso}) + \Phi_{a_{sc,i}\beta_i\mathbf{d}_i^E}^{-1}(\gamma_i) - \mathbf{s}_{1,i} \leq \mathbf{q}_i^{out} \leq \beta_i M(\mathbf{q}_i^{in} - \mathbf{q}_i^{out} - \mathbf{q}_i^{cso}) - \Phi_{-\beta_i\mathbf{d}_i^E}^{-1}(\gamma_i) + \mathbf{s}_{2,i} \tag{55}$$

$$0 \leq \mathbf{s}_{2,i} \leq \Phi_{-\beta_i\mathbf{d}_i^E}^{-1}(\gamma_i) - E\{-\beta_i\mathbf{d}_i^E\} \tag{56}$$

$$0 \leq \mathbf{s}_{1,i} \leq \Phi_{a_{sc,i}\beta_i\mathbf{d}_i^E}^{-1}(\gamma_i) - E\{a_{sc,i}\beta_i\mathbf{d}_i^E\} \tag{57}$$

3.3 | Modules - dynamic type

For the modules representing the dynamic tanks no constraints are added, but the control constraint in (38) is replaced with (58), where the upper limitation now depends on the inflows to the tank.

$$0 \leq \mathbf{q}_i^{out} \leq \overline{\mathbf{q}}_i^{out} + \mathbf{q}_i^{in} + \mathbf{q}_i^{din} \tag{58}$$

Given the replacement relies on the uncertain $\mathbf{q}^{din}$, the definitions for the CC- and ECC-MPC introduce a new slack variable with a new cost term associated with it

$$J_{CC,i} = J_{CC,i}^{base} + \boldsymbol{\rho}_S^T\mathbf{s}_{3,i} \tag{59}$$

The definition for distribution-based CC-MPC is given by (60) and (61), where the prior is the replaced constraint and the later is an added constraint on the new slack variable.

$$0 \leq \mathbf{q}_i^{out} \leq \overline{\mathbf{q}}_i^{out} + \mathbf{q}_i^{in} + E\{\mathbf{q}_i^{din}\} + \mathbf{s}_{3,i} - \sqrt{\boldsymbol{\sigma}_{q_i^{din}}}\Phi^{-1}(\gamma_i) \tag{60}$$

$$0 \leq \mathbf{s}_{3,i} \leq \sqrt{\boldsymbol{\sigma}_{q_i^{din}}}\Phi^{-1}(\gamma_i) \tag{61}$$

Tank j	2	3	4	10	11	15	16	17
Delay(min.)	20	10	4	2	5	20	3	14

TABLE 2 Delays in the Aarhus network [17]

similarly, the constraints given in (62) and (63), gives the definition for the case of the ECC-MPC.

$$0 \leq \mathbf{q}_i^{out} \leq \overline{\mathbf{q}}_i^{out} + \mathbf{q}_i^{in} - \Phi_{-\mathbf{q}_i^{din,E}}^{-1}(\gamma_i) + \mathbf{s}_{3,i} \tag{62}$$

$$0 \leq \mathbf{s}_{3,i} \leq \Phi_{-\mathbf{q}_i^{din,E}}^{-1}(\gamma_i) - E\{-\mathbf{q}_i^{din,E}\} \tag{63}$$

3.4 | Modules - connections and operation

With the modules defined, the interconnection between them and specific operation goals can be discussed. The connections come in two types; backflows and downstream connections.

3.4.1 | Backflows

Backflows of a tank i are flows going upstream to the previous tank j inside the outflow pipe. In the two types of backflow modules, this is formulated as the CSO of the backflow of tank i affecting the outflow constraint of tank j. As seen in (64) for the general case of (38), but similarly added to other module type variants.

$$0 \leq \mathbf{q}_j^{out} + \mathbf{q}_i^{cso} \leq \overline{\mathbf{q}}_j^{out} \tag{64}$$

3.4.2 | Downstream Connections

For the downstream connections, one has to consider possible flow delays and multiple sources of outflows and internal CSOs. The delays in the system can be observed in Table 2 with the tank of origin. For the receiving tank i, the tank inflow is formulated as (65), where the sets Q_c and Q_o define which CSO and outflows connect to the tank. While the matrices M_Δ and M_δ define the delays of the jth outflow.

$$\mathbf{q}_i^{in} = \sum_{j \in Q_c} \mathbf{q}_j^{cso} + \sum_{j \in Q_o} (M_{\Delta,j}\mathbf{q}_j^{out} + M_{\delta,j}\mathbf{q}_{\delta,j}^{out}) \tag{65}$$

$$M_{\Delta,j} = \begin{bmatrix} \mathbf{0}_{N_{\delta,j}} & \mathbf{0}_{N_{\delta,j}} & \cdots & \\ 1-\delta_{q,j} & \delta_{q,j} & 0 & \cdots \\ 0 & 1-\delta_{q,j} & \delta_{q,j} & \ddots \\ \vdots & \ddots & \ddots & \ddots \\ 0 & 0 & 1-\delta_{q,j} & \delta_{q,j} \end{bmatrix} \in \mathcal{R}^{H_p x H_p}, \quad M_{\delta,j} = \begin{bmatrix} \delta_{q,j} & (1-\delta_{q,j}) & 0 & \cdots \\ 0 & \ddots & \ddots & \ddots \\ \vdots & \ddots & \delta_{q,j} & (1-\delta_{q,j}) \\ \mathbf{0}_{H_p-N_{\delta,j}} & \mathbf{0}_{H_p-N_{\delta,j}} & \cdots & \mathbf{0}_{H_p-N_{\delta,j}} \end{bmatrix} \in \mathcal{R}^{H_p x N_{\delta,j}+1} \tag{66}$$

where $N_{\delta,j}$ is the number of whole sample delays, $\delta_{q,j}$ the remaining fraction of a whole sample, and $\mathbf{q}_{\delta,j}^{out}$ is the delayed flows from the last sample.

3.4.3 | Flow Inhibitors

A few of the tanks in the system has features affecting the outflow, which are not described by the general modules discussed so far. These tanks follow the constraints in (67) instead of (38). The values of the inhibition factor α_{fac} can be seen for each affected tank in Table 3.

$$0 \leq \alpha_{fac}\mathbf{q}_i^{out} \leq \overline{\mathbf{q}}_i^{out} \tag{67}$$

Tank	7	21	24	27	29	31
α_{fac}	0.2857	0.5	0.2571	0.5714	0.2	0.5714

TABLE 3 The flow inhibitor factors α_{fac} in the Aarhus network[17]

3.4.4 | Reference

For the operation of the sewer system, there is a desire to keep the outflow of tank 1 at a specific flow rate q^{ref} of 0.9 m^3/s, if possible. Therefore an extra cost and constraints are added to the module for tank 1, defined as

$$J_{D,1} = J_{D,1}^{base} + \boldsymbol{\rho}_R^T(\mathbf{r}_1 + \mathbf{r}_2) \tag{68}$$

$$-\mathbf{r}_1 \leq \mathbf{q}_1^{out} - q^{ref} \leq \mathbf{r}_2 \tag{69}$$

$$\mathbf{0} \leq \mathbf{s}_4, \mathbf{s}_5 \tag{70}$$

where $\boldsymbol{\rho}_R$ is uniformly valued at 0.01. For the CC-MPCs, the addition is the same.

3.4.5 | Spare Volume

For the system, it is desirable that the tanks are not empty. Therefore each tank description is extended with an operational lower limit to operate at, as given in (71) for a limit at some fraction α_b of the maximum volume.

$$J_{D,i} = J_{D,i}^{base} + \boldsymbol{\rho}_B^T(\mathbf{r}_{3,i}) \tag{71}$$

$$\alpha_b \overline{\mathbf{V}}_i - \mathbf{r}_{3,i} \leq \mathbf{V}_i \tag{72}$$

$$\mathbf{0} \leq \mathbf{r}_{3,i} \tag{73}$$

where the weight $\boldsymbol{\rho}_B$ is uniformly valued at 0.01, and α_b at 0.1. For the CC- and ECC-MPC, this restriction of the lower constraint is similar to their own probabilistic restriction, and therefore this extra restriction is only considered for the expectation:

$$\alpha_b \overline{\mathbf{V}}_i - \mathbf{r}_{3,i} \leq E\{\mathbf{V}_i\} \tag{74}$$

4 | RESULTS-PERFORMANCE

For the evaluation of the ECC-MPC framework, we will compare its performance against the discussed distribution-based CC-MPC. The deterministic MPC is used as a baseline for the comparison, to give a performance reference. The MPCs will all use a prediction horizon H_p of 20 samples and a sampling time of 300 seconds, giving 100 minutes of prediction. For the ECC- and CC-MPC, the confidence level γ of the quantile functions is used as 90% for all quantiles. The ECC-MPC is given an ensemble forecast of 50 independent rain scenarios, to use for the estimation. The initial volume V_0 of each tank is assumed to be known perfectly and is $1m^3$ at the start of each simulation. For the simulations, 9 sets of historical weather scenarios from the city of Aarhus were utilized. In Fig. 3, the temporal evolution of the rain events is shown, clarifying the duration of the event and its intensities in m^3/s. Likewise in Fig. 4, the spatial distribution of the rain inflow is shown, quantifying the amount of volume m^3 each tank has received per event.

4.1 | Distribution estimation approach

In the simulations, the estimation approach utilizedby the ECC-MPC is the Pearson's χ^2 goodness of fit test mentioned earlier. In this work, only two distributions have been tested for during the simulations, Normal and Uniform distributions, but could easily be extended to other well-known distributions. The uniform distribution was used as the fallback strategy, in case of estimation failure. While each probabilistic constraint is scalar, the estimation procedure used has assumed that the quantile functions within one specific module follows the same type of distribution (normal, uniform, etc.), and has estimated them simultaneous.
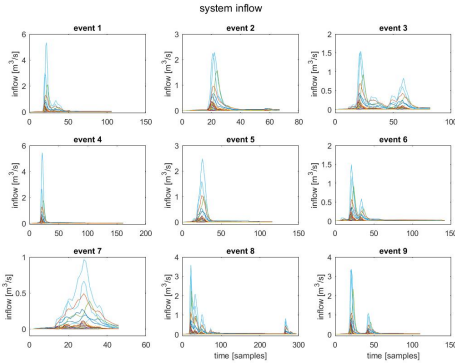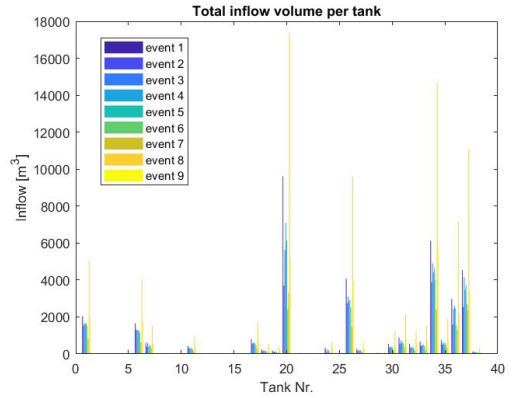
FIGURE 3 weather scenarios, temporal

FIGURE 4 weather scenarios, spatial

Simulation Nr.	1	2	3	4	5	6	7	8	9	10	11	12
Uncertainty Bounds κ	0.5	0.5	0.5	0.5	0.5	0.1	0.25	0.75	1	0.5	0.5	0.5
Scaled Bias a	0.8	0.9	1	1.1	1.2	1	1	1	1	1	1	1
Offset Bias b	0	0	0	0	0	0	0	0	0	0.005	0.01	0.1

TABLE 4 The sizes of the different types of forecast uncertainty introduced in each of the 12 simulation scenarios

4.2 | Test Scenarios

In order to evaluate the performance of the controllers, three different types of uncertainties were introduced into the rain forecast f utilized by the ECC- and CC-MPC, while the deterministic MPC is given the correct rain forecast f_0. The three types of forecast uncertainty are:

- forecast's uncertainty bound, $f \in E\{f\} \pm 3\sigma_f$

- scaled bias of the forecast expectation, $E\{f\} = af_0$

- offset bias of the forecast expectation, $E\{f\} = f_0 + b$

where the variance term σ_f is given by $\sigma_f = \frac{\kappa}{3} f_0$. Each type of uncertainty was given a default setting, such that only one type of uncertainty was being varied from simulation to simulation. In Table 4, each used combination of the three uncertainty types is shown. The default values are $\kappa = 0.5$, $a = 1.0$ and $b = 0.0$ respectively. For the simulations, the uncertainty added to the rain forecast was truncated normal distributed, in accordance with the three types of uncertainties discussed. In Fig. 5, the total CSO per event is shown for the default simulation scenario. It can be seen that both ECC- and CC-MPC are comparable in performance for the default simulation. While they both perform worse than MPC for the middle-sized events, and comparable to for small and large events, corresponding to a low loaded system and a saturated system respectively.

4.3 | Performance: Uncertainty Bounds

By varying the bounds of the uncertainty on the utilized forecasts, the effects on the controller can be evaluated. This allows us to evaluate the reliance on the certainty of the forecast. Considering the outflow of the system, we can see from Fig. 6, that the ECC-MPC operate comparably similar to CC-MPC, while providing larger outflows than MPC for the middle-sized events. Furthermore, the effects of varying the bounds appear to have only a slight effect on the performances of both ECC- and CC-MPC, with outflow generally increases as bound is increased. When focusing on the performance in the context of CSO, we have both the total CSO volume and the external CSO volume to consider. Shown for both ECC- and CC-MPC in Fig. 7 and Fig.

simulation scenario: Uncertainty size
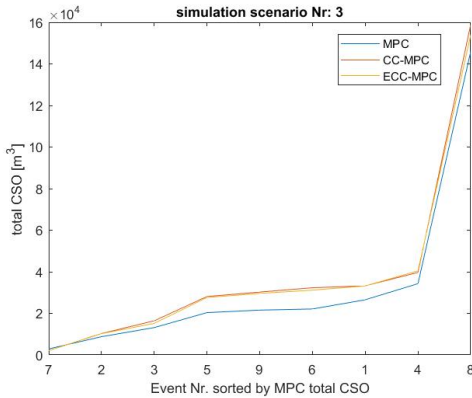
FIGURE 5 Total CSO Volume
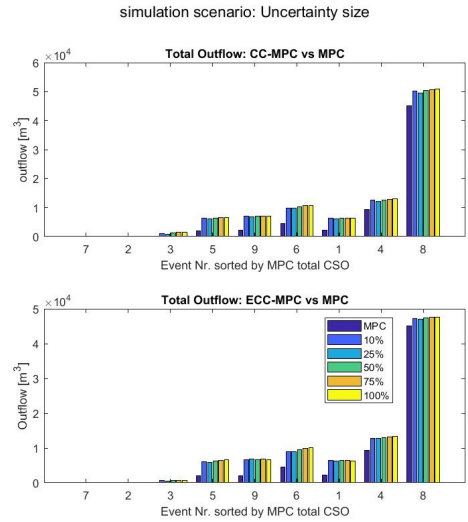
FIGURE 6 Total outflow with MPC as the baseline; for variations in uncertainty bounds

8 respectively, as percentage improvement in comparison to MPC performance. From the external CSO, we can observe clear improvements for both CC-MPCs, with a slight trend for high bounds to perform better as the event size increases. The general performance between ECC- and CC-MPC is comparable but not identical. From the total CSO, it can be seen that the price of improving the external CSO is generally a great increase in the internal CSO, rerouting the water internally leading to the observed increase in the outflow. It can further be seen that the external CSO improvement is very reliant on the spatial/temporal distribution of the rain inflow, while the total CSO only seems to depend on the event size.

4.4 | Performance: Scaled Bias

In practical applications, biases are natural to expect in the expected forecast of the distribution or ensemble. The ECC- and CC-MPC's performances under a constant scaling bias is evaluated in Fig. 9 and Fig. 10, for the total CSO and external CSO respectively. It can be seen that the general performance across events matches the performance discussed previously, with improvement in external CSO volume, at the cost of increased total CSO. The ECC- and CC-MPC are still comparable in their performance. With regard to the scaling bias, the CSO improvement has no general trend, with the exception of events with smaller percentage improvements, who shows a slight benefit of overestimating the rain forecast. From Fig. 11, the performance in the outflow volume is shown. Again, the performances are similar between the CC-MPCs and with larger outflow than the MPC.

4.5 | Performance: Offset Bias

Now considering the bias on the expectation of the forecast is a constant offset bias instead of a scaling bias. The total outflow volume with offset biases can be observed in Fig. 12. While the performance of the ECC-MPC are comparable to that of CC-MPC; they both have a clear reliance on the bias with the outflow increasing as the bias increases. The same reliance can be seen about the improvement in CSO from Fig. 13 and Fig. 14 for total and external CSO respectively. For the external CSO, the improvements show a general reliance on the bias, in the sense that the improvement drops as the bias increases; to the point of the largest bias results in a deterioration of performance.
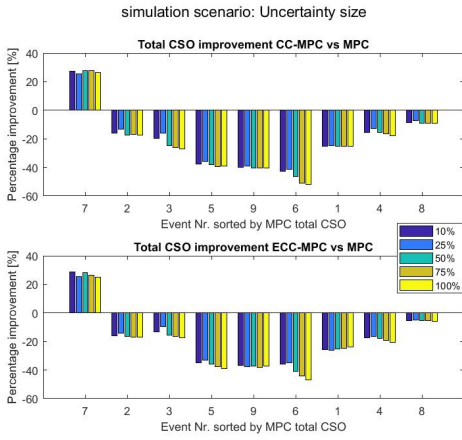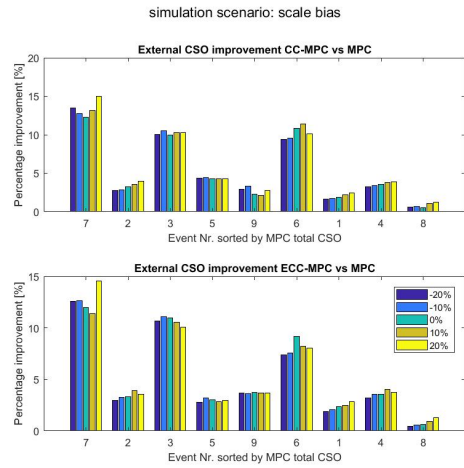
FIGURE 7 Total CSO improvement in percentages with MPC as the baseline, positive percentages representing a reduction in CSO
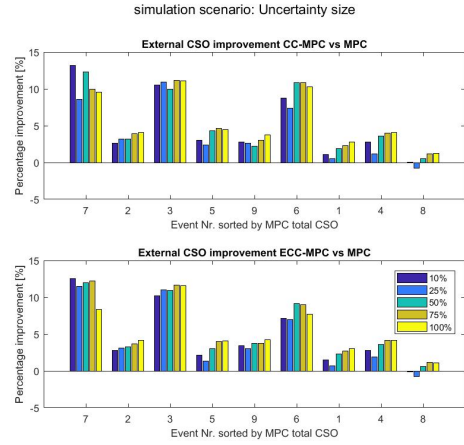
FIGURE 8 External CSO improvement in percentages with MPC as the baseline, positive percentages representing a reduction in CSO
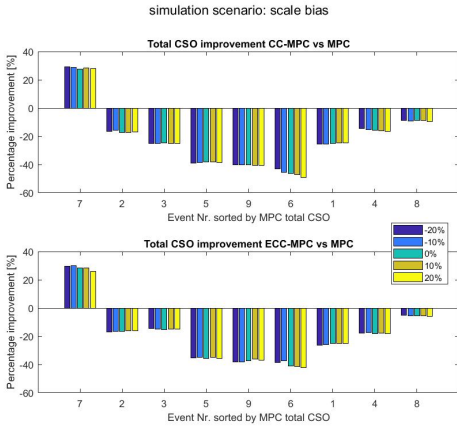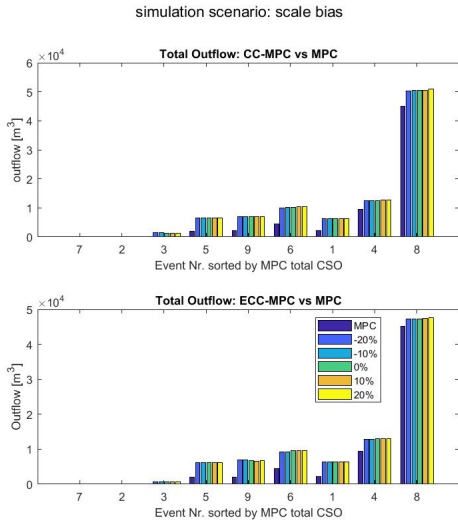

FIGURE 9 Total CSO improvement in percentages with MPC as the baseline, positive percentages representing a reduction in CSO
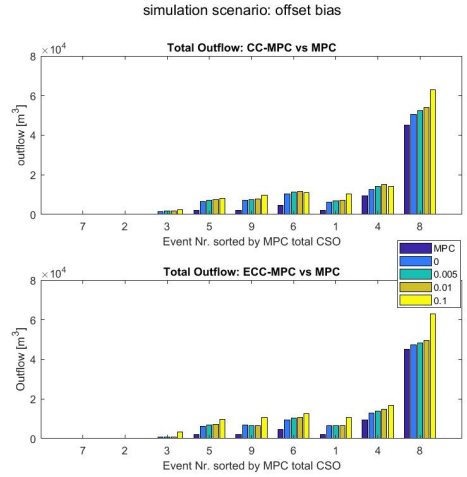

FIGURE 10 External CSO improvement in percentages with MPC as the baseline, positive percentages representing a reduction in CSO

4.6 | Reflections on the Results

The performances of both ECC- and CC-MPC show that constant offset bias is the predominant influence on their performance. While the performances appear to be less variant of the bound on the uncertainty and scaled biases. A reason for this can be the size of the scale bias is within the uncertainty bound, and that the simulations on uncertainty bound utilizes an expectation equal to the correct forecast, only resulting in more conservative solutions. While the larger offset bias might shift the correct forecast outside the bounds of the forecasts of both the ECC- and CC-MPC.
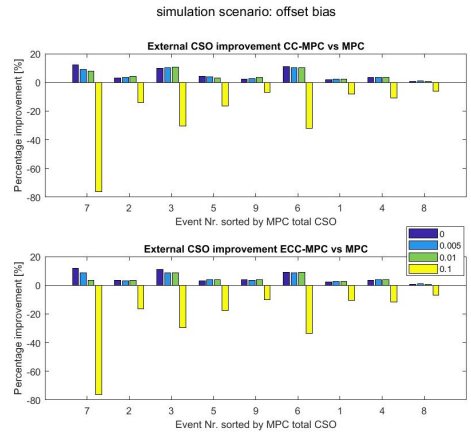
simulation scenario: scale bias

FIGURE 11 Total outflow with MPC as the baseline; for variations in scaling bias

FIGURE 12 Total outflow with MPC as the baseline; for variations in offset bias
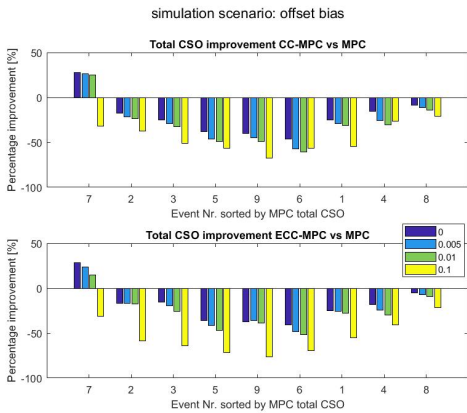
FIGURE 13 Total CSO improvement in percentages with MPC as the baseline, positive percentages representing a reduction in CSO

FIGURE 14 External CSO improvement in percentages with MPC as the baseline, positive percentages representing a reduction in CSO

In all of the simulations, the performance of both CC-MPC and ECC-MPC were comparable, but not identical to each other. This gives a good suggestion that the proposed framework should perform similar to CC-MPC at more complex system setups than linear system with normal distributed uncertainty.

Lastly a small but curious result can be observed in the general performance of both ECC- and CC-MPC w.r.t. the external CSO. The CC- and ECC-MPC perform better than the baseline MPC with a perfect forecast. While this can seem unlogical given the MPC should find the optimal solution, this is a consequence of using a finite prediction horizon. It is due to the forecast

not including the whole rain event, and is an intrinsic trade-off of all types of MPC; future information can change the optimum trajectory. Stated more practically, the MPC finds the optimal solution within the finite horizon, while CC-, and ECC- MPC finds more conservative solutions. This can results in an initial state of the next time step's optimization that is at times more favorable in the long term.

5 | CONCLUSIONS

In this paper, we have suggested a framework for handling propagation of uncertainty distributions in chance-constrained(CC) model predictive control (MPC) based on ensemble forecasts and distribution estimation. The ensemble-based CC-MPC framework (ECC-MPC) have been evaluated by simulations on a model of the sewer network of Aarhus, Denmark, and compared in performance with the performance of CC-MPC.

The simulations utilized linear models with normal distrubted forecast uncertainty, to produce a setup where both CC-MPC and ECC-MPC could easily be computed. For this particular system setup, it was found that CC-MPC and the ECC-MPC were comparable in their performances, and even shown the same responses to different changes in aspects of the uncertainties, such as expectation biases and bounds. The aspect of uncertainty which had most effect on ECC- and CC-MPC were found to be offset biases, while they were less sensitive to changes in scalling biases and uncertainty bounds.

Based on the comparable performances of the simple setup of this work, we can conclude that the ECC-MPC framework should be a suitable alternative approach to CC-MPC for more complex scenarios of distribution propagation of nonlinear models and/or non-normal distributed additive uncertainties.

References

1. Lee JH. Model Predictive Control: Review of the Three Decades of Development. *International Journal of Control, Automation, and Systems* 2011; 9(3): 415-424.

2. Qin SJ, Badgwell TA. A survey of industrial model predictive control technology. *Control Engineering Practice* 2003; 11: 733-764.

3. Gelormino MS, Ricker NL. Model Predictive Control of a Combined Sewer System. *INT. J. CONTROL* 1994; 59(3): 793-816.

4. Ocampo-Martinez C. *Model Predictive Control of Wastewater Systems*. Advances in Industrial ControlSpringer . 2010.

5. Puig V, Cembrano G, Romera J, et al. Predictive optimal control of sewer networks using CORAL tool: application to Riera Blanca catchment in Barcelona. *Water Science & Technology* 2009; 60(4): 869-874.

6. Halvgaard R, Falk AKV. Water system overflow modeling for Model Predictive Control. In: Proceedings of the 12th IWA Specialised Conference on Instrumentation, Control and Automation. ; 2017.

7. Marinaki M, Papageorgiou M. *Optimal Real-time Control of Sewer Networks*. Advances in Industrial ControlSpringer . 2005.

8. Mesbah A. Stochastic Model Predictive Control: An overview and Perspectives for Future Research. *IEEE Control Systems Magazine* 2016: 30-44. doi: 10.1109/MCS.2016.2602087

9. Grosso JM, Ocampo-Martinez C, Puig V, Joseph-Duran B. Chance-constrained model predictive control for drinking waternetworks. *Journal of Process Control* 2014; 24: 504-516.

10. Svensen JL, Niemann HH, Falk AKV, Poulsen NK. Chance-Constrained Model Predictive Control - A reformulated approach suitable for sewer networks. *Advanced Control for Applications* 2020. , Submitted.

11. Raso L, Schwanenberg D, Giesen v. dN, Overloop vP. Short-term optimal operation of water systems using ensemble forecasts. *Advances in Water Resources* 2014; 71: 200-208.

12. Evans M, Cannon M, Kouvaritakis B. Linear Stochastic MPC under finitely supported multiplicative uncertainty. In: Proc. of the 2012 American Control Conference. ; 2012.

13. Garatti S, Campi MC, Garatti S, Prandini M. The scenario approach for systems and control design. *Annual Reviews in Control* 2009; 33: 149-157.

14. Campi MC, Garatti S, Prandini M. *Scenario Optimization for MPC*: 445–463; Cham: Springer International Publishing . 2019

15. Kouvaritakis B, Cannon M. *Model Predictive Control - Classical, Robust and Stochastic*. Advances Textbooks in Control and Signal ProcessingSpringer . 2016

16. Drejer LH, Halvgaard R. Water Smart Cities Milestone 5: Offline Model Predictive Control (MPC) performance results for the Marselisborg, Aarhus case study. tech. rep., DHI; : 2020.

17. Drejer L, DHI . private communication; 2020.

18. Svensen JL, Niemann HH, Poulsen NK. Model Predictive Control of Overflow in Sewer Networks: A comparison of two methods. In: Proc. of the 4th Int. Conf. on Control and Fault-Toleran Systems. ; 2019: 412-417.

19. Danmarks-Statistik . https://www.statistikbanken.dk/BY1; 2020. Accessed: 30-09-2020.

20. Butler D, Davies JW. *Urban Drainage*. Spon Press. third ed. 2011.

21. Chow VT, Maidment DR, Mays LW. *Applied Hydrology*. McGraw-Hill . 1988.

22. Garcia L, Barreiro J, Escobar E, F. Tellez NQ, Ocampo-Martinez C. Modelling and Real-Time Control fo Urban Drainage Systems: A Review. *Advances in Water Resources* 2015; 85: 120-132.

23. Singh VP. *Hydrologic Systems. Volume 1: Rainfall-runoff modelling*. Prentice Hall . 1988.